

The role of reciprocal fusions in *MLL-r* acute leukemia: studying the chromosomal translocation t(4;11)

Dissertation

presented to the Faculty of Biochemistry, Chemistry and Pharmacy
of the Johann Wolfgang Goethe University Frankfurt
in partial fulfillment of the requirement for
the degree of Doctor of Natural Sciences
(Dr. rer. nat.)

by

Alexander Wilhelm

from Offenbach

Frankfurt am Main, 2022

(D30)

Accepted by the Faculty 14 Biochemistry, Chemistry and Pharmacy
Of the Johann Wolfgang Goethe University Frankfurt
As dissertation

Dean: Prof. Dr. Clemens Glaubitz

1st Examiner: Prof. Dr. Rolf Marschalek,
Institute of Pharmaceutical Biology, Faculty 14

2nd Examiner: Prof. Dr. Robert Fürst,
Institute of Pharmaceutical Biology, Faculty 14

Disputation:

TABLE OF CONTENT

ABSTRACT	1
ZUSAMMENFASSUNG	3
1. INTRODUCTION.....	8
1.1. Leukemia	8
1.2. <i>MLL</i> -rearranged (<i>MLL</i> -r) leukemia.....	11
1.3. t(4;11) ALL	16
1.4. Targeted treatments against t(4;11) ALL	20
1.5. Aim	25
2. MATERIAL	26
2.1. Cell lines	26
2.2. Bacterial strains	26
2.3. Oligonucleotides	27
2.4. Antibodies	27
2.5. Enzymes	28
2.6. Plasmids	28
2.7. Commercial kits	29
2.8. Chemicals and solutions	29
2.9. Buffers and media	31
3. METHODS.....	35
3.1. Sequencing.....	35
3.1.1. MACE-seq.....	35
3.1.2. ATAC-seq	36
3.2. Cell biology methods	36
3.2.1. Cultivating adherent cell lines.....	36
3.2.2. Cultivating suspension cell lines	37
3.2.3. Cell counting and viability assay.....	37

3.2.4.	Transfections using the Sleeping Beauty System	37
3.2.5.	Annexin V Assay (Flow Cytometry readout)	38
3.2.6.	Annexin V Assay (microscopic readout)	38
3.3.	Biochemical methods	39
3.3.1.	Preparation of cell lysates	39
3.3.2.	Western Blot analysis.....	39
3.4.	Bioinformatic and statistical analysis.....	39
4.	RESULTS	41
4.1.	Expression of dnTASP1 induces apoptosis in HDACi-treated t(4;11) ALL cells <i>in vitro</i>	41
4.1.1.	Generation of a dnTASP1 expressing t(4;11) pro-B ALL cell line	41
4.1.2.	Short-term expression of dnTASP1 has minor effects on HDACi-treated SEM43	
4.1.3.	Long-term expression of dnTASP1 increases HDACi-induced apoptotic levels of SEM cells <i>in vitro</i>	46
4.2.	Targeting MLL fusion proteins in patient-derived xenograft leukemia cells <i>in vivo</i> generates distinct transcriptional signatures.....	57
4.2.1.	Induction of an MLL-AF4 knock-down in proliferating PDX leukemia cells elicits altered transcriptional signatures.....	58
4.2.2.	The expression of dnTASP1 in proliferating PDX leukemia cells upregulates cell-cycle dependent genes	70
4.3.	AF4-MLL-induced chromatin and transcriptional signature persists in t(4;11) leukemia model <i>in vitro</i>.....	77
4.3.1.	A cellular t(4;11) model to study the transforming potential of transiently expressed AF4-MLL	79
4.3.2.	A cellular t(4;11) leukemic model allows to study MLL-AF4 and AF4-MLL independently.....	80
4.3.3.	AF4-MLL induces expression of pseudogenes and non-annotated genes.....	82
4.3.4.	AF4-MLL promotes clonal evolution	87
4.3.5.	Signatures of the <i>in vitro</i> cellular t(4;11) model overlap with <i>in vivo</i> gene sets of infant B-ALL patients.....	88
4.3.6.	k-means clustering indicates novel AF4-MLL-associated genes.....	89
4.4.	t(4;11) fusion proteins endorse transcription of mitochondrial genes but has no effect on mitochondrial respiration <i>in vitro</i>	91
4.4.1.	t(4;11) fusion proteins activate mitochondrial genes.....	92
4.4.2.	MLL fusion proteins have minor effects on mitochondrial respiration <i>in vitro</i> ...	93
4.5.	AF4-MLL impacts chromatin signature over time.....	96

4.5.1.	A cellular t(4;11) model to study accessibility of chromatin	96
4.5.2.	Long-term altered chromatin state upon short-term expression of AF4-MLL ...	98
4.5.3.	t(4;11) fusion proteins alter chromatin status synergistically	102
5.	DISCUSSION.....	108
5.1.	Co-targeting of MLL-AF4 and AF4-MLL synergistically induces apoptosis in t(4;11) leukemic cells <i>in vitro</i>	109
5.2.	Targeting MLL-AF4 <i>in vivo</i> in t(4;11) PDX cells down-regulates pivotal hematoma-malignant factors	114
5.3.	Expression of dnTASP1 <i>in vivo</i> in t(4;11) PDX cells de-regulates cell-cycle related genes.....	116
5.4.	Short-term expressed AF4-MLL exerts long-lasting effect on transcriptome and chromatin in cooperation with MLL-AF4.....	118
5.5.	Conclusions.....	121
6.	LIST OF ABBREVIATIONS	123
7.	LIST OF FIGURES AND TABLES	132
8.	REFERENCES.....	135
9.	STATUTORY DECLARATION.....	161
10.	CURRICULUM VITAE	162
11.	LIST OF PUBLICATIONS	164
12.	ACKNOWLEDGEMENTS	167

Parts of the thesis have been previously published in:

Wilhelm A, Marschalek R. The role of reciprocal fusions in MLL-r acute leukemia: studying the chromosomal translocation t(4;11). *Oncogene*. 2021 <https://doi.org/10.1038/s41388-021-02001-2>

and

Carlet M, Völse K, Vergalli J, Becker M, Herold T, Arner A, Liu W-H, Dill V, Fehse B, Baldus C D, Bastian L, Lenk L, Schewe D M, Bagnoli J W, Wilhelm A, Marschalek R, Jost P J, Miehting C, Riecken K, Schmidt-Supprian M, Binder V, Jeremias I. In vivo inducible reverse genetics in patients' tumors to identify individual therapeutic targets, *Nature Communications*. 2021 <https://doi.org/10.1038/s41467-021-25963-z>

ABSTRACT

The majority of B-cell precursor acute leukemias in infants are associated with the chromosomal translocation t(4;11)(q21;q23), resulting in the fusion of the mixed-lineage leukemia (*MLL*) and ALL1-fused gene of chromosome 4 (*AF4*) genes. While the fusion protein MLL-AF4 is expressed in all t(4;11) patients and essential for leukemia progression, the distinct role of the reciprocal fusion protein AF4-MLL, that is expressed in only 50-80% of t(4;11) leukemia patients (Meyer et al., 2018), remains unclear. In addition, t(4;11) leukemia could so far exclusively be generated *in vivo* in the presence of AF4-MLL and independent of the co-expression of MLL-AF4 (Bursen et al., 2010).

In a multifactorial approach inhibiting histone deacetylases (HDACs) and expressing the dominant negative mutation of Taspase1 (dnTASP1), both MLL fusion proteins were targeted simultaneously to evaluate a possible cooperative effect between MLL-AF4 and AF4-MLL during the progression of leukemia. Of note, neither HDACi nor dnTASP1 expression negatively affect endogenous MLL, but rather endorse its function hampered by the MLL fusion proteins (Ahmad et al., 2014; Bursen et al., 2004; Zhao et al., 2019). The mere expression of dnTASP1 failed to induce apoptosis, whereas dnTASP1 could elevate apoptosis levels significantly in HDACi-treated t(4;11) cells underlining the therapeutic potential of co-inhibiting both MLL fusion proteins.

Next, the impact of inhibiting either MLL-AF4 or AF4-MLL *in vivo* was resolved using whole transcriptome analysis. In PDX cells obtained by the Jeremias Laboratory (Völse, 2020) that co-expressed both t(4;11) fusion proteins, the knock-down of MLL-AF4 revealed the down-regulation of pivotal hemato-malignant factors. The expression of dnTASP1 led to massive deregulation of cell-cycle genes *in vivo*. Considering that the inhibition of particularly MLL-AF4 but not AF4-MLL impaired leukemic cell growth *in vivo* (Völse, 2020), the results of this work suggest a cooperative effect between both fusion proteins, while the loss of AF4-MLL during leukemia progression appears not essential.

Thereafter, a possible short-term role of AF4-MLL during the establishment of t(4;11) leukemia was analyzed. For this purpose, an *in vitro* t(4;11) model was constructed to investigate the transforming potential of transiently expressed AF4-MLL in cells constitutively expressing MLL-AF4, putatively reflecting the situation *in vivo*. Due to the lack of a leukemic background of the applied cell line, the aim was to investigate the long-term potential of AF4-MLL to significantly alter the epigenome rather than mimicking the development of leukemia. Strikingly, short-term-expressed AF4-MLL in cooperation with MLL-AF4 exerted durable epigenetic effects on gene transcription and chromatin accessibility. The here obtained *in vitro* data suggest a clonal evolutionary process initiated by AF4-MLL in a cooperative manner with MLL-AF4. Importantly, no long-term changes in

chromatin accessibility could be observed by the transient expression of either MLL-AF4 or AF4-MLL alone.

All in all, considering endogenous MLL, MLL-AF4 and AF4-MLL in a targeted treatment is a promising approach for a more tailored therapy against t(4;11) leukemia, and AF4-MLL is suggested to act in a cooperative manner with MLL-AF4 especially during the development of a t(4;11) leukemia.

ZUSAMMENFASSUNG

Die meisten akuten B-Zell Leukämien bei Säuglingen sind mit der chromosomalen Translokation t(4;11)(q21;q23) assoziiert, die zur Fusion der Gene für Mixed Lineage Leukemia (MLL) und ALL1-Fusion von Chromosom 4 (AF4) führt.

Die derzeitige Behandlung der t(4;11) ALL überleben nur 10-30% der Patienten, wobei die Gruppe der Säuglinge unter drei Monaten am meisten gefährdet ist (Bueno et al., 2011; Felix et al., 2000; Hess, 2004; Isoyama et al., 2002; Pui et al., 2002). Nach einer t(4;11)-Translokation erwerben transformierte Zellen eine geringe Anzahl an weiteren somatischen Mutationen, was die Potenz von chromosomalen Translokationen bei Leukämien, sowie die Notwendigkeit neuer maßgeschneiderter Therapien unterstreicht (Britten et al., 2019; Dobbins et al., 2013; Pikman and Stegmaier, 2018; Steinhilber and Marschalek, 2017).

Die Tatsache, dass AF4-MLL einen funktionellen N-Terminus des Transkriptionsverlängerungsfaktors AF4 und den C-Terminus von MLL trägt, der immer noch in der Lage ist Chromatin zu lesen und zu schreiben, legt nahe, dass AF4-MLL als epigenetischer Regulator mit einer starken transformierenden Aktivität fungieren könnte (Marschalek, 2011a; Park et al., 2010; Patel et al., 2009; Prieto et al., 2017; Rössler and Marschalek, 2013; Yokoyama, 2015; Yokoyama et al., 2013). Darüber hinaus wird der zielbestimmende N-Terminus von MLL durch AF4 ersetzt, was auf eine chromatinmodulierende Wirkung von AF4-MLL hinweist, die nicht auf die Zielgene von endogenem MLL beschränkt ist (Broeker et al., 1996; Erfurth et al., 2008; Marschalek, 2011b). Während das Fusionsprotein MLL-AF4 bei allen t(4;11)-Patienten exprimiert wird und für das Fortschreiten der Leukämie essenziell ist, wird die genaue Rolle des reziproken Fusionsproteins AF4-MLL, das nur bei 50-80% der t(4;11)-Leukämiepatienten exprimiert wird, kontrovers diskutiert (Agraz-Doblas et al., 2019; Kowarz et al., 2007; Marschalek, 2011b; Meyer et al., 2018; Muñoz-López et al., 2016; Prieto et al., 2017; Sanjuan-Pla et al., 2015; Trentin et al., 2009). Des Weiteren konnte t(4;11)-Leukämie bisher *in vivo* ausschließlich in Anwesenheit von AF4-MLL und unabhängig von der Koexpression von MLL-AF4 erzeugt werden (Prieto et al., 2017).

Ziel dieser Arbeit ist es, das Verständnis der Rolle von reziprokem AF4-MLL im Zusammenspiel mit MLL-AF4 während der Entstehung und dem Fortschreiten von t(4;11)-Leukämie voranzutreiben.

Ein großer Teil der Studien im Bereich der t(4;11)-ALL-Forschung konzentriert sich auf die Hemmung des MLL-Fusionsproteins MLL-AF4. Es fehlen Daten zur Bewertung des therapeutischen Nutzens der Hemmung des reziproken Fusionsproteins AF4-MLL allein oder zusammen mit MLL-AF4. Darüber hinaus beeinträchtigen MLL-AF4-spezifische

Wirkstoffe häufig endogenes MLL und damit die gesamte Transkriptionsmaschinerie. Der derzeitige Behandlungsplan für *MLL*-r-Leukämiepatienten, einschließlich der stark betroffenen Gruppe von Kleinkindern, besteht aus mehreren potenten Medikamenten, die oft zu schweren Nebenwirkungen oder sogar zum Tod führen (Britten et al., 2019).

In dieser Arbeit wird ein neuartiger therapeutischer Ansatz untersucht, der darauf abzielt, sowohl die MLL-Fusionsproteine zu hemmen als auch die Funktion des endogenen MLL zu erhalten. Zur Hemmung des reziproken Fusionsproteins AF4-MLL *in vitro* wurde die pro-B ALL-Zelllinie SEM, die sowohl MLL-AF4 als auch AF4-MLL exprimiert, mit einem Sleeping-Beauty-Expressionsplasmid zur induzierbaren Expression einer dominant negativen Mutante von Taspase1 (dnTASP1) transfiziert (Kowarz et al., 2015). Es konnte bereits gezeigt werden, dass die Expression von dnTASP1 die Taspase1-vermittelte Spaltung in der Nähe des C-Terminus sowohl endogenes MLL als auch AF4-MLL wirksam hemmt (Sabiani et al., 2015). Darüber hinaus ist bekannt, dass insbesondere AF4-MLL nach dnTASP1-Expression durch das Proteasom abgebaut wird, während ungespaltenes MLL weiterhin katalytisch aktiv ist (Sabiani et al., 2015; Yokoyama et al., 2013). Die kürzlich nachgewiesene Fähigkeit von Histon-Deacetylase Inhibitoren (HDAC-Inhibitoren), die dominanten Auswirkungen von MLL-AF4 durch eine Reaktivierung von endogenem MLL zu verringern (Ahmad et al., 2014), ergänzt den in dieser Studie untersuchten dualen Therapieansatz.

Während die alleinige Expression von dnTASP1 keine Apoptose auslösen konnte, erhöhte dnTASP1 in HDACi-behandelten t(4;11)-Zellen *in vitro* die Apoptoseniveaus signifikant, was auf ein therapeutisches Potenzial einer gemeinsamen Hemmung beider MLL Fusionsproteine hindeutet. Die induzierte Apoptose in mit HDACi behandelten SEM-Zellen war proportional zum Expressionsintervall von dnTASP1, wobei eine verlängerte Verabreichung von HDACis für 48 Stunden die Empfindlichkeit von SEM-dnTASP1-Zellen gegenüber Klasse I HDACi wie Mocetinostat und Entinostat verstärkte. Erhöhte Apoptosewerte nach der gleichzeitigen Behandlung mit HDACi und der Expression von dnTASP1 weisen auf eine wirksame multifaktorielle Strategie zur Hemmung sowohl der t(4;11)-Fusionsproteine als auch der Verstärkung von endogenem MLL *in vitro* hin. Um den Nutzen der AF4-MLL-Hemmung im Patienten richtig einschätzen zu können, müssen weitere Studien durchgeführt werden, die einen kürzlich postulierten (Agraz-Doblas et al., 2019) Zusammenhang zwischen AF4-MLL und einer guten Prognose von Kindern mit t(4;11)-Leukämie klären.

Als Nächstes wurde im Rahmen einer Kooperation mit der Arbeitsgruppe von Prof. Dr. Irmela Jeremias vom Helmholtz Zentrum München, insbesondere mit Kerstin Völse, sowohl MLL-AF4 als auch AF4-MLL in t(4;11) PDX Zellen *in vivo* inhibiert.

Nachdem Erhalt der zellulären Proben aus München wurde eine modifizierte 3-Ende RNA Sequenzierung durchgeführt („Massive Analysis of cDNA Ends Sequencing“ (MACE-seq)) und Transkriptomsignaturen nach Knock-down von MLL-AF4 untersucht. Hierbei ermöglichte das induzierbare Cre-ER^{T2}-Flip-System der PDX-Leukämiezellen (Carlet et al., 2021; Völse, 2020) die Inhibierung von MLL-AF4 in NSG Mäusen während der eingesetzten Proliferation der transplantierten PDX-Zellen und nach dem Auftreten von Homing- und Engraftment-Prozessen, welche als Folge der Xenotransplantationen auftreten. Dies ermöglichte zum Einen die Minimierung möglicher Sekundäreffekte und zum Anderen eine frühe und sich ausbreitende Leukämieerkrankung im Patienten zu imitieren.

In PDX-Zellen (Völse, 2020), die beide t(4;11)-Fusionsproteine exprimierten, führte der induzierte Knock-down von MLL-AF4 *in vivo* zu einer Herunterregulierung stark miteinander interagierender Onkogene, die an der Hämatopoese und B-ALL beteiligt sind. Insbesondere der herunterregulierte Transkriptionsfaktor Forkhead box protein O1 (FOXO1) ist an der Proliferation und dem Überleben in frühen Stadien der B-Zell-Differenzierung beteiligt, und seine Herunterregulierung wurde mit antileukämischer Aktivität in Xenotransplantationen in Verbindung gebracht (Wang et al., 2018). Ein weiteres nach dem Knockdown von MLL-AF4 herunterreguliertes Gen ist *recombination activating gene 1 (RAG1)*, das wie FOXO1 in Verbindung mit dem hämato-maligem Faktor IKAROS steht (Ferreirós-Vidal et al., 2013; Heizmann et al., 2013, Ferreirós-Vidal et al., 2013; Ng et al., 2009). Darüber hinaus zeigten die transkriptomischen Daten eine Korrelation zwischen der Expression von Runt-related transcription factor 1 (RUNX1) und AF4-MLL. Als ein bedeutender hämatopoetischer Transkriptionsfaktor wurde RUNX1 nach dem Knock-down von MLL-AF4 in PDX-Leukämiezellen ebenfalls signifikant herunterreguliert. RUNX1 ist ein wichtiges Ziel in t(4;11)-Leukämien, das durch MLL-AF4 aktiviert wird, mit AF4-MLL interagiert und dadurch die Expression mehrerer Zielgene initiiert (Wilkinson et al., 2013).

Die Expression von dnTASP1 in t(4;11) PDX-Zellen führte zu einer massiven Deregulierung von Zellzyklusgenen *in vivo*. Da die Hemmung insbesondere von MLL-AF4, nicht aber von AF4-MLL das Wachstum leukämischer Zellen *in vivo* beeinträchtigt (Völse, 2020), deuten die Ergebnisse dieser Arbeit auf einen kooperativen Effekt zwischen beiden Fusionsproteinen hin, während der bloße Verlust von AF4-MLL für das Fortbestehen einer t(4;11) Leukämie nicht essentiell zu sein scheint.

Anschließend wurde in dieser Arbeit eine mögliche vorübergehende Rolle von AF4-MLL während der Entstehung von t(4;11)-Leukämie untersucht. Obwohl AF4-MLL bei einer Untergruppe von t(4;11) Leukämiepatienten für das Fortbestehen der Leukämie nicht erforderlich ist, konnte bisher eine t(4;11) Leukämie *in vivo* nur mittels Expression von

humanem AF4-MLL induziert werden, wobei die Expression von humanem MLL-AF4 nicht erforderlich war (Agraz-Doblas et al., 2019; Bursen et al., 2010; Meyer et al., 2018).

Zu diesem Zweck wurde in dieser Arbeit ein *in vitro* t(4;11)-Modell konstruiert, um das transformierende Potenzial von vorübergehend exprimiertem AF4-MLL in Zellen, die zudem konstitutiv MLL-AF4 exprimieren, zu untersuchen. Dies erfolgte in Anlehnung an die mutmaßliche Situation, wie sie in einigen t(4;11) Leukämie Patienten zu finden ist und um die zugrundeliegenden Ursachen für eine mögliche Eliminierung von AF4-MLL bei fortgeschrittener Leukämie zu klären.

Um die Auswirkungen von AF4-MLL auf die Genexpression und den Chromatinstatus richtig beurteilen zu können, wurden zunächst Proben von 293T-Zellen genommen, die stabil mit einem Vektor für eine konstitutive Expression von MLL-AF4 transfiziert worden waren. Daraufhin wurden MLL-AF4 exprimierende 293T-Zellen transient mit einem Doxycyclin-induzierbaren Vektor transfiziert, der AF4-MLL exprimiert, und 24 Stunden nach der Transfektion mit Doxycyclin induziert. Nach einer 48-stündigen Doxycyclin-Induktion wurden am dritten Tag Proben von 293T Zellen geerntet, die konstitutiv MLL-AF4 und kurzzeitig AF4-MLL exprimierten. Zur Untersuchung von Langzeiteffekten wurde die Induktion der AF4-MLL-Expression an Tag 3 durch Austausch des Doxycyclin-haltigen Mediums beendet, und die Zellen wurden für weitere 25 Tage gezüchtet. Am 12. und 28. Tag des Experiments wurden zelluläre Proben entnommen, um zu untersuchen, ob sich die genomischen Signaturen sowie der Chromatinstatus aufgrund der zeitlichen Expression von AF4-MLL bis Tag 3 verändert haben.

Da die verwendeten 293T Zellen keinen leukämischen Hintergrund hatten, sollte nicht die Entwicklung einer Leukämie nachgestellt werden, sondern primär die Evaluierung eines möglichen langfristigen Effekts von AF4-MLL auf das Epigenom untersucht werden. Bemerkenswerterweise konnte gezeigt werden, dass kurzzeitig exprimiertes AF4-MLL in Zusammenarbeit mit MLL-AF4 dauerhafte epigenetische Veränderungen hervorbrachte. Die *in vitro*-Daten deuten zudem auf einen klonalen Evolutionsprozess hin, der durch AF4-MLL in Zusammenarbeit mit MLL-AF4 initiiert wird.

Beide t(4;11)-Fusionsproteine führten zudem zu einer Hochregulierung zahlreicher mitochondrialer Ziele im zellulären t(4;11)-Modell, wobei nur wenige mitochondriale Gene entweder durch MLL-AF4 oder AF4-MLL herunterreguliert wurden. Bei anschließender Messung der mitochondrialen Atmungskette mittels eines Oxygraphen wurde nur ein minimaler Effekt nach Expression von MLL-AF4 oder AF4-MLL auf das Elektronentransfersystem (ETS) von 293T Zellen bei der mitochondrialen Atmung festgestellt.

Erwähnenswerter Weise wurden keine langfristigen Veränderungen im Chromatin beobachtet bei transienter Expression eines einzelnen Fusionsproteins, MLL-AF4 oder AF4-MLL.

Zudem konnte gezeigt werden, dass AF4-MLL nicht nur zu längerfristigen Veränderungen in der Genexpression führt, sondern auch den Chromatinstatus nachhaltig beeinflusst. Darüber hinaus überstieg die AF4-MLL-induzierte Überexpression von Genen die Öffnung des Chromatins, was darauf hindeutet, dass AF4-MLL die Hochregulierung von Genen auch an Chromatin-Loci mit begrenzter Zugänglichkeit erleichtert.

Zusammengefasst konnte in dieser Arbeit gezeigt werden, dass eine zielgerichtete Therapie, welche sowohl endogenes MLL in seiner Funktion fördert als auch MLL-AF4 und AF4-MLL inhibiert einen vielversprechenden Ansatz für eine maßgeschneiderte Behandlung gegen t(4;11)-Leukämie darstellt. Zudem bekräftigen die in dieser Arbeit erhobenen Ergebnisse die Hypothese, dass AF4-MLL insbesondere während der Entwicklung einer t(4;11)-Leukämie im Zusammenspiel mit MLL-AF4 eine wichtige Rolle inne hat.

1. INTRODUCTION

1.1. Leukemia

Leukemia includes a variety of cancers within the hematopoietic system that results in irreversible changes in the red bone marrow. Identified in the 19th century by a "dirty green-yellow" staining of the red bone marrow, leukemia (from the Greek leukós for white as well as haima for blood) describes the severe proliferation of abnormal white blood cells.

Leukemias are divided into lymphoblastic leukemia (LL) and myeloid leukemias (ML) based on the affected progenitor cells (Figure 1.1.1), as well as into acute leukemias (AL) and chronic leukemias (CL) on the basis of disease progression.

In AL, a large number of dysfunctional blood progenitor cells are produced in a short period of time reducing the residual space in the bone marrow for healthy progenitor cells. Therefore, due to the rapid blood cell turnover rate, impaired hematopoiesis rapidly results in symptoms and mandates an immediate therapy to combat the otherwise deadly progression of the disease (Anderlini et al., 1996). CL, on the other hand, affects more differentiated blood cells, resulting in a much slower disease course. It is often diagnosed in patients that are not yet symptomatic.

In the United States (US) and Germany, leukemia represents the largest group of childhood cancers with approximately 30% of all cases of pediatric cancer (Krebs in Deutschland 2017/2018 - Robert Koch Institute and Zentrum für Krebsregisterdaten; Siegel et al., 2020). According to the Robert Koch Institute, leukemia occurs in Germany with an incidence of 4.6 cases per 100,000 children under the age of 18 years. Importantly, of all pediatric leukemia patients, 86% developed acute lymphoblastic leukemias (ALL) and only 14% developed acute myeloid leukemias (AML) (Figure 1.1.2) (Krebs in Deutschland 2017/2018 - Robert Koch Institute and Zentrum für Krebsregisterdaten). In contrast, in adult leukemia patients, 73% of cases are assigned to CL (Figure 1.1.2). Here, ALL and AML play a minor role with 5% and 23%, respectively. Nonetheless, leukemia contributes to only 2.2% of all adult cancer cases, which is significantly less compared to the relative amount of leukemia in children (Figure 1.1.3). Due to the overall increased incidence of leukemia in the elderly, the median age of onset of all leukemia patients was approximately 73 years (Figure 1.1.3) (Krebs in Deutschland 2017/2018 - Robert Koch Institute and Zentrum für Krebsregisterdaten).

Independent of age, the five-year overall survival was approximately 52% for ALL, 85% for CLL, 22% for AML, and 78% for chronic myeloid leukemias (CML) in 2018 (Krebs in Deutschland 2017/2018 - Robert Koch Institute and Zentrum für Krebsregisterdaten). Patients under 18 years of age had a 5-year overall survival with approximately 90% for ALL and 75% for AML in Germany and the US (Annual Report 2019 - German Childhood

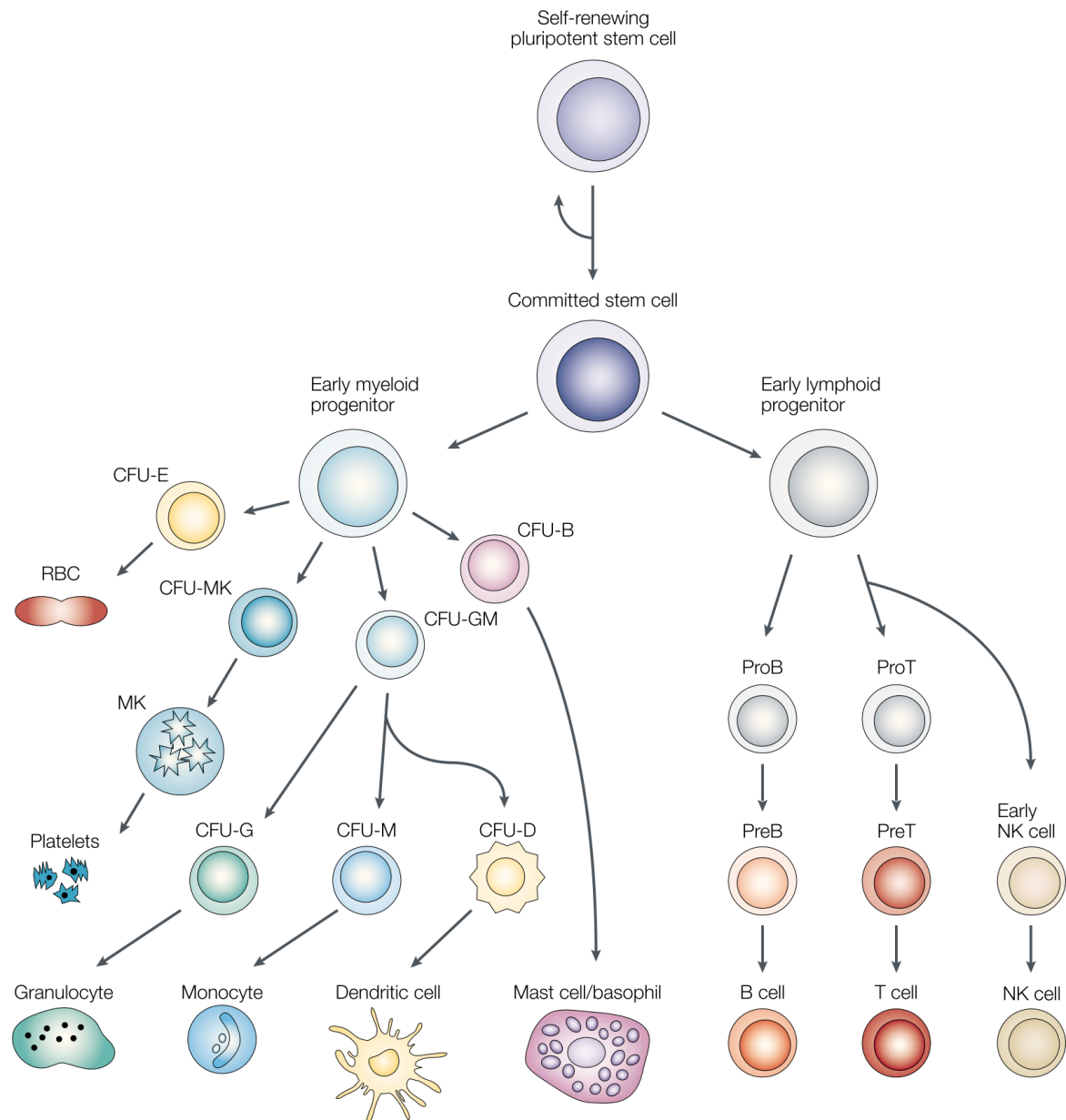


Figure 1.1.1: Hematopoietic system. Illustration of the differentiation of hematopoietic progenitor cells. Originating from a common pluripotent stem cell progenitor arise the lymphoid and the myeloid lineage. Colony-forming units for the erythroid lineage (CFU-E), red blood cell (RBC), megakaryocytic lineage (CFU-MK), dendritic lineage (CFU-D), (CFU-GM), basophilic (CFU-B), natural killer cell (NK), megakaryocyte (MK), Pro B-cell (ProB), Pre B-cell (Preb), Pro T-cell (ProT), Pre T-cell (PreT). Adapted from Stirewalt and Radich, 2003.

Cancer Registry Mainz; Siegel et al., 2020). Compared with the interval from 1981-1990 in Germany, when fifteen-year overall survival was about 70% for ALL and only 40% for AML, this value has improved significantly over time.

The underlying mechanism for the development of leukemia remains elusive. A combination of genetic as well as environmental factors is suspected to lead to mutations that transform healthy hematopoietic progenitor cells into leukemia cells.

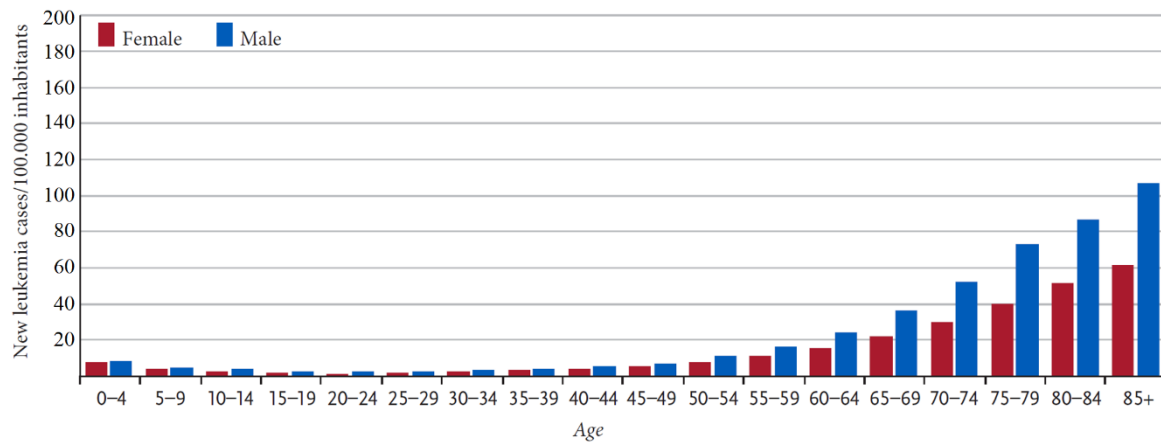


Figure 1.1.2: Age distribution of leukemia patients. Age-specific rate of new leukemia cases by sex per 100.000 inhabitants in Germany 2017 and 2018. Adapted from Krebs in Deutschland 2017/2018 - Robert Koch Institute and Zentrum für Krebsregisterdaten.

Compared to solid tumors, DNA double-strand (dsDNA) breaks are the major cause for the onset of chromosomal translocations, a genetic hallmark that drives the onset of hematological malignant tumors, and in particular the onset of *MLL-r* leukemias (Gillert et al., 1999; Reichel et al., 1998, 1999, 2001). DNA repair of dsDNA breaks by the Non-homologous-end-joining (NHEJ) is also visible when analyzing chromosomal breakpoints at the genomic level, as small deletions, inversions or duplications can be found in nearly every patient (Meyer et al., 2018). Affecting entire chromosomal segments, chromosomal translocations shift genetic material intra- or inter-chromosomally. Further on, leukemias differ from solid tumors in a lower somatic mutation burden and particularly in a lower prevalence of cross-cancer oncogenic mutations (Dobbins et al., 2013).

The balanced reciprocal translocation that frequently occurs in AL involves two chromosomes exchanging chromosomal segments without loss of genetic material (Meyer et al., 2018). In this type of translocation, a resulting homology of the two mutant chromosomes to the two homologous intact chromosomes is claimed to account for an approximately 20-fold higher risk of developing AL in individuals with Down syndrome (Robison et al., 1980; Yang et al., 2002; Zipursky et al., 1987).

From a clinical perspective, the heterogeneous course of disease between ALL, AML, CML and chronic lymphoid leukemias (CLL) demands a more sophisticated classification of leukemias. A more relevant classification of leukemia in the clinics is the characterization of leukemic cells based on the degree of differentiation that can be evaluated by the expression of unique markers at the cell surface (Bene et al., 1995). Thereafter, the group of B-cell lineage ALL is separated into pro-B, common-B, and pre-B ALL whereas the group of T-cell lineage ALL can be further specified as early T-cell precursor (ETP), pre-T, pro-T, cortical-T and mature-T ALL.

Further on, chromosomal translocations in leukemia patients represent an important clinical marker. While ALL and AML patients have an overall good prognosis, certain chromosomal translocations are associated with very aggressive and difficult to treat types of leukemia. The heterogeneous phenotypes can be explained by the site of double-strand break leading to the translocation of chromosomal segments with unique genetic activity.

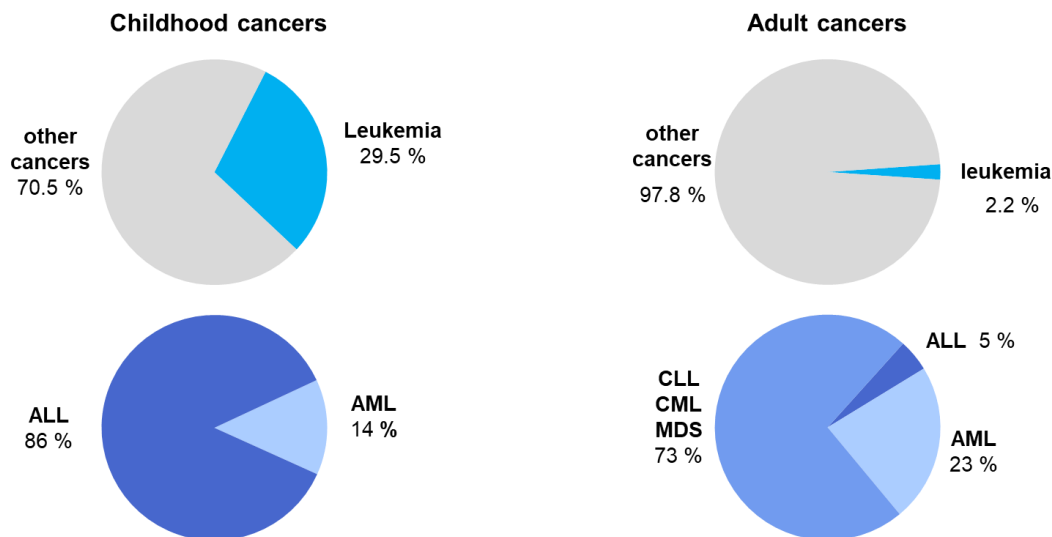


Figure 1.1.3: Incidence of leukemia patients relative to all cancer cases. Graphical Illustration of relative fraction of leukemia patients in children and adults. Data obtained from Krebs in Deutschland 2017/2018 - Robert Koch Institute and Zentrum für Krebsregisterdaten and the Deutsche Krebsforschungszentrum (DKFZ).

1.2. *MLL*-rearranged (*MLL-r*) leukemia

A special type of leukemia develops when the *MLL* (mixed lineage leukemia) gene is translocated, which often leads to exceptionally aggressive and poorly treatable leukemias (Bueno et al., 2011; Felix et al., 2000; Hess, 2004; Isoyama et al., 2002; Pui et al., 2002). *MLL*-rearranged (*MLL-r*) leukemias are eponymously characterized by the expression of surface markers of both, the lymphoid and myeloid lineage, and even lineage switches from ALL to AML (Marschalek, 2011b).

Originally identified as the orthologue of the Trithorax protein in vertebrates, the human *MLL* (or *KMT2A*) gene consists of a total of 37 exons (Meyer et al., 2006; Nilson et al., 1996). Alternative splicing at exon 2 or between exon 15 and exon 16 result in several

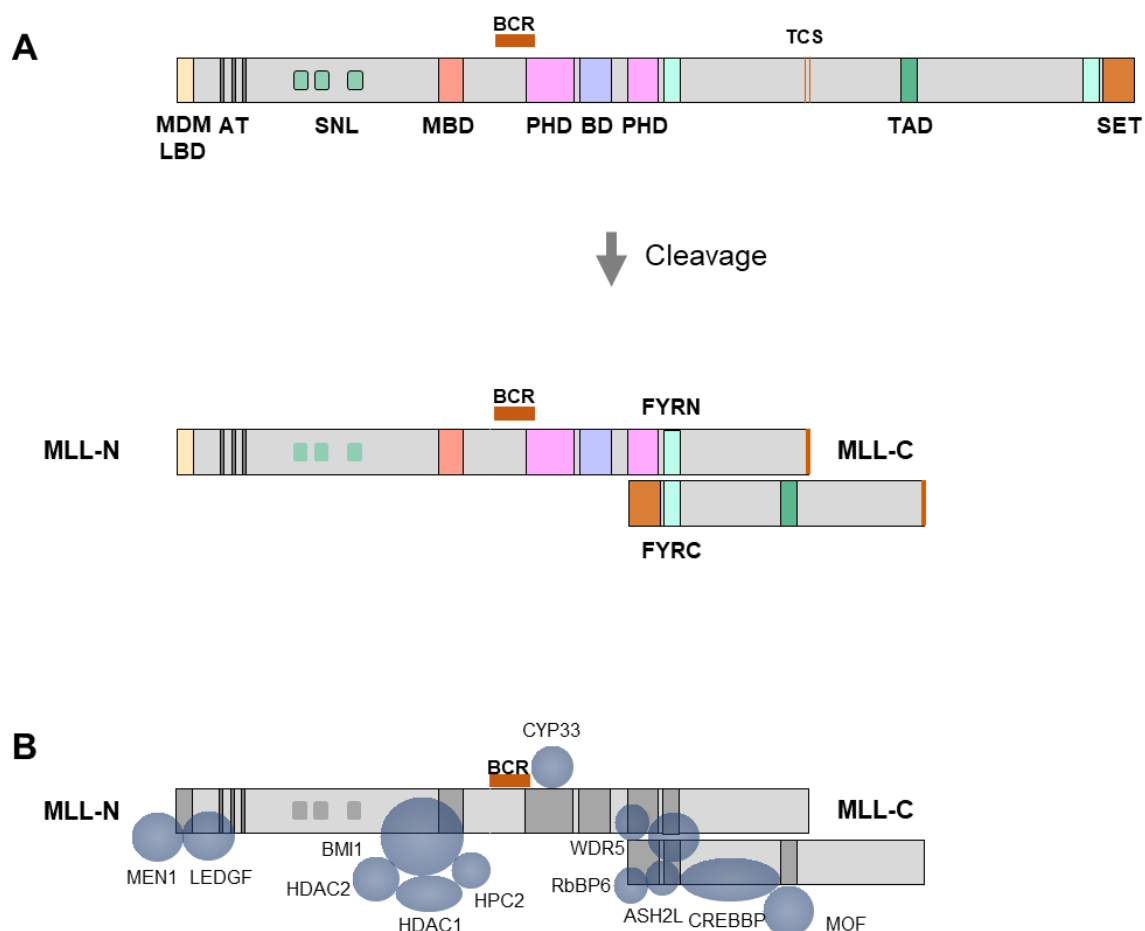


Figure 1.2.1: Functional domains of the mixed lineage leukemia (MLL) protein.

Graphical illustration of the proteolytic cleavage of the MLL protein by threonine aspartase 1 (TASP1) at the TASP1 cleavage site (TCS) (A) and reconstitution of the MLL-N and MLL-C fragment (B). MLL domains: Multiple Endocrine Neoplasia I (Menin1) Binding Motif (MDM), the Lens Epithelium-Derived Growth Factor (LEDGF) binding domain (LBD), nuclear localization site (SNL), methyl-CpG binding domain (MBD), plant homology domains (PHD), bromodomain (BD), transactivation domain (TAD), N-terminal MLL FY-rich domain (FYRN), C-terminal MLL FY-rich domain (FYRC), Su(var)3-9,enhancer-of-zeste, trithorax (SET), break-point cluster region (BCR). MLL-associated proteins: MEN1, LEDGF, Histone deacetylase 1 (HDAC1), Histone deacetylase 2 (HDAC2), heredity Prostate Cancer Protein 2 (HPC2), B Lymphoma Mo-MLV Insertion Region 1 Homolog (BMI1), cyclophilin33 (CYP33), MLL associates with WD Repeat Domain 5 (WDR5), RB Binding Protein 6, Ubiquitin Ligase (RbBP6), ASH2 Like, Histone Lysine Methyltransferase Complex Subunit (ASH2L), CREB-binding protein (CREBBP), Males Absent of the First (MOF)

large transcripts with a size of approximately 4,005 amino acids (Rössler and Marschalek, 2013).

The MLL protein is an universal transcriptional coactivator that plays an essential role in regulating genes during embryonic development and during hematopoiesis and consists of many conserved functional domains (Figure 1.2.1 A) (Djabali et al., 1992; Ernst et al., 2004). The Multiple Endocrine Neoplasia I (Menin1) Binding Motif (MDM) and the Lens Epithelium-Derived Growth Factor (LEDGF) binding domain (LBD) are found in the N-

terminus of MLL. Responsible for the localization of MLL to the nucleus, two speckled nuclear localization sites (SNLs) are found in the N-terminus of MLL (Yano et al., 1997). For specific binding to target genes, MLL contains three AT hooks interacting with AT-rich DNA (Broecker et al., 1996). In addition, a methyl-CpG binding domain (MBD) is located in the N-terminus, which specifically binds unmethylated CpG DNA and thus causes the inactivation of target genes by protecting them from DNA methylation (Figure 1.2.1 A+B) (Erfurth et al., 2008). The study by Erfurth et al. was able to demonstrate this in particular for *HOXA* genes, whose overexpression represents an important marker for the prognosis of *MLL-r* leukemia patients (Agraz-Doblas et al., 2019; Kühn, 2017). MLL further possesses four plant homology domains (PHD) with zinc finger motifs that are interrupted by a bromodomain (BD) between PHD domains 1-3 and PHD domain 4 (Figure 1.2.1 A). Importantly, H3K4me3 signatures and Cyclophilin33 (CYP33) act as antagonists for binding to the PHD 3 domain (Marschalek, 2016; Park et al., 2010; Rössler and Marschalek, 2013; Xia et al., 2003). The PHD 3 domain interaction with CYP33 results in the inactivation of target promoters bound to MLL (Marschalek, 2016). This essential regulatory molecular switch is therefore also referred to as the "CYP33 switch". Binding of CYP33 to the PHD 3 domain initiates conformational changes that result in the binding of Histone deacetylase 1 (HDAC1) and Histone deacetylase 2 (HDAC2), and Polycomb proteins such as C-Terminal Binding Protein 1 (CtBP), Heredity Prostate Cancer Protein 2 (HPC2), and B Lymphoma Mo-MLV Insertion Region 1 Homolog (BMI1), which results in the inactivation of MLL target genes (Marschalek, 2016; Xia et al., 2003; Yokoyama, 2015). Here, the PHD3 domain located in the C-terminal fragment of MLL, which binds to CP33, cooperates with the MBD located in the N-terminal fragment of MLL via the associated BMI1, CtBP, and HPC2 (Fig. 1.2.1 B).

The MLL protein is hydrolyzed post-translationally by the endopeptidase Threonine Aspartase 1 (Taspase1) at the Taspase1 cleavage site (TCS) and divided into an 320 kDa N-terminal fragment and a 180 kDa C-terminal fragment (Hsieh et al., 2003a) (Figure 1.2.1 B). Immediately after hydrolysis, both fragments reconstitute via the dimerization domains N-terminal MLL FY-rich domain (FYRN) and C-terminal MLL FY-rich domain (FYRC) (Hsieh et al., 2003a; Pless et al., 2011; Yokoyama et al., 2002). Subsequently, the non-covalently bound complex in the nucleus assembles with additional proteins to form a high molecular weight complex that interacts with histones as well as nucleosomes (Marschalek, 2011b; Yokoyama et al., 2002). The transactivation domain (TAD) in the C-terminal fragment of MLL allows binding of histone acetyltransferases (HATs), Males Absent of the First (MOF) and CREB-binding protein (CREBBP), which act as transcription co-regulators (Figure 1.2.1 B) (Bannister and Kouzarides, 1996; Dou et al., 2005). Binding

of MOF induces H3K27 as well as H3K9 acetylation of histones (Dou et al., 2005; Ernst et al., 2001; Milne et al., 2002).

The C-terminal part of MLL mediates the histone methyltransferase activity of MLL through the Su(var)3-9, enhancer-of-zeste, trithorax (SET) domain. Here, MLL associates with WD Repeat Domain 5 (WDR5) to recruit ASH2 Like, Histone Lysine Methyltransferase Complex Subunit (ASH2L) as well as RB Binding Protein 6, Ubiquitin Ligase (RbBP6), resulting in dimethylation of H3K4 (Marschalek, 2016; Patel et al., 2009; Yokoyama, 2015). *MLL*-rearranged (*MLL-r*) leukemia plays a major role in children, especially in infants, and few translocation partners of MLL are associated with moderate progression (Balgobind et al., 2009; Szczepański et al., 2010). Notably, *MLL-r* leukemias often lack secondary mutations (Agraz-Doblas et al., 2019; Sanjuan-Pla et al., 2015; Zheng, 2013). Despite the generally good prognosis for LL in children under the age of 18, the event-free survival drops remarkably below 50% for ALL in infants ((Dreyer et al., 2015; Pieters et al., 2007, 2019).

Examining the age distribution of *MLL-r* leukemias from 2345 analyzed patient samples revealed that the poor prognosis of ALL in infants is related to the very high frequency of

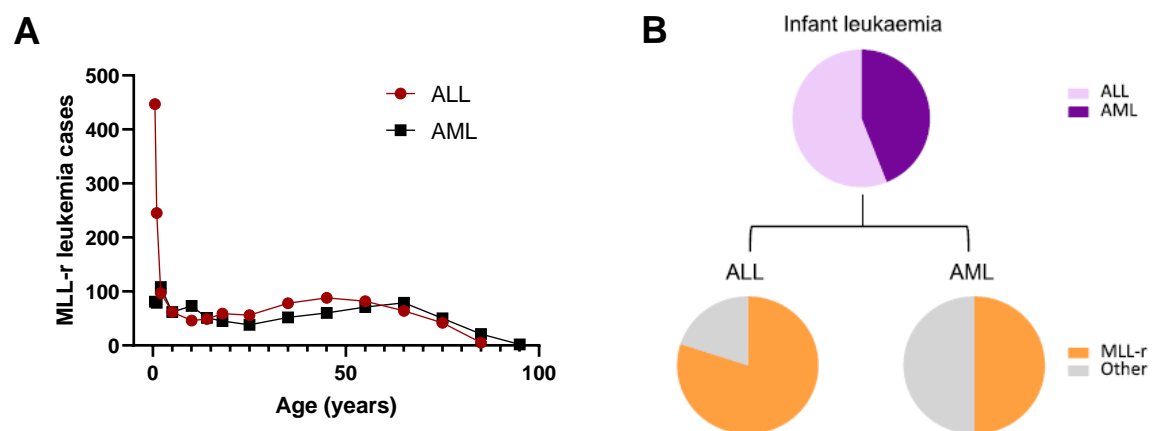


Figure 1.2.2: Age distribution of *MLL-r* leukemia cases. Graphical illustration of age distribution of ALL and AML patients ($n=2345$) (data obtained from Meyer et al., 2018) (A). Relative fraction of *MLL-r* leukemia cases of total ALL and AML infant cases (adapted from Rice and Roy, 2020) (B).

MLL-r ALL in this age group (Figure 1.2.2 A) (Meyer et al., 2018). This accumulation is unique to ALL at this level of severity, however, AML is also found at the highest incidences in infants and children 1 to 2 years of age. The relative fraction of *MLL-r* leukemia of diagnosed leukemias in infants is approximately 70-80% in infant ALL and 50% in infant

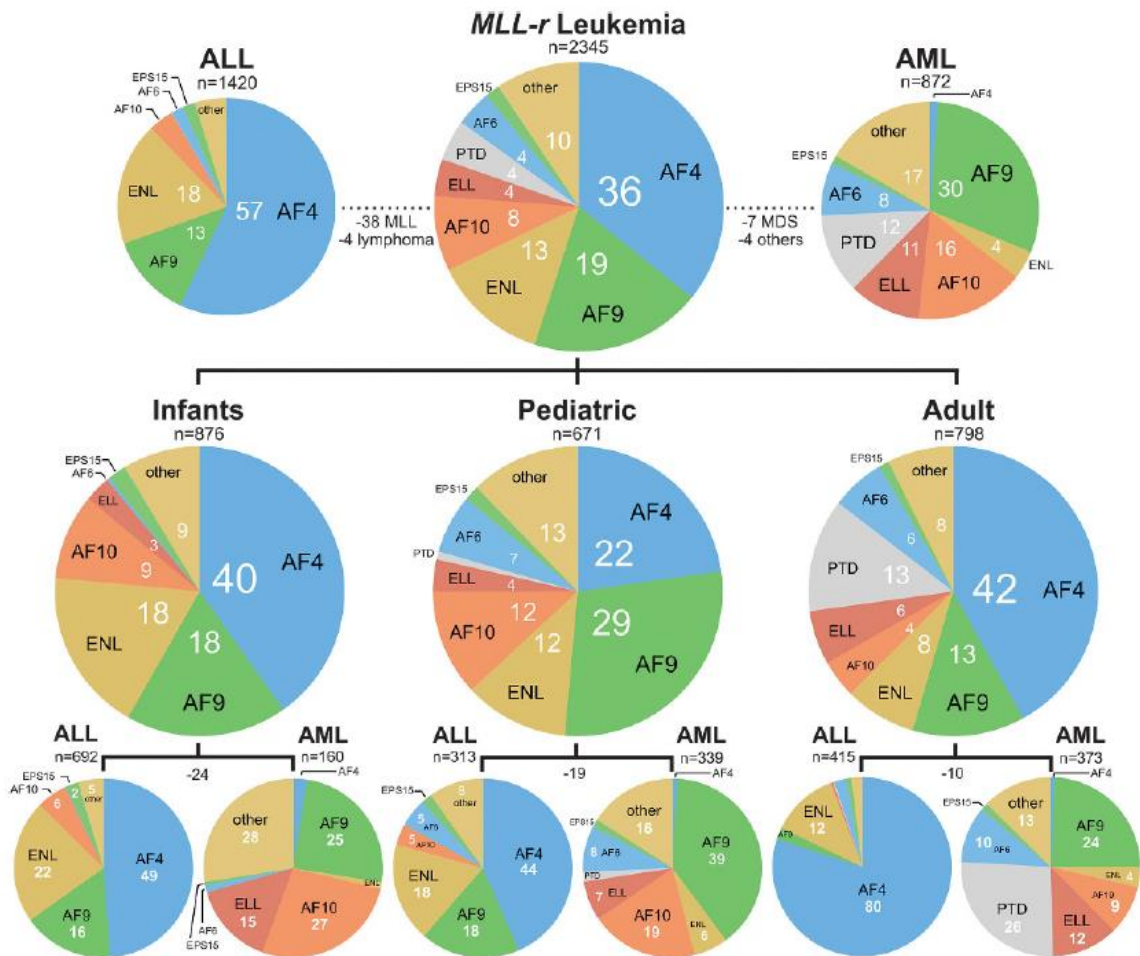


Figure 1.2.3: Translocation partner genes of MLL according to age and lineage. Graphical illustration of the most prominent translocation partner genes of MLL. White numbers indicate percentages of translocation partner genes in infants, children, adults as well as ALL and AML cases, respectively. Negative numbers represent non-ALL or -AML cases. Adapted from Meyer et al., 2018.

AML as demonstrated by several studies (Figure 1.2.2 B) (Harrison et al., 2010; Hilden et al., 2006; Pieters et al., 2007).

A comprehensive study of the genomic breakpoints within the *MLL* gene as well as associated chromosomal translocation partner genes of MLL identified in total 135 different *MLL-r* translocation partners (Meyer et al., 2018). This enormous quantity of translocation partners, when fused to *MLL*, can all cause leukemias, and indicates the enormous transforming power of the genetically modified *MLL* alleles.

Nevertheless, Meyer et al showed that over 90% of all *MLL-r* leukemias originate from only 9 different translocation partners. The translocation partner genes *AF4* and *AF9* are particularly prominent in ALL with 57% and AML with 30% of all *MLL-r* leukemia cases. In addition to *AF4* and *AF9*, the translocation partners *AF6*, *AF10*, *ELL*, and *ENL* were also frequently detected (Figure 1.2.3). Spanning all ages, *AF4* is the most frequent

translocation partner in *MLL-r* ALL in infants, children and adults. For AML, *AF9* and *AF10* account for more than half of the occurring cases in infants and children (Figure 1.2.3). Notably, partial internal tandem duplication of *MLL* (*MLL-PTD*) at exon 3-9 and 3-11 occurs particularly in older AML cases (Meyer et al., 2018; Sun et al., 2017). Across ALL and AML, a large functional correlation can be observed between the *MLL* translocation partners *AF4*, *AF9*, *ENL*, and *AF10* (Figure 1.2.3). They are all members of the super elongation complex orchestrating transcription elongation and, with the exception of *MLL-PTD* in adult AML cases, represent more than 50% of all and AML cases. Remarkably, translocation partner genes related to transcription elongation constitute more than 90% in ALL cases independent of age (Figure 1.2.3).

Besides the high prevalence of different translocation partners of *MLL*, the site of DNA double-strand breaks in the *MLL* gene varies even within reciprocal translocations with the same partner gene. The translocations in the *MLL* gene occur in breakpoint cluster regions (BCR) (Figure 1.2.1). More than 93% of translocations occur between *MLL* exon 9 and *MLL* intron 11, although a smaller fraction of rearrangements occur between *MLL* introns 21 and 23 (Meyer et al., 2013). In addition, the breakpoint distribution differs between infants, where the breakpoint primarily occurs in *MLL* intron 11, especially for *MLL-AF4*, *MLL-ENL*, and *MLL-ENL* translocations, and adults, where breakpoints are mostly found in *MLL* intron 9 (Meyer et al., 2013, 2018). Of note, patients carrying the breakpoint in *MLL* intron 11 have been shown to have a worse prognosis compared to patients with breakpoint in *MLL* intron 9 (Emerenciano et al., 2013). It is assumed that the aberration of the PHD domain in the *MLL* protein ranging from *MLL* intron 11 to 16 results in an overall dismal prognosis in patients with breakpoint in *MLL* intron 11 (Figure 1.2.1) (Rössler and Marschalek, 2013).

1.3. t(4;11) ALL

The *ALL-1 fused gene on chromosome 4 (AF4)* gene (or *AF4/FMR2 Family Member 1 (AFF1)* gene) is the most common translocation partner of *MLL* in *MLL-r* ALL and resides in chromosome 4 q21 (Benedikt et al., 2011; Chen et al., 1993; Gu et al., 1992; Meyer et al., 2018). The analysis of breakpoints in patients with a t(4;11) translocation revealed a BCR in the *AF4* gene ranging from exon 3 to exon 7 (Gillert et al., 1999). The *AF4* gene codes for a 10.5 kb mRNA transcript containing either exon 1a or 1b due to splicing events and is translated into a 131 kDa protein (Chen et al., 1993; Nakamura et al., 1993; Nilson et al., 1997). *AF4* forms a nuclear transcriptional activator involved in RNA elongation and is expressed in all cell types (Chen et al., 1993; Frestedt et al., 1996; Melko et al., 2011).

It is assigned to the AF4, LAF4, AF5q31 und FMR2 (ALF) protein family including Fragile X Mental Retardation 2 Protein (FMR2), lymphoid nuclear protein related to AF4 (LAF4), and Major CDK9 Elongation Factor-Associated Protein (MCEF) (Chen et al., 1993; Frestedt et al., 1996; Gu et al., 1996; Nilson et al., 1997; Taki et al., 1999). In line with the observation that t(4;11) translocations predominantly occur in ALL (Meyer et al., 2018), knock-out experiments with *Af4* in mice affected B- and T-cell development significantly, while the myeloid lineage appeared to be unaffected (Isnard et al., 2000).

All ALF-family proteins contain five conserved domains (Figure 1.3.1) (Bursen et al., 2004). The N-terminal homology domain (NHD) is located at the N-terminus of AF4. For a proper regulation of the expression levels of AF4, the ALF domain orchestrates the proteasomal degradation of AF4 by the interaction with seven in absentia homologue 1 (SIAH1) and seven in absentia homologue 2 (SIAH2) (Bursen et al., 2004). In contrast to the ALF domain, the phosphoserine (pSer)-domain is associated to transcriptional activation of AF4 target genes (Bursen et al., 2004; Ma and Staudt, 1996; Nilson et al., 1997; Prasad et al., 1995). Notably, the majority of breakpoints in the *AF4* gene are found at exon 3 and hence separating the transcriptional inactivating ALF domain from the transcriptional activating pSer domain (Figure 1.3.1) (Bursen et al., 2004). Further conserved domains of the *AF4* gene are the nuclear localization sequence (NLS) and the C-terminal homology domain (Figure 1.3.1).

The impact on the transcriptome of the MLL protein is sophisticatedly regulated by intrinsic control mechanisms (Marschalek, 2016). The wild-type MLL protein is equipped on the one hand in the C-terminal fragment with an associated CYP33 isomerase that acts in interplay with N-terminal MBD-associated Polycomb proteins as a transcriptional repressor. Moreover, it carries in the N-terminal fragment the TAD domain and its associated CREBBP and MOF mediating HAT activity, and the SET domain that is capable of

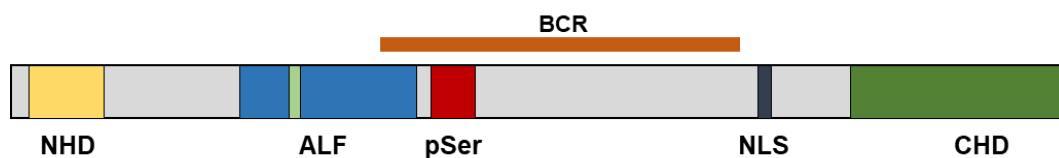


Figure 1.3.1: Functional domains of the ALL-1 fused gene on chromosome 4 (AF4) protein. Graphical illustration of the AF4 protein. AF4 domains: N-terminal homology domain (NHD), AF4, LAF4, AF5q31 und FMR2 (ALF) domain, phosphoserine (pSer)-domain, nuclear localization sequence (NLS), C-terminal homology domain (CHD), breakpoint cluster region (BCR).

methylyating H3K4 (Figure 1.3.2 A). This balanced regulatory machinery is interrupted in case of the commonly occurring breakpoint within *MLL* intron 11 (Meyer et al., 2018).

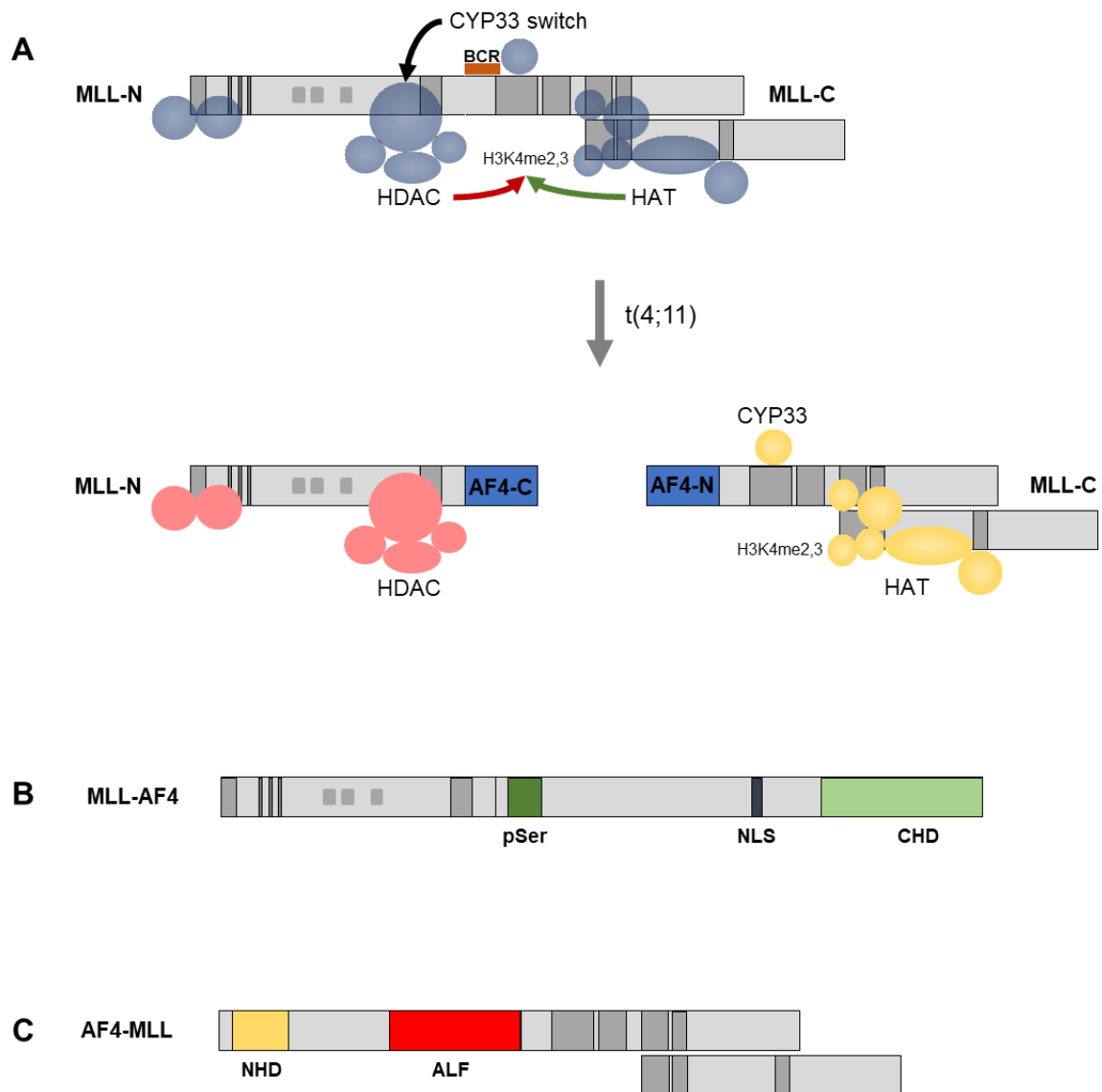


Figure 1.3.2: t(4;11) translocation results in the fusion proteins MLL-AF4 and AF4-MLL. Graphical illustration of the inter-domain regulation of the activity of endogenous MLL (involved domains highlighted in blue) (A). Involved domains are separated upon t(4;11) chromosomal translocation in to the N-terminal part of MLL (domains highlighted in red) and the C-terminal part of MLL (domains highlighted in yellow) binding to the C-terminal part of the AF4 gene (AF4-C) and the N-terminal part of the AF4 gene (AF4-N), respectively. Graphical illustration of the MLL-AF4 fusion protein (B) and the AF4-MLL fusion protein (C). AF4 domains: N-terminal homology domain (NHD), AF4, LAF4, AF5q31 und FMR2 (ALF) domain, phosphoserine (pSer)-domain, nuclear localization sequence (NLS), C-terminal homology domain (CHD), break point cluster region (BCR).

Hence, the MLL fusion proteins in t(4;11) leukemia acquire new biological properties not only by genetic material of the translocation partner gene AF4 but also by the interruption of inter-domain communication within the *MLL* gene (Figure 1.3.2 A). As a consequence, for MLL-AF4, the N-terminal part of *MLL* lacks the inhibitory impulse of the CYP33 but is capable of binding to chromatin regions and transcription factors at wild-type MLL targets

via MEN1 and LEDGF1 that are associated to the MBD and LBD (Figure 1.3.2 A). For AF4-MLL, activating HAT activity is provided by the PAD domain with its associated CREBBP and MOF, and H3K4_{me2/3} signatures are written by associated proteins at the N-terminal SET domain (Marschalek, 2016). Moreover, both t(4;11) fusion-proteins are characterized to exert a superior stability when compared to the wild-type MLL protein (Bursen et al., 2004; Krivtsov et al., 2008; Lin et al., 2010). While MLL-AF4 gains further stability by the capability of the C-terminal part of AF4 to interact with further proteins of the super elongation complex (SEC), AF4-MLL seems to circumvent SIAH1- and SIAH2-mediated proteasomal degradation, resulting in an extraordinary prolonged half-life of up to 96 h (Figure 1.3.2 B+C) (Bursen et al., 2004).

MLL-AF4 that is expressed in nearly all t(4;11) leukemia patients and is described in the literature to play a dominant role in the development and persistence of t(4;11) leukemia (Krivtsov et al., 2008; Marschalek, 2011b; Sanjuan-Pla et al., 2015). However, for AF4-MLL which is expressed in only 45-80% of t(4;11) patients, the molecular function and therapeutic potential in ALL is discussed controversially (Agraz-Doblas et al., 2019; Kowarz et al., 2007; Muñoz-López et al., 2016; Prieto et al., 2017; Sanjuan-Pla et al., 2016; Trentin et al., 2009). It remains unclear whether AF4-MLL is required during early stages of leukemia and how the missing expression of AF4-MLL during disease progression can be explained. In 2019, a study from Agraz-Doblas et al., linked the expression of AF4-MLL with overexpressed *HOXA* genes and an overall better treatment outcome for infant B-cell precursor (BCP) ALL patients (Agraz-Doblas et al., 2019). While the association between low expression of *HOXA* genes and a poor survival has been observed and elucidated before, the further association with the expression of AF4-MLL was contradictory to data obtained in numerous international studies between 2006 and 2020 (Kühn et al., 2016; Stam et al., 2006, 2010a; Trentin et al., 2009; Völse, 2020). Additionally, a cooperative effect of AF4-MLL and MLL-AF4 leads to elevated hemato-endothelial specification during human embryonic stem cell differentiation (Bueno et al., 2019). Similarly, the expression of both t(4;11) fusion proteins *in vitro* resulted in growth transformation paired with a higher resistance to apoptosis and an elevated cell cycling capacity (Gaussmann et al., 2007). Vice versa, the knock-down of either MLL-AF4 or AF4-MLL in t(4;11) cell lines led to a G2/M cell cycle arrest and elevated apoptosis upon the loss of MLL-AF4 while no changes in cell cycle or apoptosis could be observed upon the loss of AF4-MLL (Kumar et al., 2011). Importantly, ALL could so far exclusively be induced *in vivo* in the presence of AF4-MLL independent of the expression of MLL-AF4 (Bursen et al., 2010).

Hence, further studies are urgently required to elucidate the distinct roles of each MLL fusion protein in t(4;11) leukemia.

1.4. Targeted treatments against t(4;11) ALL

B-Cell Acute Lymphoblastic Leukemia (B-ALL) is the most common type of cancer in children (Pui and Evans, 2013). Especially in infants and children, the t(4;11) translocation is the most common chromosomal translocation in ALL (Caslini et al., 2000; Eguchi et al., 2006; Meyer et al., 2018).

Treatment of t(4;11) ALL is survived by only 10-30% of patients, with the group of infants under three month of age being most at risk (Bueno et al., 2011; Felix et al., 2000; Hess, 2004; Isoyama et al., 2002; Pui et al., 2002). This particularly aggressive form of leukemia urgently demands novel treatments and clearly contrasts other types of leukemia, whose highly successful treatment, with a subtype-spanning survival rate of more than 90%, is one of the greatest success stories in cancer therapy in the last decades (Cools, 2012).

A well-known example in the history of leukemia therapy of a highly successful management tailored to the specific leukemia subtype is the Philadelphia chromosome with its t(9;22)(q34;q11)-reciprocal translocation. This translocation is responsible for approximately 95% of all CML cases (Druker, 2002). It results in the formation of the BCR-ABL fusion protein, which leads to uncontrolled overexpression of the ABL protein. After it was established that the entire transformative activity is dependent on tyrosine kinase activity (Lugo et al., 1990), specific kinase inhibitors were subsequently implemented very successfully in the therapy of patients with a BCR-ABL translocation.

Following a t(4;11) translocation, transformed cells acquire virtually no further somatic mutations highlighting the potency of chromosomal translocations in leukemias (Dobbins et al., 2013). This suggests the need for tailored therapies adapted to the particular fusion proteins for individual leukemia as overlapping key mutations shared by many other cancers are less frequent and the amount of possible druggable targets limited (Britten et al., 2019; Pikman and Stegmaier, 2018; Steinhilber and Marschalek, 2017).

Importantly, promising immunotherapies such as chimeric antigen receptor T-cell (CAR-T) therapy are especially restricted in infants by the limited feasibility to extract sufficient amount of T-cells (Breese et al., 2021; von Stackelberg et al., 2016). Yet, even more problematic is a recently identified MLL-specific immune escape upon CAR-T cell therapy (Gardner et al., 2016). Gardner et al. observed that B-ALL patients developed CD19 negative AML within one month of CD19 CAR-T cell therapy.

Targeting t(4;11) fusions proteins, numerous compounds are currently in development to treat t(4;11) leukemia. Yet, the majority of treatment approaches primarily target MLL-AF4. Over the last decades, a variety of MEN1 inhibitors have evolved. MEN1 binds at the MDM near the N-terminus to MLL (Murai et al., 2011; Yokoyama et al., 2005). Together with MLL, it is essential for the formation of the super elongation complex and it mediates the binding of MLL to target genes (Chandrasekharappa and Teh, 2003; Chandrasekharappa et al.,

1997; Yokoyama and Cleary, 2008; Yokoyama et al., 2004). MEN1 was further shown to be an essential cofactor for MLL-associated leukemogenesis (Yokoyama et al., 2005). The inhibition of MEN1 by a dominant negative inhibitor resulted in the down-regulation of the HOX cofactor Meis Homeobox 1 (MEIS1) that in turn led to the inhibition of cell proliferation (Caslini et al., 2007). MEN1 inhibitors further revealed the induction of apoptosis and differentiation of leukemia cells harboring MLL translocations (Grembecka et al., 2012). Subsequently, another MEN1 inhibitor displayed responsiveness particularly to cell lines carrying MLL rearrangements and in a patient-derived xenograft (PDX) model, it could significantly reduce leukemia burden even after several rounds of engraftments with MLL-r ALL (Krivtsov et al., 2019). Exemplarily, MEN1 is required for the clinical relevant expression of HOXA genes (Artinger et al., 2013; Jude et al., 2007; Maillard et al., 2009; Nakamura et al., 2002; Yokoyama et al., 2004). Similar results could be obtained in t(4;11) PDX models for several other MEN-1 inhibitors (Borkin et al., 2015; Klossowski et al., 2020). Currently the potential of MEN1 inhibition is evaluated in the clinic (Wang et al., 2020), but so far limited data is available, especially for the high risk t(4;11) leukemia subtype.

Next, the inhibition of Dot1-like protein (DOT1L) constitutes a further targeted approach against t(4;11) leukemia. The histone methyltransferase DOT1L methylates lysine 79 of histone 3 (H3K79) and contributes to leukemogenesis by binding to numerous translocation partners of MLL, such as AF4, AF9, AF10 and ENL (Barry et al., 2010; Bitoun et al., 2007; Deshpande et al., 2012; Godfrey et al., 2019; Mueller et al., 2007; Okada et al., 2005; Reisenauer et al., 2009; Zhang et al., 2006). Nevertheless a limited efficacy was observed in clinical trials in adult AL (Stein et al., 2018). However, a clinical study in children with a median age of 4.2 years with *MLL*-r leukemia demonstrated a limited improvement since only a temporal reduction in peripheral or bone marrow blasts of only 40% of the patients could be observed (Shukla et al., 2016).

The inhibition of BET family proteins including BRD2, BRD3, BRD4 and BRDT represents another epigenetic therapy approach. The t(4;11) translocation leads to the separation of the bromodomain that is located between the PHD 1-3 and PHD 4 domain (Figure 1.2.1 and Figure 1.3.2). BRD4 has been associated with self-renewal ability and pluripotency of embryonic stem cells (Di Micco et al., 2014). The bromodomain of BRD recognizes histone acetylations and is part of the SEC (Di Micco et al., 2014). Inhibiting BET resulted in the reduction of CMYC and STAT5 phosphorylation (Ott et al., 2012). The chromatin reading capacity of BRD4 is believed to promote the aberrant transcription elongation in t(4;11) leukemia and thereafter a study in t(4;11) cells and patients resulted in elevated apoptosis levels (Dawson et al., 2011). Yet, multiple studies reported a limited efficacy of BET-inhibition due to resistance in human and mouse leukemia cells to BET inhibitors that could

be associated with a co-elevated Wnt/ β -catenin signaling (Filippakopoulos et al., 2010; Fong et al., 2015; Weisberg et al., 2007).

Table 1.4.1: Strategies to inhibit MLL fusion proteins. (adapted from Steinhilber and Marschalek 2017)

	Binding of ENL/AF9 <small>(Barretto et al., 2014; Srinivasan et al., 2004)</small>	MLL FYRN/ FYRC <small>(Pless et al., 2011)</small>	Tasp-ase1 <small>(Bursen et al., 2004; Sabiani et al., 2015)</small>	HDACi <small>(Ahmad et al., 2014, 2015; Stumpel et al., 2012; Zhao et al., 2019)</small>	Anti-sense oligos <small>(Kumar et al., 2011; Marschalek, 2011a; Thomas et al., 2005)</small>	DOT1Li <small>(Daigle et al., 2013; Godfrey et al., 2019)</small>	BETi <small>(Dawson et al., 2011; Filippakopoulos et al., 2010; McCalmont et al., 2020; Mirguet et al., 2013; Picaud et al., 2013)</small>	SETi <small>(Cao et al., 2014; Milne et al., 2002)</small>	MEN1/ LEDGFi <small>(Borkin et al., 2015; Čermáková et al., 2014; Klossowski et al., 2020; Krivtsov et al., 2019; Shi et al., 2012)</small>
MLL			Green	Green					Red
AF4	Red			Light Red		Red	Red		
MLL-AF4				Red	Light Red	Red	Light Red		Red
AF4-MLL		Red		Light Red		Red		Red	

Targeting the SET-domain (Cao et al., 2014; Milne et al., 2002), the inhibition of LEDGF (Čermáková et al., 2014), or inhibition of the AF9 binding domain of AF4 (Barretto et al., 2014; Srinivasan et al., 2004), constitute further targeted strategies to combat MLL fusion proteins, that, however, all co-target endogenous MLL or AF4 (Table 1.4.1). As a key regulator in gene expression during hematopoiesis and embryonic development, and an important nuclear transcriptional activator involved in RNA elongation that is expressed in all cell types, the de-regulation of MLL and AF4, respectively, constitutes a major drawback of these approaches (Chen et al., 1993; Djabali et al., 1992; Ernst et al., 2004; Frestedt et al., 1996; Melko et al., 2011). Contrarily, the inhibition of HDACs (Ahmad et al., 2014, 2015; Stumpel et al., 2012), the inhibition of Taspase1 (Bursen et al., 2004; Sabiani et al., 2015; Zhao et al., 2019), and the N-terminal MLL FYRN and the C-terminal counterpart MLL-FYRC (Pless et al., 2011), target either MLL-AF4 or AF4-MLL but additionally either endorse endogenous MLL and AF4 or lack any respective inhibitory function.

The Inhibition of HDACs has been shown to be useful in the therapy of hematopoietic diseases, especially ALLs, but so far have not widely been applied in the therapy of leukemias due to their lack of specificity and general toxicity (Balasubramanian et al., 2009; Bolden et al., 2006; Ceccacci and Minucci, 2016; Eckschlager et al., 2017; Haery et al.,

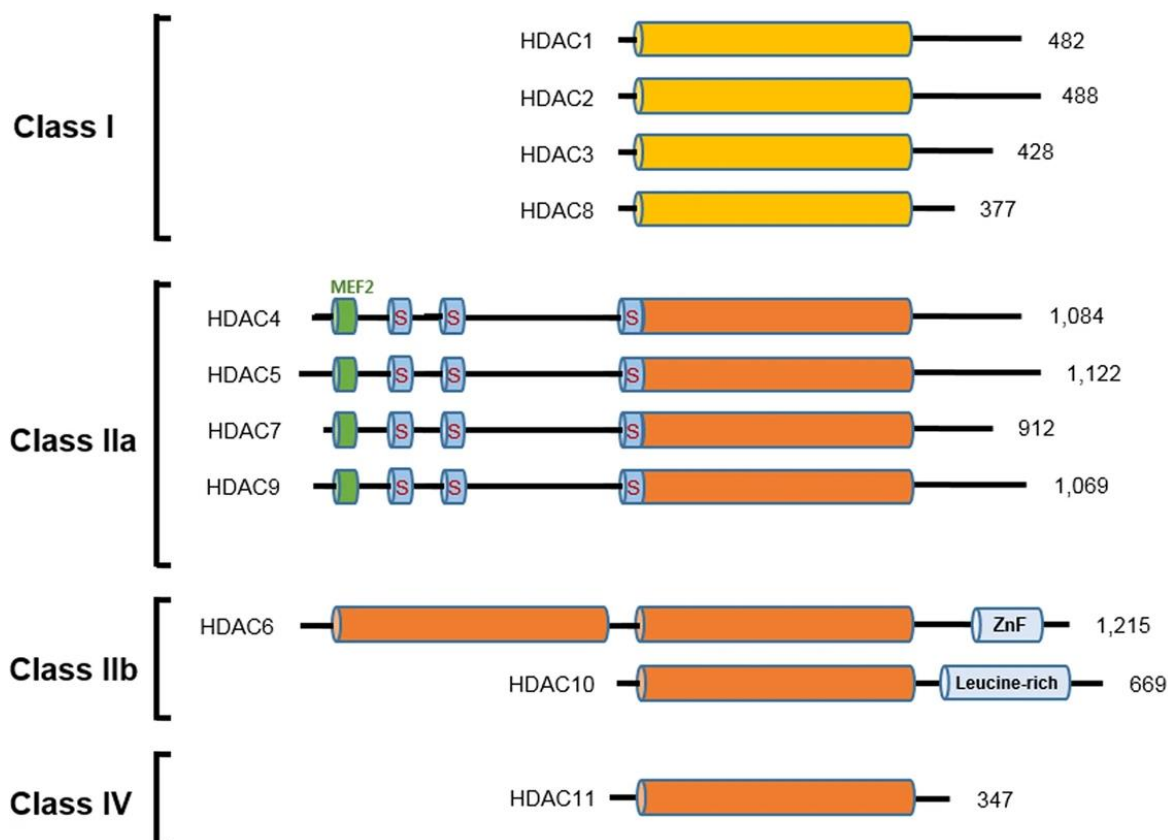


Figure 1.4.1.: Histone deacetylase (HDAC) isoforms. Graphical scheme illustrates catalytic domains (for Class I in yellow and for Class II-IV in orange), binding motifs for Myocyte enhancer factor-2 (MEF) (green) and for 14-3-3 (marked with a red “S” in blue cylinder) Adapted from Park and Kim, 2020.

2015; Vega-García et al., 2018). Moreover, HDACi are known to induce apoptosis in human leukemia cells (Bernhard et al., 2001; Kawagoe et al., 2002). In particular, overexpression of HDACs is observed in ALLs and they are considered to have an oncogenic function (Garcia-Manero et al., 2008; Haery et al., 2015).

Recently, a study of Ahmad et al. revealed a peculiarity of HDACi by demonstrating that HDACis are able not only to stabilize endogenous MLL but also to break the dominant effect of MLL-AF4 (Ahmad et al., 2014). Using a reporter assay, a dominant role of MLL-AF4 in the activation of an MLL target promoter was observed that could be replaced by endogenous MLL. Despite the extensive work and clinical trials with HDACi in cancer research over the last decades, it is nevertheless important to point out their toxicity and associated side effects. HDACs can be clustered into Class I, IIa, IIb and IV according to shared conserved domains (Figure 1.4.1). A key to enhance the efficacy of HDACi therapy in cancer is iso-type specific inhibition that is believed to reduce the toxicity of the treatment significantly (Balasubramanian et al., 2009). Regarding the very poor treatment outcomes of patients with the high-risk t(4;11) ALL and the very limited treatment options, currently

available HDACi compounds could nevertheless potentially already supplement a non-targeted combinational therapy (Suraweera et al., 2018).

The inhibition of Taspase1 represents besides HDACi the second approach that additionally is capable of endorsing endogenous MLL. While a variety of therapeutic approaches exist to inhibit MLL-AF4, AF4-MLL as a target for therapy of t(4;11) leukemias is poorly understood. Based on stability studies showing that AF4-MLL is significantly more stable than endogenous MLL, an alternative degradation process of the reciprocal fusion protein was identified in the laboratory of Prof. Marschalek (Bursen et al., 2004). A conserved SIAH binding site was identified in the N-terminus of all AFF1 family genes, which could be held responsible for the steady state (Bursen et al., 2004; House et al., 2003). The predicted applicability to the AF4-MLL fusion protein owing to the carriage of the N-terminal portion of the AF4 gene was confirmed in SIAH knock-down experiments, which furthermore did not affect endogenous MLL (Bursen et al., 2004). Moreover, proteolysis of the AF4 MLL protein was demonstrated to be prevented by processing of Taspase1 at the CS1/CS2 binding sites in the C-terminal part of MLL (Bursen et al., 2004; Hsieh et al., 2003a, 2003b; Yokoyama et al., 2002). This provided the basis for a possible specific degradation of AF4-MLL without affecting endogenous MLL. In a follow-up study in the laboratory of Prof. Marschalek, a dominant-negative mutant of *taspase1* was developed with the purpose of specifically degrading AF4-MLL (Sabiani et al., 2015). In stability studies, it has been demonstrated that after expression of dnTASP1 in 293T cells overexpressing AF4-MLL, that AF4-MLL was proteasomally degraded due to inhibition of Taspase1 and the prevented proteolytic processing (Sabiani et al., 2015). In addition, Sabiani et al. observed that endogenous MLL is not affected by proteasomal degradation after dnTASP1 expression. The inhibition of Taspase1 further is associated with an enhanced stability of endogenous MLL, as reported by Zhao et al. omitting proteolytic cleavage led to increased stability of endogenous MLL and the replacement of MLL fusion proteins from chromatin in leukemic cells (Zhao et al., 2019).

In summary, especially the administration of HDACi and the inhibition of Taspase1 represent promising treatment approaches, combining the endorsement of endogenous MLL with targeted inhibition of MLL-AF4 and AF4-MLL, respectively.

1.5. Aim

About 70 to 90% of infants with t(4;11) leukemia die and current treatments often still rely on unspecific treatments such as chemotherapeutic drugs that additionally lead to an overall high therapy-related mortality near 10% (Dreyer et al., 2015; Felix et al., 2000, 2000; Hess, 2004; Isoyama et al., 2002; Pieters et al., 2007, 2019; Pui et al., 2002).

The aim of this work is to improve the understanding of the role of reciprocal AF4-MLL during the progression of t(4;11) leukemia, since conflicting data on a possible association between AF4-MLL expression and poor prognosis for t(4;11) patients emerged (Agraz-Doblas et al., 2019; Stam et al., 2006, 2010a; Trentin et al., 2009; Völse, 2020). Next, the work aims to elucidate the impact of the interaction between MLL-AF4 and AF4-MLL during the progression of leukemia as AF4-MLL was demonstrated to be essential for the development of leukemia *in vivo*, but is not expressed in all t(4;11) patients (Bursen et al., 2010; Meyer et al., 2018).

Considering that AF4-MLL carries a functional N-terminus of the transcription-elongation factor AF4 and the C-terminus of MLL that is still capable of chromatin reading and writing, suggests AF4-MLL to act as an epigenetic regulator with a potent transforming activity (Marschalek, 2011a; Park et al., 2010; Patel et al., 2009; Prieto et al., 2017; Rössler and Marschalek, 2013; Yokoyama, 2015; Yokoyama et al., 2013). Furthermore, the target-determining N-terminus of MLL is replaced by AF4, indicating a chromatin modulating effect of AF4-MLL that is not restricted to target genes of endogenous MLL (Broeker et al., 1996; Erfurth et al., 2008; Marschalek, 2011b). Thereafter, this work further aims to unravel whether AF4-MLL might be primarily involved during leukemogenesis and becomes redundant for leukemia onset.

2. MATERIAL

2.1. Cell lines

Table 2.1.:Cell lines

Name	Description	Source
HEK-293T	Human embryonic kidney cells. It represents a derivative of cell line 293 and additionally carries a plasmid with a mutant of the temperature-sensitive gene of the SV40 T antigen. S1 adherent cell line.	ATCC® CRL-3216™ DSMZ ACC 635
NALM6	Human leukemia precursor B cells extracted from peripheral blood of a patient with ALL. S1 suspension cell line.	DSMZ ACC 128
SEM	Human B cell precursor leukemia cell line. It was isolated from a 5-years female relapse patient. S1 suspension cell line.	DSMZ ACC546

2.2. Bacterial strains

Table 2.2.:Bacterial strains

Name	Description	Source
TOP10F	F'[lacIq Tn10(tetR)] mcrA Δ(mrr-hsdRMS-mcrBC) φ80lacZΔM15 ΔlacX74 deoR nupG recA1 araD139 Δ(ara-leu)7697 galU galK rpsL(StrR) endA1 (www.openwetware.org)	Invitrogen
	Human B cell precursor leukemia cell line. It was isolated from a 5-years female relapse patient. S1 suspension cell line.	

2.3. Oligonucleotides

Table 2.3.:Oligonucleotides

Name	Description
GAPDH_For	GGTCACCAGGGCTGCTTTTA
GAPDH_Rev	CGTTCTCAGCCTTGACGGTG
MLL 8•3	CCCAAACCACTCCTAGTGAG
MLL 13•5	CAGGGTGATAGCTGTTTCGG
AF4•3	GTTGCAATGCAGCAGAAGCC
AF4•5	ACTGTCACTGTCCTCACTGTCA
Tasp1_For	CGACGGAGAGCATGTGTGT
Tasp1_Rev	ACAATGAGGAGTTTCTATTTTCATCC
dnTasp1_Rev	GCTTGTCGTCATCGTCTTTGT
EF1a.SF3	GCCTCAGACAGTGGTTCAAAG
T7_For	TAATACGACTCACTATAGGG
TCE_SF	CCTGGAGCCAATTCCAACCTCT
SV40PA.Avr.R	CCTAGGTACCACATTTGTAGAGGTT
BGH.R	CCTAGGCCAGCTGGTTCTTTCCGCCTCAGAA
BGH.SR	AGGCACAGTCGAGGCTGAT
GFP_For	ACATGTTGAGCAAGGGCGAGGAGCTGT
GFP_Rev	AGATCTTTCGAACGTCTCTCATGGGGCCAGGAT TCTCCT
GAPDH*3	CTTCACCACCATGGAGGAAGG
GAPDH*5	CCTGCTTCACCACCTTCTTG
pITRS.SF	GTCTCATGAGCGGATACATA
pITRS.SR	CGCCGCAGCCGAACGACCGA
Taspase*5	GTTCACTGGGCTCTCCAGGCGGCA

2.4. Antibodies

Table 2.4.1.: Primary antibodies

Description	Name	Dilution	Species	Source
Anti-Actin	A2066	1/1000 WB	Rabbit	Sigma-Aldrich
Anti-MLL-C	#61295	1/1000 WB	Rabbit	Active Motive

Anti-MLL-N	A300086A	1/1000 WB	Rabbit	Bethyl Labs
Anti-AF4-N	A302-344	1/1000 WB	Rabbit	Bethyl Labs
Anti-AF4-C	ab174216	1/500 WB	Rabbit	Abcam
Anti-Vinculin	V9131	1/5000 WB	Mouse	Sigma-Aldrich
Anti-Tubulin	T5168	1/5000 WB	Mouse	Sigma-Aldrich

Table 2.4.2.: Secondary antibodies

Description	Dilution	Species	Source
Anti-rabbit	1/10.000	Rabbit	Bio-Rad
Anti-mouse	1/10.000	Mouse	GE-Healthcare

2.5. Enzymes

Table 2.5.:Enzymes

Name	Source
Alkalic phosphatase	New England Biolabs
DNA-Ligase	Roche
RNase A	Sigma-Aldrich
Benzonase	Invitrogen
T4-DNA-Ligase	New England Biolabs
Restriction Enzymes	New England Biolabs
T4-DNA-Quick-Ligase	New England Biolabs
Super Script Reverse Transcriptase III	Invitrogen
Proteinase Inhibitor Cocktail	Roche

2.6. Plasmids

Table 2.6.:Plasmids

Name	Source
pSBtet::dnTASP1	Dr. Samaneh Sabiani
pSBtet::MLL-AF4	This study
pSBtet::Luc	Dr. Eric Kowarz

SB100xco	Dr. Eric Kowarz
pSBtet::AF4-MLL	This study
pSBbi::MLL-AF4	Dr. Denise Löscher

2.7. Commercial kits

Table 2.7.:Commercial kits

Name	Source
NucleoSpin® Plasmid-Purification	Macherey-Nagel
NucleoSpin® Gel and PCR Clean-up	Macherey-Nagel
RNeasy Mini-kit	Qiagen
PureYield™ Plasmid MidiPrep System	Promega
Pierce™ BCA Protein Assay Kit	Thermo Fisher Scientific
QIAquick Gel Extraction Kit	Qiagen
Qubit RNA HS Assay Kit	Invitrogen
NC-3000 Mitochondrial Potential Assay	Chemometec
NC-3000 Viability Assay	Chemometec
NC-3000 Vitality Assay	Chemometec
NC3000 Cell Cycle Assay	Chemometec
Q5 Polymerase Kit	New England Biolabs
Bioanalyzer High Sensitivity DNA Kit	Agilent

2.8. Chemicals and solutions

Table 2.8.:Reagents

Name	Source
1,4-Dithiotreitol	Invitrogen
2-Mercaptoethanol	Carl-Roth GmbH & Co. KG
4-(2-hydroxyethyl)-1-piperazineethanesulfonic acid	Carl-Roth GmbH & Co. KG
Accutase	Capricorn
Acetic acid	Carl-Roth GmbH & Co. KG
Acrylamide	Carl-Roth GmbH & Co. KG

Agar	Carl-Roth GmbH & Co. KG
Agarose	Invitrogen
Ammoniumchloride	Carl-Roth GmbH & Co. KG
Ammoniumperoxide sulfate	Carl-Roth GmbH & Co. KG
Aminocaproic acid	Sigma-Aldrich Chemie GmbH
Ampicillin	Carl-Roth GmbH & Co. KG
Bacto Trypton	Oxoid
Bovine Serum Albumin	Carl-Roth GmbH & Co. KG
Bromphenol blue	Sigma-Aldrich Chemie GmbH
CaCl ₂	Merck KGaA
Camptothecin	Alfa Aesar
CAPS	Carl-Roth GmbH & Co. KG
Chloramphenicol	Carl-Roth GmbH & Co. KG
Complete Protease Inhibitor Cocktail	Roche Diagnostics GmbH
Dacinostat	Syndax Pharmaceuticals
Dexamethasone	Cayman Chemicals
Dimethyl sulphoxide (DMSO)	Sigma Aldrich Chemie GmbH
Doxycycline	Sigma-Aldrich Chemie GmbH
Droxinostat	Syndax Pharmaceuticals
EDTA	Carl-Roth GmbH & Co. KG
Entinostat	Syndax Pharmaceuticals
Ethanol	Carl-Roth GmbH & Co. KG
Ethidium bromide	Carl-Roth GmbH & Co. KG
Glycerol	Carl-Roth GmbH & Co. KG
Glycine	Carl-Roth GmbH & Co. KG
HCl (32%)	Carl-Roth GmbH & Co. KG
Isopropanol	Carl-Roth GmbH & Co. KG
Methanol	Carl-Roth GmbH & Co. KG
MgCl ₂	Carl-Roth GmbH & Co. KG
Milk powder	Carl-Roth GmbH & Co. KG
Mocetinostat	Syndax Pharmaceuticals
NaCl	Carl-Roth GmbH & Co. KG
NaF	Carl-Roth GmbH & Co. KG
NaOAc	Merck KGaA
Penicilin/Streptomycin	Gibco/Merck KGaA
Phenylmethylsulfonyl fluoride	Sigma Aldrich Chemie GmbH
Polyethyleneimine	Sigma Aldrich Chemie GmbH

RedDot2	Biotium
Sodium deoxycholate	Sigma Aldrich Chemie GmbH
Sodium dodecyl sulfate	Biomol
Sodium hydroxide	Carl-Roth GmbH & Co. KG
Sodium phosphate	Carl-Roth GmbH & Co. KG
TEMED	Sigma Aldrich Chemie GmbH
Tris	Carl-Roth GmbH & Co. KG
Triton X-100	Sigma Aldrich Chemie GmbH
Tween 20	Sigma Aldrich Chemie GmbH
V-CF405 M	Biotium
Yeast extract	Oxoid

2.9. Buffers and media

Table 2.9.1.: Buffers

Name	Ingredients (Source)
Anode buffer I for semi-dry Western Blot (pH 10.4)	300 mM Tris 20% Methanol
Anode buffer II for semi-dry Western Blot (pH 10.4)	25 mM Tris 20% Methanol
ATAC-seq 2xTD buffer	20 mM Tris-HCl (pH 7.4) 10 mM MgCl ₂ 20 % Dimethyl Formamide
ATAC-seq Resuspension buffer I	10 mM Tris-HCl (pH 7.4) 10 mM NaCl 3 mM MgCl ₂ 0.1% NP40 0.1% Tween-20 0.01% Digitonin
ATAC-seq Resuspension buffer II	10 mM Tris-HCl (pH 7.4)

	10 mM NaCl
	3 mM MgCl ₂
	0.1% Tween-20
	25 µL 2x TD buffer
	2.5 µL transposase 26 (100 nM final)
	16.5 µL PBS
ATAC-seq Transposition mix	0.5 µL 1% Digitonin
	0.5 µL 10% Tween-20
	5 µL H ₂ O
	25 mM Tris
Cathode buffer for semi-dry Western Blot (pH 9.4)	40 mM Aminocaproic acid
	20% Methanol
Collection gel buffer for SDS-PAGE	1 M Tris (pH 6.8)
	20 mM Tris/HCl (pH 6.8)
	200 mM DTT
Laemmli buffer (2x)	4% SDS
	20% Glycerine
	0.2% Bromphenol blue
	150 mM NaCl
	5 mM EDTA (pH 8.0)
	50 mM Tris (pH 8.0)
	1% NP-40 (IGEPAL CA-630)
Lysis buffer for Western blot	0.1% SDS
	2 mM PMSF
	0.5% Sodium deoxycholate
	10 mM NaF
	1x PI-Cocktail
	10 mM CAPS
Matsudaira buffer for Western blot (pH 11.0)	15% Methanol
Phosphate buffered saline (PBS)	(Capricorn)

SDS-running buffer	3.03g Tris 14.4 g Glycine 1g SDS Ad. 1L H ₂ O
Separation gel buffer for SDS-PAGE	1 M Tris (pH 8.8) 15 g Glycine
Stripping buffer for Western Blot (pH 2.2)	1 g SDS 10 mL Tween20 Fill up to 1L with H ₂ O
TBE buffer	100 mM Tris 500mM H ₃ BO ₃ 2.5 mM EDTA
TBST solution for Western Blot	10 mM Tris/HCl (pH 7.5) 150 mM NaCl 0.1% Tween 20

Table 2.9.2.: Media

Name	Ingredients (Source)
Cultivation medium of HEK293T cells	DMEM (Gibco)
	10% FCS
	1% L-Glutamine
	1% Pen/Strep
Cultivation medium of SEM and NALM6 cells	RPMI-1640 (Gibco)
	10% FCS
	1% L-Glutamine
	1% Pen/Strep
Opti-MEM	Gibco
YT agar	1% Bacto agar
	0.5% NaCl
	0.5% Yeast Extract

YT medium

1.2% Bacto Trypton

0.5% NaCl

0.5% Yeast Extract

3. METHODS

3.1. Sequencing

3.1.1. MACE-seq

Massive analysis of cDNA ends (MACE-seq) was conducted with total RNA extracted from 293T cells to evaluate transcriptomic alterations *in vitro* upon the constitutive or induced expression, by the administration of 1 µg/mL Doxycycline, of t(4;11) fusion genes. Three biological replicates at 4 different time points of distinct expression patterns of t(4;11) fusion proteins were analyzed and compared to mock-transfected 293T cells.

All cellular samples were lysed, stored in liquid nitrogen and subsequently total RNA isolated. The NucleoSpin RNA, Mini kit (Macherey Nagel) was used for RNA isolation and RNA isolates were DNaseI-treated applying the RQ1 RNase-Free DNase Kit (Promega). RNA quality was assessed with the automated microfluidic electrophoresis TapeStation (Agilent).

The MACE-libraries were prepared at GenXPro GmbH using the Massive Analysis of cDNA Ends (MACE) Library Preparation Kit (v2.0) by GenXPro GmbH, as previously described (Nold-Petry et al., 2015). Initially, cDNA was generated using Oligo (dT) primers containing distinct Oligo IDs per sample for subsequent pooling of up to 24 samples. Following pooling, the cDNA was fragmented to an average size of 200 bp using the sonicator Biorupter Plus (Diagenode, Belgium) and cDNA size distribution was monitored using the automated microfluidic electrophoresis station LabChip GXII Touch HT platform (PerkinElmer, USA). The poly(A) containing cDNA fragments were purified by solid phase reversible immobilization (SPRI) beads (Agencourt AMPure XP, USA), end repaired and ligated to distinct 8-base pair UMI Adapters (also known as TrueQuant adapters). Subsequently, the library containing labelled and fragmented cDNA was amplified by PCR, purified by SPRI beads (Agencourt AMPure XP, USA) and sequenced strand-specific using the HiSeq2500 (Illumina, USA).

Protein-protein interactions of de-regulated genes from MACE-seq data were visualized and predicted by STRING Protein-protein interaction networks functional enrichment analysis (www.string-db.org). Heat-maps were generated using the MORPHEUS versatile visualization and analysis software from the Broad Institute (www.software.broadinstitute.org/morpheus).

For visualizing MACE-seq data, volcano plots were generated that show the statistical significance (FDR) against the magnitude of change (log-2 fold change) using the software PRISM 8.0.1 (GraphPad).

3.1.2. ATAC-seq

The Assay for Transposase-Accessible Chromatin using sequencing (ATAC-seq) was conducted in 293T cells that express t(4;11) fusion genes either constitutively or upon the induction with 1 µg/mL Doxycycline. Cells were carefully harvested and centrifuged at 500 RCF for 5 minutes and resuspended in cold PBS. Next, cells were counted and cellular viability determined using the Casy cell counter. 50,000 cells were centrifuged at 500 RCF for 5 minutes at 4°C and the supernatant carefully aspirated. Each cellular sample was resuspended by pipetting up and down 3 times in pre-cooled 50 µL ATAC-seq Resuspension Buffer I. After incubating cells for 3 minutes on ice, 1 mL of cold ATAC-seq Resuspension Buffer II was added and tubes inverted 3 times prior to pelleting nuclei by centrifugation at 500 RCF for 10 minutes at 4°C. Next, supernatant was removed and nuclei resuspended in 50 µL of ATAC-seq Transposition mix by pipetting up and down six times. Each transposition reaction was incubated at 37°C for 30 min in a thermomixer at 1000 rpm. All further steps were conducted at GenXPro GmbH that applied an Illumina HiSeq for analysis.

For visualizing ATAC-seq data, volcano plots were generated that show the statistical significance (FDR) against the magnitude of change (log-2 fold change) using the software PRISM 8.0.1 (GraphPad).

3.2. Cell biology methods

3.2.1. Cultivating adherent cell lines

HEK293T cells were maintained in an incubator at 37°C in a humidified atmosphere with 5% CO₂ and sub-cultured every 2-3 days. For this purpose, the medium of adherent 293T cells was aspirated, followed by the detachment of cells by the administration of 1 ml each of Accutase per 10 cm cell culture plate. Using a 1000 µL micro-pipette, the cellular suspension was further pipetted up and down to overcome remaining cell-cell contacts and an estimated quantity of cells maintained that lead to a cellular confluency of approx. 20-30% when attached to the 10 cm dish. Finally, 9 mL cultivating medium for 293T cells (serum-containing DMEM) was applied to inhibit the detachment activity of Accutase and to provide optimal cultivating conditions.

3.2.2. Cultivating suspension cell lines

SEM cells were maintained in an incubator at 37°C in a humidified atmosphere with 7.5% CO₂ and sub-cultured every 3-4 days. Here, cells were centrifuged at 400 RCF for 5 minutes, followed by the aspiration of the supernatant and the passaging of a quantity of cells that result in at least 40-50% confluency. Finally, cultivating medium for SEM cells was refilled.

3.2.3. Cell counting and viability assay

Cells were counted with capillary-based Casy TT cell counter. 50 µL of well-resuspended cell suspensions were added to a tube containing 10 mL of Casy-Ton.

After several rounds of careful inverting of the tube, cells were counted and the viability of the cells determined according to the manufacturers manual. All measurements were conducted as triplicates.

3.2.4. Transfections using the Sleeping Beauty System

On the first experimental day, 1×10^6 cells were plated per 10 cm cell culture dish. On the next day, the cultivating medium was renewed and two transfection solutions prepared within 60 minutes. Solution A contains 180 µL of PBS and 36 µL of the transfection agent polyethylene imine and Solution B 180 µL PBS, 9.5 µg of Sleeping Beauty plasmid DNA (Kowarz et al., 2015) containing the gene of interest and 0.5 µg DNA of the SB100xco plasmid containing the transposase that mediates a stable integration of the gene of interest into the genome.

For a transient transfection, the 0.5 µg DNA of the SB100xco was replaced with PBS. Both, Solution A and Solution B, were stored at room temperature during the 60 minutes incubation step with new cultivating medium. After the respective incubation, Solution B was transferred dropwise into the tube containing Solution A while vortexing. The mixture was incubated for 15 minutes and subsequently added dropwise to the cells. Cells were incubated for 48 hours and the transfection efficacy microscopically evaluated. Next, in case of a stable transfection, several rounds of selection steps were initiated (2 µg/mL puromycin for 24 hours or 8 µg/mL Blasticidin for 48 hours) to obtain a homogeneously transfected cell population.

3.2.5. Annexin V Assay (Flow Cytometry readout)

The Annexin V Assay using the BD FACSVerse™ Flow Cytometer was conducted with SEM-Mock and SEM-dnTASP1 cells that were both treated for 48 h with Entinostat, Mocetinostat and Dacinostat at IC-50 conditions, and 1 µg/mL Doxycycline to induce dnTASP1. Doxycycline-induced SEM cells that were treated with 0.1% DMSO served as mock control.

SEM cells were initially counted and the cellular viability determined using the Casy TT cell counter. 3×10^5 cells were selected per sample and centrifuged at 400 RCF for 5 minutes at room temperature. Next, the pellet was resuspended in a mixture of 2 µg/mL Pacific Blue (Invitrogen, USA) and 0.1% SYTOX Red (Invitrogen, USA) in 200 µL Annexin-V Binding buffer and the mixtures subsequently incubated for 15 minutes at room temperature protected from light. Finally, samples were gently mixed and kept on ice until the Flow cytometry measurements. The 405 nm and 640 nm laser of the Flow Cytometer were applied to analyze 1×10^5 cells per sample. Each sample was measured in three biological replicates.

3.2.6. Annexin V Assay (microscopic readout)

The microscopic-based Annexin V Assays was conducted with the image cytometer Nucleocounter NC-3000 (ChemoMetec, Denmark). The manufacturers manual was adapted to SEM-Mock and SEM-dnTASP1 cells that either contain a green or red backbone fluorescence, respectively (ChemoMetec A/S., 2003).

Prior to conducting the Annexin V Assay, SEM cells were treated for 48 h with Entinostat, Mocetinostat or Dacinostat at IC-50 concentrations and with 1 µg/mL Doxycycline for the induction of dnTASP1. Doxycycline-induced SEM cells that were treated with 0.1% DMSO served as mock control.

Initially, SEM cells were counted and cellular viability determined with the the Casy TT cell counter. 3×10^5 cells were taken per sample and centrifuged at 400 RCF for 5 minutes at room temperature. The pellet was resuspended in a mixture of 2 µg/mL Annexin V-CF405M (Biotium, USA) and 0.1% of the the dead-cell stain Sytox Red (ThermoFisher) or RedDot2 (Biotium, USA) in 100 µL Annexin Binding buffer (Biotium, USA) and protected from light incubated at room temperature for 15 minutes. Subsequently, samples were gently mixed and protected from light kept on ice. Cells were exposed to the 405 and 633 lasers with emission filters set at 448/45 nm and 630 LP. Each sample was measured in three biological replicates.

3.3. Biochemical methods

3.3.1. Preparation of cell lysates

Cells were centrifuged at 1000 rpm for 5 minutes and washed once with PBS. Next, 1×10^6 cells were resuspended in 20 μ L Lysis buffer and incubated for 45 minutes at 4°C on a rotor at 12 rpm. Subsequently, lysed cells were centrifuged at 14,000 rpm at 4°C for 30 minutes. The protein-containing supernatant was transferred into a 1,5 mL tube and supplemented with 4x Laemmli buffer to a final concentration of 1x Laemmli buffer. The cell lysate was incubated at 95°C for 5 minutes in a thermos shaker at 1000 rpm and either immediately loaded onto a gel or stored at -20°C.

3.3.2. Western Blot analysis

Prior to the Western Blot, proteins were separated by sodium dodecyl sulfate-polyacrylamide gel electrophoresis (SDS-PAGE) (Biorad) using Tris-Glycine gels that were supplemented with 0.5% Trichloroethanol for absolute proteins quantification. Proteins were transferred from the SDS-PAGE gel to a polyvinylidene fluoride (PVDF) membrane (Abcam, USA) in a tank blot (Biorad) for 2 h at 100 Volts at 4°C.

Next, the membrane was blocked in 5% BSA/TBS-T for 1 h on a shaker at room temperature. The primary antibody diluted 5% BSA/TBS-T was added and the membrane incubated at 4°C overnight. The membrane was 5 times washed with TBS-T with 5 minutes of incubation between each washing step. The secondary antibody diluted in 5% milk/TBS-T was applied for 1 h at room temperature, followed by 5 washing steps accordingly to the previous washing steps with TBS-T. Finally, protein bands were visualized by a chemiluminescent assay using an enhanced chemiluminescent (ECL) kit (Biorad). Images were taken with the ChemiDoc™ XRS+ system from Biorad.

3.4. Bioinformatic and statistical analysis

The bioinformatic analysis of the MACE-seq experiments was conducted in accordance to the analysis pipeline for MACE libraries by GenXPro GmbH. Distinct Oligo IDs and UMIs on each transcript allowed initial demultiplexing followed by the removal of PCR-duplicates. Remaining reads were trimmed for high-quality as well as adapter-free sequences and aligned with Bowtie 2 to the human reference genome (Genome Reference Consortium Human Build 38 patch release 13, GRCh38.p13:

https://www.ncbi.nlm.nih.gov/assembly/GCF_000001405.39) resulting in 31,415 different genes. The sequencing data, considering sequencing depth and RNA composition, was normalized with the median of ratios method by DESeq2. Besides log₂ fold-changes, p-values and false discovery rates were calculated to account for single or multiple hypothesis testing, respectively.

The output data from the and ATAC-seq and MACE-seq experiments generated with the Bioconductor software were analyzed with Microsoft EXCEL and additionally the FILEMAKER Database program was used for differential gene expression analysis (Wilhelm and Marschalek, 2021). Additionally, the distance of the closest peak to a neighbor gene as well as the peak location relative to annotation was determined by a data analysis workflow including motif enrichment (HOMER), fingerprinting and peak calling (MACS) in cooperation with GenXPro GmbH.

Gene set enrichment analysis (GSEA) was performed to compare the effect of MLL-AF4 knock-down of the t(4;11) PDX model for patient 707 and 763 with published transcriptomics data from t(4;11) leukemia patients (Stam et al., 2010a) (GEO database: GSE19475). Significant genes were selected according to Lin et al. (Lin et al., 2016), ($p \leq 0.05$, $FDR \leq 0.1$, fold change ≥ 2). The GSEA software of UC San Diego and the Broad Institute (version 4.0.1) was used for analysis according to Subramanian et al. and Mootha et al. (Mootha et al., 2003; Subramanian et al., 2005). Permutation testing was performed with a permutation test with a total of 1000 gene set specific permutations.

k-means clustering was either based on the assumption of a continuous differential gene expression upon expression of AF4-MLL or the assumption of a direct correlation between differential genes expression and AF4-MLL expression. To endorse the statistical strength of each generated cluster de-regulated genes with an $FDR > 0.25$ were excluded from analysis. Using the MEV software, in total 20 clusters were generated. Clusters indicating an immediate response were required to meet the conditions that day 0 unequal day 3, day 12, and day 28 as well as that d3, d12 and day 28 are equal. Moreover, the selection of clusters mimicking a delayed adaptation was based on the condition that day 0 equals d3, day 12 equals day 28, but day 0 and day 3 unequal day 12 and day 28. Contrarily, clusters to model a short-term effect of AF4-MLL were selected after the assumption that expression data of day 3 exceeds or undercuts the expression of d0, day 12 and day 28. Four of the best fitting clusters of each model were used for pathway enrichment analyses and knowledge-based STRING network analysis.

Further on, Student's t tests and equivalence tests were conducted with GraphPad Prism 8 (GraphPad, Dotmatics, USA) and Excel 2016 (Microsoft, USA). Differences with $p < 0.05$ were considered significant in a student's t test, or equivalent in a 95% equivalence test.

4. RESULTS

4.1. Expression of dnTASP1 induces apoptosis in HDACi-treated t(4;11) ALL cells *in vitro*

A large portion of studies in t(4;11) ALL-related research focus on the inhibition of the MLL fusion protein MLL-AF4. Data on evaluating the therapeutic benefit of inhibiting the reciprocal fusion protein AF4-MLL alone or together with MLL-AF4 is missing. Additionally, MLL-AF4-targeting compounds often affect endogenous MLL and hence the overall transcription machinery (see chapter 1.4). The current treatment plan for MLL-r leukemia patients including the highly-affected group of infants consists of several potent drugs that often lead to severe side effects or even death (Britten et al., 2019).

In this work, a novel therapeutic approach is evaluated that aims to both inhibit MLL fusion proteins and to maintain the function of endogenous MLL. For the inhibition of the reciprocal fusion protein AF4-MLL *in vitro*, the pro-B ALL cell line SEM, that expresses both MLL-AF4 and AF4-MLL, was transfected with a Sleeping Beauty expression plasmid for inducible expression of a dominant negative mutant of Taspase1 (dnTASP1) (Fig. 4.1.1.1 A). The expression of dnTASP1 was shown to effectively inhibit the Taspase1-mediated cleavage near the C-terminus in endogenous MLL as well as in AF4-MLL (Sabiani et al., 2015). Moreover, it was demonstrated that particularly AF4-MLL was degraded by the proteasome upon dnTASP1 expression, while uncleaved MLL continues to be catalytically active (Sabiani et al., 2015; Yokoyama et al., 2013). The recently shown ability of HDAC inhibitors to reduce dominant effects of MLL-AF4 through a re-activation of endogenous MLL (Ahmad et al., 2014) complements the dual therapeutic approach evaluated in this study (Fig. 4.1.1.1 A).

Here, dnTASP1-expressing SEM cells were treated with several HDACi to evaluate the co-inhibition of MLL-AF4 and AF4-MLL while preserving the activity of endogenous MLL as a potential treatment approach for t(4;11) leukemia.

4.1.1. Generation of a dnTASP1 expressing t(4;11) pro-B ALL cell line

The protein Taspase1 hydrolyses MLL at specific sites near its C-terminal end and initiates its hetero-dimerization. Interfering this processing step has minor effects on the activity of MLL, while AF4-MLL that shares the identical Taspase1 cleavage sites is degraded by the proteasome in its uncleaved form (Sabiani et al., 2015; Yokoyama et al., 2013). In this study, a dominant-negative mutant of Taspase1 was overexpressed in SEM cells to inhibit

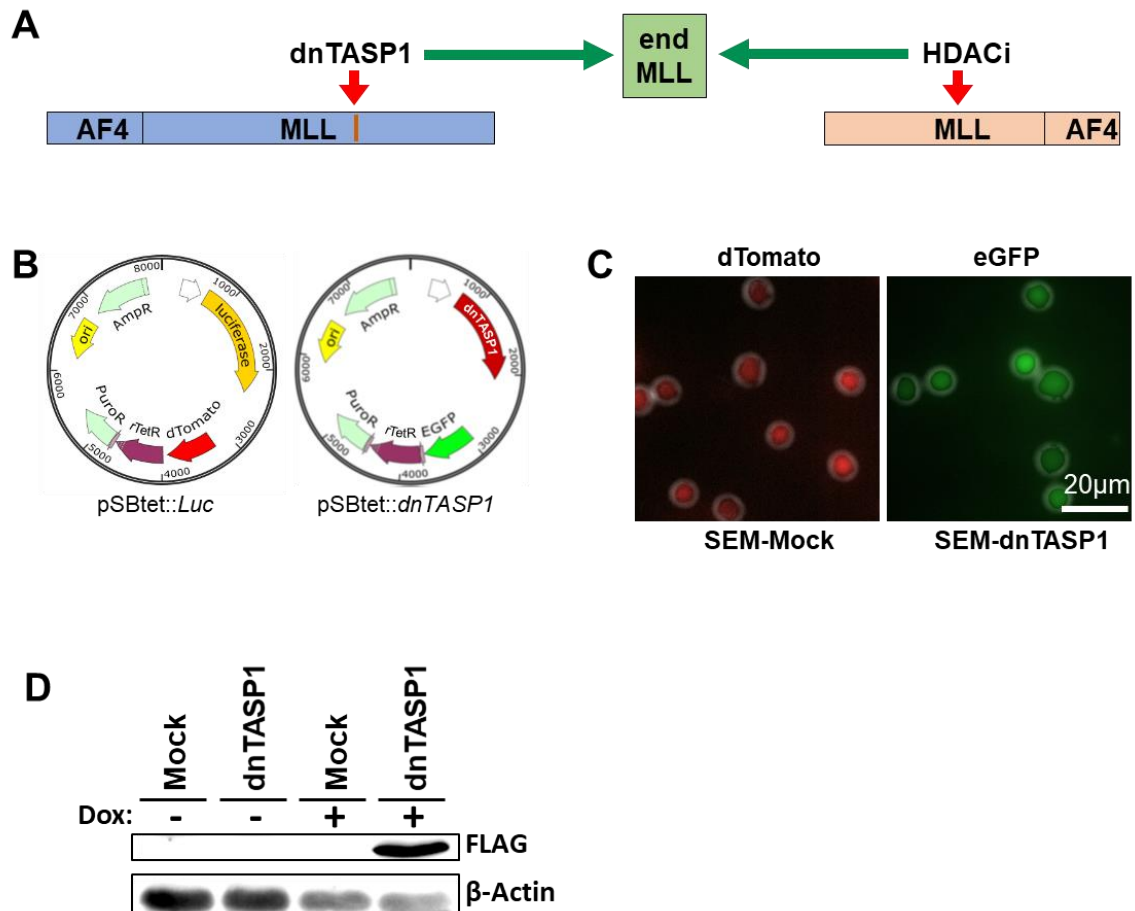


Figure 4.1.1.1: Generation of an inducible dnTASP1-expressing t(4;11) pro-B ALL cell line. Scheme of the dual therapeutic approach targeting the fusion proteins MLL-AF4 and AF4-MLL (A). endMLL = endogenous MLL. Sleeping Beauty vectors pSBtet::dnTASP1 and pSBtet::Luc were introduced into the pro-B ALL cell line SEM to mediate Doxycycline-inducible expression of dnTASP1 (SEM-dnTASP1) and Luciferase (SEM-Mock), respectively (B). AmpR = Ampicilin resistance cassette, ori = origin of replication, PuroR = Puromycin resistance cassette, rTetR = reverse Tet repressor, white arrow = TCE promoter. The stable integration of the Sleeping Beauty vectors into SEM cells could be evaluated microscopically on the basis of constitutively expressed dTomato (SEM-Mock) and eGFP (SEM-dnTASP1) (C). The expression of Luciferase and the FLAG-tagged dnTASP1 upon the induction with 1 μ g/mL Doxycycline for 24 h was confirmed by a Western-Blot of FLAG and probing for β -actin served as loading control.

Taspase1-mediated cleavage due to the lack of effective Taspase1 inhibitors (Sabiani et al., 2015).

Using transposable elements for transgene integration, my colleague Allesia Kühn stably transfected SEM cells with an optimized Sleeping Beauty transposon system for inducible overexpression of either dnTASP1 (SEM-dnTASP1) or Luciferase (SEM-Mock) (Kowarz et al., 2015). The optimized Sleeping Beauty vector system was applied for the generation of all transgenic cell lines in this work. In contrast to retro- or lentiviral systems, the Sleeping

Beauty system allows, essential for the work with MLL, a scalable number of integrations and has no limitation in size of the gene of interest.

For the generation of SEM-dnTASP1 cells and SEM-Mock cells, the tetracycline-inducible Sleeping Beauty vectors pSBtet::*dnTASP1* and pSBtet::*Luc*, respectively, were used that vary in backbone fluorescence and selection markers (Fig. 4.1.1.1 B). The pSBtet::*dnTASP1* and the pSBtet::*Luc* vector carry aside from the inducible TCE promoter for the gene of interest a RPBSA promoter for constitutive expression of a puromycin resistance cassette as well as eGFP and dTomato, respectively. Hence, the entire process of developing stable dnTASP1- or Luciferase- expressing SEM cells, from the evaluation of transfection efficacy to several rounds of antibiotic selection, can be monitored by fluorescence microscopy. After 3 rounds of selection with puromycin, the respective fluorophores were detectable in all Luciferase- and dnTASP1-expressing SEM cells (Fig. 4.1.1.1 C). In addition to the verification of the background fluorescence, the proper expression of the dnTASP1 protein was confirmed by Western Blot (Fig. 4.1.1.1 D). The co-capturing of endogenous Taspase1 was prevented by using a primary antibody against the c-terminal FLAG tag of dnTASP1.

In summary, SEM cells carrying inducible expression cassette for dnTASP1 for the inhibition of AF4-MLL *in vitro* were generated using an optimized Sleeping Beauty System.

4.1.2. Short-term expression of dnTASP1 has minor effects on HDACi-treated SEM

MLL-AF4 mainly affects transcription by acting on promoters directly (Marschalek, 2011b, 2019). Recently, it could be shown on the basis of a 5-LO promoter reporter assay, that MLL-AF4 in contrast to wild-type MLL can strongly activate promoters in the presence of HDACs (Ahmad et al., 2014). However, the same study revealed that HDAC class I inhibitors stimulate 5-LO promoter activity in a wild-type MLL-dependent manner while MLL-AF4 dependent promoter activation was significantly reduced. Ahmad et al. concluded that upon HDACi, endogenous MLL is capable of replacing the hitherto dominant MLL-AF4-mediated promoter activation (Ahmad et al., 2014).

Here, the effect of class 1 HDACs on abrogation of the dominant promoter-activating effects of MLL-AF4 by reactivating wild-type MLL in t(4;11) leukemia cells was tested to determine whether HDACi may complement the dual therapeutic approach in conjunction with the expression of dnTASP1.

Currently, there are numerous HDAC inhibitors in different phases of clinical trials available that can inhibit various combinations of HDACs. Ahmad et al. have demonstrated that the

inhibition of HDAC1-3 was sufficient to disrupt the dominance mediated by MLL-AF4 over wild-type MLL to activate the 5-LO promoter. Therefore, all tested HDACi in this study belong exclusively to class 1 HDAC inhibitors with a focus on the inhibition of HDAC1-3 (Ahmad et al., 2014). The selection of the most suitable HDACi for this study was primarily based on the ability to boost endogenous MLL-mediated promoter activation and on the decrease of the dominant promoter-binding by MLL-AF4. A further selection criteria for suitable HDAC inhibitors for this study relied on synergistic effects on 5-LO promoter activation when HDAC1 and HDAC3, HDAC2 and HDAC3, as well as HDAC1, HDAC2 and HDAC3 were knocked-down together (Ahmad et al., 2014). Hence, a selection of compounds that are sensitive to particular combinations of HDACs could further specify the particular role of individual HDACs on the affinity of MLL to promoters.

The class 1 HDAC inhibitors Entinostat (MS-275), Mocetinostat (MGCD0103) and Droxinostat (NS 41080) fulfilled all these criteria best. Entinostat is highly sensitive to HDAC1 and has a moderate inhibitory effect on HDAC3. It is not sensitive to further HDACs, in particular not to class 1 HDAC2 or HDAC8. Entinostat effectively abrogated MLL-AF4 related 5-LO promoter activation and strongly increased wild-type MLL related promoter activation (Ahmad et al., 2014). The highest activation of wild-type MLL-mediated promoter activation of all tested HDACi in the study from Ahmad et al. was achieved with Mocetinostat (Ahmad et al., 2014). It primarily inhibited HDAC1 and HDAC2, but also weakly HDAC3. The inhibitory effect on MLL-AF4 was comparable to Entinostat. The third class 1 HDAC inhibitor in this work, Droxinostat, was primarily selected due to its specific inhibition of HDAC3. It was significantly less potent than Entinostat or Mocetinostat, but could also confer the highest binding affinity to the 5-LO promoter to wild-type MLL compared to MLL-AF4 when high molar concentrations were applied (Ahmad et al., 2014). The pan HDAC inhibitor Dacinostat (LAQ824) was examined serving as a reference to class HDAC inhibitors that merely inhibit HDAC1 to HDAC3.

Initially, the sensitivity of the four selected HDAC inhibitors was evaluated in SEM cells (Fig. 4.1.2.1 A). Both, SEM-Mock and SEM-dnTASP1 cells, were initially induced with 1 µg/ml Doxycycline. After 24 h, the HDACi were applied at indicated concentrations for another 24 h followed by viability measurements and IC-50 values could be calculated for Entinostat (17 µM), Mocetinostat (2.5 µM) as well as Dacinostat (0.1 µM). Droxinostat was excluded due to no reduction in the viability of both SEM cell lines at the high concentration of 10 µM. Overall, no significant difference in viability nor in cellular growth was recognizable in SEM-dnTasp1 cells in comparison to SEM-Mock cells upon treatment with the HDAC inhibitors (Fig. 4.1.2.1 A).

A subsequent cell cycle analysis highlighted how the inhibition of HDACs severely affected SEM cells (Fig. 4.1.1 B+C). Doxycycline-induced SEM-Mock and SEM-dnTASP1 cells

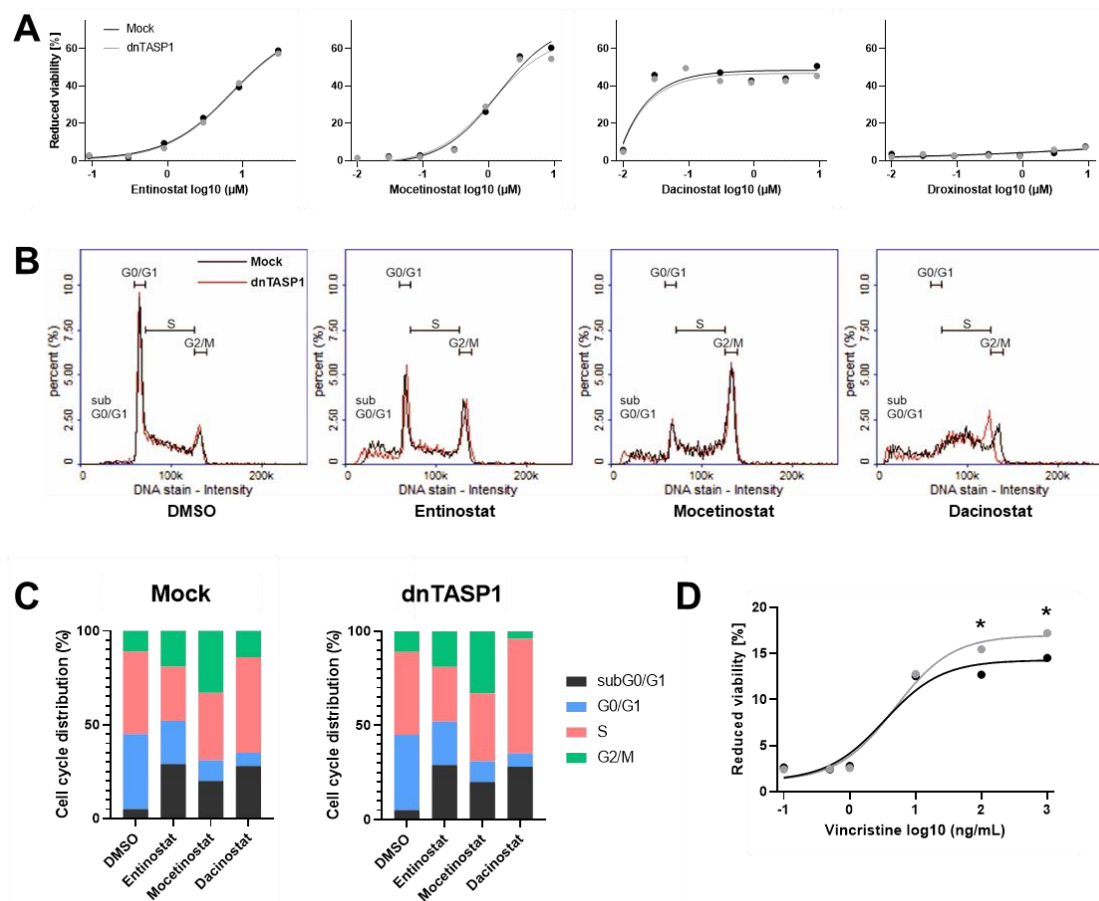


Figure 4.1.2.1: No difference in viability of HDACi-treated SEM cells upon short-term expression of dnTASP1. Viability assay of HDACi-treated SEM-Mock and SEM-dnTASP1 cells (A). Entinostat, Mocetinostat, Dacinostat and Droxinostat were administered for 24 h at indicated concentrations to 24 h Doxycycline-pre-induced SEM-Mock and SEM-dnTASP1 cells. While Entinostat (IC-50: 17 μM), Mocetinostat (IC-50: 2.5 μM) and Dacinostat (IC-50: 0.1 μM) significantly reduced the viability of SEM cells at concentrations up to 1 μM, the application of Droxinostat resulted in almost no reduction in viability at comparable concentrations. Cell cycle analysis of HDACi-treated SEM cells based on DAPI intensity (B) enabled the quantification of cells in sub-G0/G1-, G0/G1-, S- and G2/M-phase (C). Viability assay of SEM-Mock and SEM-dnTASP1 cells treated with different concentrations of Vincristine (D). Representative pictures out of three biological replicates shown. Statistical significance was calculated by two-sided ttest. Asterisks indicate p-values as *(p < 0.05).

were treated with Entinostat, Mocetinostat and Dacinostat at IC-50 concentrations. Overall, no significant changes in cell cycle could be measured upon the expression of dnTASP1. G0/G1 cells represent 40% and S-phase cells 44% of the total SEM-Mock and SEM-dnTASP1 population upon DMSO treatment (Fig. 4.1.1.B+C). The relative number of G0/G1 cells are significantly decreased upon HDACi with 23% for Entinostat, 11% for Mocetinostat and only 7% for Dacinostat.

The sub-G0/G1 cell population is an indicator for DNA fractionation, and thus, for apoptosis as well as for partial relaxation of DNA during necrosis. Sub-G0/G1 cells are defined as

the cell population emerging at lower DNA stain intensities than G0/G1 cells. HDACi resulted in a 2- to 3-fold increase of cells in the sub-G0/G1 phase when compared to the DMSO control (Fig. 4.1.2.1 B+C). SEM-Mock and SEM-dnTASP1 cells in G2/M phase were found to be approx. 3-fold enriched upon the treatment with Mocetinostat (33%) in comparison to the DMSO control (11%). Only minor changes in G2/M populations were observed for Entinostat (SEM-Mock: 19%; SEM-dnTASP1: 19%) and Dacinostat (SEM-Mock: 14%, SEM-dnTASP1: 4%).

The short-term expression of dnTASP1 seemed to have only a minor effect on HDACi-treated SEM cells as no significant differences in viability and cell cycle assays were observed. Therefore, as a control experiment, HDACi treatment was replaced by Vincristine (VCR) for assessing the benefit of the expression of dnTASP1 in SEM cells in a short-term manner. The cytostatic VCR inhibits mitosis and is also widely used in the treatment of ALL and particularly in the treatment protocol of t(4;11) ALL patients (Bohannon et al., 1963; Committees et al., 1968). VCR was applied to Doxycycline-induced SEM-Mock and SEM-dnTASP1 cells. A moderate but significant decrease ($p < 0.05$) in viability of SEM-dnTASP1 cells could be obtained with 100 and 1000 ng/ml VCR in comparison to SEM-Mock cells (Fig. 4.1.2.1 D).

In summary, the expression of dnTASP1 reduced the viability of SEM cells, when administered together with the cytostatic VCR treatment. However, no difference in viability and cell cycle was obtained upon expression of dnTASP1 for 24 h in HDACi-treated SEM cells.

4.1.3. Long-term expression of dnTASP1 increases HDACi-induced apoptotic levels of SEM cells *in vitro*

MLL fusion proteins in general, but particularly AF4-MLL are associated with a very long half-life (Bursen et al., 2004; Marschalek, 2015). Since AF4-MLL is additionally associated with sophisticated epigenetic reprogramming activities, long-term experiments to unravel the therapeutic potential of AF4-MLL seem to be more adequate. High-levels of AF4-MLL are expected to remain upon short-term expression of dnTASP1. This might explain the lacking differences in viability and cell cycle between short-term treated SEM-Mock and SEM-dnTASP1 cells as observed in chapter 3.1.2. Thereafter, in this chapter, dnTASP1 was long-term induced with Doxycycline for 28 days in HDACi-treated SEM cells and the therapeutic potential of the co-treatment evaluated on the basis of altered apoptosis levels.

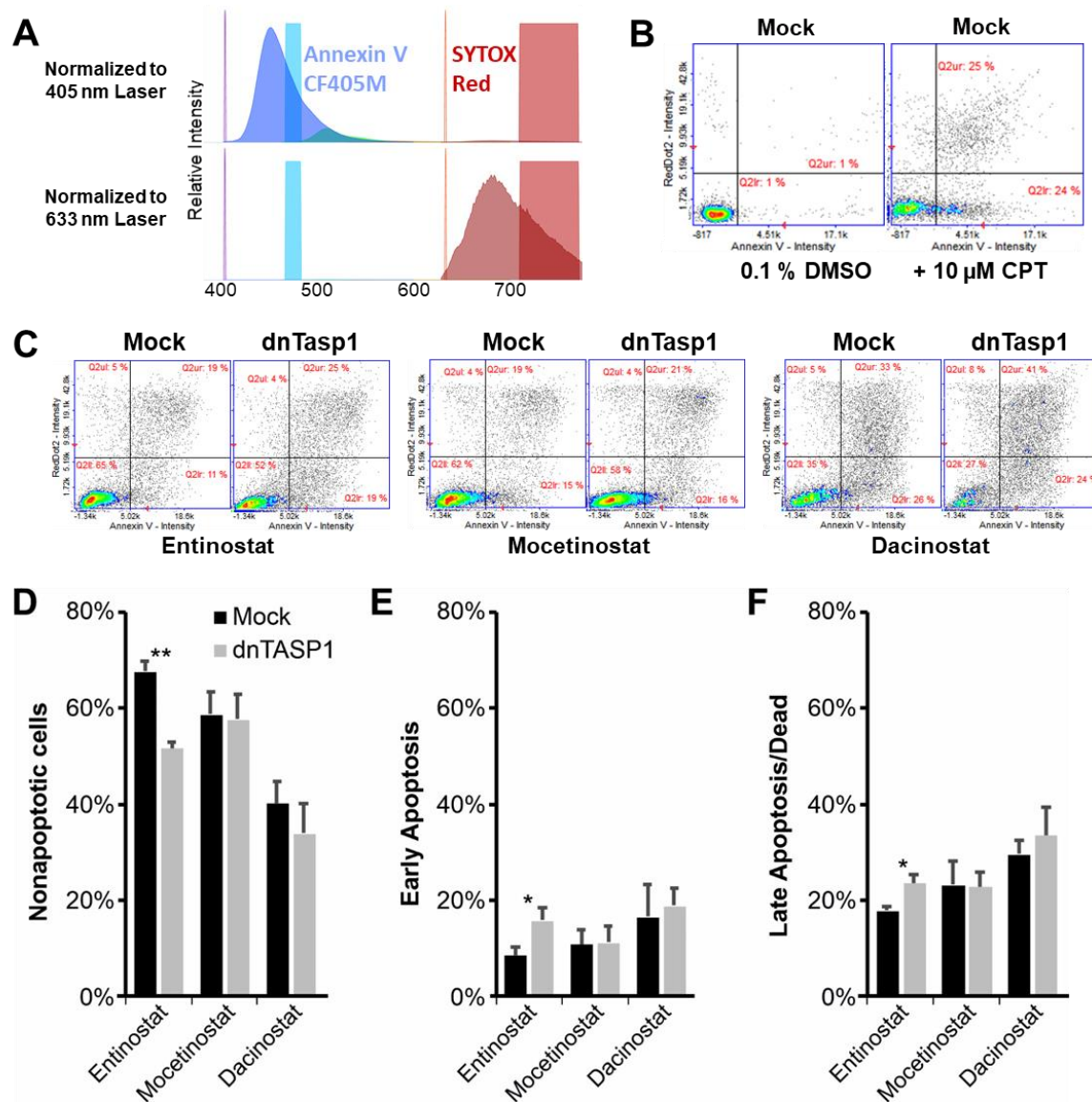


Figure 4.1.3.1: SEM cells respond individually to different HDACi after 28 days expression of dnTASP1. Inter-fluorophore cross-talk was assessed by plotting emissions of Annexin V-CF405M and SYTOX red normalized to the 405 nm and 633 nm lasers and filters of the Nucleocounter NC3000 (Chemometec) (A). The back-bone fluorescence of SEM-Mock (dTomato) and SEM-dnTASP1 (eGFP) were included in the intensity blot and showed no cross-talk to the applied fluorophores. The measuring window of the microscopically based Annexin V Assay was evaluated by comparing apoptosis levels of DMSO- and camptothecin (CPT)-treated SEM cells (B). The representative density scatter plots of SEM cells maintained for 28 days in medium containing 1 μ g/mL Doxycline and treated with 17 μ M Entinostat, 2.5 μ M Mocetinostat and 0.1 μ M Dacinostat (C). Quantification of nonapoptotic cells (D), early apoptotic cells (E) and late apoptotic cells (F). $n = 3$ biological replicates per sample. Values represent the mean \pm standard deviation. Statistical significance was calculated by two-sided ttest. Asterisks indicate p-values as * ($p < 0.05$) and ** ($p < 0.01$).

For a reliable maintenance of permanent expression of dnTASP1, Doxycycline was added to SEM-cells every 48 h, since the expression of dnTASP1 after adding 1 µg/ml Doxycycline can be detected via Western Blot up to 5 days post induction (data not shown).

Annexin V apoptosis assays were evaluated microscopically using the cell analyzer NucleoCounter® NC-3000™. The dTomato and eGFP fluorescence back-bone signal of SEM-Mock and SEM-dnTASP1 cells, respectively, required a careful selection of proper dyes for the Annexin V Assay to circumvent inter-fluorophore cross-talk. Conjugated Annexin V-CF405M in combination with SYTOX Red as dead-cell-stain met the criteria best and no interference is expected in excitation and emission spectra (Fig. 4.1.3.1 A). Noteworthy, the highest-possible collection efficiency of the NC-3000 for Annexin V-CF405M was relatively low with only 16%, which could reduce the detection capacity of apoptotic cells. Nevertheless, after careful consideration of numerous available fluorophores and the given microscopy settings, the CF405M conjugate represented the most suitable candidate.

SEM-Mock cells treated with the apoptosis inducer camptothecin (CPT) served as a positive control for evaluation of the adapted Annexin V Assay (Fig. 4.1.3.1 B). In comparison to SEM-Mock cells that were treated with 0.1% DMSO, CPT treatment resulted in significantly more early apoptotic cells (24%) and late apoptotic/dead cells (25%). Notably, the microscopic readout resulted in a particularly narrow measurement window in density scatter plots for detected CF405M intensities of CPT-treated SEM cells (Fig. 4.1.3.1 B). Upon the expression of dnTASP1 for 28 days, the HDAC inhibitors Entinostat, Mocetinostat and Dacinostat were applied at IC-50 concentrations for another 24 h prior to determination of apoptosis levels (Fig. 4.1.3.1 C). Density scatter plots of SEM cells treated with HDACi show poor separation between non-apoptotic and early-apoptotic cells, consistent with the CPT control. Instead of two clearly separated populations, a circular population with an elongated tail to the right appears. Yet, a synergistic effect of the co-treatment of dnTASP1 and Entinostat could be demonstrated for the first time (Fig. 4.1.3.1 D). Not only the amount of non-apoptotic cells was significantly decreased ($p < 0.05$) in SEM-dnTASP1 cells, but also *vice versa* the early-apoptotic ($p < 0.05$) and late apoptotic/dead population ($p < 0.05$). The apoptosis levels of SEM-dnTASP1 cells treated with Dacinostat pointed in a similar direction, but high standard deviations prevented a clear statement, while Mocetinostat treatment exhibited no visible effect.

Apoptosis data obtained from the Nucleocounter NC3000 (Chemometec) partially show a synergistic effect of HDACi and dnTASP1 co-therapy. Although, insufficient separation of populations in the density scatter plots of SEM cells and high standard deviations argue for an alternative strategy than a microscopy-based evaluation.

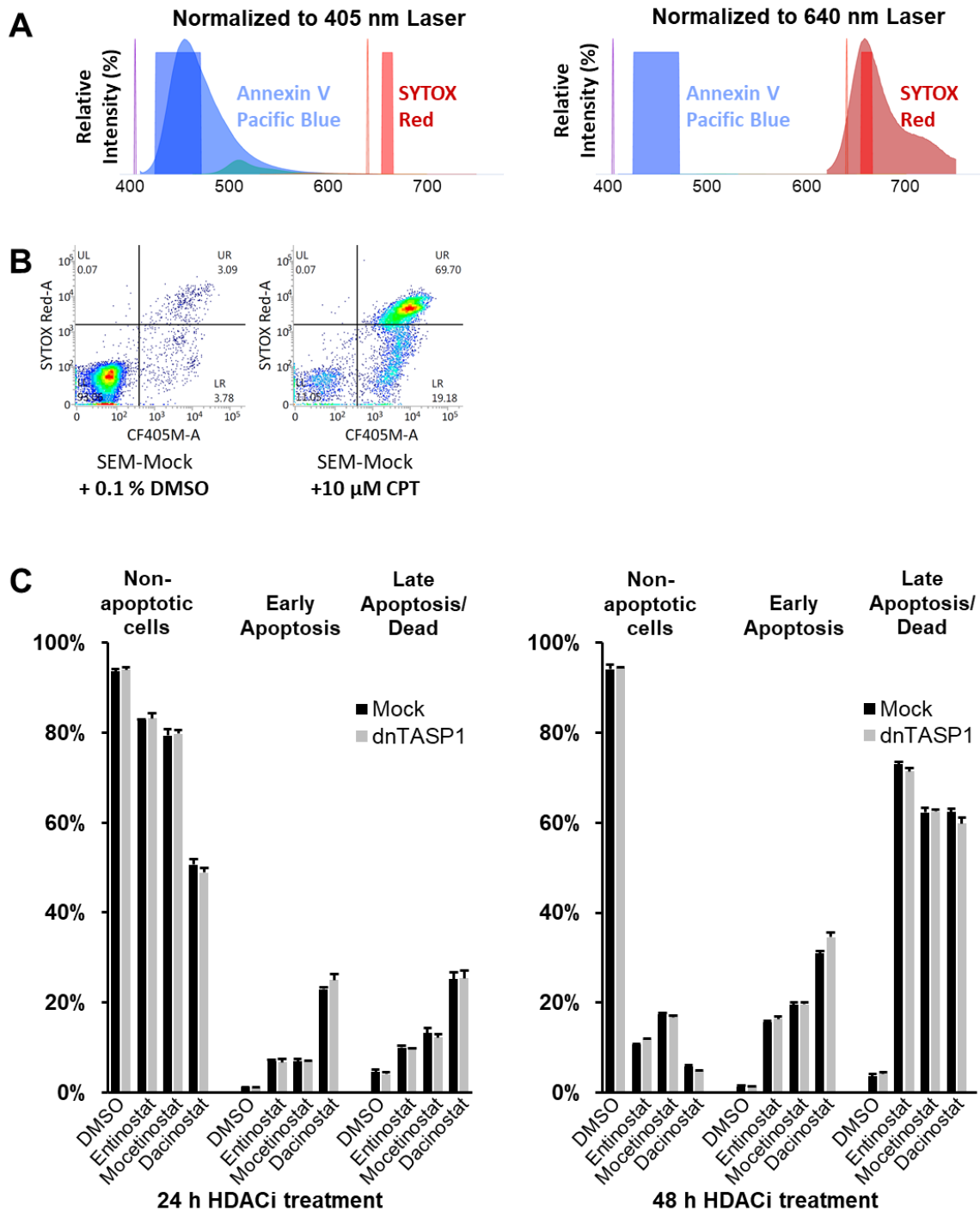


Figure 4.1.3.2: Flow Cytometry based Annexin V Assay design for SEM cells. Emission spectra of Annexin V-Pacific Blue and SYTOX red are plotted normalized to the 405 nm and 640 nm lasers and filters of flow cytometer (A). The emission spectra plot further contains the back-bone fluorescence of SEM-Mock (dTomato) and SEM-dnTASP1 (eGFP). Representative density scatter plots of DMSO- and camptothecin (CPT)-treated SEM-Mock cells (B); and Entinostat-treated SEM cells (C). Quantification of SEM-Mock and SEM-dnTASP1 cells maintained in Doxycycline-free medium and treated with Entinostat, Mocetinostat and Dacinostat accordingly to Fig. 4.1.3.1 for either 24 h or 48 h (D). Samples were analyzed in cooperation with Wai Lam Kwan. $n = 3$ biological replicates per sample. Values represent the mean \pm standard deviation.

Hence, the microscopy-based readout of the Annexin-V Assay was subsequently replaced by Flow Cytometry. The Flow Cytometer BD FACS Verse enabled a better adaptation of fluorophores and the optics of the instrument (Fig. 4.1.3.2 A). The analogues of Annexin-V conjugate CF405M and RedDot 2, Pacific Blue and Sytox Red, were applied. The Flow Cytometer achieved high collection efficiencies of 51% for Pacific Blue and 27% for Sytox Red.

Compared to 4% early apoptotic cells and 3% late apoptotic/necrotic cells in the DMSO control, 19% and 70%, were obtained for CPT-treated SEM cells, respectively (Fig. 4.1.3.2 B). Moreover, the density scatter plots of the Flow Cytometry data allowed a significantly more precise distinction between non-apoptotic and apoptotic SEM cells compared to the NC3000.

SEM-Mock and SEM-dnTASP1 cells were treated exclusively with the three HDAC inhibitors without the addition of Doxycycline to exclude secondary effects of HDACi (Fig. 4.1.3.2 C). Quantification of apoptotic levels revealed comparable sensitivity of non-induced SEM-Mock and SEM-dnTASP1 cells to Entinostat, Mocetinostat or Dacinostat treatment (Fig. 4.1.3.2 C).

Next, SEM cells were long-term induced with doxycycline for 21 days and the three HDACis were applied at IC-50 concentrations on days 0, 5, 12, and 19 (Fig. 4.1.3.3 A). The sample from day 0 was treated with HDACis only. Apoptosis assays were conducted either 24 h after treatment with HDACis (samples collected on days 1, 6, 13, and 20) or 48 h post-treatment with HDACis (samples collected on days 2, 7, 14, and 21).

The density plots of long-term Doxycycline-induced SEM cells 24 h (day 20) and 48 h (day 21) after HDACi treatment illustrate clearly separated populations of non-apoptotic cells, early apoptotic cells and late apoptotic cells allowing the adequate determination of apoptosis levels of dual-treated SEM cells (Fig. 4.1.3.3 B+C). Upon treatment with Entinostat, Mocetinostat or Dacinostat for 24h more than half of the cells still remained in the non-apoptotic phase (Fig. 4.1.3.3 B). However, 48 h after administering the three HDACi, the majority of cells were already in the apoptotic phase, independent of the applied HDACi hampering the evaluation of a possible synergistic effect of the co-treatment (Fig. 4.1.3.3 C). Importantly, the flow-cytometry based read-out of the Annexin V Assay revealed significant differences in apoptosis levels for all applied HDACi between SEM-Mock and SEM-dnTASP1 cells in comparison to the previously conducted microscopic readout (see chapter 2.1.2).

The quantification of apoptotic SEM cells upon inducing dnTASP1 for three weeks revealed a highly significant increase of apoptotic levels when treated for 24 h with Entinostat ($p < 0.01$), Mocetinostat ($p < 0.001$) and Dacinostat ($p < 0.001$) or for 48 h with Entinostat ($p < 0.01$), Mocetinostat ($p < 0.001$) and Dacinostat ($p < 0.05$) (Fig. 4.1.3.4 A). HDACi-treated

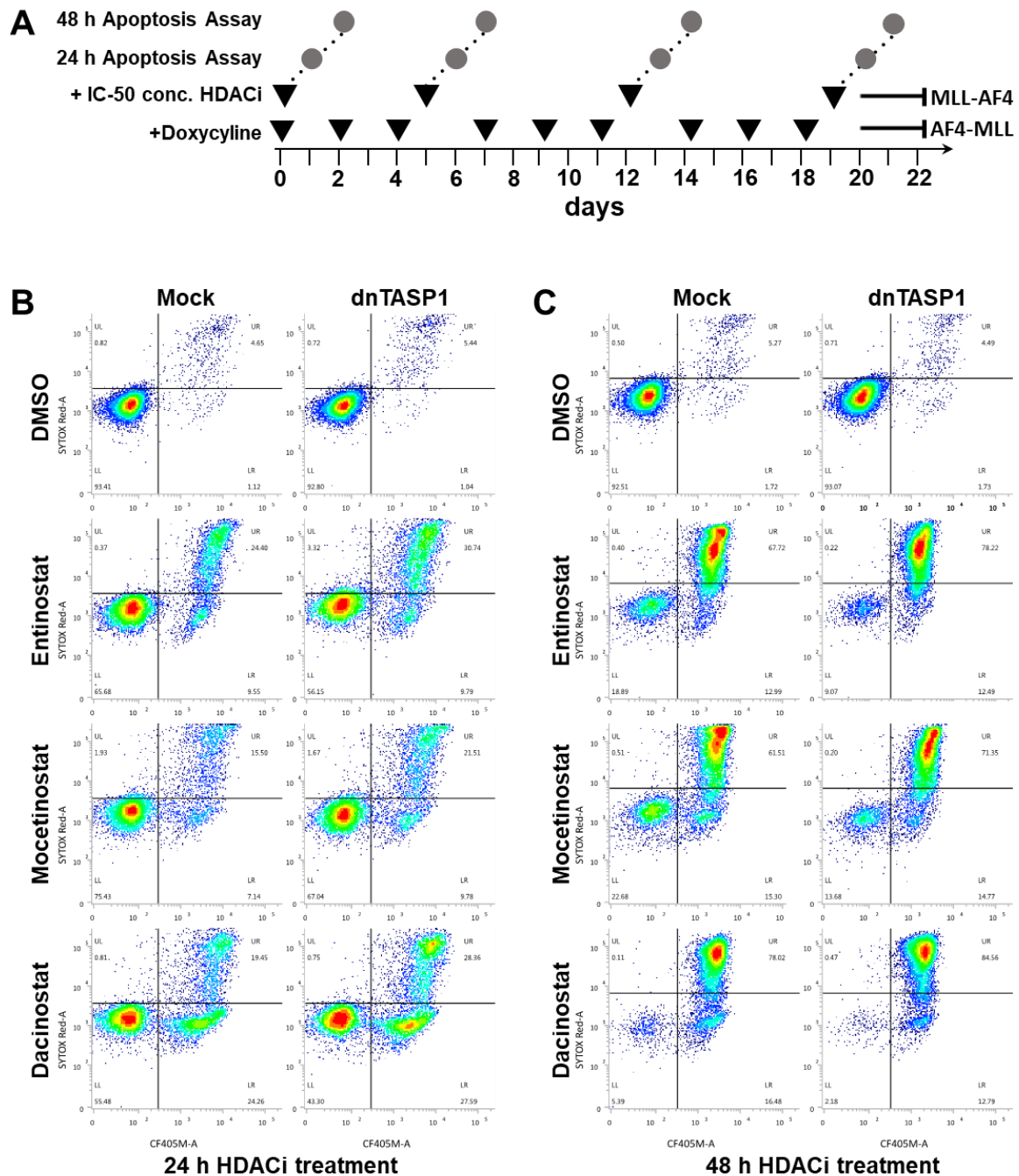


Figure 4.1.3.3: Determination of dnTASP1 expression and HDACi-treatment intervals to induce apoptosis in SEM cells. Graphical illustration of the experimental setup of apoptosis assays conducted at several time points (A). SEM-Mock and SEM-dnTASP1 cells were maintained in medium containing 1 $\mu\text{g}/\text{mL}$ Doxycycline and apoptosis assays performed 24 h and 48 h after the administration of HDACis at day 1 and 2, 6 and 7, 13 and 14; and 20 and 21, respectively. Density scatter plots of SEM cells at day 20 and day 21 treated for 24 h and 48 h with HDACis, respectively. Samples were analyzed in cooperation with Wai Lam Kwan.

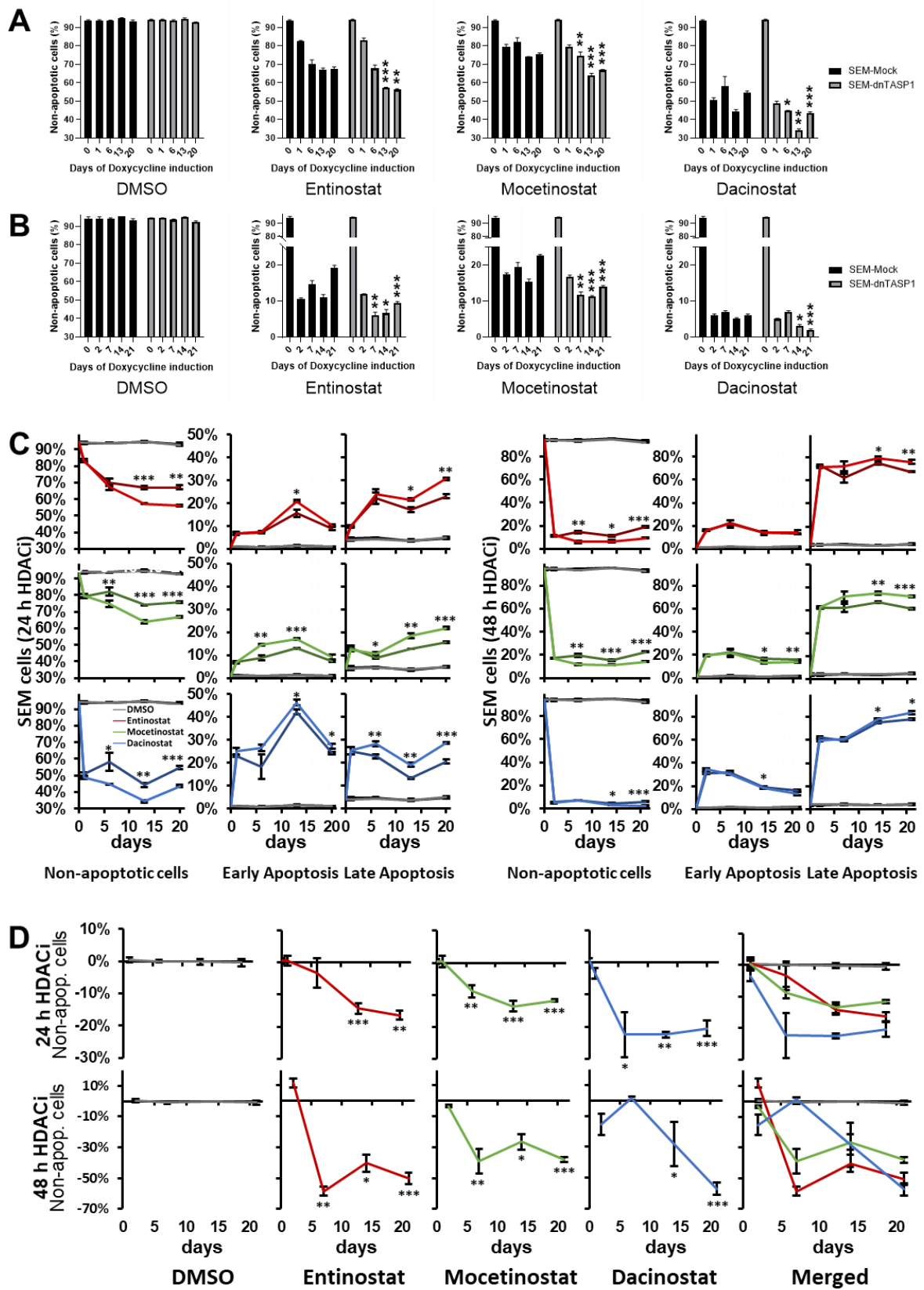
SEM cells undergo apoptosis to significantly elevated levels upon the expression of dnTASP1 for at least 6 days for Mocetinostat ($p < 0.01$) and Dacinostat ($p < 0.05$), and 13 days ($p < 0.001$) for Entinostat. The long-term inhibition of AF4-MLL alone seems to have

minor effects on apoptosis since no increase in apoptotic levels was observed for dnTASP1-expressing SEM cells over time when treated with DMSO (Fig. 4.1.3.4 A).

Only few SEM cells remained in a non-apoptotic state upon 48 h treatment with Entinostat, Mocetinostat or Dacinostat (Fig. 4.1.3.4 B). A significant decrease of non-apoptotic SEM cells was observed from day 7 onwards for Entinostat ($p < 0.01$) and Mocetinostat ($p < 0.01$); and from day 14 onwards for Dacinostat ($p < 0.05$) of dnTASP1 induction. Three weeks of dnTASP1 expression resulted in highly significant increased levels of apoptosis in SEM cells treated with Entinostat ($p < 0.001$), Mocetinostat ($p < 0.001$) and Dacinostat ($p < 0.001$). Apoptosis Assays performed 48 h post-treatment with HDACi support the observation of elevated apoptotic SEM-dnTASP1 cells in comparison to SEM-Mock cells obtained 24 h after administration of HDACi (Fig. 4.1.3.4 A+B). Yet, overall low levels of non-apoptotic SEM cells of less than 20% limit the measuring range considerably in the 48 h treatment setup for all three HDAC inhibitors.

The reduction of non-apoptotic SEM-dnTASP1 cells upon treatment with Entinostat for 24 h on day 13 was mainly caused by an increase of early-apoptotic SEM-dnTASP1 cells on that day (Fig. 4.1.3.4 C). The week after, on day 20, early-apoptotic SEM-dnTASP1 were not over-represented in comparison to SEM-Mock cells and the main driver was the elevated amount of late-apoptotic and necrotic SEM-dnTASP1 cells. Similarly, there are significantly more early-apoptotic SEM-dnTASP1 cells upon Mocetinostat treatment for 24 h on day 6 and day 13, but not on day 20 (Fig. 4.1.3.4 C). Moreover, with increasing duration of the expression of dnTASP1 rises the impact of elevated late-apoptotic and necrotic Mocetinostat-treated SEM-dnTASP1 cells. Contrarily, a non-gradual development from day 6 to day 21 was observed for treatment for 24 h with the pan-HDACi Dacinostat (Fig. 4.1.3.4 C). Levels of early-apoptotic, late apoptotic and necrotic SEM-dnTASP1 were constantly elevated 6 days upon the induction of dnTASP1. The decrease in non-apoptotic SEM-dnTASP1 by Dacinostat was mainly caused due to an increased amount of late apoptotic and necrotic cells. The treatment with HDACi for 48 h converts the majority of SEM cells into the late apoptotic and necrotic phase (Fig. 4.1.3.4 C). The expression of dnTASP1 moderately elevates levels of late apoptotic and necrotic SEM cells for Entinostat (day 15: $p < 0.05$, day 21: $p < 0.01$) Mocetinostat (day 15: $p < 0.01$, day 21: $p < 0.001$) and Dacinostat (day 15: $p < 0.05$, day 21: $p < 0.05$). Contrarily, a very limited effect upon dnTASP1 expression was obtained for early-apoptotic cells for all three HDACi (Fig. 4.1.3.4 C).

Accordingly, the relative decrease of non-apoptotic SEM-dnTASP1 cells is comparable on day 6 (-22.44%, $p < 0.05$), day 13 (-22.49%, $p < 0.01$) and day 20 (-20.47%, $p < 0.001$) for 24 h treatment with Dacinostat (Fig. 4.1.3.4 D). Thereafter, the pan-HDACi Dacinostat demonstrated its greatest effect in co-treated SEM cells already 6 days upon expression



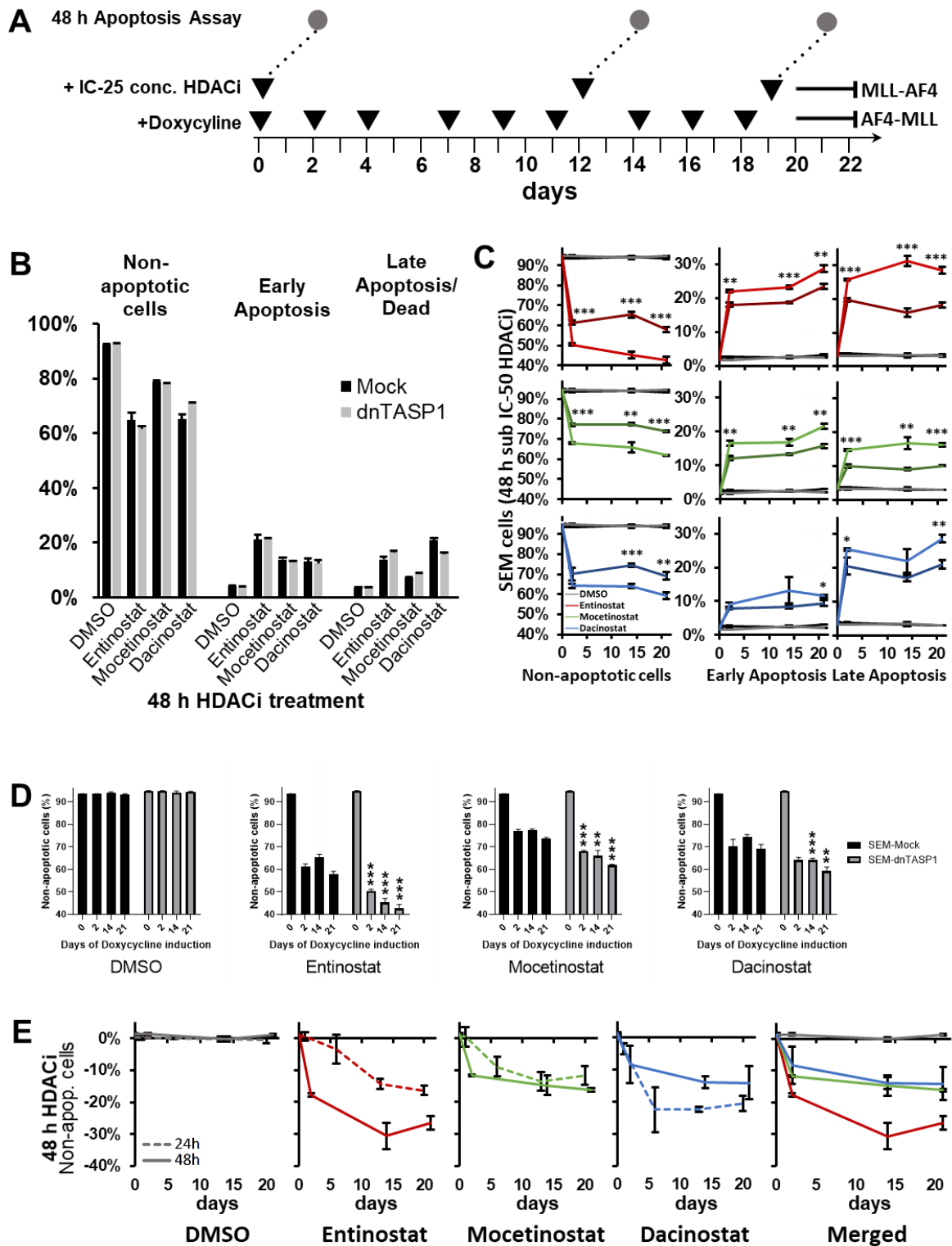
of dnTASP1. Conversely, the effect of dnTASP1 expression gradually increased for Entinostat treatment for 24 h from day 3 (3.37%, $p > 0.05$) to day 13 (14.25%, $p < 0.001$) and

Figure 4.1.3.4: HDACi-treated SEM cells respond in a delayed manner to dnTASP1 expression. Annexin V Assays conducted in Doxycycline-induced SEM-Mock and SEM-dnTASP1 cells 24 h (A) or 28 h (B) after HDACi treatment. Days of dnTASP1-expression are displayed on the x-axis. See Fig. 4.1.3.3 for a more detailed experimental scheme. Illustration of absolute levels of non-apoptotic, early- and late-apoptotic SEM cells that were induced with Doxycycline either 24 h or 48 h after the treatment with HDACi (C). Relative effect of dnTASP1 expression on apoptosis in HDACi-treated SEM cells (D). $n = 3$ biological replicates per sample. Samples were analyzed in cooperation with Wai Lam Kwan. Values represent the mean \pm standard deviation. Statistical significance was calculated by two-sided ttest. Asterisks indicate p-values as *($p < 0.05$), **($p < 0.01$) and ***($p < 0.001$).

day 20 (16.38%, $p < 0.01$) (Fig. 4.1.3.4 D). For the 24 h treatment with Mocetinostat, the relative decrease of non-apoptotic SEM-dnTASP1 cells was on day 13 (-13.56%, $p < 0.001$) and day 20 (-11.71%, $p < 0.001$), approx. 1.4-fold higher compared to day 6 (-8.88%, $p < 0.01$) (Fig. 4.1.3.4 D). The relative decreases of non-apoptotic SEM cells treated for two days with HDACi peak for Entinostat at -58.59% (day 7, $p < 0.01$) for Mocetinostat at -39.17% (day 7, $p < 0.01$) and Dacinostat at -57.12% (day 21, $p < 0.001$). Gradual and non-gradual tendencies obtained with the 24 h treatment could not be reproduced after 48 h HDACi treatment. As indicated by the large standard deviations, considerable low amounts of remaining non-apoptotic SEM-Mock and SEM-dnTASP1 cells seemed to hamper the readout of the Annexin V Assay.

Therefore, the 48 h HDACi treatment was re-conducted at IC-25 optimized concentrations for a prolonged treatment (Fig. 4.1.3.5 A). Apoptosis assays were performed at day 2, day 14 and day 21 of serial induction with Doxycycline after 48 h HDACi treatment. HDACi concentrations that render 25% of cells in an apoptotic state (IC-25) proved to enable the most adequate measuring range for the Annexin V Assay using SEM cells (data not shown). Thus, the 48 h HDACi treatment was re-conducted with 3 μM Entinostat, 0.6 μM Mocetinostat and 0.03 μM Dacinostat. Equal responsiveness of SEM-Mock and SEM-dnTASP1 cells to HDACi could be confirmed treating SEM cells with HDACi and DMSO for 48 h (Fig. 4.1.3.5 B). Differences in non-apoptotic, early- and late apoptotic cells were not significant for all HDACi.

The optimized HDACi treatment for 48 h revealed a considerable decrease of non-apoptotic SEM cells that express dnTASP1 already on experimental day 2 (Fig. 4.1.3.5 C+D). Highly significant changes were obtained for class 1 HDACi Entinostat (day 2 to day 21: $p < 0.001$) and Mocetinostat (day 2 to day 21: $p < 0.001$) (Fig. 4.1.3.5 D). A significant reduction of non-apoptotic SEM-cells could be detected for Dacinostat on day 14 ($p < 0.001$) and day 21 ($p < 0.01$). Noteworthy, this reduction albeit not significant was also observed as early as day 2 with Dacinostat.



Taking a deeper look to the distribution of apoptotic phases demonstrates differences between class 1 and pan-HDACi in the 48 h treatment setting. The prolongation to 48 h led to an immediate significant increase of late apoptotic and necrotic cells treated with Entinostat at day 2 (day 2 to day 21: $p < 0.001$) (Fig. 4.1.3.5 C+D). The relative increase of

Figure 4.1.3.5: The prolonged HDACi treatment of SEM cells elicits an immediate response to dnTASP1 expression. Graphical Illustration of the experimental setup of apoptosis assays conducted upon the administration of HDACi at IC-25 concentrations and distinct intervals of Doxycycline induction (A). Annexin V Assay performed in SEM-Mock and SEM-dnTASP1 treated with HDACi and DMSO for 48 h (B). Distribution of non-apoptotic, early- and late-apoptotic SEM cells upon 48 h treatment with HDACis at IC-25 concentrations (C+D). Relative effect of dnTASP1 expression on apoptosis in SEM cells treated with HDACis for 48 h (E). n = 3 biological replicates per sample. Samples were analyzed in cooperation with Wai Lam Kwan. Values represent the mean \pm standard deviation. Statistical significance was calculated by two-sided t-test. Asterisks indicate p-values as *(p < 0.05), **(p<0.01) and ***(p<0.001).

late-apoptotic SEM-dnTASP1 was already elevated to 30.7% on day 2 (SEM-Mock: 19.71%, SEM-dnTASP1: 25.76%) and peaked with 96% on day 14 (SEM-Mock: 15.91%, SEM-dnTASP1: 31.15%), followed by 56% on day 21 (SEM-Mock: 18.11%, SEM-dnTASP1: 28.33%) (Fig. 4.1.3.5 C). Comparable pronounced increases of late-apoptotic and necrotic SEM cells upon dnTASP1 expression were obtained with Mocetinostat starting with 47% on day 2 (SEM-Mock: 10.05%, SEM-dnTASP1: 14.78%), followed by 84% on day 14 (SEM-Mock: 9.12%, SEM-dnTASP1: 16.77%), and 60% on day 21 (SEM-Mock: 10.18%, SEM-dnTASP1: 16.33%) (Fig. 4.1.3.5 C). Moreover, early apoptotic SEM-dnTASP1 were significantly increased throughout all measuring points when treated with Entinostat (day 2: p<0.01, day 14: p<0.001, day 21: p<0.01) and Mocetinostat (day 2 to day 21: p<0.01). Contrarily, Dacinostat showed only minor effects for early apoptotic cells with a low but significant increase on day 21 (p<0.05) (Fig. 4.1.3.5 C). Moderate relative increases of necrotic or late apoptotic SEM cells expressing dnTASP1 were obtained with Dacinostat on day 2 with 25.09% (SEM-Mock: 20.33%, SEM-dnTASP1: 25.43%), day 14 with 30.24% (SEM-Mock: 16.83%, SEM-dnTASP1: 21.92%), and day 21 with 36.56% (SEM-Mock: 20.90%, SEM-dnTASP1: 28.54%).

The relative reduction of non-apoptotic SEM cells of 17.79% at day 2, 30.58% at day 14 and 26.50% at day 21 (all p>0.001) was observed upon the expression of dnTASP1 (Fig. 4.1.3.4 E). For Mocetinostat, a relative change of -11.78% on day 2 (p<0.001), -14.77% on day 14 (p<0.01) and -16.20% on day 21 (p<0.001) was observed. The treatment with pan-HDACi Dacinostat revealed a relative reduction of -8.31% on day 2 (p>0.05), -13.96% on day 14 (p<0.001) and -14.11% on day 21 (p<0.01). In contrast to the HDACi treatment at IC-50 for 24 h, an immediate response to dnTASP1 expression was observed in SEM cells treated with HDACi for 48 h at IC-25 concentrations (Fig. 4.1.3.4 E). Furthermore, apoptosis levels gradually increased with a prolonged expression of dnTASP1 for all three HDACi. While the relative effect of dnTASP1 expression upon the administration of Dacinostat for 48 h was slightly lower compared to the 24 h setting at IC-50 concentrations,

the sensitivity of SEM cells upon dnTASP1 expression to the administration of Mocetinostat and, in particular, Entinostat for 48 h was profoundly elevated (Fig. 4.1.3.4 E).

All in all, the microscopy based apoptosis assay of the NC3000 showed limited usability for SEM cells, while a Flow Cytometry based readout proved to be highly applicable to detect a dnTASP1 induced increase in HDACi-treated SEM cells undergoing apoptosis. Induced apoptosis levels in HDACi-treated SEM cells were proportional to the expression interval of dnTASP1. Administering HDACis for 48 h elicits an immediate response to dnTASP1 expression and enhanced the sensitivity of SEM-dnTASP1 cells to class I HDACi Mocetinostat and particularly Entinostat.

4.2. Targeting MLL fusion proteins in patient-derived xenograft leukemia cells *in vivo* generates distinct transcriptional signatures

In collaboration with the Jeremias Laboratory from the Helmholtz Center München, the effect of down-regulation of MLL-AF4 and AF4-MLL *in vivo* during progression of leukemia was investigated.

An *in vivo* t(4;11) model system was generated on the basis of the inducible knock-down Cre-ER^{T2} Flip system that was established by the members of the Jeremias Laboratory: Michaela Carlet, Jenny Vergalli and Birgitta Heckl. Here, MLL fusion proteins were targeted by the expression of either dnTASP1 or shRNA targeting MLL-AF4 in PDX cells in NSG mice (Carlet et al., 2020; Völse, 2020) (Fig. 4.2.1.1 A). The inducibility of the (t4;11) PDX model allows the inhibition of MLL-AF4 in mice when tumor burden increases emitting secondary effects during cellular homing and engraftment; and moreover, imitating a growing leukemia condition in patients. Further on, distinct fluorescent markers enable a competitive readout for the inducible gene of interest (GOI) (Carlet et al., 2020).

I brought to this collaboration the expertise of our laboratory in the study of *MLL-r* leukemia, in the molecular biology part by helping with the design of the constructs for the expression of dnTASP1 and in the bioinformatics part by designing and analyzing the RNA-seq experiments. The Jeremias Laboratory contributed its broad knowledge with *in vivo* PDX models in the context of pediatric cancer research and established the competitive inducible knock-down system in the PDX leukemia models. All related experiments in mice of this collaboration were conducted by Kerstin Völse (Völse, 2020). The next two chapters deal with my *in vivo* transcriptomics analyses upon inhibition of either MLL-AF4 (chapter 2.2.1) or AF4-MLL (chapter 2.2.2).

4.2.1. Induction of an MLL-AF4 knock-down in proliferating PDX leukemia cells elicits altered transcriptional signatures

The expression of the fusion protein MLL-AF4 is found in all patients with t(4;11) leukemia, but its effect on gene expression *in vivo* is unknown. Therefore, transcriptomic changes were studied in this work by MACE-seq analysis using PDX leukemia cells after knocking-down MLL-AF4.

The establishment of the inducible overexpression/knock-down Cre-ER^{T2} Flip system in PDX leukemia cells was conducted by Kerstin Völse from the Jeremias Laboratory and required two consecutive transduction steps (Carlet et al., 2020; Völse, 2020). First, serially passaged PDX cells were transduced to express mCherry and the Tamoxifen (TAM) inducible Cre-ER^{T2} enzyme (Fig. 4.2.1.1 A). Subsequently, mCherry-sorted PDX cells were amplified in NSG mice and re-isolated for transduction with two different knock-down vectors carrying the Cre-ER^{T2} Flip system: a control vector bearing constitutively expressed iRFP in sense orientation, constitutively T-Sapphire and control shRNA in anti-sense orientation; and the MLL-AF4 knock-down vector carrying constitutively expressed mTagBFP in sense orientation, constitutively eGFP and shRNA targeting MLL-AF4 in anti-sense orientation (Fig. 4.2.1.1 A). Upon iRFP and mTagBFP sorting, respectively, and amplification in separate mice, both PDX cells were transplanted in a 1:1 ratio into a single NSG mouse for a competition readout (Fig. 4.2.1.1 A). After cell engraftment and homing as soon as ALL PDX cells were proliferating, TAM was administered to initiate recombination mediated by Cre-ER^{T2}. TAM-Induced expression of control shRNA and shRNA targeting MLL-AF4 can be monitored by the co-expressed T-Sapphire and eGFP, respectively. By quantifying the ratios of both fluorophores, the effect of the expression of MLL-AF4 for tumor progression can be revealed.

Transcriptomic analyses upon MLL-AF4 knock-down in PDX cells were conducted from donors either expressing both MLL fusion proteins or exclusively expressing MLL-AF4. Specimens from t(4;11) patient ALL-707 expressed MLL-AF4 and AF4-MLL, whereas the specimen of patient ALL-763 lacked the expression of AF4-MLL, as detected by RT-PCR using primers specifically detecting MLL-AF4 and AF4-MLL, respectively (Völse, 2020). PDX cells from donor ALL-707 and ALL-763 were selected for down-stream analysis of gene expression profiles.

Upon receiving the cellular samples prepared from Kerstin Voelse, a modified 3'-end RNA sequencing method Massive Analysis of cDNA Ends Sequencing (MACE-seq) was conducted, and subsequently the transcriptional signatures upon MLL-AF4 knock-down analyzed. Considering the false discovery rate (FDR) and the log-2 fold-change of shRNA

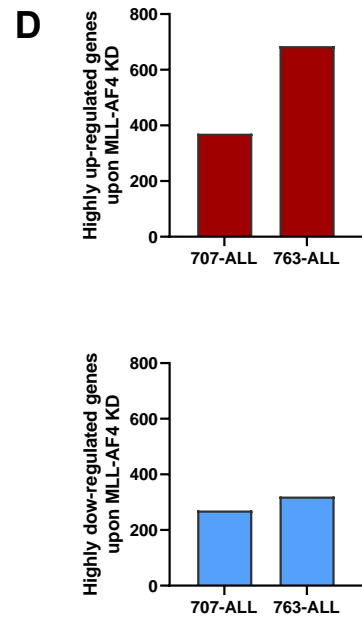
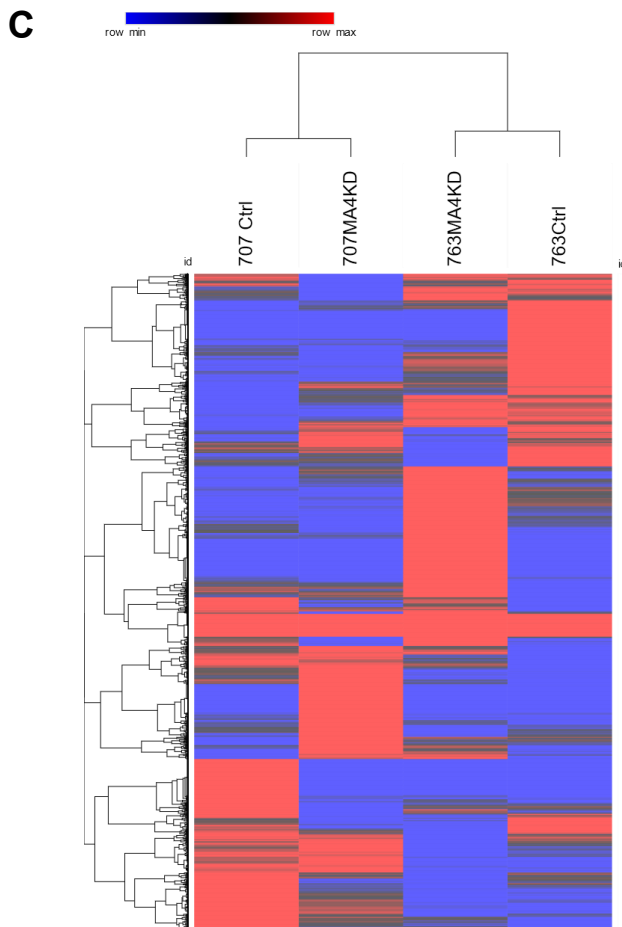
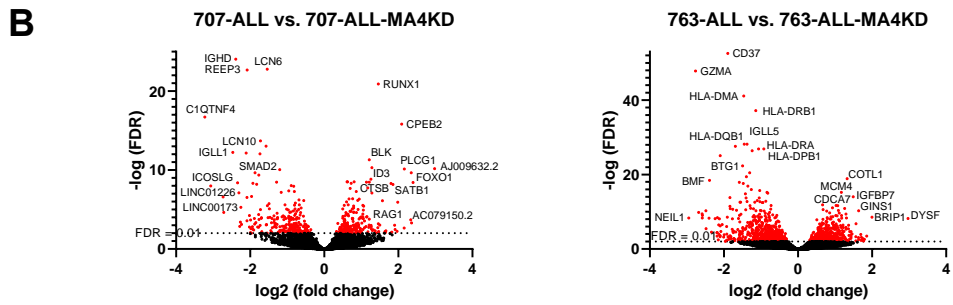
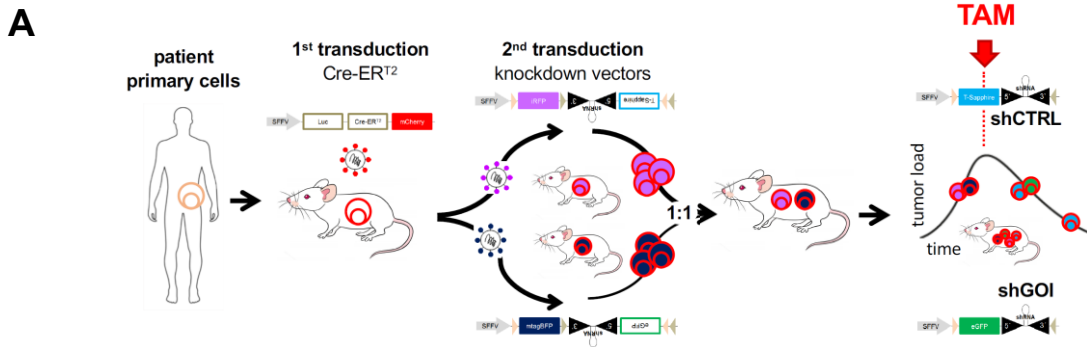


Figure 4.2.1.1: Induced MLL-AF4 knock-down alters transcription of PDX leukemia cells *in vivo*. Graphical illustration of the experimental setup of the t(4;11) PDX model on the basis of the inducible knock-down Cre-ER^{T2} Flip system (adapted from Carlet et al. 2020 and Völse, 2020) (A). All preceding experiments in mice were conducted by Kerstin Voelse (Jeremias Laboratory, Helmholtz Center München). Volcano plots highlight significantly de-regulated genes using ALL-763 and ALL-707 cells (B). Clustering of de-regulated genes upon MLL-AF4 knock-down illustrated by a heat-map analysis (C). Quantification of highly de-regulated genes of 707-ALL and 763-ALL cells (\log_2 values ± 1 , $p < 0.05$) (D).

control versus MLL-AF4 knock-down sample, highly significant up- or down-regulated targets could be revealed in a Volcano Plot (Fig. 4.2.1.1 B). An almost balanced situation of significantly up- and down-regulated genes upon MLL-AF4 knock-down was observed for ALL-707 cells. The *Runt-related transcription factor 1 (RUNX1)* was the strongest down-regulated gene in ALL-707 cells upon *MLL-AF4* knock-down. *RUNX1* regulates the differentiation of hematopoietic stem cells and constitutes a major target in t(4;11) leukemia. It is activated by MLL-AF4, but also interacts with AF4-MLL and thereby initiates expression of several gene targets (Wilkinson et al., 2013). Noteworthy, knocking-down MLL-AF4 in ALL-763 cells that lack AF4-MLL had only a negligible effect on *RUNX1* transcription. Moreover, the *cytoplasmic polyadenylation element binding protein 2 (CPEB2)* involved in cell cycle regulation was down-regulated upon MLL-AF4 knock-down. The most down-regulated target in ALL-707 cells is the lncRNA AJ009632.2 with a not yet further described function.

Targets involved in stem cell differentiation: the *B-lymphoid tyrosine kinase (BLK)*, *special AT-rich sequence-binding protein-1 (SATB1)* and *inhibitors of DNA binding 3 (ID3)*; the *recombination activating gene 1 (RAG1)* that is involved in pre-B cell allelic exclusion and orchestrates immunoglobulin V-D-J recombination; the *transcription factor Forkhead box protein O1 (FOXO1)* and the *lysosomal cysteine protease gene for cathepsin B (CTSB)*, that plays an important role in proteolysis, are all significantly down-regulated in ALL-707 cells upon *MLL-AF4* knock-down.

Importantly, CPEB2, BLK, SATB1, CTSB and ID3 are all associated to B-ALL. *BLK* is a proto-oncogene involved in cell proliferation and differentiation that plays a role in B-cell receptor (BCR) signaling and B-cell development (Kim et al., 2017). Moreover, *BLK* is down-regulated upon the deletion of *Ikaros family zinc finger protein 1 (IKZF1)* (Iacobucci et al., 2012). *SATB1* is a global chromatin regulator that directs hematopoietic stem cell differentiation and is induced in the lymphoid lineage (Satoh et al., 2013).

The negative outcome marker CPEB2 that constitutes a top-upregulated gene in t(4;11) leukemia patients and is associated with elevated H3K79me3 marks (Geng et al., 2012;

Kerry et al., 2017). Here, upon MLL-AF4 knock-down in the ALL-707 PDX model it was significantly down-regulated.

Additionally, the *Recombination activating gene 1 (RAG1)* is also down-regulated in ALL-707 cells upon MLL-AF4 knock-down. Its expression is associated with high proliferation in B-ALL and it acts as a repressor of *BLK*-inducing *IKZF1* (Han et al., 2019).

Both, *phospholipase C, gamma 1 (PLCG1)* and *AC079150.2*, a pseudogene that is associated to *PLCG1*, are two further down-regulated targets on that list. Mediating the synthesis of inositol 1,4,5-trisphosphate (IP3) and diacylglycerol (DAG), *PLCG1* is involved in intracellular signaling cascades and cell migration.

For ALL-763 cells lacking the expression of AF4-MLL, a knock-down of MLL-AF4 resulted in significantly more up-regulated genes protruding in the Volcano Plot compared to down-regulated genes (Fig. 4.2.1.1 B). The greatest down-regulated target is *dysferlin (DYSF)* that plays a role in skeletal muscle repair and has not yet been associated with B-ALL. *BRCA1 interacting helicase 1 (BRIP1)* that participates in DNA repair, the *go-ichi-ni-san (GINS) complex subunit 1 (GINS1)* that is involved in the initiation and elongation of cellular DNA replication, *Insulin like growth factor (IGF) binding protein 7 (IGFBP7)* regulating IGFs, the *F-actin binding protein coactosin-like protein (COTL1)* that is involved in cytoskeleton regulation, *minichromosome maintenance complex competent 4 (MCM4)* that initiates genome replication and constitutes a key component of the pre-replication complex and the *CMYC* responsive gene *cell division cycle associated 7 (CDCA7)* that participates in *MYC proto-oncogene (MYC)*-mediated cell transformation and apoptosis are further significantly down-regulated targets for ALL-763 upon MLL-AF4 knock-down (Fig. 4.2.1.1 B). Of note, *GINS1*, *IGFBP7* and *CDCA7* have all been associated to B-ALL previously. *GINS1* has been shown to promote drug resistance and cell cycle transit in leukemia cells *in vitro* (Hsieh et al., 2020). *IGFBP7* is related to the L-Asparaginase resistance as it promotes the interaction of ALL cells with bone-marrow stroma cells (Holleman et al., 2004; Laranjeira et al., 2012). The Myc-induced *CDCA7* is overexpressed in B-ALL with a so far unknown function in B-ALL (Jiménez-P et al., 2018).

The top significant up-regulated genes upon the knock-down of *MLL-AF4* in ALL-707 cells co-expressing AF4-MLL are coding for the *immunoglobulin heavy constant delta (IGHD)*, that constitutes an antigen receptor present on most peripheral B-cells, the *receptor expression-enhancing protein 3 (REEP3)* that binds microtubules and orchestrates proper cell division, for extracellular *lipocalins*, *lipocalin 6 (LCN6)* and *lipocalin 10 (LCN10)*, that bind to small hydrophobic molecules and the secreted protein *complement C1q tumor necrosis factor-related protein 4 (C1QTNF4)* (Fig. 4.2.1.1 B). Further on, the genes of *immunoglobulin lamda like polypeptide 1 (IGLL1)* that is part of the pre-B-cell receptor, the *SMAD family member 2 (SMAD2)* that acts as a transcriptional modulator and signal

transducer, the *inducible T cell costimulatory ligand (ICOSLG)* that induces T-cell proliferation and B-cell differentiation as well as antibody secretion and the *long intergenic non-protein coding RNA 173 (LINC00173)* were all significantly up-regulated for ALL-707 upon MLL-AF4 knock-down. Previous studies already addressed *C1QTNF4*, *IGLL1*, *SMAD2* and *LINC00173* a role in B-ALL. *C1QTNF4* binds to Nucleolin that promotes execution of the hematopoietic stem cell program (Mahotka et al., 2018; Vester et al., 2021). *IGLL1* was characterized to be weakly expressed in MLL-r B-ALL (Chen et al., 2016). *SMAD2* cooperates with *SMAD Family member 4 (SMAD4)* in the growth inhibitory TGF- β pathway. Higher expression of phosphorylated *SMAD2* has been reported in childhood B-ALL as a major signal transducer for transmission of TGF- β intracellular signaling (Rouce et al., 2016). Moreover, the non-coding RNA *LINC00173* is involved in blood homeostasis and influences hematopoietic stem cells (Cruz-Miranda et al., 2019; Schwarzer et al., 2017).

The knock-down of *MLL-AF4* caused in ALL-763 cells highly significantly up-regulated genes as indicated by $-\log$ FDR values beyond 20 (Fig. 4.2.1.1 B). The up-regulated genes for *tetraspanin 26 (CD37)* that codes for a B-cell surface antigen that is involved in tumor suppression and B-cell maturation (Wang et al., 2014), *granzyme A (GZMA)* that is an abundantly found proteases in the cytosolic granules of cytotoxic T-cells and *immunoglobulin lambda like polypeptide 5 (IGLL5)* that is a critical component of the pre-B-cell receptor, the *B-cell translocation Gene 1 (BTG1)* that is involved in cellular differentiation and growth and genes for several human leukocyte antigens (HLAs), all fulfilled the criteria of a $-\log$ FDR larger than 20. Notably, HLAs particularly corresponding to MHC class II are found beyond top up-regulated targets, such as the *HLA class II alpha chain paralogues HLA-DM Alpha (HLA-DMA)* and *HLA-DR Alpha (HLA-DRA)* as well as *HLA class II beta chain paralogues HLA-DR Beta 1 (HLA-DRB1)*, *HLA-DQ Beta 1 (HLA-DQB1)* and *HLA-DP Beta 1 (HLA-DPB1)*. Moreover, further up-regulated genes are coding for the *B-cell CLL/Lymphoma 2 (BCL2)-modifying factor (BMF)* that is a pro-apoptotic regulator and involved in numerous cellular pathways, and for the *Nei like DNA glycosylase 1 (NEIL1)* that plays a role in the DNA repair pathways and constitutes the most up-regulated gene with a 7.5-fold increased expression upon MLL-AF4 knock-down. Besides the strong hematopoietic correlation of up-regulated genes in ALL-763 cells, the genes *GZMA*, *HLA-DMA* and *BTG1* have additionally been correlated with B-ALL. *GZMA* constitutes a *RUNX1* target gene and is additionally crucial for sensitivity towards glucocorticoids mediating dexamethasone induced apoptosis in pre-B ALL cells (Li et al., 2021; Myoumoto et al., 2007; Ruike et al., 2007; U et al., 2004; Yamada et al., 2003). *HLA-DMA* is overexpressed in primary B-ALL cells, but it generally correlated with numerous types of leukemia (Fleischmann et al., 2014; Klitz et al., 2012; Taylor et al., 2008;

Thompson et al., 2014). Noteworthy, HLA-class II-positive leukemia patients were associated with an overall better survival (Takeuchi et al., 2019). Correlated with several HLA genes, *BTG1* acts as a tumor suppressor and its loss is linked to resistance towards glucocorticoids such as Dexamethasone (van Galen et al., 2010). Further on, deletions in *BTG1* were shown to act as drivers of leukemogenesis (Waanders et al., 2012).

A large-scale snapshot of the genomic activity of both ALL-707 and ALL-763 of either control and *MLL-AF4* knock-down samples revealed the overall differences in expression levels across the four samples ((Fig. 4.2.1.1 C). The clustering of de-regulated targets illustrates a higher proportion of up-regulated genes for ALL-763 upon *MLL-AF4* knock-down compared to the ALL-763 control sample. This is further highlighted by the imbalance in the Volcano Plot (Fig. 4.2.1.1 B) due to a larger proportion of highly significant up-regulated genes found in ALL-763 upon *MLL-AF4* knock-down. Among the 31,414 total reads of the MACE analysis, 777 genes were more than two-fold up-regulated for ALL-763 upon *MLL-AF4* knock-down (Fig. 4.2.1.1 D). Thereof, 685 genes have a p-value < 0.05. Considerably less prominent were the down-regulated genes for ALL-763 upon *MLL-AF4* knock-down with 382 genes in total and 320 genes with a p-value <0.05. For ALL-707, the ratio of at least 2-fold up- and down-regulated genes upon *MLL-AF4* knock-down was more balanced with 425 to 325, and 370 to 270 taking into consideration a p-value <0.05, respectively (Fig. 4.2.1.1 D).

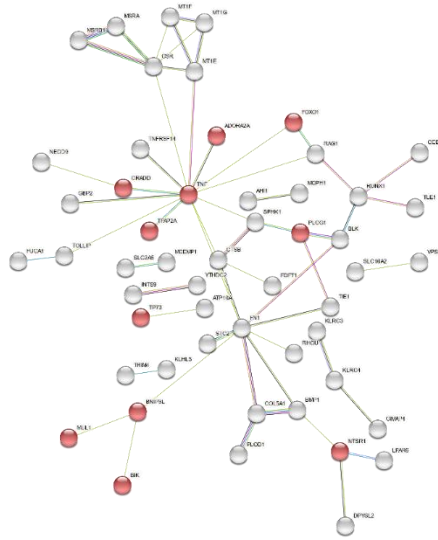
Next, the physical and functional interactions of genes that are at least two-fold up- or down-regulated with a FDR smaller than 0.25 were analyzed. Using the STRING database, networks on the basis of physically interacting proteins as well as collaborating but not physically interacting proteins were drawn (Fig. 4.2.1.2 B and D, Fig. 4.2.1.3 B and D). For a better assessment of the proteins within each network, the twenty most de-regulated genes for ALL-707 and ALL-763 cells were plotted in rank order (Fig. 4.2.1.2 A and C, Fig. 4.2.1.3 A and C). Further on, each network was tested for particularly relevant pathways including biological processes derived from gene ontology data and Kyoto Encyclopedia of Genes and Genomes (KEGG) pathways.

The STRING network of proteins encoded by down-regulated genes upon *MLL-AF4* knock-down for ALL-707 cells is characterized by tumor necrosis factor (TNF), the glycoprotein fibronectin 1 (FN1) and the B-lymphoid kinase (BLK) which constitute elementary connecting nodes to numerous other proteins in the network (Fig. 4.2.1.2 B). A key biological process of this network is the *positive regulation of apoptotic process* (GO-term GO:0043065; FDR = 0.0455). Its members, highlighted by red nodes, are often directly interacting with TNF (Fig. 4.2.1.2 B). Further listed proteins are FOXO1 and PLCG1, that are both top down-regulated targets of ALL-707 (Fig. 4.2.1.2 A) and cooperate with the RUNX1 interaction partners RAG1 and BLK (Wang et al., 2018).

A Top down-regulated genes in ALL-707-MA4-KD

Gene	log2FC	FDR
(shC/ shMA4)		
AJ009632.2	2.98	6.76E-11
KLRC3	2.40	3.71E-09
SH3D21	2.36	4.89E-04
FOXO1	2.35	2.16E-10
AC079150.2	2.33	2.00E-04
PLCG1	2.16	7.17E-11
TIGD7	2.16	2.19E-03
CPEB2	2.09	1.52E-16
AL355297.2	1.99	1.18E-06
MED12L	1.96	5.67E-03
LINC01943	1.91	3.35E-03
CELSR1	1.90	9.71E-04
SATB1	1.85	6.76E-09
YTHDC2	1.83	1.69E-02
TLE1	1.83	7.32E-03
INTS9	1.80	4.87E-09
TNFRSF14	1.80	9.39E-03
ZNF154	1.78	1.15E-02
MT2P1	1.67	5.08E-03
MT1E	1.65	8.02E-03

B



C Top down-regulated genes in ALL-763-MA4-KD

Gene	log2FC	FDR
(shC/ shMA4)		
DYSF	2.97	6.51E-09
BRIP1	2.00	2.89E-09
FGD6	1.86	3.35E-04
CENPI	1.79	2.68E-03
FBXO48	1.77	7.49E-03
ADAM22	1.76	1.79E-03
PRKAG2-AS1	1.76	2.79E-03
ENOSF1	1.74	3.60E-03
TMEM177	1.71	8.08E-04
SCAMP5	1.70	4.85E-03
HTRA3	1.70	1.24E-04
ACRV1	1.64	2.82E-03
GINS1	1.64	5.64E-11
RPL12P25	1.63	8.27E-04
MNS1	1.60	1.54E-02
LY6E	1.57	1.72E-07
MTND1P26	1.56	4.92E-04
AC024940.2	1.56	6.42E-03
GPT2	1.50	2.74E-02
IGFBP7	1.49	9.96E-15

D

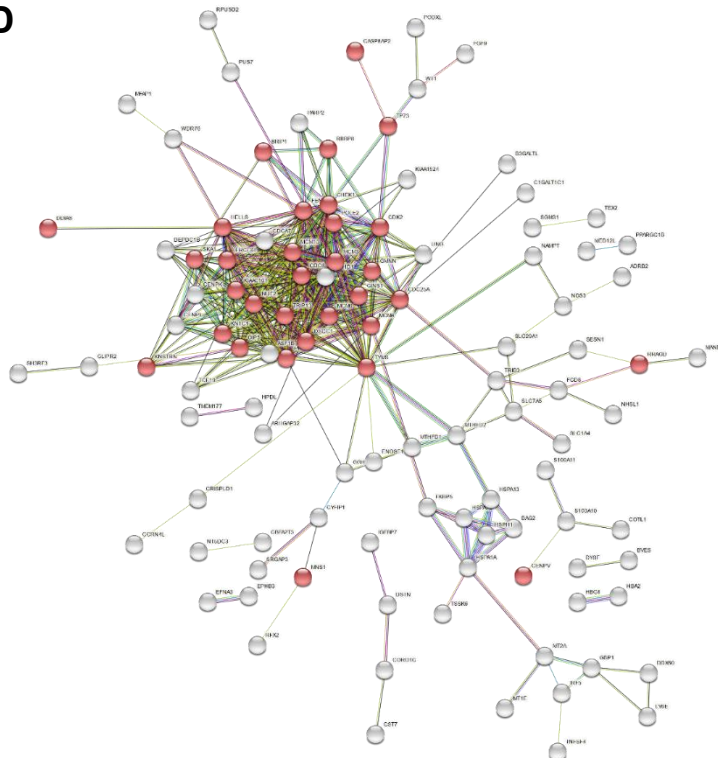


Figure 4.2.1.2: Top down-regulated genes upon MLL-AF4 knock-down in PDX leukemia cells. List of top down-regulated targets in ALL-707 and ALL-763 cells, respectively (FDR <0.25) (A+C). Illustration of physical and functional interactions (STRING database network) of top down-regulated targets of ALL-707 cells (B) and ALL-763 cells (log2 values ± 1 and FDR <0.25) (D). Key annotated pathways in ALL-707 cells the *positive regulation of apoptotic process* (GO-term GO:0043065; FDR = 0.0455) (C) and in ALL-763 cells the *cell cycle* ((GO:0007049, FDR = 0.0001) are highlighted in red (D).

For ALL-763, the STRING network is twice as large as for ALL-707. Here, a highly visible subset of proteins stands out that interact particularly strongly with each other and have little connections to the rest of the proteins of the network (Fig. 4.2.1.2 D). Besides the very high branching among each other, most of that subset of proteins is involved in cell cycle related processes. Not only the process *cell cycle* (GO:0007049, FDR = 0.0001) that is highlighted in red (Fig. 4.2.1.2 D), but also further processes related to cell cycle such as *cell cycle process* (GO:0022402, FDR = 0.0128), *mitotic cell cycle* (GO:0000278, FDR = 0.0048), *mitotic cell cycle process* (GO:1903047, FDR = 0.0117) and *DNA replication* (GO:0006260, FDR = 8.08×10^{-7}) overlap with the subset of proteins within the STRING network for ALL-763 cells. Protruding within the cell cycle related proteins by numerous interactions to non-cell-cycle related proteins of the ALL-763 down-regulated network upon MLL-AF4 knock-down is the thymidylate synthase (TYMS) that is involved in maintaining the pool of dTMP.

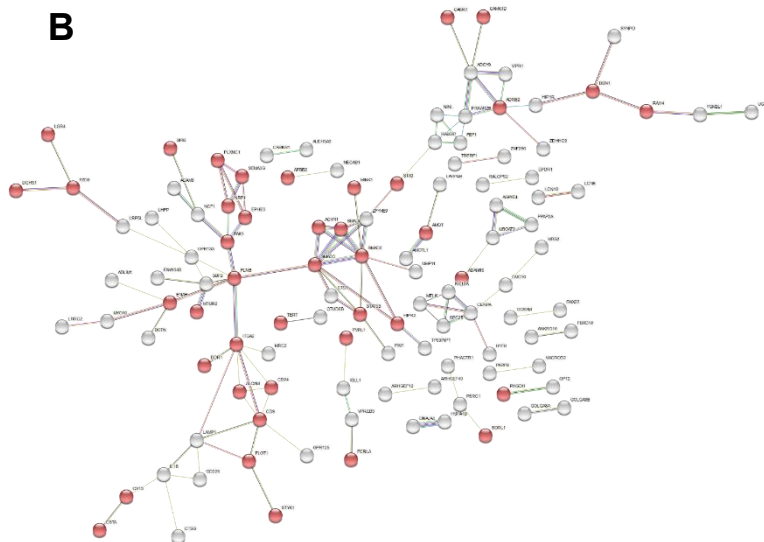
Further cell cycle related targets in the network are cyclin-dependent kinases (CDKs), minichromosome maintenance complex components (MCMs), in particular the highly significant MCM4, cell division cycle proteins (CDCs), centromere proteins (CENPs), checkpoint kinase 1 (CHK1), thyroid hormone receptor interactor 13 (TRIP13), NUF2 component of NDC80 kinetochore complex (NUF2), DNA polymerase Epsilon 2, accessory subunit (POLE2), GINS complex subunit 1 (GINS1), PCNA-associated factor encoded by the KIAA0101/PCLAF gene, kinetochore associated 1 protein (KNTC1), DNA replication and sister chromatid cohesion 1 (DSCC1), Opa interacting protein 5 (OIP5), Geminin DNA replication inhibitor (GMNN), lymphoid specific helicase (HELLS) and the highly significant BRIP1. Furthermore, the two cell-cycle related targets GINS1 and CENPI are listed as top-down-regulated targets for ALL-763 upon MLL-AF4 knock-down (Fig. 4.2.1.2 C). Of note, the FDRs of the top 10 down-regulated targets FYVE, RhoGEF and PH domain containing protein 6 (FGD6), CENPI, F-Box protein 48 (FBXO48), ADAM Metallopeptidase domain 22 (ADAM22), the lncRNA protein kinase AMP-activated non-catalytic subunit gamma 2 (PRKAG2) antisense RNA 1 (PRKAG2-AS1), the mitochondrial protein enolase superfamily member 1 (ENOSF1), the transmembrane protein 177 (TMEM177) and the secretory carrier membrane protein 5 (SCAMP5) are slightly above 0.01 and hence not particularly mentioned in the Volcano plot (Fig. 4.2.1.2 C).

The ALL-707-related STRING network of up-regulated genes upon MLL-AF4 knock-down is characterized by long strands of single chains of proteins related to cell differentiation and developmental processes (Fig. 4.2.1.3 B). Key nodes in the process of *cell differentiation* (GO:0030154, FDR = 0.0154) that is emphasized in red, are Filamin B (FLNB) that plays a role in the actin cytoskeleton through the interaction to glycoprotein Ib,

A Top up-regulated genes
in 707-MA4-KD

Gene	log2FC (shC/ shMA4)	FDR
C1QTNF4	-3.22	1.95E-17
NECTIN1	-3.06	1.04E-08
EPHB3	-2.73	2.60E-07
DDR1	-2.71	2.27E-05
IGLL1	-2.47	5.75E-13
IGHD	-2.39	8.92E-25
ICOSLG	-2.34	4.08E-09
LINC01226	-2.30	7.55E-08
B3GNT5	-2.28	1.34E-03
MTMR2	-2.26	3.92E-04
LINC00173	-2.25	5.24E-06
STYK1	-2.23	7.61E-04
RHPN1	-2.11	7.08E-13
VAT1L	-2.09	2.62E-04
GCHFR	-2.09	2.89E-07
REEP3	-2.08	2.15E-23
MSRB3	-2.02	1.68E-03
SERINC2	-2.02	5.72E-05
MRC2	-2.00	1.12E-02
NECAB1	-1.99	8.29E-03

B



C Top up-regulated genes
in 763-MA4-KD

Gene	log2FC (shC/ shMA4)	FDR
NEIL1	-2.95	4.77E-09
GZMA	-2.77	1.49E-48
DTX1	-2.68	1.53E-10
SYTL2	-2.59	3.58E-10
SCIMP	-2.58	4.77E-09
ITGA6	-2.58	9.41E-10
PPIC	-2.49	5.63E-11
GIMAP8	-2.48	3.53E-06
CDHR3	-2.40	5.42E-09
BMF	-2.39	3.80E-19
RIN2	-2.33	2.96E-05
COL6A3	-2.24	6.83E-09
GRAMD1C	-2.19	4.13E-05
MS4A1	-2.19	3.37E-04
PLA2G2C	-2.18	3.97E-05
LINC00494	-2.18	4.04E-09
AC139713.2	-2.15	3.45E-03
TTC21A	-2.14	3.46E-07
RAD51-AS1	-2.13	1.26E-04
IGLC5	-2.12	7.87E-09

D

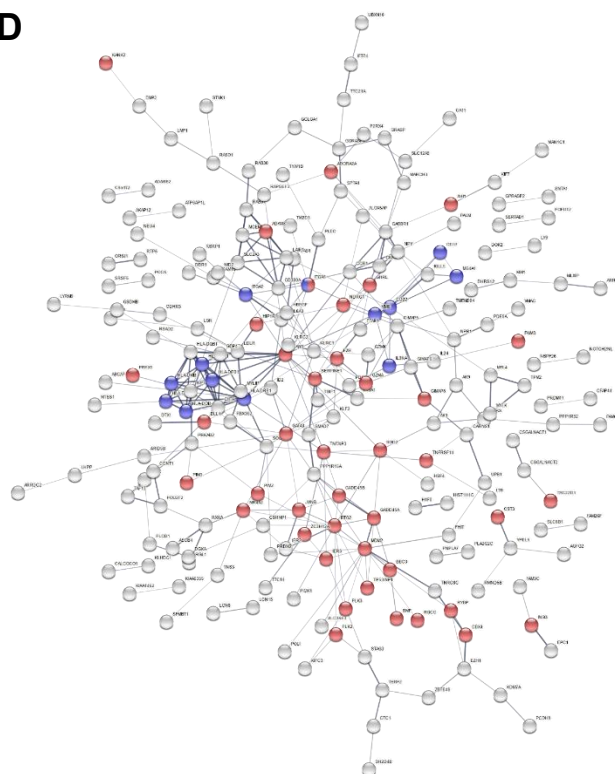


Figure 4.2.1.3: Top up-regulated genes upon MLL-AF4 knock-down in PDX leukemia cells. List of top up-regulated targets in ALL-707 and ALL-763 cells (FDR < 0.25) (A+C). Illustration of physical and functional interactions (STRING database network) of top up-regulated targets of ALL-707 cells (B) and ALL-763 cells (log2 values ± 1 and FDR < 0.25) (D). Key annotated pathways, for ALL-707 cells the process *cell differentiation* (GO:0030154, FDR = 0.0154) (C), and for ALL-763 the *regulation of cell death* (GO:0010941, FDR = 0.0421) are highlighted in red. The Krypto Encyclopedia of Genes and Genomes (KEGG) pathway the *hematopoietic cell lineage* (hsa04640, FDR = 3.76×10^{-6}) is depicted in blue for ALL-763 cells (D).

the signal transducers and transcriptional regulators SMAD2 and SMAD3, the alpha subunit of a transmembrane receptor integrin subunit alpha 2 (ITGA2), the tetraspanin CD9 and the serine/threonine p21 (RAC1)-activating kinase 1 (PAK1). Also processes related to developmental processes, such as developmental process (GO:0032502, FDR = 0.0172), cellular developmental process (GO:0048869, FDR = 0.0154) and regulation of developmental process (GO:0050793, FDR = 0.0191) are significantly connected to this ALL-707-related STRING network. The two receptor tyrosine kinases, the discoidin domain receptor tyrosine kinase 1 (DDR1) and the serine/threonine/tyrosine kinase 1 (STYK1) that both orchestrate the cellular communication with its microenvironment as well as the Ephrin type-b receptor 3 (EPHB3), are not only involved in regulating cell differentiation but also constitute top up-regulated targets for ALL-707 upon *MLL-AF4* knock-down (Fig. 4.2.1.3 A). Other significant targets not yet further specified among the top 10 up-regulated genes are the immunoglobulin nectin cell adhesion molecule 1 (NECTIN1), the long intergenic non-protein coding RNA 1226 (LINC01226), the membrane protein UDP-GlcNAc:BetaGal Beta-1,3-N-Acetylglucosaminyltransferase 5 (B3GNT5) and the lipid phosphatase Myotubularin Related Protein 2 (MTMR2).

The STRING network for ALL-763 with up-regulated targets has the highest number of connected targets compared to the other STRING networks upon *MLL-AF4* knock-down, specifically ALL-707 with up- and down-regulated targets and ALL-763 with down-regulated targets, respectively (Fig. 4.2.1.2 + Fig. 4.2.1.3). There are numerous biological processes significantly correlated to this STRING network, such as the process for regulation of cellular metabolic process (GO:0031323, FDR = 0.0455), the process for regulation of developmental process (GO:005079, FDR = 0.0404) that co-emerges in the STRING network for ALL-707 up-regulated targets upon *MLL-AF4* knock-down, the process of programmed cell death (GO:0043067, FDR = 0.0253), the regulation of the apoptotic process (GO:0042981, FDR = 0.0439) and the process for regulation of cell death (GO:0010941, FDR = 0.0421). The latter, highlighted in red, is characterized by central connection points such as the nuclear E3 ubiquitin ligase mouse double minute 2 proto-oncogene (MDM2) that targets p53 for proteasomal degradation, the BTG anti-proliferation factor 2 (BTG2) that regulates the transition from G1/S of the cell cycle with antiproliferative properties, the TNF alpha induced protein 3 (TNFAIP3) that is induced by TNF and inhibits TNF-mediated apoptosis, the transcription factor GATA binding protein 3 (GATA3) that is a regulator of T-cell development and the surface glycoprotein intercellular adhesion molecule 1 (ICAM1) (Fig. 4.2.1.3 D).

Noteworthy, this STRING network has numerous genes listed that are involved in the differentiation of hematopoietic cells. These genes could be identified within the STRING network by the Krypto Encyclopedia of Genes and Genomes (KEGG) as highlighted in blue

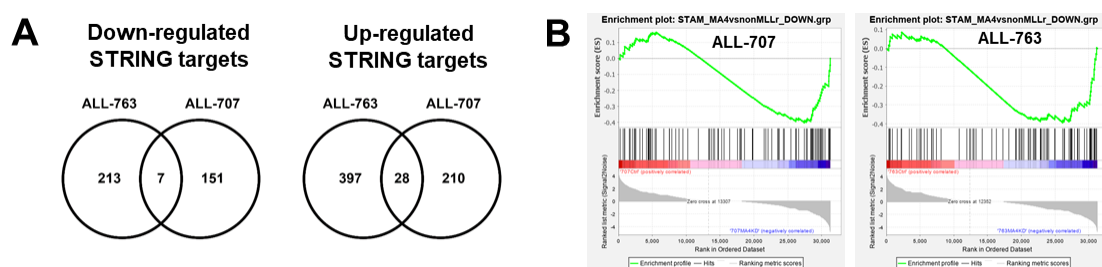


Figure 4.2.1.4: t(4;11) PDX cells share physical and functional targets upon MLL-AF4 knock-down independent of the expression of AF4-MLL. STRING networks originated from either up- or down-regulated genes of ALL-707 and ALL-763 cells were analyzed for overlapping targets (A). Gene set enrichment analysis (GSEA) compared ALL-707 and ALL-763 expression data upon MLL-AF4 knock-down with a published gene set (Stam et al., 2010) of down-regulated genes in ALL patients carrying MLL-AF4 compared to non-MLL-r ALL patients.

(Fig. 4.2.1.3 D). 13 genes were found to be significantly related to the KEGG pathway Hematopoietic cell lineage (hsa04640, FDR = 3.76×10^{-6}), that comprises surface markers particularly expressed by hematopoietic cells undergoing differentiation processes. Among these, numerous HLA-Ds, the B-lymphocyte cell adhesion molecule CD22 and the transmembrane glycoprotein membrane metalloendopeptidase (MME), that constitutes a major cell surface marker of ALL, stand out. Remarkably, the surface glycoprotein ICAM1 that is assigned to the biological process of cell death serves as a key connector within the KEGG pathway Hematopoietic lineage. It binds on the one hand to the cluster of several HLA-Ds and on the other hand to MME that is further connected to CD22, CD37 and the B-lymphocyte-specific membrane protein Membrane spanning 4-domains A1 (MS4A1) as well as to the interleukin 3 receptor subunit alpha (IL3RA) and the integrin subunit alpha 6 (ITGA6) that additionally belongs to the process of cell death (Fig. 4.2.1.3 D). Related to the process of cell death, GZMA, BMF and ITGA6 are further classified as the top up-regulated genes for ALL-763 upon MLL-AF4 knock-down (Fig. 4.2.1.3 C+D). Further genes on that list are the Deltex E3 Ubiquitin Ligase 1 that constitutes a regulator of Notch-signalling pathway, the synaptotagmin like 2 protein (SYTL2), the SLP Adaptor And CSK Interacting Membrane Protein (SCIMP) that is involved in MHC class II signal transduction in B cells, the peptidylprolyl isomerase C (PPIC), GTPase, IMAP Family Member 8 (GIMAP8) and cadherin related family member 3 (CDHR3).

Next, STRING networks for ALL-707 and ALL-763 cells of either up- or down-regulated genes upon *MLL-AF4* knock-down were examined for shared targets that are physically and functionally correlated (Fig. 4.2.1.4 A). Of 213 down-regulated targets for ALL-763 and 151 targets for ALL-707, only 7 genes are present in both STRING networks. This accounts for 3% of all ALL-763 and 5% of all ALL-707 related genes. Commonly down-regulated proteins are the tumor protein p77 (TP73) that is a tumor suppressor and p53 like

transcription factor involved in cellular responses to stress and development, the cytoskeleton associated protein LIM domain and actin bindin 1 (LIMA1), the metallothionein 1E (MT1E) and the processed pseudogene of metallothionein 2 (MT2P1), TMEM177, the ubiquitin E3 ligase SH3 domain containing ring finger 3 (SH3RF3) and the mediator complex subunit 12L (MED12L) that is a major coactivator for gene specific transcription of RNA polymerase II dependent genes. Except for TMEM177 that constitutes a top-down-regulated target for ALL-763, none of the shared down-regulated genes were particularly protruding in ALL-763 or ALL-707 related lists or networks. Besides MED12L that was shown to be over-expressed in relapse pediatric B-ALL cases (Bhatia et al., 2021) the distinct effect on B-ALL for all other targets is unknown yet.

A total of 28 shared up-regulated targets could be observed representing 7% of all ALL-763 and 13% of all ALL-707 related genes (Fig. 4.2.1.4 A). The shared up-regulated genes STYK1, IGHD, LINC00173, C1QTNF4, ITGA2, DDR1 and CDHR3 are additionally all top up-regulated genes for either ALL-763 or ALL-707. A remarkable subset of commonly up-regulated genes are related to autophagy and apoptosis, such as DEPP autophagy regulator 1 (DEPP1), the mediator of apoptosis BCL2 binding component 3 (BBC3) that together with the ALL-707 related BMF constitute regulators of BCL-2 and a target of p53 (Townsend et al., 2015), the immediate early response 3 gene (IER3) and the anti-proliferative and pro-apoptotic tumor protein p53 inducible nuclear protein 1 (TP53INP1). The leukocyte receptor tyrosine kinase (LTK) that plays a role in cell growth and differentiation and the lncRNA jumonji domain containing 1C antisense RNA 1 (JMJD1C-AS1) that inhibits the histone H3 lysine 9 (H3K9) demethylase jumonji are further important shared up-regulated targets.

Subsequently, gene set enrichment analyses (GSEA) were conducted to elucidate complex correlations between individual genes. Herein, all genes of the MACE-seq database obtained from ALL-707 or ALL-763 after the knock-down of MLL-AF4 were examined for association with published t(4;11)-ALL related gene lists (Fig. 4.2.1.4 B). The here selected reference gene list exclusively consists of genes that were downregulated in patients with t(4;11) ALL compared to patients with non-*MLL*-r ALL (Stam et al., 2010a).

The GSEA revealed enrichment scores for either ALL-707 of -0.40 (FDR = 0.031) and for ALL-763 of -0.39 (FDR = 0.036), respectively (Fig. 4.2.1.4 B). Strikingly, this indicates a strong correlation between up-regulated genes upon *MLL-AF4* knock-down of the t(4;11) PDX model and up-regulated genes of ALL patients in the absence of MLL. Genes from the reference list of Stam et al. *DDR1*, *GCHFR*, and *IGLL1* or the genes *DTX1*, and *MS4A1* are all top-20 up-regulated genes in the PDX model upon MLL-AF4 knock-down for ALL-707 or ALL-763 cells, respectively. Moreover, genes of the reference list with a high correlation to the knock-down of *MLL-AF4* that are shared between ALL-707 and ALL-763

are *DDR1*, *DTX1*, *CD27 Molecule (CD27)* that codes for a key B-cell regulator, *T-Cell Leukemia/Lymphoma 1 AKT Coactivator B (TCL1B)*, *Nidogen 2 (NID)* that is involved in cell-adhesion, *Pleckstrin Homology And RhoGEF Domain Containing G4B (PLEKHG4B)*, *Purinergic Receptor P2Y14 (P2RY14)* that is a member of the G-protein coupled receptors, *Joining Chain of Multimeric IgA and IgM (JCHAIN)* that links monomer units of IgA and IgM, *Differentially Expressed in FDCP 8 Homolog (DEF8)*, *Zinc Finger E-Box Binding Homeobox 1 (ZEB1)* and *CD52 molecule (CD52)*.

All in all, the induced *MLL-AF4* knock-down elicits altered transcriptional signatures in proliferating PDX leukemia cells that either express both fusion proteins *MLL-AF4* and *AF4-MLL* or exclusively *MLL-AF4*.

4.2.2. The expression of dnTASP1 in proliferating PDX leukemia cells upregulates cell-cycle dependent genes

After studying the effect of *MLL-AF4* inhibition *in vivo*, the impact of *AF4-MLL* inhibition was investigated in PDX cells *in vivo* that constitutively express dnTASP1 mediating proteasomal degradation of *AF4-MLL* (Sabiani et al., 2015).

The dnTASP1-expressing PDX leukemia cells were established by Kerstin Völse from the Jeremias Laboratory (Völse, 2020) (Fig. 4.2.2.1 A). *MLL-AF4* and *AF4-MLL* expressing ALL-707 PDX cells were transduced with either a control shRNA or a dnTASP1 expressing cassette and the cells injected into NSG mice (Völse, 2020). The expression of the FLAG-tagged dnTASP1 mutant was confirmed via Western Blot eight weeks after injection (Völse, 2020).

In general, the amount of significantly up-regulated genes was increased upon the expression of dnTASP1 (Fig. 4.2.2.1 B), since the major fraction of de-regulated genes with $FDR < 0.01$ were up-regulated. The gene for *H2A histone family member X variant histone H2A (H2AFX)* that is involved in chromatin remodeling and the gene *high-mobility group protein B2 (HMGB2)* that codes for a non-histone chromatin-associated protein are identified in the Volcano Plot within the group of up-regulated genes with a $-\log(FDR) < 30$ (Fig. 4.2.2.1 B). Most of the highly significant and up-regulated genes upon dnTASP1 expression were associated to cell-cycle processes, such as the genes for *Ubiquitin Conjugating Enzyme E2 C (UBE2C)* that constitutes a promoter of cell cycle progression, *Aurora Kinase B (AURKB)* that associates with microtubules during mitosis and *Polo Like Kinase 1 (PLK1)* that is involved in cell cycle regulation via phosphorylation of *Cyclin B1 (CCNB1)*, that itself is also up-regulated upon dnTASP1 expression. Further cell-cycle related and up-regulated genes are coding for *the Cyclin Dependent Kinase 1 (CDK1)* that

constitutes an M-phase promoting factor and cell cycle regulator; and is regulated by *MYC*, *Tubulin Beta 4B Class IVb (TUBB4B)* that constitutes a major player in microtubule cytoskeleton organization, *Kinesin Family Member C1 (KIFC1)* that is associated to mitotic spindle assembly, *CDC28 Protein Kinase Regulator Subunit 2 (CKS2)* that is capable of binding to cyclin-dependent kinases (CDKs), *CCNB1* that plays a role in G2/M transition, *Nucleolar And Spindle Associated Protein 1 (NUSAP1)* that organizes microtubules, *Cell Division Cycle 25B (CDC25B)* that induces progression of mitosis, *Sperm Associated Antigen 5 (SPAG5)* that orchestrates mitotic spindles, *Ribonucleotide Reductase Regulatory Subunit M2 (RRM2)* that codes for the cell-cycle regulated M2 protein, *Cell Division Associated 3 (CDCA3)* that mediates degradation of WEE1 kinase and initiates mitosis, the *Centromere Protein A (CENPA)* that is a centromere-specific histone H3, *Proline And Serine Rich Coiled-Coil 1 (PSRC1)* that encodes for a protein that is involved in mitosis and is regulated by the tumor suppressor protein p53 and ,finally, *Spindle Pole Body Component 25 (SPC25)* that is involved in spindle checkpoint activity.

Importantly, *HMGB2*, *UBE2C*, *AURKB*, *PLK1*, *CDK1*, *CKS2*, *CCNB1*, *CDC25B* and *CDCA3* have all been associated to B-ALL previously. *HMGB2* and its pseudogene are overexpressed in pediatric ALL patients (Almamun et al., 2015). Moreover, CAR-T cells to treat ALL patients overexpress *HMGB2* that was also correlated to high expression of cell cycle genes (Bai et al., 2021). Additionally, single-cell RNA-seq (scRNA-seq) data revealed that *HMGB2* was significantly increased in relapsed infant ALL patient samples (Guest et al., 2019). While promoting cell cycle progression, the up-regulated *UBE2C* is a frequently methylated gene in ALL and its knock-down is further associated with L-asparaginase-mediated resistance in pediatric ALL cells (Dunwell et al., 2010). Next, the up-regulated *AURKB* gene was shown to act as a negative regulator of the EHMT1/2 co-regulator complex and to be over-expressed in relapsed B-ALL patients (Poulard et al., 2019). The up-regulated kinase *PLK1* was demonstrated not only to be over-expressed in pediatric B-ALL patients, but also that its knock-down caused cell death of B-ALL cells *in vitro* and *in vivo* (Goroshchuk et al., 2020; Kannan et al., 2019). This was further confirmed in a study comparing conserved signatures between fetal blood progenitors and ALL blasts to identify genes critical for disease maintenance, *PLK1* was identified as a key gene for survival of t(4;11) ALL cells (Symeonidou et al., 2021). Next, regulated by *MYC*, Cdk1-dependent cell cycle progression was identified to be the main driver of *MYC*-controlled tumorigenesis in pediatric B-ALL (Yang et al., 2018). Notably, WEE1 G2 Checkpoint Kinase (*WEE1*) was also observed to be upregulated that was described to phosphorylate CDK1. Similarly, the kinase *CKS2* is induced by *MYC* and is overexpressed in *MLL-r* leukemia (Grey et al., 2018). Further on, the cell cycle regulators *CCNB1* and *CDC25* were shown to be overexpressed in SEM cells and in B-ALL patient samples (Consolaro et al., 2015; Ghelli

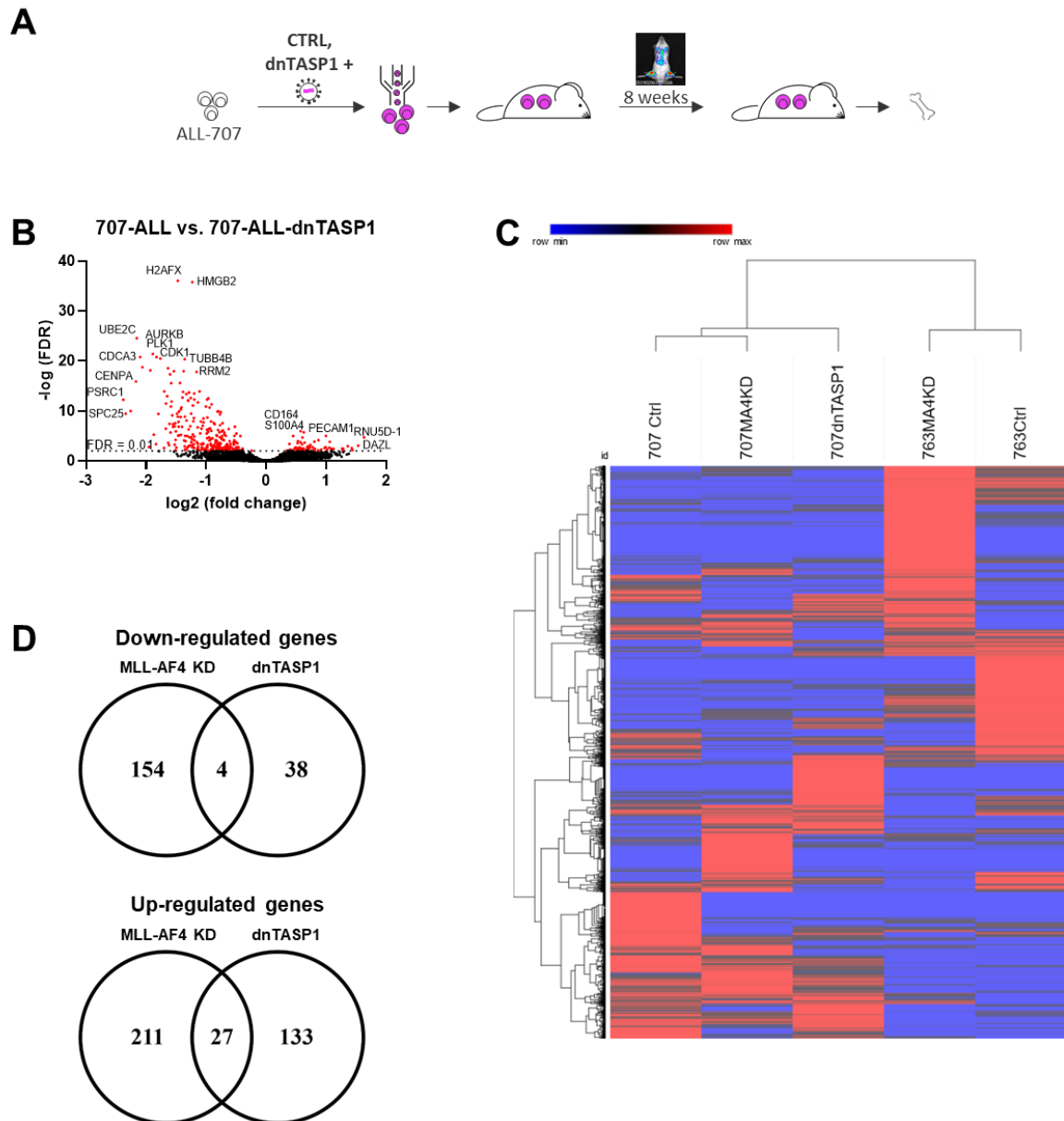


Figure 4.2.2.1: Expression of dnTASP1 increases amount of significantly up-regulated genes *in vivo*. Graphical illustration of experimental setup of constitutive dnTASP1 overexpression in PDX cells *in vivo* (adapted from Carlet et al. 2020 and Völse, 2020) (A). All preceding experiments in mice were conducted by Kerstin Voelse (Jeremias Laboratory, LMU, Munich). Significantly de-regulated genes are highlighted in a Volcano plot (B). Heat-map analysis illustrates clustering of de-regulated genes upon dnTASP1 expression in ALL-707 cells (C). Quantification of shared de-regulated genes (\log_2 values ± 1 , $p < 0.05$) in ALL-707 cells that either express dnTASP1 or upon induced MLL-AF4 knock-down (D).

Luserna Di Rorà et al., 2018). Importantly, *CDC25*, that is phosphorylated by Aurora-A has been characterized to dephosphorylate and activate *CDK1* (Davezac et al., 2002, 2002; Dutertre et al., 2004), that is also up-regulated upon dnTASP1 expression *in vivo*.

A considerably smaller portion of down-regulated genes upon dnTASP1 expression are protruding in the Volcano Plot, due to $-\log(\text{FDR})$ values below 6 (Fig. 4.2.2.1 B). *CD164* that orchestrates adhesion, migration and proliferation in hematopoietic progenitor cells, and *S100 Calcium Binding Protein A4 (S100A4)* that is involved in cell cycle progression and differentiation demonstrate the smallest FDR of all down-regulated genes. The gene for *Deleted in Azoospermia Like (DAZL)* that encodes for an mRNA-binding protein in germ cells and RNA and *the snRNA 5UD Small Nuclear 1 (RNU5D-1)* are the two top-down-regulated genes upon dnTASP1 expression (Fig. 4.2.2.1 B). Further, the down-regulated gene of *Platelet And Endothelial Cell Adhesion Molecule 1 (PECAM1)* that encodes for a surface protein involved in intercellular junctions peaks in the Volcano Plot.

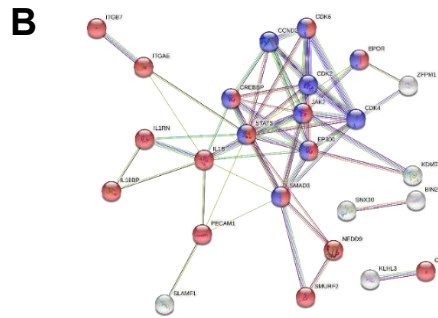
S100A4 is the only down-regulated cell-cycle gene upon the expression of dnTASP1 and has been associated to B-ALL. Inhibition of *S100A4* resulted in anti-leukemic effects in B-ALL cells and it was also shown to be highly overexpressed in patients with acute leukemia (Alanazi et al., 2020; Guo et al., 2021). The surface protein PECAM1 was described to be highly over-expressed in B-ALL associated non-classical monocytes and in patient-derived ALL cells (Chen et al., 2015; Witkowski et al., 2020).

A heat-map of dnTASP1 expressing ALL-707 cells revealed a similar ratio of total up- and down-regulated genes compared to ALL-707 cells upon MLL-AF4-knock-down (Fig. 4.2.1.1 C). A greater portion of up-regulated genes upon dnTASP1 expression as shown for significantly deregulated genes in the Volcano Plot could not be observed in the heat-map analysis. Comparing the effects between an induced MLL-AF4 knock-down and the expression of dnTASP1, a minor overlap of highly de-regulated genes (> 2 -fold change, $p < 0.05$) was observed in ALL-707 cells that either inhibit MLL-AF4 or AF4-MLL, respectively (Fig. 4.2.1.1 D).

Next, a STRING network analysis confirmed the observed strong correlation between up-regulated genes upon dnTASP1 expression and cell cycle regulation (Fig. 4.2.2.2 C+D). With a total number of 97 genes, almost the entire STRING network was shown to be correlated to cell cycle processes (GO:0007049, $\text{FDR} = 3.25 \times 10^{-68}$). Moreover, cell-cycle related genes demonstrated a very high branching among each other. The top-20 list of up-regulated genes upon dnTASP1 expression consists of genes whose outstanding up-regulation was already detected in the Volcano Plot such as *CDK1*, *PLK1*, *AURKB*, *CDCA3*, *UBE2C*, *CENPA*, *SPC25* and *PSRC1* (Fig. 4.2.2.2 C). The genes for *Cyclin F (CCNF)* a member of the F-box protein family that orchestrates cell cycle progression, *Maternal Embryonic Leucine Zipper Kinase (MELK)* that is involved in cell cycle and particularly the phosphorylation of *CDC25B*, *Suppressor APC Domain Containing 2 (SAPCD2)* that promotes cell proliferation and mitotic spindle orientation and the cell cycle-regulated kinase Aurora Kinase A (*AURKA*) constitute the top four up-regulated genes

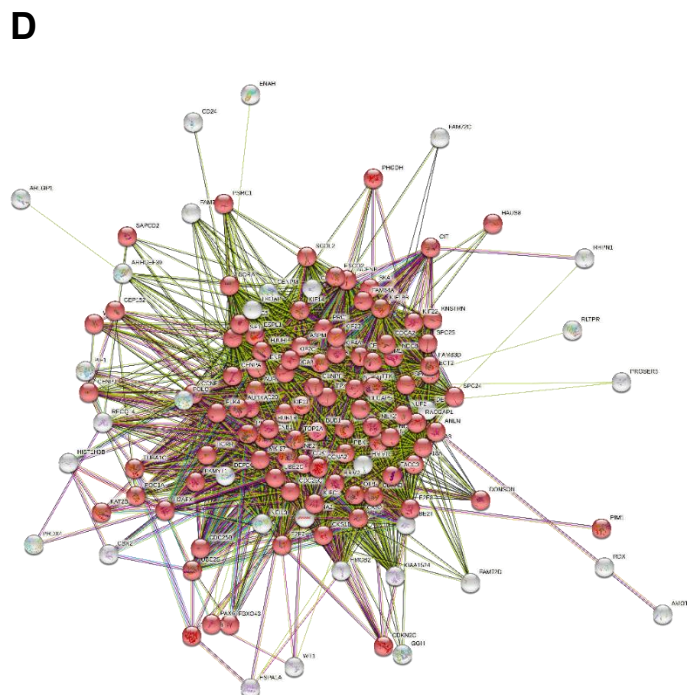
A Top down-regulated genes in 707-dnTASP1

Gene	log2FC (shC/ dnT1)	FDR
RNU5D-1	1.63	1.95E-05
DAZL	1.53	8.68E-04
SORBS2	1.44	7.27E-03
KDM7A	1.43	2.86E-03
SMAD3	1.38	3.90E-02
ZHX3	1.36	1.15E-03
BIN2	1.34	5.12E-02
TPMT	1.28	1.74E-02
CCND2	1.28	3.69E-03
SNX30	1.28	9.09E-03
SERPINF1	1.27	3.59E-03
C3orf58	1.25	1.37E-01
RNU5A-1	1.22	5.51E-02
RNU5B-1	1.22	1.73E-02
IL18BP	1.18	6.07E-02
KLHL3	1.18	7.15E-02
JAK2	1.17	3.67E-02
RNU4ATAC	1.15	4.48E-02
MARCH2	1.14	1.85E-02
SLAMF1	1.12	3.84E-03



C Top up-regulated genes in 707-dnTASP1

Gene	log2FC (shC/ dnT1)	FDR
CCNF	-1.67	3.37E-12
MELK	-1.67	3.65E-07
SAPCD2	-1.69	1.19E-14
AURKA	-1.70	2.60E-03
CDK1	-1.76	3.16E-21
MTMR2	-1.78	1.11E-02
KIF23	-1.80	3.96E-10
PLK1	-1.83	1.64E-21
FBXO43	-1.83	4.60E-04
KIF18A	-1.87	5.70E-06
AURKB	-1.89	3.70E-22
CCNB1	-1.93	7.72E-19
PHGDH	-1.95	1.65E-03
KIFC1	-2.06	1.78E-19
CDCA3	-2.10	1.64E-21
UBE2C	-2.15	2.73E-25
CENPA	-2.17	1.30E-16
PIF1	-2.26	1.06E-10
SPC25	-2.34	3.45E-10
PSRC1	-2.38	5.83E-13



upon dnTASP1 expression in ALL-707 cells with FDRs smaller than 0.01. Further top-up-regulated genes encode for the phosphoinositide lipid phosphatase *Myotubularin Related Protein 2 (MTMR2)*, the *Kinesin Family Member 23 (KIF23)* that is responsible for transporting chromosomes during cell division, another *F-Box carrying protein F-Box Protein 43 (FBXO43)* that is involved in the regulation of cell cycle progression, *Kinesin*

Figure 4.2.2.2: Cell-cycle-related genes are significantly up-regulated upon expression of dnTASP1 *in vivo*. List of top up- (A) and down-regulated targets (B) in ALL-707 cells upon the expression of dnTASP1 *in vivo* (FDR <0.25). Illustration of physical and functional interactions (STRING database network) of top up- (B) and down-regulated targets (D) of dnTASP1-expressing ALL-707 cells (log2 values ± 1 and FDR <0.25). Key annotated pathways, for up-regulated genes *cell cycle processes* (GO:0007049, FDR = 3.25×10^{-68}) highlighted in red (D), and for down-regulated genes the *surface receptor signaling* (GO:0007166, FDR = 0.0059) highlighted in red and Positive regulation of cell cycle process (GO:0090068, FDR = 0.0385) highlighted in blue.

Family Members 18A (KIF18A) and C1 (KIFC1), Cyclin B1 (CCNB1) that interacts with *MELK, CDK1, FOXM1* and *CDC25B, Phosphoglycerate Dehydrogenase (PHGDH)* that is associated to the L-serine synthesis and the PIF1 5'-To-3' DNA Helicase (PIF1) that orchestrates the maintenance of DNA integrity and is also involved in the maintenance of telomeric DNA (Fig. 4.2.2.2 C).

Especially the cell-cycle-related genes *MELK* and *AURKA* are associated to B-ALL. *MELK* is overexpressed in ALL cell lines and highly methylated in pediatric ALL patients (Almamun et al., 2015; Deo, 2017). Furthermore, inhibition of *MELK* resulted in down-regulation of *FOXM1* that plays a role in the sensitivity of B-ALL treatments (Alachkar et al., 2014; Consolaro et al., 2015). Moreover, inhibition of *MELK* decreases expression levels of co-up-regulated *CCNB1* and *CDK1* (Zhang et al., 2018).

Highly branched genes of this STRING network, not belonging to cell cycle-related processes, are Hyaluronan mediated motility receptor (HMMR), Trophinin associated protein (TROAP), DEP domain-containing protein 1A (DEPDC1), Karyopherin subunit alpha 2 (KPNA2), Ubiquitin-conjugating enzyme E2 T (UBE2T), Endonuclease 8-like 3 (NEIL3) and DNA polymerase theta (POLQ).

For down-regulated genes upon dnTASP1 expression, STRING network analysis revealed a marked association to the biological process cell surface receptor signaling (GO:0007166, FDR = 0.0059) (Fig. 4.2.2.2 B). The major branching points of receptor-signaling related genes are *Signal Transducer And Activator of Transcription 3 (STAT3)*, *SMAD Family Member 3 (SMAD3)* that is associated to signal transduction and transcriptional regulation, *Janus Kinase 2 (JAK2)* that is associated to growth factor and cytokine signaling and the pro-inflammatory cytokine *Interleukin 1 Beta (IL1B)*.

Importantly, besides the tremendous enrichment of up-regulated genes upon dnTASP1 expression in cell cycle processes, a subset of down-regulated genes were associated to the biological process Positive regulation of cell cycle process (GO:0090068, FDR = 0.0385). Particularly, the Cyclin Dependent Kinase (CDK2) constitutes the key node of targets positively regulating cell cycle. There it is surrounded by *IL1B*, the histone acetyltransferase *E1A Binding Protein P300 (EP300)*, *Cyclin Dependent Kinase 4 (CDK4)*

and Cyclin D2 (CCND2). Noteworthy, CCND2 associates together with Cyclin D1 and D3 to CDK4 and CDK6 to promote cell cycle progression, and it is a target of *STAT5* and *MYC*. Genes from *Pathways in cancer* of the KEGG network (hsa05200, FDR = 5.89×10^{-6}) are also enriched and protrude with a very high branching among each other (Fig. 4.2.2.2 B). With Cyclin Dependent Kinase 6 (CDK6), Erythropoietin Receptor (EPOR), CREBBP, JAK2, STAT3, EP300 and SMAD3, half of the targets related to cancer are also involved in surface receptor signaling. In addition, the targets related to *Pathways in cancer* CCND2, CDK2 and CDK4 are also related to *positive regulation of cell cycle progress*. Of note, the targets CREBBP, CDK6, EPOR, EP300, STAT3 and IL1B constitute a substantial part of the STRING network but are only moderately down-regulated upon dnTASP1 expression (Fig. 4.2.2.2 B).

All of the top-20 down-regulated genes upon dnTASP1 expression in ALL-707 cells show FDR values close to 0.01 (Fig. 4.2.2.2 A). Following the two-most down-regulated genes *RNU5D-1* and *DAZL*, top-down-regulated genes are the *non-receptor protein tyrosine kinase Sorbin And SH3 Domain Containing 2 (SORBS2)*, *Lysine Demethylase 7A (KDM7A)* that in contrast to the methyl transferase MLL demethylates lysines of histones, and *SMAD Family Member 3 (SMAD3)* that codes for a signal transducer and transcriptional regulator. Of note, SMAD2 and SMAD4 are both up-regulated in ALL-707 upon the induced knock-down of MLL-AF4. The genes for transcription factor *Zinc Fingers And Homeoboxes 3 (ZHX3)*, the *Binding Integrator 2 (BIN2)* that is associated to phospholipid binding and phagocytosis, *Thiopurine S-Methyltransferase (TPMT)* that is associated to methylation of thiopurine, *CCND2* that together with CCND1 and CCND3 associates to CDK4 and CDK6 to promote cell cycle progression and additionally is a target of *STAT5* and *MYC*, and *Sorting Nexin Family Member 30 (SNX30)* that plays a role in protein transport are listed in the top-10-down-regulated genes upon dnTASP1 expression (Fig. 4.2.2.2 A). Further on, the remaining genes of the top-20 down-regulated genes are *Serpin Family F Member 1 (SERPINF1)* that is involved in the inhibition of angiogenesis, *Divergent Protein Kinase Domain 2A (C3orf58)*, three regulatory RNAs of the snRNA class, *RNU5A-1*, *RNU5B-1* and *RNU4ATAC*, *Interleukin 18 Binding Protein (IL18BP)* that counteracts IFN-gamma production by preventing IL18 to bind to its receptor, *Kelch Like Family Member 3 (KLHL3)* and *Membrane Associated Ring-CH-Type Finger 2 (MARCH2)* that both play a role in ubiquitination, *Janus Kinase 2 (JAK2)* that is associated to growth factor and cytokine signaling, and *Signaling Lymphocytic Activation Molecule Family Member 1 (SLAMF1)* that is involved in the signaling of hematopoietic stem cells (Fig. 4.2.2.2 A). In particular, *TPMT*, *CCND2* are *SERPINF1* play a role in B-ALL. While the S-Methyltransferase TPMT is a favorable prognostic factor in ALL (Moriyama et al., 2021; Relling et al., 1999; Schmiegelow et al., 1995), *SERPINF1* has been shown to be over-

expressed in *MLL-r* leukemia (Mullighan et al., 2007). Additionally, Cyclin D2 is a key driver in proliferation of B-ALL cells (Geng et al., 2015; Ketzer et al., 2022).

Overall, numerous de-regulated genes seem to be associated with C-MYC that codes for a pivotal transcription factor in hematopoiesis (Delgado and León, 2010; Gómez-Casares et al., 2013; Langdon et al., 1986). In particular, the de-regulated CDK1, PLK1, cyclin D2 (*CCND2*) and CDC28 (*CKS2*) are all linked to C-MYC.

The expression of dnTASP1 often resulted in the up-regulation of cell-cycle genes independent of a promoting or inhibitory function as observed for CDK1 (Figure 4.2.2.1 and Figure 4.2.2.2). It has been described as a main driver of C-MYC controlled tumorigenesis in pediatric B-ALL and plays an important role in the mitotic checkpoint (Davidson and Niehrs, 2010; Yang et al., 2018). However, also *WEE1* that phosphorylates CDK1 causing a delay in G2/M transition, and, *vice versa*, *CDC25B* and *CDC25C* that promotes mitotic entry by de-phosphorylating CDK1 were up-regulated upon dnTASP1 expression (Heald et al., 1993; Watanabe et al., 1995; Zhong et al., 2017).

The expression of dnTASP1 further up-regulated mutually regulated cell-cycle genes such as *PLK1*, *AURKA* and *CCNB1*. In cooperation with *MYC*, *PLK1* is a known oncogenic transformation factor that highly interacts with cyclin B1 (*CCNB1*) and *AURKA*. Orchestrating mitotic progression, *AURKA* itself interacts with cyclin B1 but also phosphorylates *PLK1* (Asteriti et al., 2015; Dutertre et al., 2004; Hirota et al., 2003), and *PLK1* is also capable of phosphorylating *CCNB1* (Fu et al., 2008; Major et al., 2004). The up-regulated dnTASP1 target clusters *WEE1*, *CDK1* and *CDC25B* are linked to the cluster of *Plk1*, *CCNB1* and *AURKA* by the association of *CDC25B* with *AURKA* (Dutertre et al., 2004; Hirota et al., 2003; Zhong et al., 2017).

In summary, the first transcriptional *in vivo* data for leukemic cells expressing dnTASP1 revealed a profound overexpression of cell-cycle-related genes. Moreover, the majority of de-regulated genes with an FDR <0.01 are up-regulated indicating that dnTASP1 acts in a leukemic background as a transcriptional activator.

4.3. AF4-MLL-induced chromatin and transcriptional signature persists in t(4;11) leukemia model *in vitro*

AF4-MLL is known to have a chromatin-opening function due to the MLL portion at the C-terminus, which is expected to induce a profound effect on global transcription through the transcription-elongating AF4 at the N-terminus and the concomitant lack of the target-gene-defining N-terminus of MLL (Marschalek, 2015). Contrarily, MLL-AF4, carries the N-

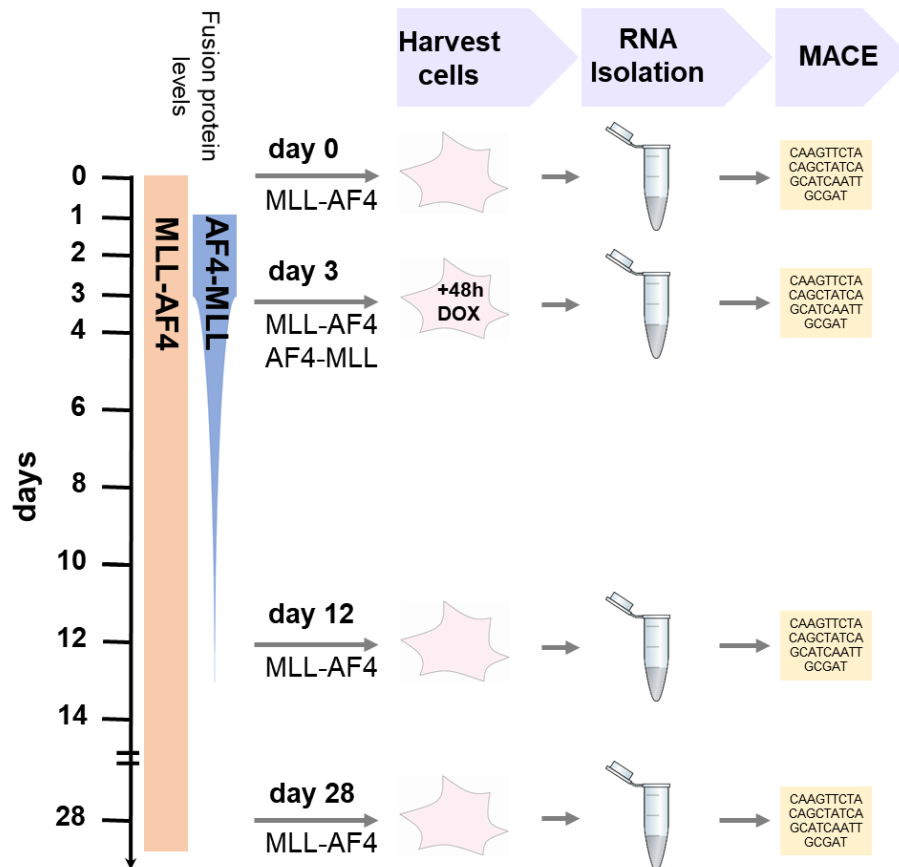


Figure 4.3.1.1: A cellular t(4;11) model to study transcriptional signatures upon short-term expression of AF4-MLL. Gene expression signatures were assessed first when only MLL-AF4 is expressed (day 0), upon the co-expression of both MLL-fusion proteins (day 3), and 9 and 25 days after short-term expression of AF4-MLL, respectively (day 12 and day 28). MACE-seq analysis was conducted with harvested RNA of 293T cells of each experimental time-point. n = 3 biological replicates per sample.

terminus of MLL and its chromatin remodeling ability is presumably limited to target genes of wild-type MLL. However, the role of MLL fusion proteins in early phase of disease development and for disease progression remains unclear.

There is only a single published functional study that succeeded in the development of a t(4;11) leukemia *in vivo* using human MLL fusion genes (Bursen et al., 2010). It demonstrated that the AF4-MLL fusion protein is indispensable for the development of a t(4;11) leukemia in mice. Subsequently, during disease progression, only the expression of MLL-AF4 is detectable in all t(4;11) leukemia patients, while a subset of patients lack the expression of AF4-MLL (Agraz-Doblas et al., 2019; Kowarz et al., 2007; Sanjuan-Pla et al., 2016; Trentin et al., 2009). Remarkably, a recent study revealed that the co-expression of MLL-AF4 and AF4-MLL is highly associated with a better disease outcome when compared to the expression of MLL-AF4 alone (Agraz-Doblas et al., 2019).

Hence, in this work, it the capability to induce persistent changes in chromatin and gene transcription by either MLL-AF4 or AF4-MLL was evaluated using a cellular t(4;11)

leukemia model to elucidate the underlying rationale for a putative elimination of AF4-MLL in advanced leukemia.

4.3.1. A cellular t(4;11) model to study the transforming potential of transiently expressed AF4-MLL

The absence of AF4-MLL expression in a subset of t(4;11) leukemia patients indicates AF4-MLL-induced effects that play a role in the development rather than maintenance of advanced leukemia. As almost no further secondary mutations are found in t(4;11) leukemia, particularly in infants, long-term changes in the genomic landscape after short-term AF4-MLL expression may suggest its possible involvement in the temporal transformation of a cell into a leukemic cell (Agraz-Doblas et al., 2019; Sanjuan-Pla et al., 2015; Zheng, 2013). Thus, in this work, a cellular t(4;11) model was designed based on constitutively expressed MLL-AF4 and short-term induced expression of AF4-MLL. Particularly, gene expression signatures were compared when both MLL fusion proteins are expressed together and well after short-term expression of AF4-MLL with the stage of constitutive expression of MLL-AF4 only.

The cellular t(4;11) model was designed to obtain cellular samples for MACE-seq analysis to determine differential gene expression on four different time-points that vary in the expression of MLL-AF4 and AF4-MLL (Fig. 4.3.1.1). To properly assess the impact of AF4-MLL on gene expression, initially, RNA was harvested of 293T cells that were stably transfected with a vector for a constitutive expression of *MLL-AF4*, referred to as day 0 (Fig. 4.3.1.1). Harvested RNA from day 0 constitute an important reference as changes in the gene signature can be clearly assigned to MLL-AF4 when compared to Mock cells that merely express Luciferase. Additionally, MLL-AF4 expressing 293T cells were transiently transfected on day 0 with an Doxycycline-inducible vector expressing *AF4-MLL*. and induced with 1 µg/mL Doxycycline 24 h post transfection. Upon 48 h Doxycycline induction, RNA was harvested on day 3 from cells constitutively expressing MLL-AF4 and a peak expression of AF4-MLL. For the investigation of long-term effects, the induction of AF4-MLL expression was terminated on day 3 by replacing Doxycycline-containing media and the cells were grown for another 25 days. On day 12 and on day 28 of the experiment, RNA was harvested to evaluate whether genomic signatures are altered due to the temporal expression of AF4-MLL until day 3 (Fig. 4.3.1.1).

Considering the long half-life of 48 h of the fusion protein (Bursen et al., 2004), on day 12, approximately 1.56% of AF4-MLL is expected to remain in the cell compared to day 3. Accordingly, on day 28, this relative amount drops to negligible low 0.006%.

4.3.2. A cellular t(4;11) leukemic model allows to study MLL-AF4 and AF4-MLL independently

For a rapid generation of the cellular t(4;11) model, MLL fusion proteins were cloned into specific vectors of the Sleeping Beauty transposon system (Fig. 4.4.1.1 A). For the constitutive expression of MLL-AF4, the pSBbi::*MLL-AF4* vector was transfected bearing *MLL-AF4* with *MLL* exons 1-10 and AF4 exon 4-20 under the control of the EF1 α -promoter. For the inducible expression of *AF4-MLL*, the pSBtet::*AF4-MLL* vector were applied that

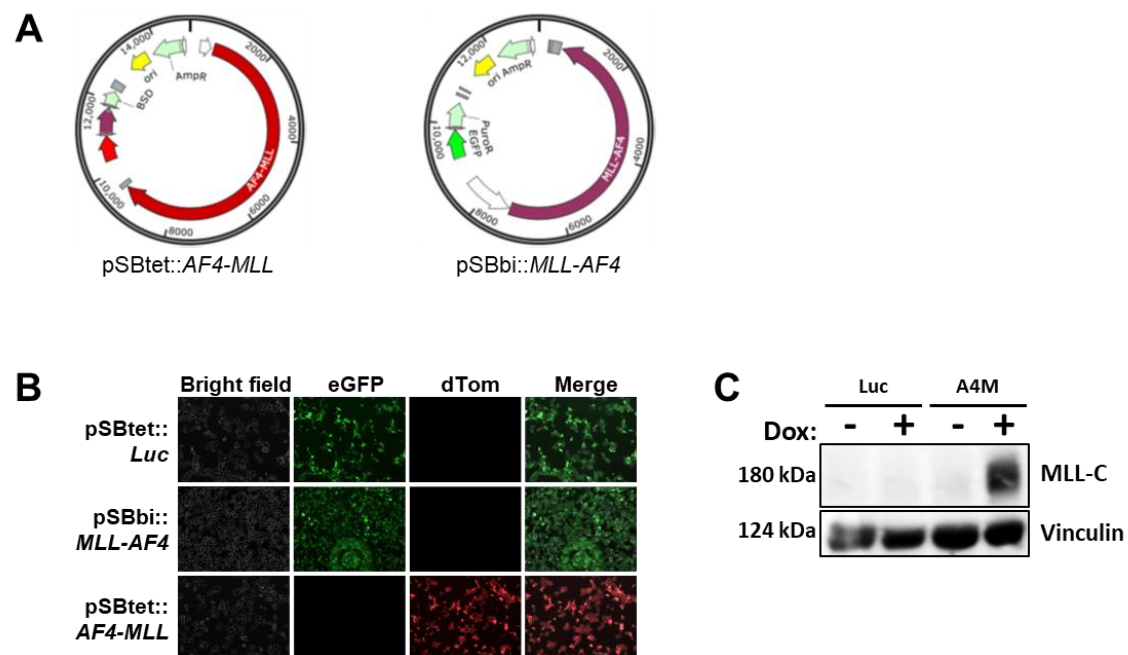


Figure 4.3.2.1: Cloning of t(4;11) fusion genes and generation of cellular t(4;11) model. Vector maps of applied Sleeping Beauty Vectors for inducible or constitutive expression of t(4;11) fusion transgenes (A). The vector for inducible expression of AF4-MLL, pSBtet::*AF4-MLL*, constitutively expresses a Blasticidine resistance cassette (BSD) and the dTomato protein. *AF4-MLL* is under control of the inducible TCE-promoter (white arrow). The vector for constitutive expression of MLL-AF4, pSBbi::*MLL-AF4*, constitutively expresses a Puromycine resistance cassette (PuroR) and the protein EGFP (EGFP). The TCE-promoter (white arrow) mediates constitutive expression of *MLL-AF4*. Integrity of Sleeping Beauty vectors was confirmed by evaluating the dTomato- and EGFP-backbone fluorescence, respectively (adapted from Wilhelm & Marschalek, 2021) (B). The inducibility of *AF4-MLL* upon the administration of 1 μ g/mL Doxycycline for 24 h was confirmed by a Western-Blot of the C-terminus of MLL (adapted from Wilhelm & Marschalek, 2021) (C). Equal loading of each sample was evaluated by probing for Vinculin.

carries AF4-MLL with AF4 exon 1-3 and MLL exons 12-37, under the control of the Doxycycline-inducible TCE-promoter. The vector pSBtet::*Luc* contains a Doxycycline-inducible Luciferase and was used for the generation of a Mock control. Of note, both Sleeping Beauty vectors carrying a MLL fusion protein further differ in the use of Puromycin

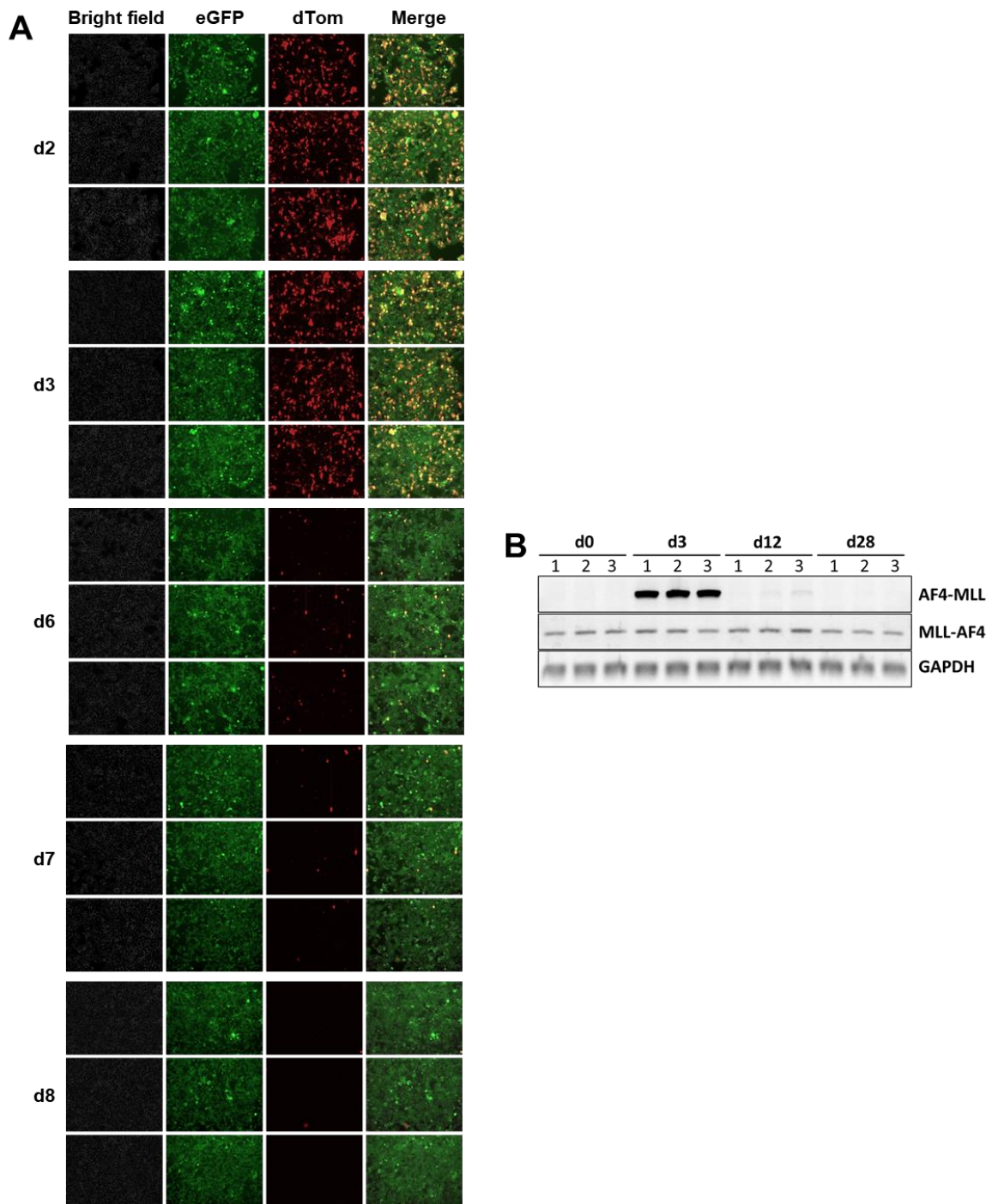


Figure 4.3.2.2: Presence of t(4;11) fusion transgene vectors throughout experimental time points. 293T cells carrying the pSBtet::*AF4-MLL* vector are detectable until day 7 as indicated by the dTomato signal (d7), while the EGFP backbone fluorescence of the pSBbi::*MLL-AF4* vector is detectable throughout all experimental time points (adapted from Wilhelm & Marschalek, 2021) (A). RT-PCR experiments indicate the presence of RNA transcripts of *MLL-AF4* and *AF4-MLL* at each experimental time point (adapted from Wilhelm & Marschalek, 2021) (B). Equal loading of RNA was confirmed by a GAPDH control. n = 3 biological replicates per sample.

and Blasticidin as selection markers and constitutively expressed eGFP and dTomato as backbone fluorescence signal, respectively (Fig. 4.4.1.1 A). The non-leukemic HEK293T cell line (ATCC CRL-3216) was used for the generation of the *in vitro* t(4;11) model.

Initially, the integrity of pSBbi::*MLL-AF4*, pSBtet::*AF4-MLL* and pSBtet::*Luc* vectors was confirmed by assessing the respective backbone fluorescence (Fig. 4.4.1.1 B). Next, the optimal administration of Doxycycline to induce AF4-MLL temporarily was evaluated (data not shown). A peak of AF4-MLL induction was observed already 48 h after the administration of 1 µg/mL Doxycycline. This was subsequently confirmed by Western Blot using an antibody that exclusively detects the C-terminus of MLL (Fig. 4.4.1.1 C).

Due to the transient character of the transfection with pSBtet::*AF4-MLL* vector, the reduction of dTomato positive cells from day 3 to day 6 confirms the expected significant drop of cells carrying Sleeping Beauty vectors integrated into the genome (Fig. 4.3.2.2 A). Therefore, newly synthesized AF4-MLL can be excluded from day 8 onwards, as 293T cells carrying the pSBtet::*AF4-MLL* vector showed no or a very limited promoter leakiness (data not shown). The overall presence of either MLL-AF4 or AF4-MLL RNA transcript in the cells at each of the four time-points was determined via RT-PCR (Fig. 4.3.2.2 B). MLL-AF4 RNA transcripts on the one hand could be detected at equal amounts throughout the entire experiment. However, AF4-MLL RNA transcripts on the other hand could be detected at high levels on day 3 and to a very low amount on day 12, while on day 28 it was completely absent (Fig. 4.3.2.2 B).

Thus, the absence of pSBtet::*AF4-MLL* vector-carrying 293T cells from day 8 onwards and the disappearance of AF4-MLL transcripts between day 12 and day 28 in the cellular model, confirm the exclusively transient appearance of AF4-MLL in the subsequent transcriptome analysis.

4.3.3. AF4-MLL induces expression of pseudogenes and non-annotated genes

MACE-seq analysis revealed overall comparable metrics of the RNA taken at day 0, day 3, day 12 and day 28 with total reads ranging from 5,444,783 to 5.805.637 and total entries ranging from 29,981 to 31,536 (Fig. 4.4.2.1 A). A large overlap of de-regulated genes can be observed on the one hand for day 0 and day 12 and on the other hand for day 3 and day 28 (Fig. 4.4.2.1 B).

For a more detailed view of the extent of de-regulation upon AF4-MLL expression, the signature of highly de-regulated genes with a threshold of at least 4-fold de-regulation compared to the Mock sample, was examined for each time point (Fig. 4.4.2.1 C). In accordance with the overall trend shown in the heat-map analysis (Fig. 4.4.2.1 B), total reads of de-regulated genes are highly resembling between day 0 and day 12; as well as day 3 and day 28. The largest fraction of up-regulated genes at day 0 and day 12 are

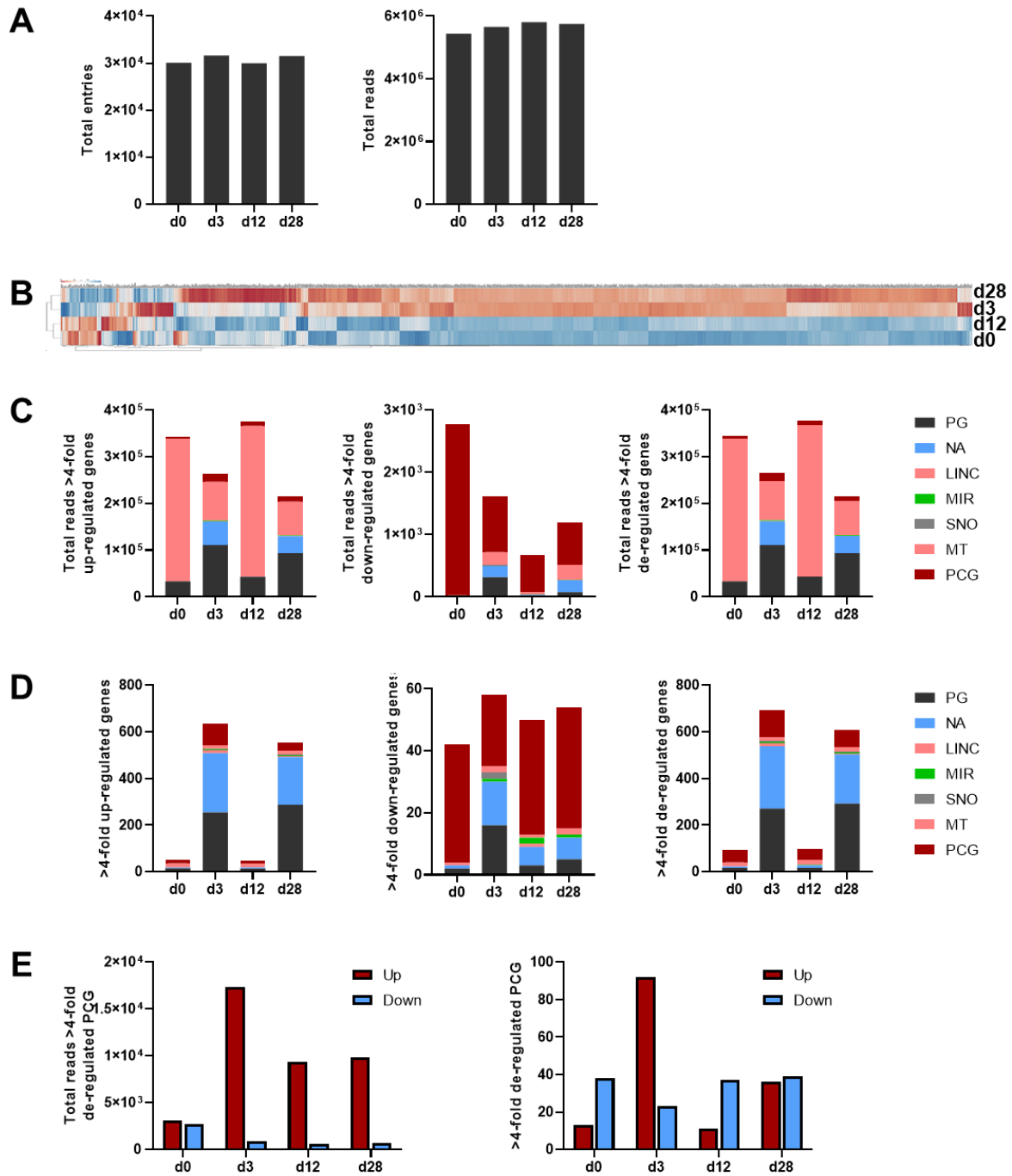


Figure 4.3.3.1: AF4-MLL promotes expression of pseudogenes and non-annotated genes. Quantification of total reads and entries of MACE-seq analysis of cellular t(4;11) model (A). Illustration of commonly regulated clusters of genes between experimental time points by Heat-map analysis (adapted from Wilhelm & Marschalek, 2021) (B). Quantitative and qualitative analysis of total reads (C) and total entries (D) of at least 4-fold de-regulated genes ($p < 0.05$) between day 0 and day 28, respectively. Genes were qualitatively categorized into pseudo- (PG), non-annotated (NA), long inter-genetic non-coding RNA (lincRNAs), microRNA (MIR), small nucleolar RNA (SNO), mitochondrial (MT) and protein-coding genes (PTG). Total reads and entries of particularly significantly up- and down-regulated PCGs (>4-fold de-regulated, $p < 0.05$) were compared at each time point (E). Quantifications were conducted with the mean of 3 biological replicates per sample.

mitochondrial (MT) genes with 305,728.51 and 323,283.14 reads, followed by pseudogenes (PG) with 33058.12 and 43329.29 reads, respectively. Protein-coding genes (PCG) are represented with 3083.6 and 9328.99 reads at day 0 and day 12, while long inter-genetic non-coding RNA (lincRNAs), microRNA (MIR), small nucleolar RNA (SNO) and non-annotated (NA) genes are all below 55 reads. While the very high abundance of MT genes resulted in overall high total reads at day 0 and day 12, other groups of genes yielded no more than 20 reads at both time points (Fig. 4.4.2.1 D). The pattern of highly up-regulated genes at day 0 and day 12 shifts utterly at day 3 when both MLL fusions are co-expressed and to a similar extent on day 28. MT genes are significantly less highly up-regulated and a significant amount of reads is derived from two additional groups of genes, PGs and NA genes (Fig. 4.4.2.1 C). With 110862.93 and 93918.47 reads for PGs and 50555.4 and 36066.71 reads for NA genes on day 3 and day 28, respectively, both groups of genes account for more than half of the signature of highly up-regulated genes. In general, the number of highly up-regulated genes at day 3 and day 28 with 634 and 554 largely exceeds total entries at day 0 and day 12 with 50 and 48, respectively (Fig. 4.4.2.1 D). This imbalance is mainly derived from highly increasing entries of PGs and NA genes accounting for more than 80% and 90% of total entries on day 3 and day 28, respectively. At day 0 and day 12, less than 39 reads of highly down-regulated PGs, NA, LINC, MIR, SNO and MT genes remain (Fig. 4.4.2.1 C). Contrarily, at day 3 and d28, 11% and 16%, of the signature of down-regulated genes is comprised of PG and NA genes, respectively. The overall number of entries of highly down-regulated genes resemble between every time point, although relatively high amounts of PGs and NA genes are notable at day 3 (Fig. 4.4.2.1 D).

The most prominent group of down-regulated genes are PCGs starting with 2,741.89 reads at day 0. Total reads of at least 4-fold up- or down-regulated PCGs are almost balanced prior to the expression of AF4-MLL on day 0 (Fig. 4.4.2.1 E). Nevertheless, emerging AF4-MLL drops highly down-regulated PCGs irreversibly to 895.68 on day 3, 597.80 on day 12 and 680.35 reads on day 28. *Vice versa*, reads of highly up-regulated PCGs are significantly increased upon the expression of AF4-MLL with 17387.73 on day 3, 9328.99 on day 12 and 9873.04 on day 28 compared to 3083.60 reads on day 0 (Fig. 4.4.2.1 E). However, entries of down-regulated PCGs are exclusively reduced at day 3. A 7-fold and 3-fold increase of up-regulated PCGs can be observed for day 3 and day 28 when compared to day 0 and day 12, respectively (Fig. 4.4.2.1 E).

The analysis of shared up-regulated genes revealed remarkable 418 overlapping genes at day 3 and day 28 mostly comprising of PGs and NA genes (Fig. 4.3.3.2 A). Relatively low amounts of highly up-regulated genes at day 0 and day 12 could be observed with 12 and 4 genes, respectively, considering that 25 up-regulated genes are shared at every time

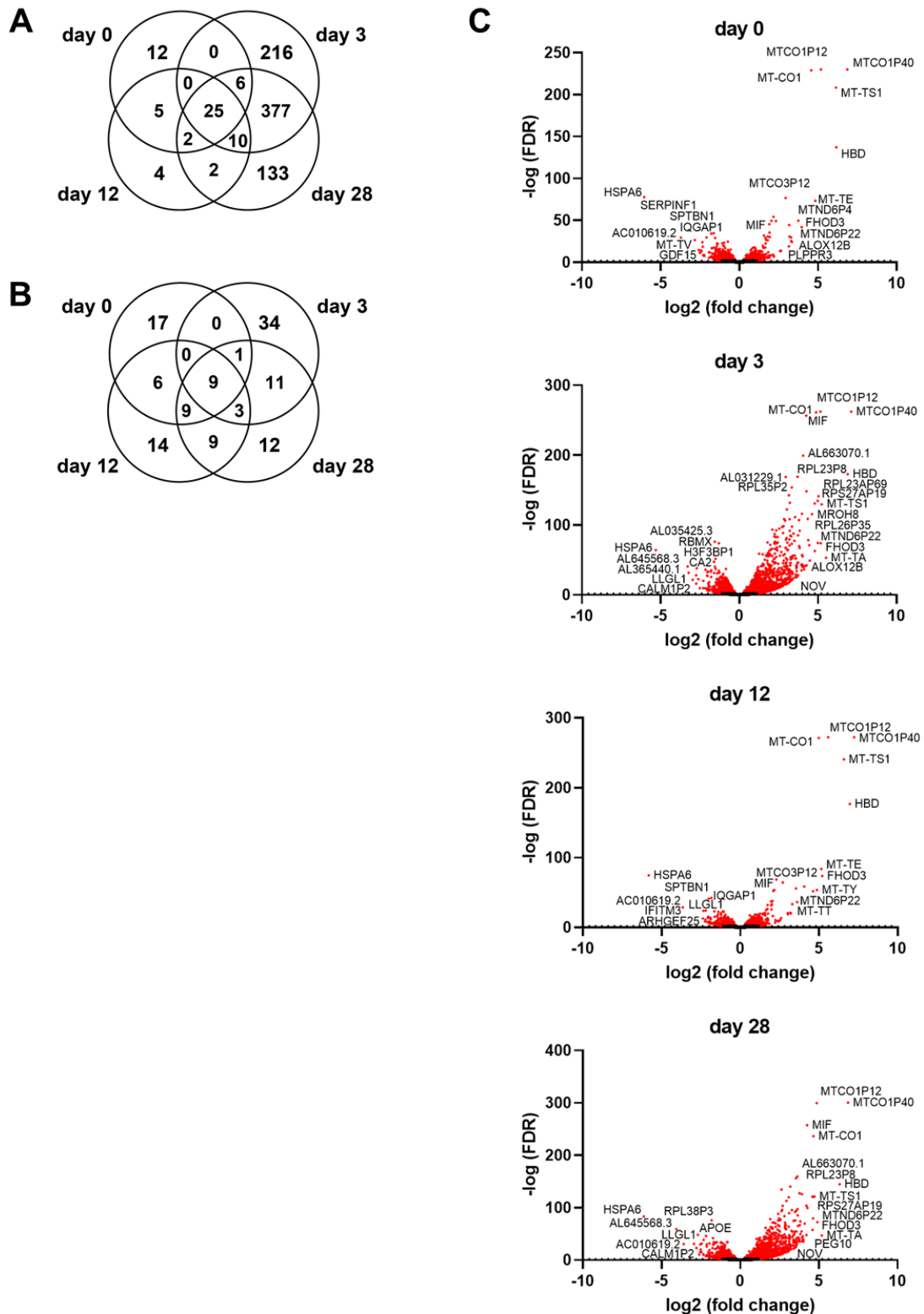


Figure 4.3.3.2: Lost AF4-MLL-induced signature of up-regulated genes reappears over time. Evaluation of shared up- (A) and down-regulated genes (B) (\log_2 values ± 2 , >10 reads, p -value < 0.05) between each experimental time point illustrated in a Venn diagram (adapted from Wilhelm & Marschalek, 2021). Illustration of highly de-regulated genes taking into account the \log_2 fold-change and the FDR (adapted from Wilhelm & Marschalek, 2021) (C). The depicted Volcano plots contain all genes of each time-point obtained by MACE-seq analysis. Quantifications were conducted with the mean of 3 biological replicates per sample.

point. To the overall less pronounced down-regulation of genes, little overlap of genes was found in the analysis of shared down-regulated genes (Fig. 4.3.3.2 B).

Complementing the analysis of highly up- and down-regulated genes, the FDR was included as a further dimension to identify particularly significant and simultaneously highly de-regulated targets (Fig. 4.3.3.2 C). A massive de-regulation of few genes with $-\log_{10}$ FDR values of nearly 300 can be observed from day 0 to day 28 leading to a poorly discernible separation of de-regulated genes with \log_2 fold changes between -2 and -1 as well as 1 and 2 (Fig. 4.3.3.2 C). With $-\log_{10}$ FDRs larger than 200, the gene for *Mitochondrially Encoded Cytochrome C Oxidase I (MT-CO1)* and its two pseudogenes *MTCO1P12* and *MTCO1P40* protrude at all four time points (Fig. 4.3.3.2 C). *MT-CO1* is associated to the cytochrome c oxidase and is involved in the mitochondrial respiratory chain. Another highly significant up-regulated target upon the expression of MLL-AF4 is the gene for *Macrophage Migration Inhibitory Factor (MIF)* that is involved in the suppression of anti-inflammatory effects. Besides numerous mitochondrial and ribosomal proteins, the gene for *Hemoglobin Subunit Delta (HBD)*, for *Arachidonate 12-Lipoxygenase, 12R Type (ALOX12B)* and for *Formin Homology 2 Domain Containing 3 (FHOD3)* are highly up-regulated at each time point. Upon the expression of AF4-MLL until day 28, the genes for *Paternally Expressed 10 (PEG10)* that codes for a retrotransposon-derived protein and *NOV or Cellular Communication Network Factor 3 (CCN3)* are specifically up-regulated. The gene for chaperone *Heat Shock Protein Family A (Hsp70) Member 6 (HSP6)*, the processed transcript *AC010619.2* and the gene for *Lethal Giant Larvae Homolog 1, Scribble Cell Polarity Complex (LLGL1)* constitute highly significantly down-regulated targets from the beginning of the expression of MLL-AF4 on day 0 until day 28 (Fig. 4.3.3.2 C).

Notably, the overexpression of anti-inflammatory MIF that is particularly up-regulated at day 3 (22-fold) and day 28 (21-fold) has been associated with poor overall survival and disease-free survival in childhood ALL patients (Sharaf-Eldein et al., 2018). Similarly, the up-regulated *PEG10* was shown to be overexpressed in B-ALL cells and it is suggested to stabilize caspase-3 and caspase-8 in B-ALL to rescue leukemic cells from TNF α -mediated apoptosis (Chunsong et al., 2006). Moreover, *PEG10*-mediated resistance to apoptosis is suggested to be further supported by the interaction with SIAH1 (Okabe et al., 2003).

All in all, the short-term expression of AF4-MLL results in a significant over-expression of not-annotated genes and pseudogenes., and an irreversible elevation of total reads of PCGs. Moreover, signatures of total and at least 4-fold up-regulated genes disappeared upon the short-term expression of AF4-MLL, but reappeared at a later time point.

4.3.4. AF4-MLL promotes clonal evolution

The previously shown analyses of MACE-seq highlighted similarities between day 3 and day 28; and a deviated intermediate time point day 12. The loss of the signature on day 12 might be explained by an initially small sub-population of AF4-MLL reprogrammed cells whose dominance could be first detected on day 28. Probably, the signature on day 12 resembles day 0 as the newly emerging dominant sub-population still counts for only a small fraction of the total cellular population.

So far, *de novo* and shut down genes were not covered by merely looking at up- and down-regulation of genes because of a missing value to refer to. Implementing newly expressed

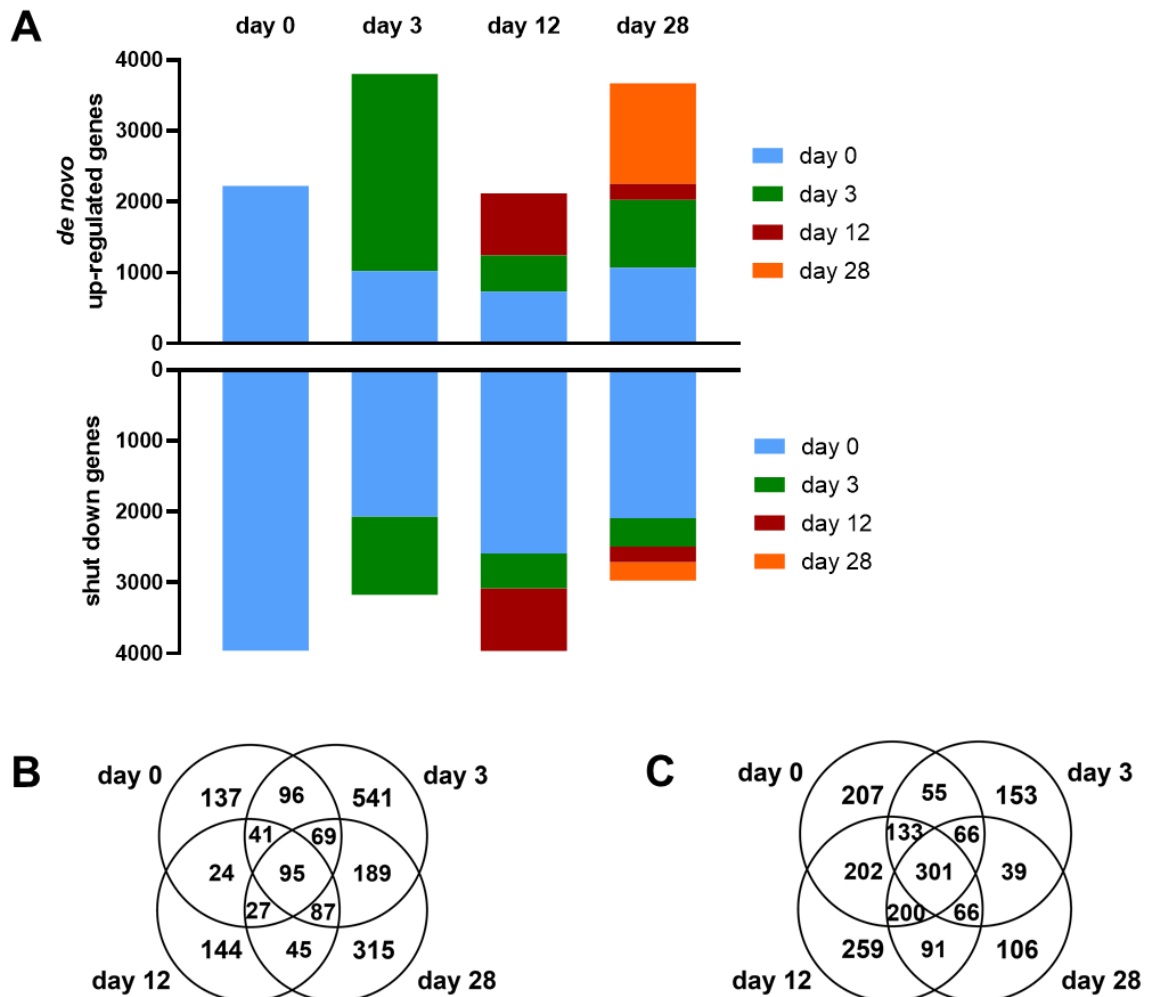


Figure 4.3.4.1: AF4-MLL activates *de novo* genes and shut down genes. Quantification of *de novo* genes and shut down genes at day 0, day 3, day 12 and day 28 (adapted from Wilhelm & Marschalek, 2021) (A). Analysis of overlapping *de novo* (B) or shut down PCGs (C) between each experimental time-point (adapted from Wilhelm & Marschalek, 2021). Quantifications were conducted with the mean of 3 biological replicates per sample.

genes or genes interrupted in expression, the hypothesis of a selection process initiated by AF4-MLL expression was tested in detail.

Of 2221 genes that are the first time expressed upon the emergence of MLL-AF4, 1021 are maintained upon the expression of AF4-MLL on day 3, 732 on day 12 and 1067 on day 28 (Fig. 4.3.4.1 A). The co-expression of both MLL fusion proteins results in 2782 *de novo* genes of which 511 and 959 are found on day 12 and day 28, respectively. Thus, the expression of AF4-MLL at day 3 resulted in a 1.25-fold increase of newly emerging genes when compared to the mere expression of MLL-AF4 at day 0 (Fig. 4.3.4.1 A). Upon the co-expression of both MLL fusion proteins at day 3, AF4-MLL-related *de novo* genes account for 73% of all *de novo* genes. Of 876 *de novo* genes on day 12 remain 227 on day 28 on which 1419 *de novo* genes could be detected. 42% of *de novo* genes at day 12 emerge for the first time whereas 35% and 24% of *de novo* genes originated at day 0 and day 3, respectively weakening the hypothesis of a AF4-MLL-induced selection process at day 3 (Fig. 4.3.4.1 A). Moreover, 66% of *de novo* genes at day 12 arose after the short-time expression of AF4-MLL. At day 28, 71% of all *de novo* genes emerged between day 3 and day 28. Importantly, 39% of *de novo* genes originated at day 28. 1419 genes newly expressed at day 28 indicate an adaptation process that is not completed 4 weeks after the short-term expression of AF4-MLL. Hence, 42% and 39% emergence of primarily emerging *de novo* genes at day 12 and day 28, respectively, suggest a clonal evolution rather than an AF4-MLL-related selection process.

Next, the analysis of *de novo* and shut down PCGs revealed that majority of *de novo* PCGs emerge at day 3 and day 28, while shut down PCGs were mainly observed at day 0 and day 12 (Fig. 4.3.4.1 B+C). Additionally, the signatures of shut down PCGs are significantly more overlapping when compared to *de novo* PCGs.

In conclusion, the short-term expression of AF4-MLL endorses the *de novo* expression and shut down of genes. The evolving signatures indicate that AF4-MLL initiates a clonal evolutionary process rather than a selection process as indicated by previous analysis (see chapter 2.3.1.2).

4.3.5. Signatures of the *in vitro* cellular t(4;11) model overlap with *in vivo* gene sets of infant B-ALL patients

Although the t(4;11) model rather focusses on the capability of AF4-MLL to alter gene transcription in a long-term fashion than to mimic leukemia development, a GSEA analysis was conducted to reveal possible correlations between de-regulated genes *in vitro* of day 3, day 12 and day 28 with *in vivo* gene sets of t(4;11) patients. Despite using non-leukemic

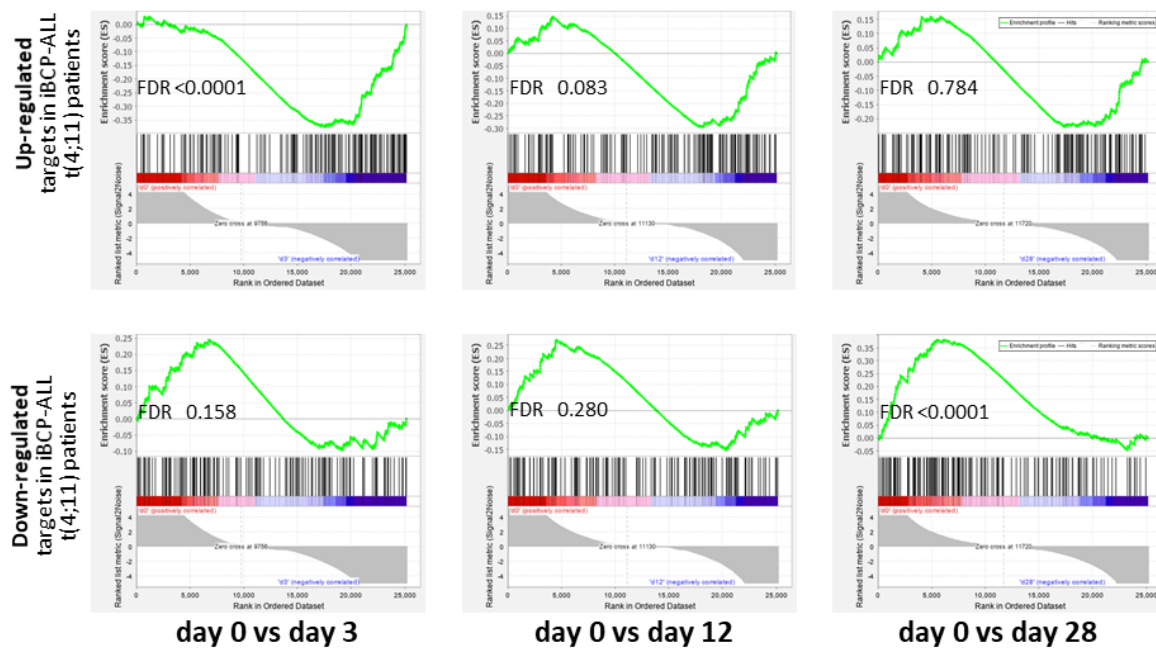


Figure 4.3.5.1: Gene expression analysis reveals correlation between *in vitro* t(4;11) model and *in vivo* gene sets of infant B-ALL patients. GSEA analysis was conducted comparing the signatures of the cellular t(4;11) leukemia model at day 3, day 12 and day 28 with de-regulated target genes observed in infant B-cell precursor ALL patients (Agraz-Doblas et al., 2019). FDR = False discovery rate.

293T cells, the co-expression of t(4;11) fusion proteins resulted in a significant correlation between the signatures of day 3, day 12 and day 28 with de-regulated target genes found in infant B-cell precursor (iBCP) ALL patients (Agraz-Doblas et al., 2019) (Fig. 4.3.5.1 A). Up-regulated t(4;11) target genes of iBCP-ALL patients on the one hand are significantly enriched to the signature of day 3 (FDR < 0.001), but lack a correlation to day 12 (FDR = 0.083) and day 28 (FDR = 0.784). Down-regulated t(4;11) target genes on the other hand, are not correlated to the signature of day 3 (FDR = 0.159) or day 12 (FDR = 0.280), but highly correlate to day 0 when compared to day 28 (FDR < 0.001) (Fig. 4.3.5.1 A).

Considering the non-leukemic background of 293T cells, GSEA analysis with iBCP-ALL patient data indicates a short-term effect of AF4-MLL on t(4;11) up-regulated genes and a long-term effect of AF4-MLL on t(4;11) down-regulated genes.

4.3.6. k-means clustering indicates novel AF4-MLL-associated genes

A screening based on k-means clustering was conducted to unravel further AF4-MLL associated genes (Fig. 4.3.6.1 A+B). Cluster selection was either based on the assumption of a continuous differential gene expression upon expression of AF4-MLL (Fig. 4.3.6.1 A)

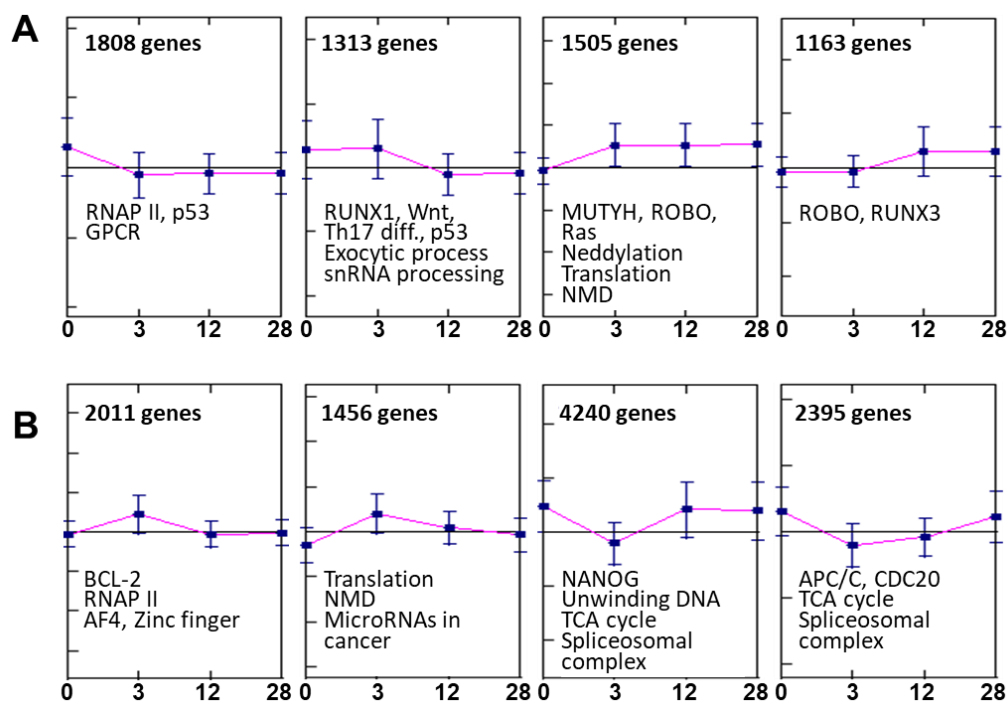


Figure 4.3.6.1: Modelling putative modes of action of t(4;11) fusion proteins during leukemogenesis using k means based clusters enables the identification of novel AF4-MLL-associated genes. Clusters were selected based on the assumption of a continuous differential gene expression upon the expression of AF4-MLL (A) or the assumption of a short-term direct correlation of AF4-MLL (B). Only genes with an FDR <0.25 were selected for the generation of clusters. Depicted genes and pathways in each cluster are derived pathway enrichment analysis of genes of the respective cluster.

or the assumption of a direct correlation between differential genes expression and AF4-MLL expression (Fig. 4.3.6.1 B).

The statistical strength of each cluster generation was further enhanced by excluding de-regulated genes with an FDR > 0.25. A continuous differential gene expression upon AF4-MLL expression was modelled assuming an immediate effect of AF4-MLL at day 3 or a delayed adaption on day 12 (Fig. 4.3.6.1 A). Hence, genes included into the cluster for an immediate response were required to meet the conditions that day 0 unequal day 3, day 12, and day 28 as well as that d3, d12 and day 28 are equal. The cluster for a delayed adaptation was based on the condition that day 0 equals d3, day 12 equals day 28, but day 0 and day 3 unequal day 12 and day 28. Contrarily, clusters modelling a short-term effect of AF4-MLL were generated by the assumption that expression data of day 3 exceeds or undercuts the expression of d0, day 12 and day 28. Four of the best fitting clusters of each model were used for pathway enrichment analyses and knowledge-based STRING network analysis (Fig. 4.3.6.1 A+B). The pathway enrichment analysis for the cluster containing 1808 genes that are constantly down-regulated immediately upon the expression of AF4-MLL revealed pathways related to RNA polymerase II (RNAP II), the

universal tumor suppressor gene p53 and G-protein coupled receptors (GPCR) (Fig. 4.3.6.1 A). 1313 genes were assigned to the cluster describing a delayed but permanent down-regulation upon short-time AF4-MLL expression. Here, pathways related to the hematopoietic transcription factor RUNX1, p53 and Wnt could be identified. Of note, the cluster with a total of 1163 delayed up-regulated genes is associated to *Runt-related transcription factor 3 (RUNX3)*-related pathways (Fig. 4.3.6.1 A). Further on, pathways linked to RNAPII, AF4, B-cell lymphoma 2 (BCL-2), nonsense-mediated decay (NMD) and miRNAs in cancer were identified within the clusters of 2011 and 1456 genes, respectively, that are directly correlated to the expression of AF4-MLL (Fig. 4.3.6.1 B). Enriched pathways related to the Spliceosomal complex, the tricarboxylic acid (TCA) cycle, anaphase promoting complex (APC/C) and the cell division cycle protein 20 homolog (CDC20) could be detected in temporarily down-regulated genes during the co-expression of both MLL fusion proteins at day 3 (Fig. 4.3.6.1 B). Key nodes in the STRING network analysis of clusters containing constantly up-regulated genes upon AF4-MLL expression are genes for *Ubiquitin C (UBC)*, *SMAD3* and numerous ribosome-related proteins. Highly connected nodes in the STRING network obtained from clusters of genes that are up-regulated particularly on day 3, are genes for *Mitogen-Activated Protein Kinase 3 (MAPK3)*, *RELA Proto-Oncogene, NF-KB Subunit (RELA)* also known as transcription factor p65 and various ribosomal proteins.

Contrarily, the STRING network of clusters for constantly down-regulated genes are characterized by the genes for *CDC20*, *Ataxia Telangiectasia Mutated Serine/Threonine Kinase (ATM)* and *Mitotic Checkpoint Serine/Threonine Kinase Budding Uninhibited By Benzimidazoles 1 (BUB1)*. Moreover, STRING networks of clusters covering short-term down-regulated genes are comprised of highly-connected genes for *Cyclin B2 (CCNB2)*, *Decapping Scavenger Enzyme (DCPS)* that is involved in pre-mRNA splicing, miRNA turnover and decapping of mRNAs, *Nucleoporin 133 (NUP133)*, *Proteasome 20S Subunit Alpha 6 (PSMA6)* and *Nucleolar Protein 58 (NOP58)*.

In summary, k-means clustering identified genes that are potentially useful in deciphering the role of AF4-MLL in t(4;11) leukemia at different temporal contexts.

4.4. t(4;11) fusion proteins endorse transcription of mitochondrial genes but has no effect on mitochondrial respiration *in vitro*

Mitochondrial genes represent a significant proportion of total reads of highly de-regulated genes in the cellular t(4;11) model, upon the expression of MLL-AF4 and AF4-MLL (Fig.

4.4.2.1 C). Despite the molecular heterogeneity between different types of ALL, the increased metabolism of leukemic cells indicate major adaptation processes in mitochondria. Therefore, in this study the expression of mitochondrial genes obtained from the MACE-seq analysis was analyzed and subsequently the role of t(4;11) fusion proteins on mitochondrial respiration evaluated.

4.4.1. t(4;11) fusion proteins activate mitochondrial genes

Differential expression of genes in mitochondria was examined in the cellular t(4;11) model to elucidate the decisive role of each t(4;11) fusion protein on individual mitochondrial genes.

The gene for *Mitochondrially Encoded TRNA-Val (MT-TV)* that constitutes a mitochondrial tRNA represents the unique down-regulated mitochondrial gene across all time points in the t(4;11) model. The constant down-regulation of *MT-TV* indicates an association to particularly MLL-AF4 (Fig. 4.4.1.1). In addition, the expression of the gene for *Mitochondrially Encoded TRNA-Ser (AGU/C) 2 (MT-TS2)* is decreased from day 0 to day 28. However, a -2.24 log₂ fold-change on day 3 compared to log₂ fold-changes of -0.31 at day 0, -1.21 at day 12 and -0.42 at day 28 suggest an involvement of AF4-MLL (Fig. 4.4.1.1). Moreover, the genes for mitochondrial tRNAs *Mitochondrially Encoded TRNA-Gly (GGN) (MT-TG)*, *Mitochondrially Encoded TRNA-Lys (AAA/G) (MT-TK)*, and *Mitochondrially Encoded TRNA-Leu (UUA/G) 1 (MT-TL1)* as well as the gene for *Mitochondrially Encoded ATP Synthase Membrane Subunit 6 (MT-ATP6)* are down-regulated at day 3 (Fig. 4.4.1.1).

Often, de-regulated mitochondrial genes are up-regulated upon the expression of MLL-AF4 and AF4-MLL (Fig. 4.4.1.1). The top up-regulated mitochondrial genes at each of the four time points are *Mitochondrially Encoded Cytochrome C Oxidase I (MT-CO1)*, *Mitochondrially Encoded NADH:Ubiquinone Oxidoreductase (MT-ND6)*, *Mitochondrially Encoded TRNA-Ile (AUU/C) (MT-TI)*, *Mitochondrially Encoded TRNA-Gln (CAA/G) (MT-TQ)* and *Mitochondrially Encoded TRNA-Ser (UCN) 1 (MT-TS1)*. While the genes for *Mitochondrially Encoded TRNA-Ala (GCN) (MT-TA)* and *Mitochondrially Encoded TRNA-Arg (CGN) (MT-TR)* are up-regulated upon AF4-MLL expression at day 3 and day 28, the genes for *Mitochondrially Encoded 12S RRNA (MT-RNR1)*, *Mitochondrially Encoded 16S RRNA (MT-RNR2)*, *Mitochondrially Encoded TRNA-Cys (UGU/C) (MT-TC)*, and *Mitochondrially Encoded TRNA-Phe (UUU/C) (MT-TF)* are constantly up-regulated upon the expression of AF4-MLL (Fig. 4.4.1.1).

Overall, both t(4;11) fusion proteins up-regulate the majority of mitochondrial targets in the cellular t(4;11) model and only few mitochondrial genes are down-regulated by either MLL-AF4 or AF4-MLL.

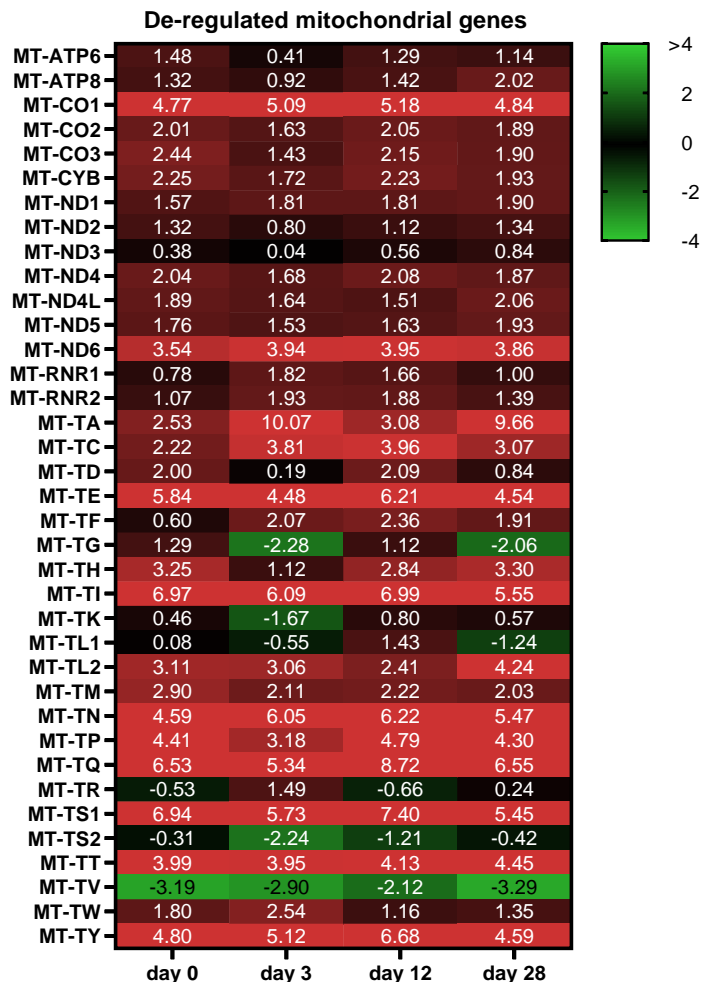
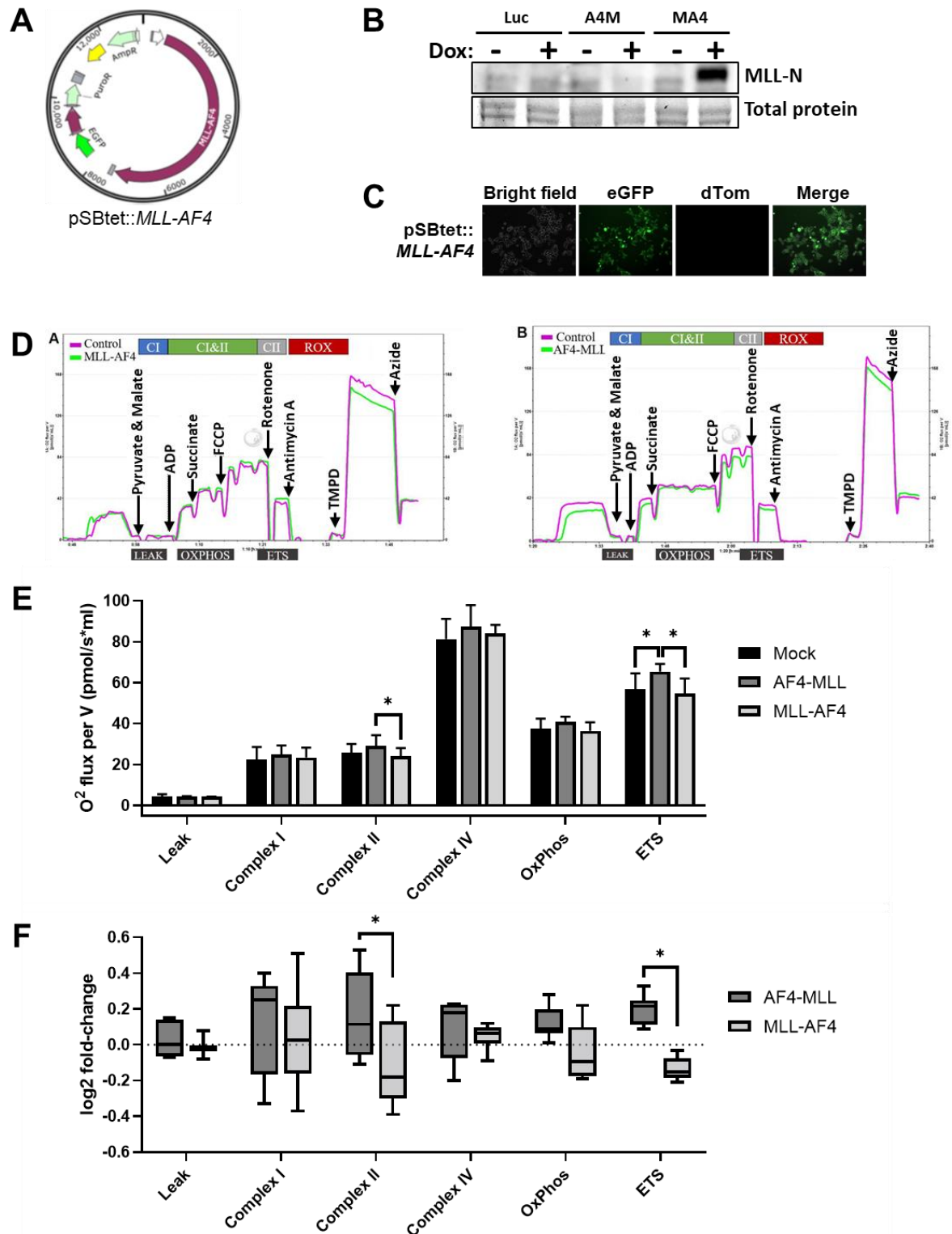


Figure 4.4.1.1: t(4;11) fusion proteins elevate expression of the majority of mitochondrial genes. Quantification of de-regulated mitochondrial genes of the cellular t(4;11) model at day 0, day 3, day 12 and day 28 illustrated in a heat-map.

4.4.2. MLL fusion proteins have minor effects on mitochondrial respiration *in vitro*

The MACE-seq analysis unraveled an overall up-regulation of mitochondrial genes upon the expression of MLL-AF4 and AF4-MLL in the cellular t(4;11) model. The impact of highly de-regulated mitochondrial genes upon the expression of MLL fusion proteins on



mitochondrial respiration remains unclear and is of particular interest to further decipher the role of MLL fusion proteins in a t(4;11) leukemia. This was addressed in this work *in vitro* by measuring mitochondrial respiration with a respirometer upon the expression of MLL-AF4 or AF4-MLL.

Figure 4.4.2.1: t(4;11) fusion proteins play a minor role in mitochondrial respiration *in vitro*. Using the Sleeping Beauty vectors *pSBtet::AF4-MLL* (see Figure 2.3.1.2) and *pSBtet::MLL-AF4* (A), 293T cells were generated expressing either MLL-AF4 or AF4-MLL. *pSBtet::MLL-AF4* constitutively expresses a Blasticidine resistance cassette (BSD) and the EGFP protein. *MLL-AF4* is under control of the inducible TCE-promoter (white arrow). The inducibility of *MLL-AF4* upon the application of 1 µg/mL Doxycycline for 24 h was confirmed by a Western-Blot of the N-terminus of MLL (adapted from Wilhelm & Marschalek, 2021) (B). Total protein staining confirmed equal loading of each sample. The presence of *pSBtet::MLL-AF4* vector in all stably transfected 293T cells was confirmed by the presence of EGFP back-bone fluorescence detected by fluorescence microscopy (adapted from Wilhelm & Marschalek, 2021) (C). Evaluation of the oxidative potential of distinct steps of the mitochondrial respiratory chain (D). A single representative experiment is shown conducted with MLL-AF4 or AF4-MLL expressing 293T cells (D). Quantification of the oxidative potential of distinct steps of the mitochondrial respiratory chain (E). Illustration of relative changes between MLL-AF4 and AF4-MLL expressing cells (F). n = 12 biological replicates per sample. Values represent the mean ± standard deviation. Samples were analyzed in cooperation with Constantin Kondak and Irene Ballesteros. Statistical significance was calculated by two-sided ttest. Asterisks indicate p-values as *(p < 0.05).

Due to the great number of de-regulated mitochondrial genes at each time point of the cellular t(4;11) model, the respiration assay was conducted accordingly in 293T cells expressing either MLL-AF4 or AF4-MLL. On the one hand, the vector *pSBtet::AF4-MLL* that was previously applied in the t(4;11) model, was stably transfected into 293T cells for Doxycycline-inducible expression of AF4-MLL (Fig. 4.3.1.1 A-C). Using the identical Sleeping beauty-based plasmid backbone of the *pSBtet::AF4-MLL* vector, the *pSBtet::MLL-AF4* vector was transfected for inducible expression of MLL-AF4 (Fig. 4.4.2.1 A). 293T cells carrying the *pSBtet::Luc* vector served as Mock control. Expression levels of MLL-AF4 upon the administration of 1 µg/mL Doxycycline were confirmed by Western Blot (Fig. 4.4.2.1 B). Prior to the mitochondrial respiration assay, fluorescence microscopy confirmed that the newly generated *pSBtet::MLL-AF4* vector was present in all 293T cells upon 3 rounds of selection with Puromycin (Fig. 4.4.2.1 C).

The effect of MLL-AF4 or AF4-MLL on mitochondrial respiration was analyzed using the O2k-FluoRespirometer (Oroboros Instruments, Innsbruck, Austria) in collaboration with the laboratory of Prof. Jochen Klein and especially the support of Constantin Kondak. Upon the induction with 1 µg/mL Doxycyclin for 48 h, cells were permeabilized and administered to the respirometer. Since the respirometer consists of two identical reaction chambers, obtained respiratory data of MLL-AF4 or AF4-MLL expressing cells were constantly compared to Mock cells that alternately occupied one of the two reaction chambers. Each respiration experiment consists of identical administration of substrates that uncouple, inhibit or promote specific steps of the mitochondrial respiratory chain. The oxygen consumption of mitochondria from MLL-AF4 and AF4-MLL expressing cells on the one hand, and Mock cells on the other hand, was measured after the injection of each substrate

into the reaction chamber (Fig. 4.4.2.1 D). In the context of the tremendous de-regulation of mitochondrial genes in the t(4;11) model, differences in oxygen consumption are restricted to specific parts of mitochondrial respiration. The maxima of oxidative phosphorylation, complex I, complex IV are not significantly altered between MLL-AF4-expressing, AF4-MLL-expressing and Mock-cells (Fig. 4.4.2.1 E+F). However, maxima of Succinate-Q oxidoreductase (complex II) and the capacity of the electron transfer system (ETS) significantly differ between the two MLL fusion proteins. In both cases, the capacity of the mitochondrial respiratory unit is increased upon the expression of AF4-MLL in comparison to MLL-AF4. While no significant difference between the maximum capacity of complex II in AF4-MLL-expressing and Mock-cells can be detected, the maxima of ETS is significantly increased when AF4-MLL is expressed compared to Mock-cells (Fig. 4.4.2.1 E+F).

In summary, the maximal oxidative capacity of ETS and complex II is different in MLL-AF4- or AF4-MLL-expressing cells. Nevertheless, overall mitochondrial respiration appears to be less impaired upon 48 h expression of MLL fusion proteins *in vitro* as indicated by the tremendous deregulation of mitochondrial genes.

4.5. AF4-MLL impacts chromatin signature over time

The brief expression of AF4-MLL for two days *in vitro* resulted in a transcriptional signature that was still significantly altered three weeks later (see chapter 2.3). This suggests that reciprocal AF4-MLL can initiate a clonal evolutionary process in concert with MLL-AF4. The underlying molecular mechanism of AF4-MLL, in addition to MLL-AF4 being known as a strong activating transcription factor, is still largely unknown. Due to an N-terminus filled by the universal transcription activator AF4 and the simultaneous omission of domains required for the recognition of wild-type MLL target genes, AF4-MLL is suspected to have a comprehensive effect on the accessibility of chromatin. Hence, this work next examined, whether the observed long-lasting effects on transcriptional signatures upon the short-time expression of AF4-MLL correlate with changes in chromatin status.

4.5.1. A cellular t(4;11) model to study accessibility of chromatin

The accessibility of the entire chromatin after the expression of t(4;11) fusion proteins was assessed by the Assay for Transposase-Accessible Chromatin using sequencing (ATAC-seq) with an approach that was in line with the previous MACE-seq experiment (see

chapter 2.3) (Fig. 4.5.1.1). Initially, the chromatin status was evaluated after the Doxycycline-induced expression of MLL-AF4 for 48 hours (day 0). Subsequently, samples were taken 48 hours upon the Doxycycline-induced expression of AF4-MLL and the constitutively expressed MLL-AF4 (day 3). For the assessment of persisting changes of accessible DNA regions, ATAC-seq was conducted with cells from experimental day 3 that were maintained for another 25 days lacking Doxycycline-induced expression of AF4-MLL (Fig. 4.5.1.1).

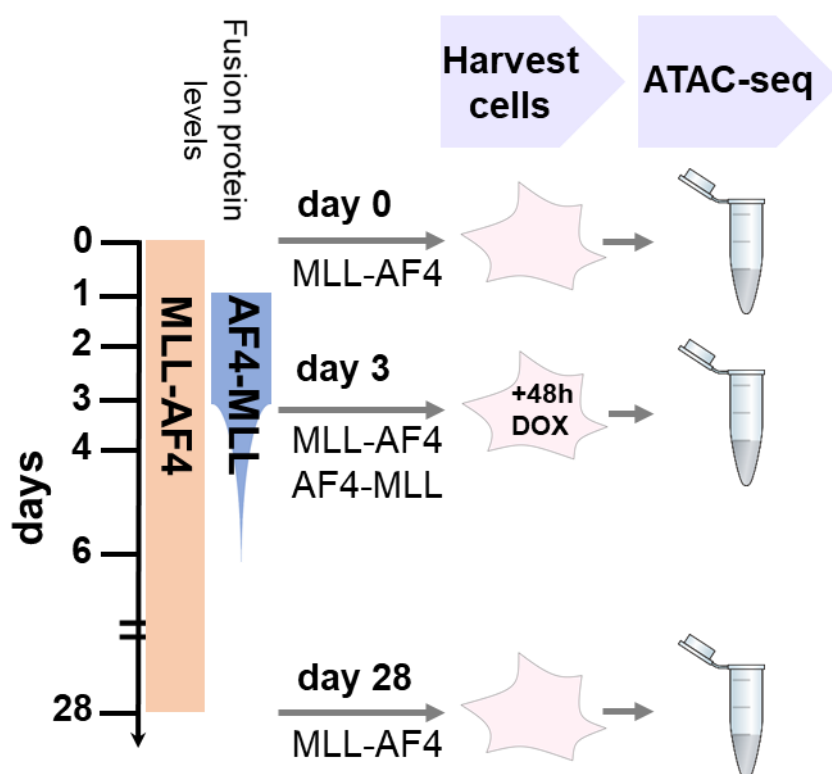


Figure 4.5.1.1: A cellular t(4;11) model to study accessibility of chromatin upon short-term expression of AF4-MLL. The approach to assess the chromatin status *in vitro* in 293T cells that constitutively express MLL-AF4 and additionally, for a 48 h interval, AF4-MLL is equivalent to the cellular t(4;11) model to study gene expression signatures. The Assay for Transposase-Accessible Chromatin using sequencing (ATAC-seq) was conducted with 293T cells that particularly express MLL-AF4 (day 0), upon the co-expression of both MLL-fusion proteins for 48 h (day 3), and 25 days after the short interval of AF4-MLL expression (day 28). n = 3 biological replicates per sample.

4.5.2. Long-term altered chromatin state upon short-term expression of AF4-MLL

Initially, peaks of ATAC-seq from day 0, day 3 and day 28 were annotated to genomic features (Fig. 4.5.2.1 A). The expression of MLL-AF4 alone at day 0 resulted in a strong relative increase of peaks in introns and a sharp relative reduction of peaks located in the promoter and transcription start site (TSS) region. Besides an increase of intergenic peaks at day 3, only minor changes in the relative distribution of genomic features could be observed upon the co-expression of both t(4;11) fusion proteins when compared to the Mock sample (Fig. 4.5.2.1 A). Of note, intergenic peaks at day 28 returned to levels as observed in the Mock sample. Focusing on the proximity of peaks to unique genes, a distinct increase of peaks with a distance to a unique gene of more than 10 kilobases can be observed at day 0 when particularly MLL-AF4 is expressed (Fig. 4.5.2.1 B). Remarkably, peaks in close proximity to unique genes dominate in the Mock sample as well as at day 3 and day 28. Overall, this indicates a MLL-AF4- rather than AF4-MLL-related effect of ATAC-seq peaks regarding genomic features and distance to neighbor genes.

Studying the accessibility of chromatin upon the expression of t(4;11) fusion proteins in comparison to the Mock sample, little comparable signatures are apparent at each time point (Fig. 4.5.2.1 C). In particular, accessible and non-accessible chromatin regions at day 0, day 3 and day 28 barely overlap. Hence, the short-time expression of AF4-MLL seems to significantly alter the pattern of accessible chromatin regions. Furthermore, a novel chromatin signature evolves three weeks after the short-time expression of AF4-MLL, that overlaps to a very limited extent to preceding signatures (Fig. 4.5.2.1 C).

Next, plotting the log₂ fold-change on the one hand and the significance of the altered accessibility of a chromatin region on the other hand, chromatin regions of mitochondrial genes, with $-\log_{10}$ p-values greater than 30, protrude particularly at day 28 (Fig. 4.5.2.1 D). In accordance with MACE-seq data from chapter 2.3, the processed transcript *AC010619.2* also protrudes on a chromatin level with significantly less accessible chromatin throughout all experimental time points. A highly-significant increase of chromatin accessibility specifically at day 0 is observable at genes coding for the *transcriptional repressors Zinc Finger E-Box Binding Homeobox 2 (ZEB2)* and *Zic Family Member 2 (ZIC2)* as well as *Protohadherin 9 (PCDH9)*; and accordingly specifically for day 3, the genes for *ER Membrane Protein Complex Subunit 4 (EMC4)*, *Neurogenin 1 (NEUROG1)* and for the transcription factor *Forkhead Box B1 (FOXB1)*; and specifically for day 28 the genes for *Tryptophan 2,3-Dioxygenase (TDO2)* and *Doublecortin Domain Containing 2C (DCDC2C)*. Increased accessible chromatin at day 0 and day 3 is also seen at genes for *Heat Shock Protein Family A (Hsp70) Member 5 (HSPA5)* that codes for an anti-apoptotic regulator and *Transcription Elongation Factor A Like 8 (TCEAL8)*; and at day

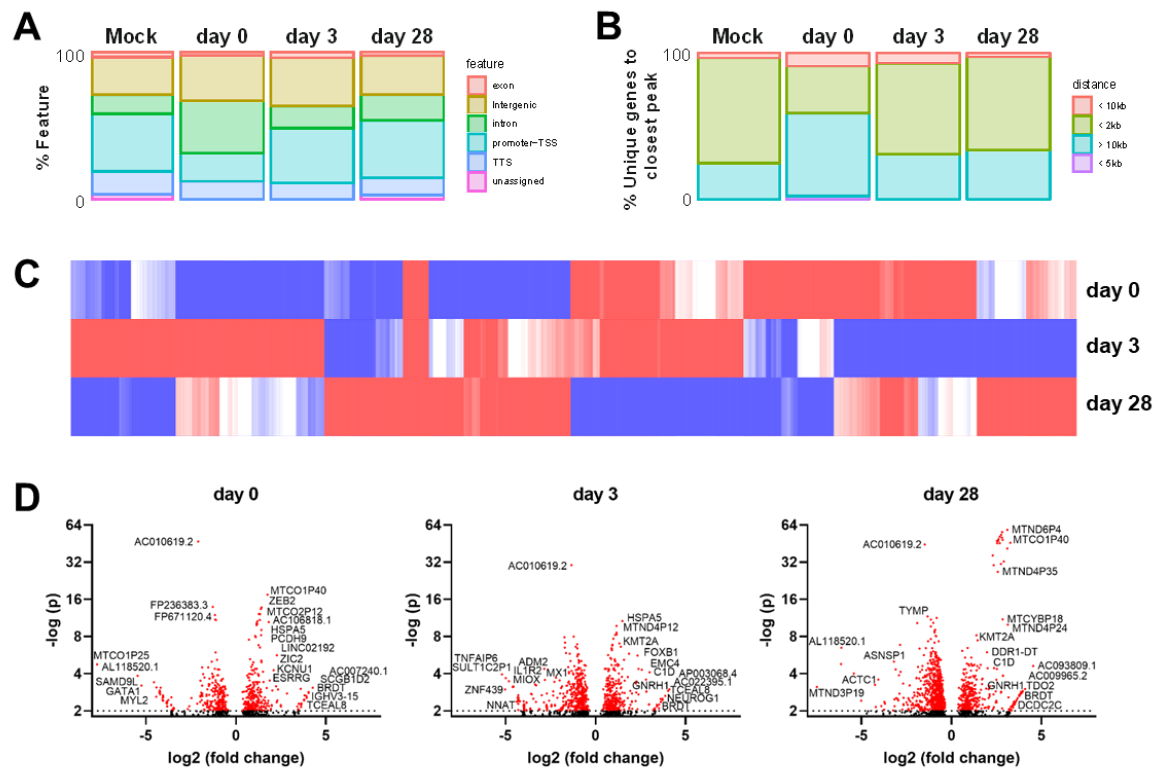


Figure 4.5.2.1: Short-term expression of AF4-MLL alters chromatin accessibility. Distribution of genomic features of accessible chromatin regions (A). The annotations for exon, intergenic, intron, promoter-transcription-start-site (TSS), transcription terminal site (TTS) and unassigned were evaluated. Proximity of peaks to unique genes (B). Distances were categorized into <10 kilobases (kb), <2 kb, > 10 kb and <5 kb proximity to a neighboring gene. Illustration of chromatin accessibility clusters between day 0, day 3 and day 28 by Heat-map analysis (C). Illustration of chromatin regions with highly altered accessibility by plotting the log₂ fold-change and the p-value (adapted from Wilhelm & Marschalek, 2021) (D). The depicted Volcano plots contain all genes of each time-point obtained by ATAC-seq analysis. Quantifications were conducted with the mean of 3 biological replicates per sample.

3 and day 28. Interestingly, an accessible chromatin state between day 0 and day 28 is observable for the gene *Bromodomain Testis Associated (BRDT)* that is associated to the bromodomain and extra-terminal domain (BET) protein family, indicating an association to specifically MLL-AF4.

Highly accessible *ZEB2*, *ZIC2*, *PCDH9*, *HSPA5* and *BRDT* are all involved in B-ALL. For *ZEB2* an interaction with *CTBP2* and *CASP8AP2* was previously demonstrated that are correlated with poor outcome and higher risk of relapse in pediatric B-cell ALL (Wang et al., 2022). Moreover, *ZEB2* is activated in SEM cells by *RUNX1* that constitutes a major target in t(4;11) leukemia (Wilkinson et al., 2013). The transcriptional repressor *ZIC2* was primarily associated to the expression of MLL-AF4 and constitutes an important player in the specification of embryonic stem cells. Of high relevance for hematopoietic disorders in general, *ZIC2* preferably binds to transcription enhancers that promote cellular

differentiation (Luo et al., 2015). Next, *PCDH9* was linked to the resistance to daunorubicin in the treatment of childhood ALL (Silveira et al., 2013). *HSPA5* is considered a chemo resistance biomarker and molecular target in B-ALL (Uckun et al., 2011). Notably, BRDT belongs to BET class of human bromodomain proteins. Inhibiting BET is suggested to be highly efficient in reducing viability of different B-ALL cells including cells with the t(4;11) translocation due to the inhibition of c-Myc and STAT5 phosphorylation (Ott et al., 2012). Less-accessible chromatin related to the expression of MLL-AF4 is observable at genes for *Sterile Alpha Motif Domain Containing 9 Like (SAMD9L)* that codes for a tumor suppressor, the transcription factor *GATA Binding Protein 1 (GATA1)* and *Myosin Light Chain 2 (MYL2)* (Fig. 4.5.2.1 D). The additional expression of AF4-MLL at day 3 results in a reduced accessible chromatin at genes for *Adrenomedullin 2 (ADM2)*, *TNF Alpha Induced Protein 6 (TNFAIP6)*, *Sulfotransferase Family 1C Member 2 Pseudogene 1 (SULT1C2P1)*, *Zinc Finger Protein 439 (ZNF439)*, *Neuronatin (NNAT)*, *Myo-Inositol Oxygenase (MIOX1)*, *Interleukin 1 Receptor Type 2 (IL1R2)* and *MX Dynamin Like GTPase 1 (MX1)*, whereas at day 28 genes for *Actin Alpha Cardiac Muscle 1 (ACTC1)*, *Asparagine Synthetase Pseudogene 1 (ASNSP1)* and *Thymidine Phosphorylase (TYMP)* protrude (Fig. 4.5.2.1 D).

Genes with less accessible chromatin upon the expression of MLL-AF4 *SAMD9L* and *GATA1*, are involved in ALL. *SAMD9L* codes for a tumor suppressor and *SAMD9L* mutations were shown to be associated with the development of pediatric ALL (Cheah et al., 2019). Additionally, the transcription factor *GATA1* was identified to be over-expressed in ALL patients (Patmasiriwat et al., 1999). The AF4-MLL-related and less accessible gene *NNAT* is down-regulated in ALL patients and inhibited in a HEK-293 reporter assay by miR-708 that constitutes a highly up-regulated target in B-ALL patients (Li et al., 2013).

Next, the signatures of de-regulated chromatin accessibility obtained from ATAC-seq as well as gene expression data derived from MACE-seq were analyzed after the expression of t(4;11) fusion proteins (Fig. 4.5.2.2 A). The expression of MLL-AF4 at day 0 is associated with an overall limited number of highly de-regulated genes. In addition, chromatin accessibility is less affected at day 0 when compared to later time points after the co-expression with AF4-MLL (Fig. 4.5.2.2 A). Gene expression and chromatin accessibility are remarkably similarly de-regulated at day 3 and day 28. Both time points, that share a co-expression with AF4-MLL between day 1 and day 3 for 48 hours, exhibit a significantly stronger pronounced de-regulation on chromatin and gene expression level when compared to the mere expression of MLL-AF4 at day 0. Remarkably, the difference in de-regulation between day 0 on the one hand and day 3 and day 28 on the other hand, is more pronounced on the transcriptional level as observed for ATAC-seq related data (Fig.

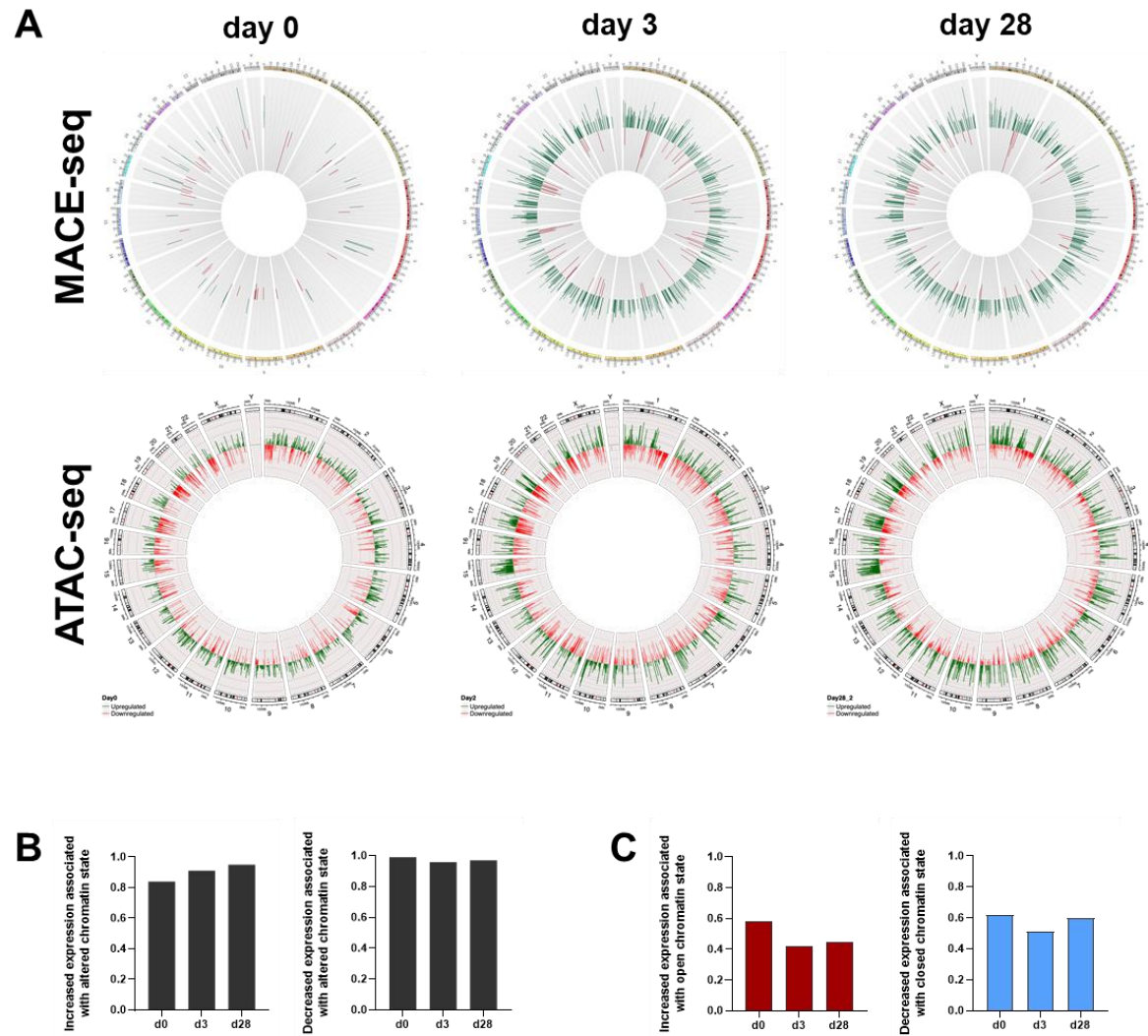


Figure 4.5.2.2: Briefly expressed AF4-MLL exerts not only a lasting effect on the transcriptome and chromatin, but also facilitates up-regulation of genes in less accessible chromatin regions. Circos plots derived from MACE-seq and ATAC-seq were compared at day 0, day 3 and day 28 (\log_2 values ± 2 , $p < 0.05$) (adapted from Wilhelm & Marschalek, 2021) (A). The de-regulation of gene expression (MACE-seq) or chromatin accessibility is illustrated for each chromosome (red = decreased gene expression and closed chromatin state; green = increased gene expression and opened chromatin state, respectively.) Determination of ratio of increased and decreased gene expression with an altered chromatin state (adapted from Wilhelm & Marschalek, 2021) (B). Determination of ratio of increased and decreased gene expression with open and closed chromatin state, respectively (D). Quantifications were conducted with the mean of 3 biological replicates per sample.

4.5.2.2 A). Thereafter, AF4-MLL-related up-regulation of gene expression exceeds the concomitant opening of the chromatin.

The extent to which de-regulation of genes is associated with altered chromatin accessibility was investigated to unravel the relatively different response of gene expression and chromatin accessibility after expression of MLL-AF4 and AF4-MLL (Fig. 4.5.2.2 B+C). First, approximately 90% of highly de-regulated genes ($\log_2 > \pm 1$, $p < 0.05$

and > 2 reads) could be identified to be located at loci with a significantly altered chromatin state ($\log_2 > \pm 1$, $p < 0.05$ and > 2 reads) (Fig. 4.5.2.2 B). The smallest overlap is observable for significantly up-regulated genes at day 0 and down-regulation of genes is generally associated to altered chromatin states at day 0, day 3 and day 28 as indicated by overlaps above 95% (Fig. 4.5.2.2 B).

Upon the relationship of either de- or increased expression to altered chromatin states in general, a second analysis correlated expression to particularly an open or a closed chromatin state (Fig. 4.5.2.2 C). Consistent with greater expression than an opening of chromatin loci upon AF4-MLL expression, a 28% and 23% decrease of up-regulated genes located at accessible chromatin loci was observed at day 3 and day 28, respectively. (Fig. 4.5.2.2 C). While AF4-MLL reduces the association of up-regulated genes to opened chromatin at both, day 3 and day 28, the ratio of decreased expression associated with a closed chromatin state is exclusively lower at day 3 (-18%). The decline detected at day 3 is almost completely recovered at day 28 with only -3% (Fig. 4.5.2.2 C).

All in all, AF4-MLL not only impacts gene expression over time, but also the accessibility of chromatin. Moreover, AF4-MLL-induced overexpression of genes exceeds chromatin opening suggesting that AF4-MLL facilitates up-regulation of genes even from chromatin loci with limited accessibility.

4.5.3. t(4;11) fusion proteins alter chromatin status synergistically

The short-term expression of AF4-MLL together with constitutively expressed MLL-AF4 induced long-term altered transcriptional and chromatin signatures, and increased expression of genes with a limited accessible chromatin (see chapter 2.3+2.5).

The interplay of both t(4;11) fusion proteins seems to promote a clonal evolutionary process that may play a key role in the development and the progression of t(4;11) leukemia. The impact of each t(4;11) fusion protein individually on chromatin remains unclear. The previously conducted ATAC-seq analysis focused on the long-lasting effect on chromatin of AF4-MLL in the presence of MLL-AF4. Therefore, the influence on chromatin accessibility by MLL-AF4 and AF4-MLL was investigated separately and a potential long-term effect on chromatin signature evaluated.

Cellular samples were analyzed at two time points by ATAC-seq upon the expression of either MLL-AF4 or AF4-MLL (Fig. 4.5.3.1). At the first time point (day 3), 293T cells carrying either the pSBbi::*MLL-AF4*, pSBtet::*AF4-MLL* or pSBtet::*Luc* vector expressed the respective t(4;11) fusion protein or Luciferase to a great extent due to the induction with

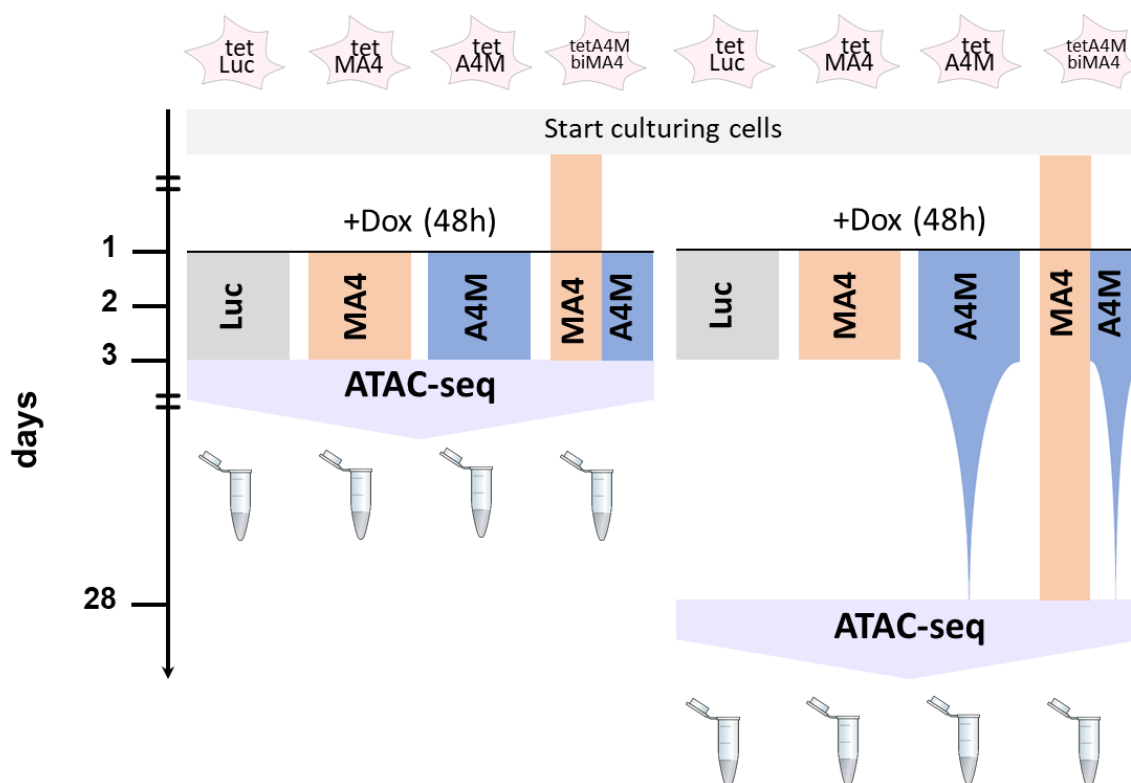
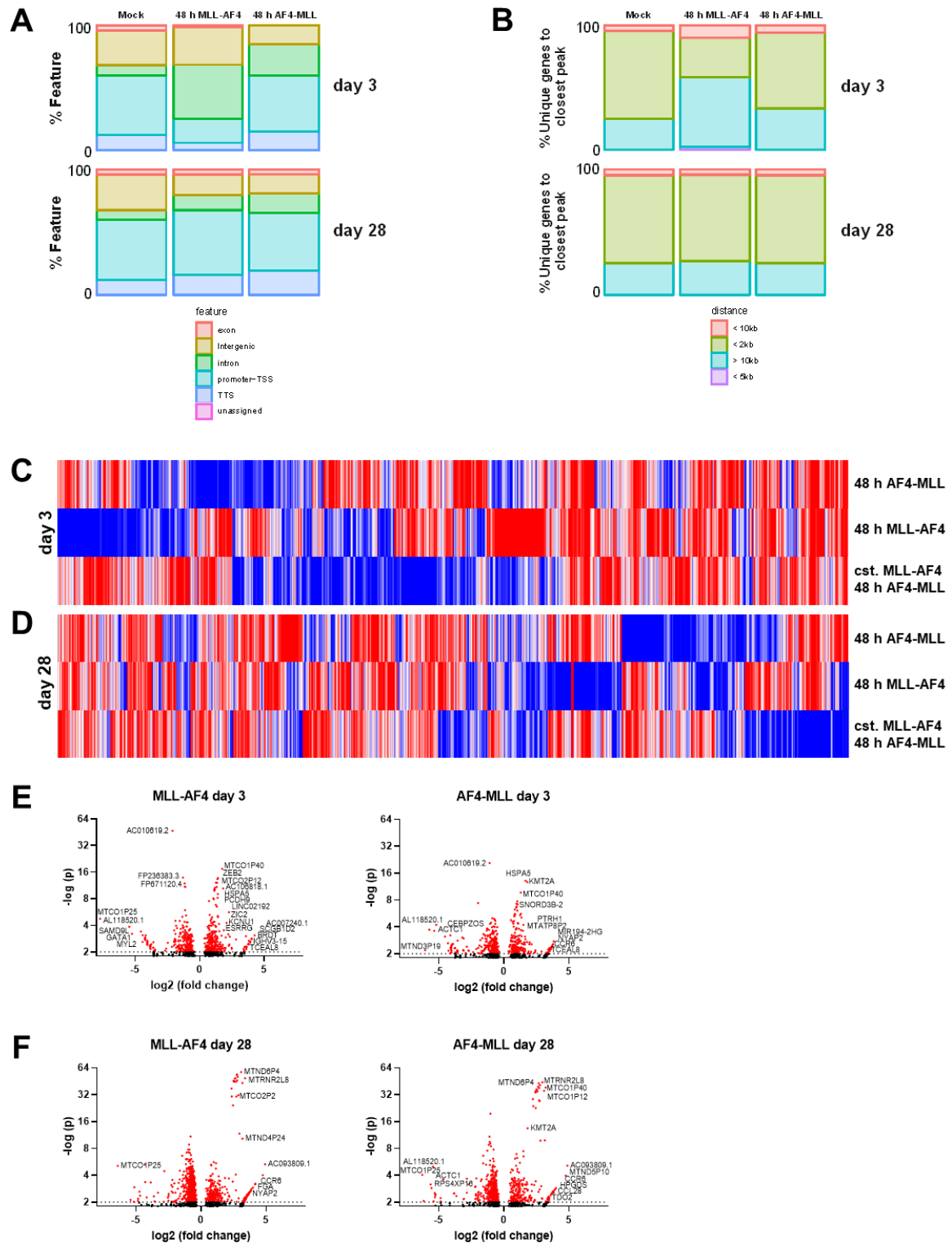


Figure 4.5.3.1: A cellular t(4;11) model to study t(4;11) fusion proteins individually. 293T cells expressing each t(4;11) fusion protein alone for a 48 h interval (day 1 to day 3) or 293T cells expressing constitutively MLL-AF4 and AF4-MLL for a 48 h interval (day 1 to day 3) were analyzed by ATAC-seq. Cellular samples were taken immediately after the 48 h interval of expression of the respective fusion protein (day 3) or 25 days later for evaluation of a long-term effect on the chromatin state (day 28). n = 3 biological replicates per sample.

Doxycycline from day 1 to day 3 for 48 hours. A potential long-term effect of each t(4,11) fusion protein on the chromatin state was assessed at day 28 using 293T cells from day 3 maintained in Doxycycline-free medium ever since (Fig. 4.5.3.1). For a more robust evaluation of MLL-AF4- or AF4-MLL-specific effects on chromatin, 293T cells combining a constitutive expression of MLL-AF4 and Doxycycline-inducible expression of AF4-MLL as applied in chapter 2.3 were included as reference.

The initially conducted ATAC-seq peak annotation revealed an increase of intronic chromatin accessibility upon the expression of MLL-AF4 at day 3 (Fig. 4.5.3.2 A). However, the effect of short-term expression of MLL-AF4 is not maintained until day 28. The distribution of annotated genomic features at day 3 and day 28 is not affected by either AF4-MLL alone or upon the co-expression of both t(4;11) fusion proteins (Fig. 4.5.3.2 A). Assigning of peaks to the nearest gene demonstrates a specific increase of opened chromatin at sites with more than 10 kilobases distance to the closest unique gene upon 48 h expression of MLL-AF4 (Fig. 4.5.3.2 B). Similarly to the increase in opened intronic chromatin, the effect is only detectable at day 3 and absent at day 28. Moreover, distances



between altered accessible chromatin sites to unique genes appear to be independent of the expression of AF4-MLL (Fig. 4.5.3.2 B). Hence, especially MLL-AF4 seems to influence on the one hand intronic chromatin and on the other hand chromatin regions distant to the closest annotated gene.

Figure 4.5.3.2: MLL-AF4 and AF4-MLL act in different ways on chromatin. Distribution of genomic features of accessible chromatin regions (A). The annotations for exon, intergenic, intron, promoter-transcription-start-site (TSS), transcription terminal site (TTS) and unassigned were evaluated. Proximity of peaks to unique genes (B). Distances were categorized into <10 kilobases (kb), <2 kb, > 10 kb and <5 kb proximity to a neighboring gene. Illustration of chromatin accessibility clusters at day 3 and day 28 by Heat-map analysis between 293T cells that either express MLL-AF4 and AF4-MLL individually or constitutively express MLL-AF4 together with a 48 h interval of AF4-MLL expression (see Fig. 4.3.4.4 for a detailed experimental scheme) (adapted from Wilhelm & Marschalek, 2021) (C+D). Illustration of chromatin regions with highly altered accessibility by plotting the log₂ fold-change and the p-value (E+F). The depicted Volcano plots contain all genes of each time-point obtained by ATAC-seq analysis. Quantifications were conducted with the mean of 3 biological replicates per sample.

In a subsequent analysis of overall chromatin accessibility, short- and long-term changes in chromatin accessibility at day 3 and day 28, respectively, are highlighted upon the expression of t(4;11) fusion proteins in comparison to the Mock control (Fig. 4.5.3.2 C+D). The opened and closed regions of chromatin differ at day 3 when MLL-AF4 or AF4-MLL is expressed alone or upon the co-expression of both fusion proteins. Further on, very limited consistency for relative changes in accessibility at distinct chromatin loci can be observed between day 3 and day 28. Of note, chromatin signatures at day 28 from cells expressing either MLL-AF4 or AF4-MLL for 48 hours overlapped moderately in comparison to the signatures from day 3, whereas cells expressing MLL-AF4 constitutively and AF4-MLL between day 1 and day 3 share areas of closed chromatin between both time points (Fig. 3.5.3.2 C+D). Thus, the expression of MLL-AF4, AF4-MLL or the co-expression of both t(4;11) fusion proteins results in distinct chromatin signatures indicating distinctive regulatory roles of either MLL-AF4 and AF4-MLL in t(4;11) ALL.

Next, the determination of highly significant de-regulated chromatin loci by plotting log₂ fold-change and the $-\log_{10}$ p-value revealed low quantitative variability between time points and cells expressing either MLL-AF4 or AF4-MLL (Fig. 4.5.3.2 E+F). In general, there is a less pronounced de-regulation of chromatin accessibility upon the expression of either MLL-AF4 or AF4-MLL as observed in the sample with co-expression (see chapter 2.3). Less accessible chromatin for either t(4;11) fusion protein can be observed at genes for AC010619.2 and MTCO1P25, and opened chromatin at genes for ACC093809.1 and C-C Motif Chemokine Receptor 6 (CCR6). Particularly less accessible chromatin upon expression of MLL-AF4 at day 3 is associated to genes for SAMD9L, GATA1 and MYL2, while opened chromatin is observable at day 3 at genes for ZEB2, ZIC2 and PCDH9 accordingly to chapter 2.3, and at day 28 to genes for Fibrinogen Alpha Chain (FGA) and Neuronal Tyrosine-Phosphorylated Phosphoinositide-3-Kinase (NYAP2). For AF4-MLL, less accessible chromatin was detected at day 3 and day 28 at the gene for Actin Alpha Cardiac Muscle 1 (ACTC1) and opened chromatin could be linked at day 3 to the genes

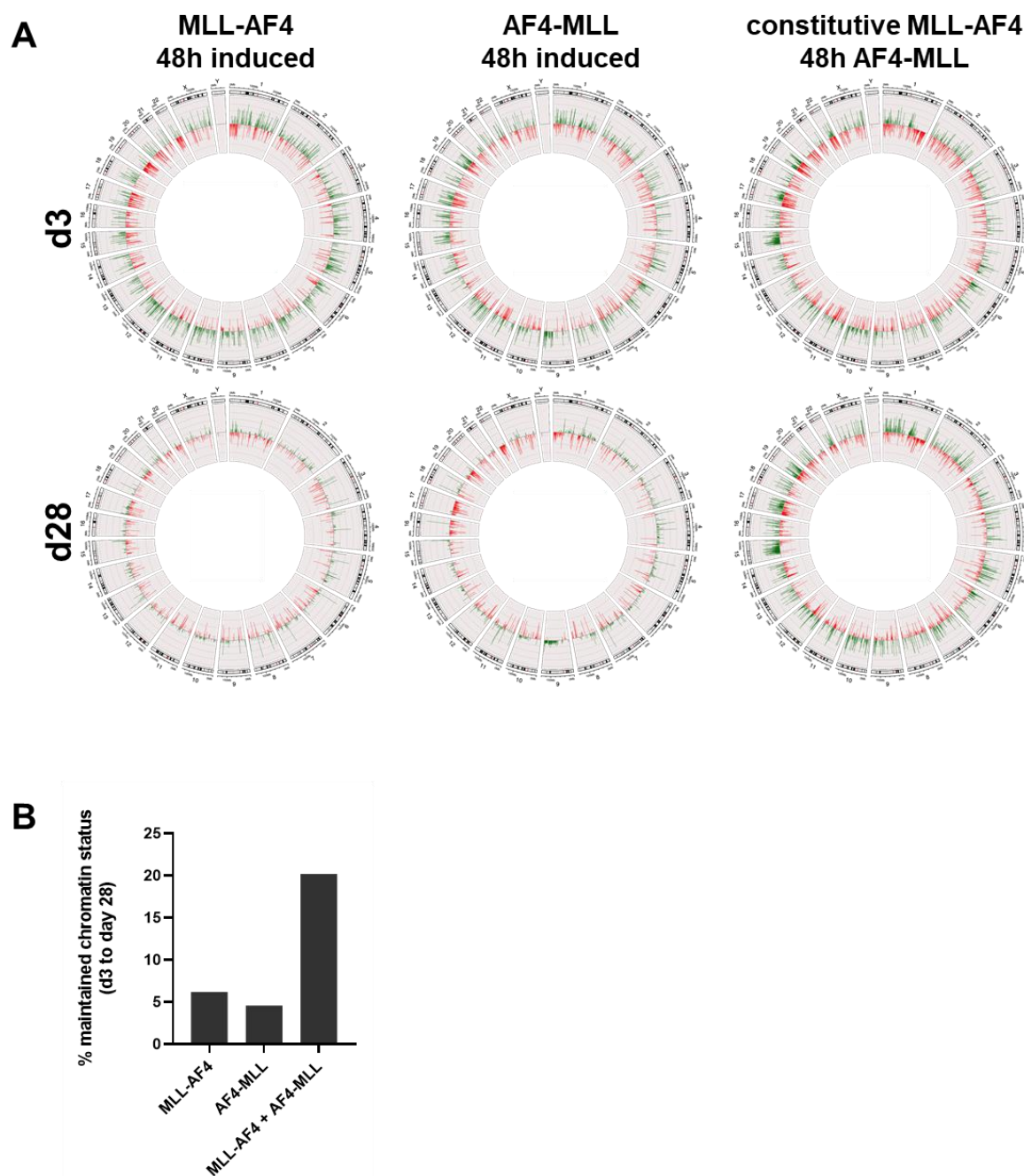


Figure 4.5.3.3: Interplay of MLL-AF4 and AF4-MLL mediate long-term impact on chromatin. Circos plots derived from ATAC-seq data were compared at day 3 and day 28 (\log_2 values ± 2 , $p < 0.05$) (adapted from Wilhelm & Marschalek, 2021) (A). The deregulation of chromatin accessibility is illustrated for each chromosome (red = decreased gene expression and closed chromatin state; green = increased gene expression and opened chromatin state, respectively.) Determination of chromatin regions with a maintained accessibility between day 3 and day 28 (B). Quantifications were conducted with the mean of 3 biological replicates per sample.

NYAP2, PTRH1 and microRNA MIR194-2HG, and at day 28 to the genes for, TDO2, C-C Motif Chemokine Ligand 28 (CCL28) and Hematopoietic Prostaglandin D Synthase (HPGDS).

Further on, a genome wide chromatin signature analysis was carried out to illustrate global differences in chromatin accessibility induced by either MLL-AF4 or AF4-MLL (Fig. 4.5.3.3 A). Immediately after peak expression of t(4;11) fusion proteins at day 3, chromatin accessibility quantitatively resembles but qualitatively differs between MLL-AF4 and AF4-MLL. Importantly, the level of highly- opened and closed chromatin sites significantly drops at day 28 for both fusion proteins indicating an exclusively short-term effect of either MLL-AF4 or AF4-MLL when expressed individually (Fig. 4.5.3.3 A). Contrarily, the short-time expression of AF4-MLL in 293T cells constitutively expressing MLL-AF4 lead to a profoundly de-regulated chromatin signature at day 28. Analyzing the amount of the chromatin status maintained from day 3 to day 28 further supports the distinct impact on chromatin due to the interplay of both fusion proteins (Fig. 4.5.3.3 B). Only 6.2% and 4.6% of genes linked with de-regulated chromatin accessibility at day 3 can be detected at day 28 for MLL-AF4 and AF4-MLL, respectively. The maintenance of genes in 293T cells that co-expressed both fusion proteins for two days is approx. 4-fold higher with 20.2% of maintained genes when compared to the individual expression of each fusion protein (Fig. 4.5.3.3 B).

All in all, neither MLL-AF4 nor AF4-MLL maintain chromatin signature from day 3 individually, while the level of de-regulated chromatin endures in case of constitutively expressed MLL-AF4 and short-term expressed AF4-MLL. Hence, an interplay between MLL-AF4 and AF4-MLL seem to promote the modification of chromatin even upon the loss of AF4-MLL for more than three weeks indicating a “hit-and-run” mode of action of AF4-MLL.

5. DISCUSSION

The translocation t(4;11)(q21;q23) leads to the most prevalent form of ALL in young children (Meyer et al., 2018). Current therapies for this particular high-risk leukemia are still very poor and new therapeutic approaches are urgently needed (Bueno et al., 2011; Felix et al., 2000; Hess, 2004; Isoyama et al., 2002; Pui et al., 2002). Importantly, approximately 30% of ALL patients under the age of 1 year carry the t(4;11) translocation (Meyer et al., 2018).

Efforts to inhibit t(4;11) fusion proteins often particularly focus on the MLL-AF4 protein (Barretto et al., 2014; Borkin et al., 2015; Cao et al., 2014; Čermáková et al., 2014; Daigle et al., 2013; Dawson et al., 2011; Filippakopoulos et al., 2010; Godfrey et al., 2019; Kumar et al., 2011; McCalmont et al., 2020; Milne et al., 2002; Mirguet et al., 2013; Picaud et al., 2013; Shi et al., 2012; Srinivasan et al., 2004; Steinhilber and Marschalek, 2017; Thomas et al., 2005). It is expressed in all t(4;11) leukemia patients and is thought to play an important role in the development and persistence of leukemia (Krivtsov et al., 2008; Marschalek, 2011b; Sanjuan-Pla et al., 2015). Contrarily, the AF4-MLL protein is expressed in only 45-80% of patients and its molecular function and therapeutic potential in ALL is significantly less understood and controversially discussed (Agraz-Doblas et al., 2019; Bursen et al., 2010; Kowarz et al., 2007; Marschalek, 2015, 2019; Muñoz-López et al., 2016; Sanjuan-Pla et al., 2016; Trentin et al., 2009).

There are conflicting data on a possible association between AF4-MLL expression and poor prognosis for t(4;11) patients. A subset of studies associate the expression of AF4-MLL with an overall better survival of t(4;11) patients and the over-expression of *HOXA* genes suggesting that inhibition of AF4-MLL is contra-indicated in the combat against t(4;11) ALL (Agraz-Doblas et al., 2019; Bueno et al., 2019). However, this association of overexpressed *HOXA* genes and AF4-MLL is refuted by other studies (Stam et al., 2006, 2010a; Trentin et al., 2009; Völse, 2020).

Additionally, there is a limited understanding of the impact of AF4-MLL at different stages of ALL. Some studies propose a non-essential and only complementary function of AF4-MLL in the development and progression of ALL, while other studies emphasize the importance of the individual expression of AF4-MLL and its interplay with MLL-AF4 (Bursen et al., 2010; Gaussmann et al., 2007; Kumar et al., 2011; Prieto et al., 2017; Sanjuan-Pla et al., 2016). As t(4;11) leukemia constitutes a disease difficult to model *in vivo*, so far only a single study was able to generate ALL *in vivo* with human MLL fusion proteins. Contradictory to the picture of a dominant role of MLL-AF4 in ALL, this type of leukemia could exclusively be generated *in vivo* in the presence of AF4-MLL and independent of the co-expression of MLL-AF4 (Bursen et al., 2010).

Hence, in this work the therapeutic benefit of AF4-MLL inhibition was evaluated towards more precise therapies for high-risk t(4;11) ALL, and the potential of AF4-MLL assessed to irrevocably alter the transcriptome and chromatin for a better understanding of the role of AF4-MLL during development and progression of ALL.

5.1. Co-targeting of MLL-AF4 and AF4-MLL synergistically induces apoptosis in t(4;11) leukemic cells *in vitro*

The frequent absence of secondary mutations in t(4;11) ALL and the extremely divergent treatment success compared to other ALLs caused by different chromosomal translocations highlights the great importance of novel tailored therapies against the fusion proteins MLL-AF4 and AF4-MLL (Agraz-Doblas et al., 2019; Sanjuan-Pla et al., 2015; Zheng, 2013).

In this work, a novel therapeutic strategy was examined targeting both MLL fusion proteins while preserving a functional wild-type MLL. For the inhibition of AF4-MLL, dnTASP1 was expressed in the pro-B t(4;11) ALL cell line SEM mediating the inhibition of Taspase1 and leading to the proteasomal degradation of AF4-MLL while uncleaved endogenous MLL remained catalytically active (Sabiani et al., 2015; Yokoyama et al., 2013). Next, for the inhibition of MLL-AF4, class 1 HDACis that have been demonstrated to reduce the dominant effect of MLL-AF4 by endorsing endogenous MLL (Ahmad et al., 2014), were administered to dnTASP1-expressing SEM cells and apoptosis levels evaluated.

For the rapid generation of stable SEM-Mock and SEM-dnTASP1 cells an optimized Sleeping Beauty System was applied (Kowarz et al., 2015). On the basis of a transposon-mediated integration of our vector system into the genome, the Sleeping Beauty System allowed a more precise incorporation of the dnTASP1 expression cassette into SEM cells when compared to the widely used lentiviral transduction approaches. Particularly, the Sleeping Beauty system enables the insertion of SB vectors into the genome mainly at TA-sites rather than a random integration into the genome and the scalability of the desired copy number of SB vectors into the genome per cell.

The inhibition of HDACs in pro-B t(4;11) cells resulted in elevated apoptosis levels when dnTASP1 was expressed (chapter 4.1). The dnTASP1-related increase of apoptosis levels increased over time accordingly to the exceptional long half-life of AF4-MLL. However, a prolonged administration of HDACis lead to a more immediate response to dnTASP1 expression and enhanced the sensitivity of dnTASP1 expressing SEM cells to class I HDACi Mocetinostat and Entinostat.

The association of HDAC1 and HDAC2 to the MBD together with Polycomb proteins BMI1, HPC2 and CtBP is orchestrated by the “CYP33 switch” (Marschalek, 2016) that binds to MLL via the PHD domain (Park et al., 2010; Rössler and Marschalek, 2013; Xia et al., 2003). In this work, the potential of inhibiting HDACs and especially the MLL-associated HDAC1 and HDAC2 was analyzed. In particular, the class 1 HDACi Entinostat that specifically inhibits HDAC1 and HDAC3 as well as Mocetinostat that exhibits a potent inhibition of HDAC1 but also HDAC2, HDAC3 and HDAC11, and the pan-HDACi Dacinostat were applied. Interestingly, class 1 HDACi that exhibit a greater isotype-specificity were capable of inducing a synergistic effect in t(4;11) cells expressing dnTASP1 to a comparable level as observed for the non-specific pan-HDACi Dacinostat (Figure 4.1.3.4 and Figure 4.1.3.5). From a clinical point of view, this constitutes a favorable situation, since the non-specific inhibition of HDACs is associated with high toxicity resulting in low tolerated doses and thus limited efficacy of compounds (Balasubramanian et al., 2009).

As such, class 1 HDACi as used by Ahmad et al represent a further development with respect to a more specific therapy (Ahmad et al., 2014). Yet, it has been shown that despite the increased specificity of class 1 HDACi, side effects such as grade 3 and higher fatigue, vomiting, diarrhea, thrombocytopenia, and neutropenia are similar in severity to non-selective pan-inhibitors (Balasubramanian et al., 2009). This results in relatively low doses that can be administered in the clinic and exclusively condition the use of HDACi in concert with other drugs due to the insufficient efficacy of current compounds in development. Therefore, widespread use of HDACi in the clinic, especially class 1, is not expected until isotype-specific and thus presumably much less toxic HDACi are developed. It should be noted here that "isotype-specific" is not "HDAC-class-specific" as it is often inaccurately used in the literature (Balasubramanian et al., 2009). The resulting potential for higher doses suggests a much more efficient therapy in the future. In addition, data from t(4;11) patients comparing the expression of different HDACs with treatment success, allow for a more accurate selection of currently available and future promising HDACi (Garcia-Manero et al., 2008).

Of note, in this study particularly the inhibition of HDAC1 and HDAC3 was covered by all applied HDACis. The here obtained data allow no further discrimination between HDAC1 and HDAC3. Nevertheless, the inhibition of HDAC3, that in comparison to HDAC1 and HDAC2 is not directly associated to MLL, might be relevant via its interactions to other HDACs (Park et al., 2010; Rössler and Marschalek, 2013; Xia et al., 2003). This is supported by the study of Ahmad et al. revealing that the knock-down of HDAC3 significantly boosted effects related to the knock-downs of either HDAC1 and HDAC2 (Ahmad et al., 2014). Hence, it remains unclear whether the inhibition of particularly the

MLL-related HDAC1 or even HDAC3 suffices to induce a synergistic effect together with dnTASP1 on t(4;11) cells. Nevertheless, the relative increase of apoptosis levels in HDACi-treated SEM cells of up to 30% upon the expression of dnTASP1 indicates the therapeutic potential of class 1 HDACs in the treatment of t(4;11) leukemic cells. Noteworthy, the here observed potent apoptotic effect of HDACs on SEM cells is in line with anti-leukemic effects demonstrated in *in vitro* and *in vivo* t(4;11)-specific studies (Bhatla et al., 2012; Garrido Castro et al., 2018; Stumpel et al., 2012).

The increased apoptosis levels of t(4;11) cells might be attributed to the inhibition of both MLL-AF4 and AF4-MLL fusion proteins, the effects on wild-type MLL by HDACi and the expression of dnTASP1, to the combined effect of MLL fusion protein inhibition and endorsement of wild-type MLL, but also to secondary effects not directly related to MLL and MLL fusion proteins.

Apoptosis data obtained from a 24 h HDACi treatment in combination with the expression of dnTASP1 over a longer period of time indicate a cooperative effect of both MLL fusion proteins, which might be disturbed by the dual-treatment approach of this study. No synergistic effect could be detected for the HDACi treatment when combined with a short-term expression of dnTASP1 (Figure 4.1.3.4). A benefit of co-treatment was primarily observed after 6 days of dnTASP1 expression, which is in line with the exceptionally long half-life of AF4-MLL of 96 h (Bursen et al., 2004). This observation is consistent with a paper that examined the effect of t(4;11) fusion proteins on cell cycle, growth behavior, and resistance to apoptosis (Gaussmann et al., 2007). Gaussmann et al. revealed a cooperative effect between MLL-AF4 and AF4-MLL in non-leukemic MEF cells by the overexpression of the two MLL fusion proteins. Cell cycle, growth, and apoptosis resistance were particularly affected when both MLL fusion proteins were co-expressed.

Notably, the inhibition of Taspase1 disrupted the proliferation and enhanced apoptosis in various cancer cells (Chen et al., 2010). Additionally, the expression of dnTASP1 in SEM cells has previously been described to alter growth behavior and the cell cycle (Sabiani et al., 2015). Here, no difference in growth and cell cycle of SEM cells upon the expression of dnTASP1 could be observed, which might be explained by the short-term character of the experiment (Figure 4.1.2.1). In contrast to enhanced apoptosis levels in non-t(4;11) leukemia cell lines (Chen et al., 2010) and in support of a cooperative effect between MLL-AF4 and AF4-MLL, the mere expression of dnTASP1 over a period of 28 days failed to induce apoptosis in SEM cells that have not been co-treated with HDACis (Figure 4.1.3.4 and Figure 4.1.3.5).

Accordingly, our cooperation partner in Munich obtained similar results with an *in vivo* t(4;11) on the basis of PDX cells carrying inducible overexpression/knock-down Cre-ER^{T2} Flip system (established by the members of the Jeremias Laboratory: Michaela Carlet,

Jenny Vergalli and Birgitta Heckl). While the induced knock-down of MLL-AF4 affected cellular growth of PDX cells *in vivo*, no effect could be detected for the mere inhibition AF4-MLL by shRNA or the expression of dnTASP1 (Völse, 2020). In a previous study by Kumar et al. inhibiting AF4-MLL via siRNA, it was concluded that AF4-MLL is dispensable for leukemic cell proliferation and survival (Kumar et al., 2011). Due to the short-term and the often not efficient nature of inhibiting proteins by siRNA, the relevance of assessing the effect of individual MLL proteins in particular the stable AF4-MLL on the development and progression of leukemic cells is limited. Nevertheless, the *in vitro* data of Kumar et al based on siRNA knock-downs are in line with the *in vivo* data of the methodologically superior *in vivo* model from Munich based on shRNA knock-down and dnTASP1 expression. Therefore, the observed elevated apoptosis levels upon the co-treatment of SEM cells in this study are in line with the observation of a cooperative effect between MLL-AF4 and AF4-MLL in MEF cells (Gaussmann et al., 2007), and the lacking induction of apoptosis by the mere expression of dnTASP1 even for up to 28 days fit *in vitro* and *in vivo* studies that inhibited the MLL fusion proteins individually (Carlet et al., 2020; Kumar et al., 2011; Völse, 2020).

Further on, a cooperation of MLL-AF4 with AF4-MLL could also be demonstrated during human embryonic stem cell differentiation, where particularly the co-expression of MLL fusion proteins led to enhanced hemato-endothelial specification (Bueno et al., 2019).

Opposing the claim of a mere inhibition of fusion proteins after HDACi and dnTASP1 co-treatment is the finding that after prolonged duration of HDACi therapy from 24 h to 48 h in combination with dnTASP1 expression, a rather surprising synergistic effect occurred as early as 2 days after dnTASP1 expression (Figure 4.1.3.5). While this is difficult to explain by the tremendous stability of AF4-MLL, it suggests that the hypothesized contemporaneous stabilization of endogenous MLL was involved. In addition to the study by Ahmad et al, which demonstrated by a report assay that HDACi can break the dominance of MLL-AF4 in target promoter activation over wild-type MLL (Ahmad et al., 2014), it was further observed that endogenous MLL was stabilized when proteolytic cleavage was omitted (Zhao et al., 2019). Importantly, Zhao et al. additionally demonstrated a displacement of MLL fusion proteins from chromatin *in vivo* upon the induced stabilization of endogenous MLL. The therapeutic potential of stabilizing endogenous MLL was further supported by the observation that the proliferation of leukemia cells could be reduced by the mere stabilization of endogenous MLL (Liang et al., 2017).

In contrast to an *in vitro* study from 2006 postulating an altered binding of unprocessed MLL to E2F and cyclins (Takeda et al., 2006), Yokoyama et al. using mouse mutant alleles incapable of intra-molecular interaction revealed that intra-molecular binding rather than

proteolytic cleavage of MLL by Taspase1 is essential for the proper activity of MLL (Yokoyama et al., 2013). Furthermore, in this study, the lack of proteolytic cleavage was not affecting the target genes of endogenous MLL *in vivo*.

Thus, stabilization of endogenous MLL by inhibition of Taspase1, in addition to enhancement of target promoter activation of endogenous MLL by HDACi, represents another possible component of the dual HDACi and dnTASP1 approach, which may explain the short-term effect after Taspase1 inhibition.

An assessment of whether inhibition of MLL-AF4 and AF4-MLL or the stabilization of endogenous MLL played a more decisive role in the synergistic effect of the co-therapy is difficult to perform with the data collected. Thereafter, the fact that Taspase1 is overexpressed in many leukemia cell lines implies the supportive character for the transformation of cells induced by MLL fusion proteins. However, this might be explained on the one hand by the previously observed reduced stability of endogenous MLL upon the proteolytic cleavage but also on the other hand by the leukemic cells' strategy to avoid the proteasomal degradation of unprocessed AF4-MLL (Bursen et al., 2004; Liang et al., 2017; Sabiani et al., 2015; Zhao et al., 2019).

Moreover, it should also be considered that secondary effects are involved in the induction of apoptosis after dnTASP1 expression due to the binding of Taspase1 to further targets beyond MLL. Taspase1 also binds to Mixed Lineage Leukemia Gene Homolog 2 (MLL2) and the transcription factor IIA (TFIIA) (Zhou et al., 2006). In addition, an *in silico* study predicted 27 further Taspase1 targets (Bier et al., 2011). The list of predicted targets comprises besides targets that are involved in transcription, developmental processes and numerous targets with unknown function also a predicted target site in the human hepatitis E virus (Bier et al., 2011).

In 2019, a complete turnaround in the assessment of AF4-MLL as a target in therapy against t(4;11) leukemia occurred with the study of Agraz-Doblas et al. (Agraz-Doblas et al., 2019). Contradicting former observations, an association between AF4-MLL expression and a good prognosis of infant t(4;11) ALL patients was reported. The novelty of this study was that in addition to the known correlation of good prognosis with increased expression of *HOXA* genes, also AF4-MLL appeared to be correlated with the former two criteria. The H3K79 activation marks found in *HOXA* genes in human embryonic stem cells co-expressing both MLL fusion proteins were hypothesized to cause the correlation of AF4-MLL expression and expressed *HOXA* genes in infant t(4;11) patients (Bueno et al., 2019). However, this observation on AF4-MLL is in clear contradiction with previous observations, which failed to show any association between *HOXA* gene signatures and the expression of AF4-MLL (Trentin, Stam, Marschalek, and Stam, Voelse). Thus, AF4-MLL inhibition by dnTASP1 expression is to be considered relevant for potential clinical application only once

this inconsistency in the data is clarified. Hence, further studies are urgently needed to clarify the role of AF4-MLL as a prognostic marker in t(4;11) patients.

The current treatment protocol for t(4;11) patients is, despite great advances in medicine, still mainly based on a chemotherapy and hematopoietic stem cell transplants (Döhner et al., 2010; Dombret and Gardin, 2016). Especially in infants that constitute the largest group of t(4;11) patients (Meyer et al., 2018), chemotherapy is associated with overall high therapy-related mortality of near 10% and only a poor treatment success (Dreyer et al., 2015; Felix et al., 2000; Hess, 2004; Isoyama et al., 2002; Pieters et al., 2007, 2019; Pui et al., 2002). Further on, only a subtype of infants seems to benefit from stem cell transplants (Mann et al., 2010). Thus, a more targeted approach as available for patients with the BCR-ABL chimeric protein is still urgently needed for t(4;11) patients. However, the absence of secondary mutations in t(4;11) patients tremendously reduces the amount of possible targets and currently available targeted therapies are still falling short of expectations in the clinic (Shukla et al., 2016; Stein et al., 2018; Steinhilber and Marschalek, 2017).

A major disadvantage for the group of infant t(4;11) patients is the restricted applicability to novel immunotherapy approaches such as chimeric antigen receptor T cell (CAR-T). Patients under the age of one year are often excluded from CAR-T cell trials due to limited feasibility to aspirate sufficient amounts of T-cells (Breese et al., 2021; von Stackelberg et al., 2016). Nevertheless, improving immunotherapies including individualized RNA-based treatments or genetically modified T cells from healthy donors genetically show promising results and possess the potential to significantly improve the treatment outcome even for high-risk leukemia patients (Beck et al., 2021; Liu et al., 2016; Maude et al., 2018; Qasim et al., 2017).

In conclusion, the increased apoptosis levels after co-treatment with HDACi and expression of dnTASP1 suggest a potent and multifactorial strategy to inhibit both t(4;11) fusion proteins and boost endogenous MLL *in vitro*. However, to properly assess the benefit of AF4-MLL inhibition, it is essential to wait for further studies clarifying a previously postulated association of AF4-MLL and a good prognosis of infants with t(4;11) leukemia.

5.2. Targeting MLL-AF4 *in vivo* in t(4;11) PDX cells down-regulates pivotal hemato-malignant factors

The effect of MLL-AF4 inhibition on the transcriptome of t(4;11) leukemic cells *in vivo* is largely unknown. The analysis of differential gene expression when tumor burden increases imitating a growing leukemia *in vivo* is of great significance for a better

understanding of the underlying molecular mechanisms of MLL fusion proteins during the progression of t(4;11) leukemia.

In this work, MACE-seq analysis was conducted with PDX leukemia cells received from Kerstin Völse from our cooperation with the Jeremias Laboratory, that were harvested from mice upon the knock-down of MLL-AF4 by shRNA or upon the expression of dnTASP1 inhibiting AF4-MLL (Carlet et al., 2020; Völse, 2020).

In comparison to the ALL-707 PDX cells co-expressing both MLL fusion proteins, significantly less genes associated to hematopoietic regulation or B-ALL studies were observed in ALL-763 PDX cells that exclusively express MLL-AF4.

Yet, the knock-down of MLL-AF4 in ALL-707 PDX cells resulted in the down-regulation of highly interacting oncogenes involved in hematopoiesis and B-ALL. In particular, the down-regulated transcription factor FOXO1 is involved in the proliferation and survival at early stages of B-cell differentiation and its down-regulation has been associated with anti-leukemic activity in xenografts (Wang et al., 2018). The expression of FOXO1 is further orchestrated by IKAROS that is derived from the *IKZF1* gene. It primes gene expression of multipotent progenitors towards the lymphoid lineage including FOXO1 (Ferreirós-Vidal et al., 2013; Ng et al., 2009). Further on, the expression of IKAROS is related to poor prognosis in B-ALL (Mullighan et al., 2009). Another down-regulated gene upon MLL-AF4 knock-down is *RAG1* whose expression is linked to IKAROS, but also FOXO1 (Ferreirós-Vidal et al., 2013; Heizmann et al., 2013). Noteworthy, involved in B-cell receptor signaling, the oncogenes *PLCG1*, and its so far not described pseudogene *AC079150.2*, and *BLK* are all significantly down-regulated upon MLL-AF4 knock-down in ALL-707 cells (Kim et al., 2017; Liu et al., 2014). Notably, the expression of BLK is additionally linked to IKAROS (Iacobucci et al., 2012).

Moreover, the transcriptomic data indicated a correlation between the expression of RUNX1 and AF4-MLL. As a crucial hematopoietic transcription factor, RUNX1 was also highly significantly down-regulated upon MLL-AF4 knock-down in ALL-707 PDX cells (Figure 4.2.1.1.). RUNX1 constitutes a major target in t(4;11) leukemias that, activated by MLL-AF4, also interacts with AF4-MLL and thereby initiates expression of several target genes (Wilkinson et al., 2013). However, in ALL-763 PDX cells that lack AF4-MLL, the expression of RUNX1 was only slightly de-regulated upon the knock-down of MLL-AF4. Accordingly, in cord blood-derived CD34 positive murine hematopoietic stem/progenitor cells, RUNX1 was approximately 2.5 fold up-regulated upon the ectopically expression of AF4-MLL (Prieto et al., 2017).

The down-regulation of RUNX1 and especially the triangle *FOXO1*, *RAG1* and *IKZF1* that all are tightly interacting with each other and play a major role in the gene expression signature of B-cells, suggests a significant effect on t(4;11) leukemic cells.

In addition to the transcriptomic analysis, our cooperation partner further evaluated growth behavior of 707-ALL PDX cells upon MLL-AF4 knock-down using a competitive system (Carlet et al., 2021; Völse, 2020). Here, knock-down and control PDX cells were injected together in a single mouse enabling a less error-prone and highly sensitive read out (Völse, 2020). 28 days of MLL-AF4 knock-down resulted in a significant diminished growth of leukemic cells in mice in comparison to the control PDX cells. Moreover, MLL-AF4 appeared to be essential for leukemia maintenance in PDX cells either expressing exclusively MLL-AF4 or both MLL fusion proteins (Carlet et al., 2020; Völse, 2020). Notably, the PDX cells used for transcriptomic analysis were derived from a single patient and therefore the data must be interpreted with caution. Nevertheless, the obtained transcriptomic data of de-regulated hemato-malignant factors from the *in vivo* t(4;11) model imitating a growing leukemia, were consistent with previous *in vivo* studies in particular when both MLL fusions were expressed. Hence, the revealed differentially expressed genes may support the understanding of the underlying mechanism of MLL fusion proteins during t(4;11) leukemia progression.

5.3. Expression of dnTASP1 *in vivo* in t(4;11) PDX cells de-regulates cell-cycle related genes

The effect of inhibiting Taspase1 in t(4;11) leukemic cells *in vivo* on the transcriptome remains unclear. In collaboration with Kerstin Völse from the Jeremias Laboratory that provided PDX cells upon the expression of dnTASP1, a profound de-regulation of genes related to the cell cycle could be detected by MACE-seq analysis.

The observed de-regulation of numerous key regulatory genes that are involved in the cell-cycle are often mutually regulated and have also previously been associated with t(4;11) leukemia (Almamun et al., 2015; Consolaro et al., 2015; Deo, 2017; Dutertre et al., 2004; Ghelli Luserna Di Rorà et al., 2018; Goroshchuk et al., 2020; Heald et al., 1993; Hirota et al., 2003; Jiménez-P et al., 2018; Kannan et al., 2019; Watanabe et al., 1995; Yang et al., 2018; Zhong et al., 2017). Key regulators of cell cycle such as PLK1, CDK1, AURKA, MYC, CDC25B and cyclin B1 were down-regulated in dnTASP1-expressing 707-ALL PDX cells that express both t(4;11) fusion proteins (Figure 4.2.2.1 and Figure 4.2.2.2).

In parallel to the transcriptomic analysis, the growth behavior of 707-ALL PDX cells either expressing dnTASP1 or shRNA cassettes to obtain a knock-down of AF4-MLL was analyzed (Völse, 2020). Of note, neither the expression of dnTASP1 nor shRNA mediating an AF4-MLL knock-down affected the growth behavior of t(4;11) PDX cells. Thereafter, the here detected changes in cell-cycle gene expression appear to be insufficient to alter

progression of t(4;11) leukemic cells *in vivo*. This is in line with here obtained *in vitro* apoptosis data of SEM cells expressing dnTASP1 for 28 days (Figure 4.1.3.4 and Figure 4.1.3.5). The mere expression of dnTASP1 over time was not sufficient to induce apoptosis. Yet, significantly elevated apoptosis levels could be observed in dnTASP1-expressing SEM cells co-treated with HDACi indicating, as discussed in chapter 4.2, a cooperative effect of both MLL fusion proteins in t(4;11) leukemia progression.

The inhibition of Taspase1 by expressing dnTASP1 not only causes the proteasomal degradation of AF4-MLL but also results in the accumulation of unprocessed endogenous MLL (Bursen et al., 2004; Sabiani et al., 2015). Thus, the evaluation of the impact of the highly de-regulated cell-cycle genes upon dnTASP1 expression on t(4;11) leukemia progression requires a multifactorial analysis considering unprocessed endogenous MLL and MLL fusion proteins.

A differently regulated cell-cycle has been previously observed upon the expression of AF4-MLL in interplay with MLL-AF4 *in vitro* (Gaussmann et al., 2007). Since ALL-707 PDX cells also express both MLL fusion proteins, it seems plausible, that the here obtained alterations in cell cycle can be linked to the inhibition of AF4-MLL. Further on, a previous study with Taspase1^{-/-} mice detected a de-regulated expression of cell-cycle genes (Takeda et al., 2006). An up-regulation of cyclin D1 and D2, and p16 was observed that mediated the down-regulation of cyclins/CKDs such as cyclin E1, E2, A2, B1 and B2 *in vivo*. In contrast to Taspase1^{-/-} mice, in this work, the expression of dnTASP1 in a t(4;11) leukemia context resulted in the down-regulation of cyclin D2 *in vivo*. Remarkably, the cyclin D2 constitutes the only down-regulated cyclin in the *in vivo* t(4;11) model, whereas in Taspase1^{-/-} mice particularly cyclin D2 was up-regulated in comparison to all other down-regulated cyclins (Takeda et al., 2006). In addition to cyclin D, also cyclin B1 was reciprocally regulated in a t(4;11) context *in vivo*. Here, upon the expression of dnTASP1, cyclin B1 and numerous of its cell-cycle related interaction partners such as PLK1, AURKA, CDC25B and CDC25C were all up-regulated (Figure 4.2.2.1 and Figure 4.2.2.2) (Asteriti et al., 2015; Dutertre et al., 2004; Hirota et al., 2003; Zhong et al., 2017). Thus, the expression of cyclin B1 and D2 might be de-regulated in an AF4-MLL dependent manner, however further studies are required to draw further conclusions. Especially, the technically different approaches of Taspase1^{-/-} mice and leukemic PDX cells expressing dnTASP1 limit the comparability of gene expression data. Further on, transcriptomics data of dnTASP1-expressing PDX cells are derived from a single patient and need to be carefully interpreted.

Hence, the inhibition of Taspase1 de-regulated cell-cycle genes significantly, but was not affecting growth of leukemic cells *in vivo*. This suggests a cooperative effect of MLL-AF4 and AF4-MLL rather than a significant role of accumulated unprocessed endogenous MLL

or AF4-MLL for the growth of t(4;11) leukemic cells. Of high value to further elucidate the distinct roles of MLL-AF4 and AF4-MLL during t(4;11) leukemia progression, the altered expression of cell-cycle genes could not particularly be addressed to the inhibition of AF4-MLL or the accumulation of unprocessed endogenous MLL in this work.

A future transcriptomic analysis of dnTASP1-expressing PDX cells that either express MLL-AF4 alone or both t(4;11) fusion proteins could address whether unprocessed MLL or AF4-MLL is the key driver of de-regulated cell-cycle genes in progressing t(4;11) cells *in vivo*.

5.4. Short-term expressed AF4-MLL exerts long-lasting effect on transcriptome and chromatin in cooperation with MLL-AF4

t(4;11)-leukemia is challenging to model *in vivo* (Milne, 2017). So far, only a single study succeeded in the induction of a t(4;11) leukemia in mice (Bursen et al., 2010). Here, the presence of human AF4-MLL was required independent of the expression of human MLL-AF4 that alone failed to initiate the development of a leukemia. While the role of MLL-AF4 seems essential for leukemia progression, as indicated by the expression of MLL-AF4 in all t(4;11) patients and the inhibition of t(4;11) leukemia cell growth upon the knock-down of exclusively MLL-AF4 *in vivo* (Meyer et al., 2018; Völse, 2020), is the distinct role of AF4-MLL for leukemia onset controversially discussed (Bueno et al., 2019; Bursen et al., 2010; Kumar et al., 2011; Marschalek, 2019; Prieto et al., 2017; Völse, 2020). Despite different phenotypes observed upon the co-expression of both MLL fusion proteins, the presence of AF4-MLL appears to be not essential as indicated by not in frame 3'-MLL translocations or the absent expression of AF4-MLL in approximately 50 – 80% of t(4;11) patients and a presumably lacking impact on the growth of t(4;11) leukemia cells *in vivo* (Andersson et al., 2015; Downing et al., 1994; Kowarz et al., 2007; Meyer et al., 2018; Rego and Pandolfi, 2002). Moreover, a recent study correlated the expression of AF4-MLL with a high expression of *HOXA* genes that in turn resulted in an overall better treatment outcome (Agraz-Doblas et al., 2019). However, the consequence of expressing AF4-MLL to up-regulate *HOXA* genes has not been seen by several other previous studies and hence needs to be further validated (Kowarz et al., 2007; Stam et al., 2007, 2010b; Trentin et al., 2009; Völse, 2020) as it is of utmost importance for the risk assessment of t(4;11) patients and the development of more targeted therapies.

The aim of this work, besides the assessment of a novel targeted treatment approach against t(4;11) leukemia focusing on the role of both MLL fusion proteins during leukemia progression, was to elucidate the role of AF4-MLL during leukemia development.

Considering that the highly-stable AF4-MLL carries a functional N-terminus of the transcription-elongation factor AF4 and the C-terminus of MLL that is still capable of chromatin reading and writing, suggests an epigenetic regulator with a potent transforming activity (Marschalek, 2011a; Park et al., 2010; Patel et al., 2009; Prieto et al., 2017; Rössler and Marschalek, 2013; Yokoyama, 2015; Yokoyama et al., 2013). Furthermore, the target-determining N-terminus is replaced by AF4 indicating a chromatin modulating effect of AF4-MLL that is not restricted to target genes of endogenous MLL (Broeker et al., 1996; Erfurth et al., 2008; Marschalek, 2011b).

Hence, in this work the potential of AF4-MLL to exert a long-lasting effect on the chromatin and the transcriptome was elucidated to evaluate the hypothesis that AF4-MLL is essential particularly for a short interval during leukemogenesis and possibly obsolete for the onset of leukemia (Wilhelm and Marschalek, 2021). Using a cellular t(4;11) model that constitutively expressed MLL-AF4 but AF4-MLL exclusively for a short period of time, transcriptomic and chromatin accessibility analyses were conducted at different time points to evaluate the long-lasting effect of AF4-MLL.

As early as 1976, Peter Nowell proposed in *Science* his theory of “clonal evolution of tumor cell populations” (Nowell, 1976). In particular, he suggested that “tumor progression results from acquired genetic variability within the original clone allowing sequential selection of more aggressive sublines”. Accordingly, the long-term altered chromatin and transcriptome signatures obtained in this work seem to be established by an underlying clonal evolutionary process in the sense of a sequential selection that started with the short-term expression of AF4-MLL rather than an initially assumed single-step positive selection (Marschalek, 2019).

Focusing on highly de-regulated protein-coding genes only, shortly after the co-expression of MLL fusion proteins, a clear peak could be observed that was maintained over time above the expression levels observed before the short-term expression of AF4-MLL (Figure 4.3.3.1 E). In particular, the entries of highly up-regulated PCGs were still 3-fold increased 25 days post-expression of AF4-MLL in comparison to a 7-fold increase immediately after the co-expression situation. Yet, in favor for a positive selection process, the signature of all genes, that were at least 4-fold de-regulated, disappeared several days after the co-expression of both MLL fusion proteins and re-emerged to a later time point (Figure 4.3.3.1 B - D). The mere quantification of all highly differentially expressed genes and the statistical strength of the level of de-regulation suggests that the signature obtained at the latest time-point upon short-term expression of AF4-MLL, day 28, is derived from the signature obtained immediately after the co-expression of both MLL fusion proteins at day 3 (Figure 4.3.3.1 and Figure 4.3.3.2).

However, a deeper look into *de novo* and shut down genes rather suggests a clonal evolutionary process initiated upon the co-expression of MLL-AF4 and AF4-MLL than an initially hypothesized positive selection (Marschalek, 2019) (Figure 4.3.3.2). *De novo* gene analysis revealed a large fraction of genes primarily emerged at experimental day 12 and day 28, respectively (Figure 4.3.3.3). Of note, experimental day 12 and day 0 as well as day 3 and day 28, respectively, appeared to be similar considering the amount of total de-regulated genes (Figure 4.3.3.1). Nevertheless, in case of a positive selection process upon the co-expression of both MLL fusion proteins, the fraction of *de novo* genes re-emerging at day 28 would be assumed to profoundly overlap with the signature from day 3. Thus, the overall maintenance of *de novo* genes throughout all experimental days paired with 70%, 42% and 39% *de novo* genes emerging primarily at day 3, day 12 and day 28, respectively, support a clonal evolutionary process rather than a positive selection upon the short-term expression of AF4-MLL in interplay with MLL-AF4 (Figure 4.3.3.3). Thus, the previously assumed function of AF4-MLL to act as a “can-opener” on chromatin could be supported in a non-leukemic cellular background *in vitro*.

Next, a cooperative effect between MLL-AF4 and AF4-MLL could be determined leading to long-term epigenetic modulations (Figure 4.3.3.1), since the expression of either AF4-MLL or MLL-AF4 alone failed to induce a long-term signature on the chromatin (Figure 4.5.3.3). However, referencing previous loss-of-function studies and results of this work of co-targeting AF4-MLL that also demonstrate a lacking effect upon AF4-MLL inhibition alone on apoptosis or growth (Kumar et al., 2011; Völse, 2020), on the absent differences in chromatin signatures is inaccurate. The mentioned studies and the first part of this work focus on the consequences of inhibiting exclusively AF4-MLL during leukemia progression, while the transcriptome and chromatin analyses exclusively investigate a long-term epigenetic imprinting potential of the fusion proteins. Nevertheless, the data is consistent with a gain-of-function study of Prieto et al., that failed in CD34+ murine hematopoietic stem/progenitor cells to render any hematological or phenotypic sign of disease upon the expression of exclusively AF4-MLL (Prieto et al., 2017). Hence, a clonal evolutionary process is suggested that requires a cooperation of both MLL fusion proteins.

Despite using a non-leukemic cell line and the *in vitro* design of the study, the observed long-term effect of AF4-MLL in interplay with MLL-AF4 may serve as an explanation for the clinical situation observed in t(4;11) patients in addition to a putative correlation to *HOXA* gene signatures (Agraz-Doblas et al., 2019; Bueno et al., 2019; Stam et al., 2007, 2010b; Trentin et al., 2009; Völse, 2020). Particularly in the presence of both fusion proteins, a peak in de-regulation of gene expression and chromatin accessibility was observed. Of note, the study was not aiming to mimic leukemia development, but rather to unravel the potential of AF4-MLL in combination with MLL-AF4 to alter the chromatin and gene

transcription over time. Thereafter, the obtained MACE-seq and ATAC-seq data in this study support the supposed role of AF4-MLL to act on the chromatin as a “can-opener” that might play an important role during leukemogenesis (Marschalek, 2011a, 2015, 2019) (Figure 4.5.2.2). Consequently, the observed overall better prognosis of t(4;11) patients expressing AF4-MLL could be related to an AF4-MLL driven increased metabolic activity of leukemia cells. While, tremendously up-regulated genes might promote the oncogenic transformation of pre-leukemic hematopoietic cells it appears less plausible to be beneficial for the onset of leukemia. Thereafter, the poor treatment outcome of t(4;11) patients (Bueno et al., 2011; Felix et al., 2000; Hess, 2004; Isoyama et al., 2002; Pui et al., 2002), might be also derived from a shut down of genes upon the loss of AF4-MLL expression that are not particularly relevant for the oncogenic metabolism resulting in more resilient leukemia cells. Alternatively, considering the low load of somatic mutations in t(4;11) patients (Dobbins et al., 2013), leukemic cells with an elevated transcriptional activity may also exert a greater amount of targetable biological mechanisms.

Remarkably, MACE-seq and ATAC-seq analyses further revealed a significant up-regulation of mitochondrial genes when MLL-AF4 is expressed but also upon the co-expression with AF4-MLL (Figure 4.4.1.1.). Yet, a subsequent mitochondrial respiration assay could not detect any differences upon the expression of MLL-AF4 or AF4-MLL. Unfortunately, the experiments to investigate the effect of co-expression of both MLL fusion proteins on mitochondrial respiration beyond several others could not be completed due to the COVID-19 pandemic. Moreover, AF4-MLL-induced enhanced transcription levels that became more independent of the accessibility of chromatin (Figure 4.5.2.2) or vastly up-regulated pseudogenes and not-annotated genes (Figure 4.3.3.1) represent hitherto novel and possibly important observations that need to be further characterized in future studies. In summary, short-term expressed AF4-MLL in cooperation with MLL-AF4 exerts long-lasting epigenetic effects *in vitro* that presumably are following a clonal evolutionary process of sequential genetic selection processes. The data of the *in vitro* t(4;11) model suggest transforming activities of AF4-MLL that may take place during leukemogenesis but appear to be obsolete for disease progression.

5.5. Conclusions

In this study, a multifactorial approach was tested inhibiting HDACs and expressing dnTASP1 to target both MLL fusion proteins and to simultaneously stabilize endogenous MLL *in vitro*.

The expression of dnTASP1 in t(4;11) cells alone failed to induce apoptosis, whereas dnTASP1 significantly elevated apoptosis levels in HDACi-treated t(4;11) cells. Thus, the *in vitro* results underline the therapeutic potential of endorsing endogenous MLL in combination with co-inhibiting both MLL fusion proteins during t(4;11) leukemia progression.

Furthermore, upon receiving cellular samples from Kerstin Völse, for the first time, the transcriptome of t(4;11) PDX cells either expressing dnTASP1 or upon the knock-down of MLL-AF4 was analyzed *in vivo*. Despite the low number of samples, the knock-down of MLL-AF4 revealed the down-regulation of pivotal hemato-malignant factors and the expression of dnTASP1 led to massive deregulated cell cycle genes *in vivo*.

Finally, in a cooperative manner with MLL-AF4, transiently expressed AF4-MLL exerts long-lasting epigenetic effects and seems to be capable of inducing an evolutionary process of sequential genetic selection processes *in vitro*. These findings collectively suggest AF4-MLL to be primarily involved in the development of leukemia.

6. LIST OF ABBREVIATIONS

ACTC1	Actin Alpha Cardiac Muscle 1, Actin Alpha Cardiac Muscle 1
ADAM22	ADAM Metallopeptidase domain 22
ADM2	Adrenomedullin 2
AF4	ALL-1 fused gene on chromosome 4, ALL-1 fused gene on chromosome 4, ALL1-fused gene of chromosome 4
AFF1	AF4/FMR2 Family Member 1
AL	acute leukemia
ALF	AF4, LAF4, AF5q31 und FMR2
ALL	acute lymphoblastic leukemia
ALOX12B	Arachidonate 12-Lipoxygenase, 12R Type
AML	acute myeloid leukemia
APC/C	anaphase promoting complex
ASH2L	ASH2 Like, Histone Lysine Methyltransferase Complex Subunit
ASNSP1	Asparagine Synthetase Pseudogene 1
ATM	Ataxia Telangiectasia Mutated Serine/Threonine Kinase
AURKA	Aurora Kinase A
AURKB	Aurora Kinase B
B3GNT5	UDP-GlcNAc:BetaGal Beta-1,3-N-Acetylglucosaminyltransferase 5
B-ALL	-Cell Acute Lymphoblastic Leukemia
BBC3	BCL2 binding component 3
BCL-2	B-cell lymphoma 2
BCR	breakpoint cluster regions
BD	bromodomain
BET	bromodomain and extra-terminal domain
BIN2	Binding Integrator 2
BLK	B-lymphoid kinase, B-lymphoid tyrosine kinase
BMF	B-cell CLL/Lymphoma 2 (BCL2)-modifying factor
BMI1	B Lymphoma Mo-MLV Insertion Region 1 Homolog
BRDT	Bromodomain Testis Associated
BRIP1	BRCA1 interacting helicase 1
BTG1	B-cell translocation Gene 1
BTG2	BTG anti-proliferation factor 2
BUB1	Budding Uninhibited By Benzimidazoles 1
C1QTNF4	complement C1q tumor necrosis factor-related protein 4
C3orf58	Divergent Protein Kinase Domain 2A

CAR-T	chimeric antigen receptor T-cell
CBP	CREB-binding protein
CCL28	C-C Motif Chemokine Ligand 28
CCN3	Cellular Communication Network Factor 3
CCNB1	cyclin B1, Cyclin B1, Cyclin B1
CCNB2	Cyclin B2
CCND2	cyclin D2, Cyclin D2
CCNF	Cyclin F
CCR6	C-C Motif Chemokine Receptor 6
CD27	CD27 Molecule
CD37	tetraspanin 26
CD52	CD52 molecule
CDC	cell division cycle protein
CDC20	cell division cycle protein 20 homolog
CDC25B	Cell Division Cycle 25B
CDCA3	Cell Division Associated 3
CDCA7	cell division cycle associated 7
CDHR3	cadherin related family member 3
CDK	cyclin-dependent kinase, cyclin-dependent kinase
CDK1	Cyclin Dependent Kinase 1
CDK2	Cyclin Dependent Kinase
CDK4	Cyclin Dependent Kinase 4
CDK6	Cyclin Dependent Kinase 6
CENP	centromere protein
CENPA	Centromere Protein A
CHK1	checkpoint kinase 1
CKS2	CDC28 Protein Kinase Regulator Subunit 2
CL	chronic leukemia
CLL	chronic lymphoid leukemia
CML	chronic myeloid leukemia
COTL1	F-actin binding protein coactosin-like protein
CPEB2	cytoplasmic polyadenylation element binding protein 2
CPT	camptothecin
CtBP	C-Terminal Binding Protein 1
CTSB	lysosomal cysteine protease gene for cathepsin B
CYP33	cyclophilin33
DAG	diacylglycerol

DAZL	Deleted in Azoospermia Like
DCDC2C	Doublecortin Domain Containing 2C
DCPS	Decapping Scavenger Enzyme
DEF8	Differentially Expressed in FDCP 8 Homolog
DEPDC1	DEP domain-containing protein 1A
DEPP1	DEPP autophagy regulator 1
dnTASP1	Taspase1
DOT1L	Dot1-like protein
DSCC1	DNA replication and sister chromatid cohesion 1
DYSF	dysferlin
EMC4	ER Membrane Protein Complex Subunit 4
ENOSF1	enolase superfamily member 1
EP300	E1A Binding Protein P300
EPHB3	Ephrin type-b receptor 3
EPOR	Erythropoietin Receptor
ETP	T-cell precursor
FBXO43	F-Box carrying protein F-Box Protein 43
FBXO48	F-Box protein 48
FGA	Fibrinogen Alpha Chain
FGD6	FYVE, RhoGEF and PH domain containing protein 6
FHOD3	Formin Homology 2 Domain Containing 3
FLNB	Filamin B
FMR2	Fragile X Mental Retardation 2 Protein
FN1	glycoprotein fibronectin 1
FOXB1	Forkhead Box B1
FOXO1	transcription factor Forkhead box protein O1
FYRC	C-terminal MLL FY-rich domain
FYRN	N-terminal MLL FY-rich domain
GATA1	GATA Binding Protein 1
GATA3	GATA binding protein 3
GIMAP8	IMAP Family Member 8
GINS	go-ichi-ni-san
GINS1	GINS complex subunit 1, go-ichi-ni-san (GINS) complex subunit
GMNN	Geminin DNA replication inhibitor
GOI	gene of interest
GSEA	gene set enrichment analyses
GZMA	granzyme A

H2AFX	2A histone family member X variant histone H2A
H3K79	lysine 79 of histone 3
H3K9	histone H3 lysine 9
HAT	histone acetyltransferase
HBD	Hemoglobin Subunit Delta
HDAC	histone deacetylase
HDAC1	Histone deacetylase 1
HDAC2	Histone deacetylase 2
HELLS	lymphoid specific helicase
HLA	human leukocyte antigen
HLA-DMA	HLA class II alpha chain paralogues HLA-DM Alpha
HLA-DPB1	HLA-DP Beta 1
HLA-DQB1	HLA-DQ Beta 1
HLA-DRA	HLA-DR Alpha
HLA-DRB1	HLA class II beta chain paralogues HLA-DR Beta 1
HMGB2	high-mobility group protein B2
HMMR	Hyaluronan mediated motility receptor
HPC2	Heredity Prostate Cancer Protein 2
HPGDS	Hematopoietic Prostaglandin D Synthase
HSP6	Heat Shock Protein Family A (Hsp70) Member 6
HSPA5	Heat Shock Protein Family A (Hsp70) Member 5
iBCP	infant B-cell precursor
ICAM1	intercellular adhesion molecule 1
ICOSLG	inducible T cell costimulatory ligand
ID3	inhibitors of DNA binding 3
IER3	immediate early response 3 gene
IGF	Insulin like growth factor
IGFBP7	Insulin like growth factor (IGF) binding protein 7
IGHD	immunoglobulin heavy constant delta
IGLL1	immunoglobulin lamda like polypeptide 1
IGLL5	immunoglobulin lambda like polypeptide 5
IKZF1	Ikaros family zinc finger protein 1
IL18BP	Interleukin 18 Binding Protein
IL1B	Interleukin 1 Beta
IL1R2	Interleukin 1 Receptor Type 2
IL3RA	interleukin 3 receptor subunit alpha
IP3	inositol 1,4,5-trisphosphate

ITGA2	integrin subunit alpha 2
ITGA6	integrin subunit alpha 6
JAK2	Janus Kinase 2, Janus Kinase 2
JCHAIN	Joining Chain of Multimeric IgA and IgM
JMJD1C-AS1	jumonji domain containing 1C antisense RNA 1
KDM7A	Lysine Demethylase 7A
KEGG	Krypto Encyclopedia of Genes and Genomes, Kyoto Encyclopedia of Genes and Genomes
KIF18A	Kinesin Family Members 18A
KIF23	inesin Family Member 23
KIFC1	Kinesin Family Members C1, Kinesin Family Member C1
KLHL3	Kelch Like Family Member 3
KNTC1	CNA-associated factor encoded by the KIAA0101/PCLAF gene, kinetochore associated 1 protein
KPNA2	Karyopherin subunit alpha 2
LAF4	lymphoid nuclear protein related to AF4
LBD	Lens Epithelium-Derived Growth Factor binding domain
LCN10	lipocalin 10
LCN6	lipocalins, lipocalin 6
LEDGF	Lens Epithelium-Derived Growth Factor
LIMA1	LIM domain and actin bindin 1
LINC00173	long intergenic non-protein coding RNA 173
LINC01226	intergenic non-protein coding RNA 1226
lincRNAs	inter-genetic non-coding RNA
LL	lymphoblastic leukemia
LLGL1	Lethal Giant Larvae Homolog 1, Scribble Cell Polarity Complex
LTK	leukocyte receptor tyrosine kinase
MAPK3	Mitogen-Activated Protein Kinase 3
MARCH2	Membrane Associated Ring-CH-Type Finger 2
MBD	methyl-CpG binding domain
MCEF	Major CDK9 Elongation Factor-Associated Protein
MCM	minichromosome maintenance complex component
MCM4	minichromosome maintenance complex competent 4
MDM	Multiple Endocrine Neoplasia I Binding Motif
MDM2	ouse double minute 2 proto-oncogene
MED12L	mediator complex subunit 12L
MEIS1	Meis Homeobox 1

MELK	Maternal Embryonic Leucine Zipper Kinase
Menin1	Multiple Endocrine Neoplasia I
MIF	Macrophage Migration Inhibitory Factor
MIOX1	Myo-Inositol Oxygenase
MIR	microRNA
ML	myeloid leukemia
MLL	mixed-lineage leukemia
MLL-r	MLL-rearranged
MME	membrane metalloendopeptidase
MOF	Males Absent of the First, Males Absent of the First
MT	mitochondrial
MT1E	metallothionein 1E
MT2P1	metallothionein 2 pseudogene 1
MT-ATP6	Mitochondrially Encoded ATP Synthase Membrane Subunit 6
MT-CO1	Mitochondrially Encoded Cytochrome C Oxidase I, Mitochondrially Encoded Cytochrome C Oxidase I
MTMR2	Myotubularin Related Protein 2, Myotubularin Related Protein 2
MT-ND6	Mitochondrially Encoded NADH:Ubiquinone Oxidoreductase
MT-RNR1	Mitochondrially Encoded 12S RRNA
MT-RNR2	Mitochondrially Encoded 16S RRNA
MT-TA	Mitochondrially Encoded TRNA-Ala (GCN)
MT-TC	Mitochondrially Encoded TRNA-Cys (UGU/C)
MT-TF	Mitochondrially Encoded TRNA-Phe (UUU/C)
MT-TG	Mitochondrially Encoded TRNA-Gly (GGN)
MT-TI	Mitochondrially Encoded TRNA-Ile (AUU/C)
MT-TK	Mitochondrially Encoded TRNA-Lys (AAA/G)
MT-TL1	Mitochondrially Encoded TRNA-Leu (UUA/G) 1
MT-TQ	Mitochondrially Encoded TRNA-Gln (CAA/G)
MT-TR	Mitochondrially Encoded TRNA-Arg (CGN)
MT-TS1	Mitochondrially Encoded TRNA-Ser (UCN) 1
MT-TS2	Mitochondrially Encoded TRNA-Ser (AGU/C) 2
MT-TV	Mitochondrially Encoded TRNA-Val
MX1	MX Dynamin Like GTPase 1
MYL2	Myosin Light Chain 2
NA	non-annotated
NECTIN1	nectin cell adhesion molecule 1
NEIL1	Nei like DNA glycosylase 1

NEIL3	Endonuclease 8-like 3
NEUROG1	Neurogenin 1
NHD	N-terminal homology domain
NHEJ	Non-homologous-end-joining
NID	Nidogen 2
NLS	nuclear localization sequence
NMD	nonsense-mediated decay
NNAT	Neuronatin
NOP58	Nucleolar Protein 58
NUF2	NUF2 compoment of NDC80 kinetochore complex
NUP133	Nucleoporin 133
NUSAP1	Nucleolar And Spindle Associated Protein 1
NYAP2	Neuronal Tyrosine-Phosphorylated Phosphoinositide-3-Kinase
OIP5	Opa interacting protein 5
P2RY14	Purinergic Receptor P2Y14
PAK1	serine/threonine p21 (RAC1)-activating kinase 1
PCDH9	Protohadherin 9
PCG	Protein-coding gene
PDX	patient-derived xenograft
PECAM1	Platelet And Endothelial Cell Adhesion Molecule 1
PEG10	Paternally Expressed 10
PG	pseudogenes
PHD	plant homology domain
PHGDH	Phosphoglycerate Dehydrogenase
PIF1	PIF1 5'-To-3' DNA Helicase
PLCG1	phospholipase C, gamma 1
PLEKHG4B	Pleckstrin Homology And RhoGEF Domain Containing G4B
PLK1	Polo Like Kinase 1
POLE2	DNA polymerase Epsilon 2, accessory subunit
POLQ	polymerase theta
PPIC	peptidylprolyl isomerase C
PRKAG2-AS1	protein kinase AMP-activated non-catalytic subunit gamma 2 (PRKAG2) antisense RNA 1
pSer	phosphoserine
PSMA6	Proteasome 20S Subunit Alpha 6
PSRC1	Proline And Serine Rich Coiled-Coil 1
RAG1	recombination activating gene 1

RbBP6	RB Binding Protein 6, Ubiquitin Ligase
REEP3	receptor expression-enhancing protein 3
RELA	RELA Proto-Oncogene, NF-KB Subunit
RNAP II	77
RNU5D-1	snRNA 5UD Small Nuclear 1
RRM2	Ribonucleotide Reductase Regulatory Subunit M2
RUNX1	Runt-related transcription factor 1
RUNX3	Runt-related transcription factor 3
S100A4	S100 Calcium Binding Protein A4
SAMD9L	Sterile Alpha Motif Domain Containing 9 Like
SAPCD2	Suppressor APC Domain Containing 2
SATB1	special AT-rich sequence-binding protein-1
SCAMP5	secretory carrier membrane protein 5
SCIMP	SLP Adaptor And CSK Interacting Membrane Protein
scRNA-seq	single-cell RNA-seq
SEC	super elongation complex
SERPINF1	Serpin Family F Member 1
SET	Su(var)3-9,enhancer-of-zeste, trithorax
SH3RF3	SH3 domain containing ring finger 3
SIAH1	seven in absentia homologue 1
SIAH2	seven in absentia homologue 2
SLAMF1	Signaling Lymphocytic Activation Molecule Family Member 1
SMAD2	SMAD family member 2
SMAD3	SMAD Family Member 3, MAD Family Member 3
SMAD4	SMAD Family member 4
SNL	speckled nuclear localization site
SNO	small nucleolar RNA
SNX30	Sorting Nexin Family Member 30
SORBS2	Sorbin And SH3 Domain Containing 2
SPAG5	Sperm Associated Antigen 5
SPC25	Spindle Pole Body Component 25
STAT3	Signal Transducer And Activator of Transcription 3
STYK1	serine/threonine/tyrosine kinase 1
SULT1C2P1	Sulfotransferase Family 1C Member 2 Pseudogene 1
SYTL2	synaptotagmin like 2 protein
TAD	transactivation domain
Taspase1	Threonine Aspartase 1

TCA	tricarboxylic acid
TCEAL8	Transcription Elongation Factor A Like 8
TCL1B	T-Cell Leukemia/Lymphoma 1 AKT Coactivator B
TCS	taspase1 cleavage site
TDO2	Tryptophan 2,3-Dioxygenase
TMEM177	transmembrane protein 177
TNF	tumor negrosis factor
TNFAIP3	TNF alpha induced protein 3
TNFAIP6	TNF Alpha Induced Protein 6
TP53INP1	tumor protein p53 inducible nuclear protein 1
TP73	tumor protein p77
TPMT	Thiopurine S-Methyltransferase
TRIP13	thyroid hormone receptor interactor 13
TROAP	Trophinin associated protein
TSS	transcription start site
TUBB4B	Tubulin Beta 4B Class IVb
TYMP	Thymidine Phosphorylase
TYMS	tymidylate synthase
UBC	Ubiquitin C
UBE2C	Ubiquitin Conjugating Enzyme E2 C
UBE2T	Ubiquitin-conjugating enzyme E2 T
US	United States
WDR5	WD Repeat Domain 5
WEE1	WEE1 G2 Checkpoint Kinase
ZEB1	Zinc Finger E-Box Binding Homeobox 1
ZEB2	Zinc Finger E-Box Binding Homeobox 2
ZHX3	Zinc Fingers And Homeoboxes 3
ZIC2	Zic Family Member 2
ZNF439	Zinc Finger Protein 439

7. LIST OF FIGURES AND TABLES

Figures

Figure 1.1.1: Hematopoietic system

Figure 1.1.2: Age distribution of leukemia patients

Figure 1.1.3: Incidence of leukemia patients relative to all cancer cases

Figure 1.2.1: Functional domains of the mixed lineage leukemia (MLL) protein

Figure 1.2.2: Age distribution of *MLL-r* leukemia cases

Figure 1.2.3: Translocation partner genes of MLL according to age and lineage

Figure 1.3.1: Functional domains of the ALL-1 fused gene on chromosome 4 (AF4) protein

Figure 1.3.2: t(4;11) translocation results in the fusion proteins MLL-AF4 and AF4-MLL

Figure 1.4.1.: Histone deacetylase (HDAC) isoforms

Figure 4.1.1.1: Generation of an inducible dnTASP1-expressing t(4;11) pro-B ALL cell line

Figure 4.1.2.1: No difference in viability of HDACi-treated SEM cells upon short-term expression of dnTASP1

Figure 4.1.3.1: SEM cells respond individually to different HDACi after 28 days expression of dnTASP1

Figure 4.1.3.2: Flow Cytometry based Annexin V Assay design for SEM cells

Figure 4.1.3.3: Determination of dnTASP1 expression and HDACi-treatment intervals to induce apoptosis in SEM cells

Figure 4.1.3.4: HDACi-treated SEM cells respond in a delayed manner to dnTASP1 expression

Figure 4.1.3.5: The prolonged HDACi treatment of SEM cells elicits an immediate response to dnTASP1 expression

- Figure 4.2.1.1: Induced MLL-AF4 knock-down alters transcription of PDX leukemia cells *in vivo*
- Figure 4.2.1.2: Top down-regulated genes upon MLL-AF4 knock-down in PDX leukemia cells
- Figure 4.2.1.3: Top up-regulated genes upon MLL-AF4 knock-down in PDX leukemia cells
- Figure 4.2.1.4: t(4;11) PDX cells share physical and functional targets upon MLL-AF4 knock-down independent of the expression of AF4-MLL
- Figure 4.2.2.1: Expression of dnTASP1 increases amount of significantly up-regulated genes *in vivo*
- Figure 4.2.2.2: Cell-cycle-related genes are significantly up-regulated upon expression of dnTASP1 *in vivo*
- Figure 4.3.1.1: A cellular t(4;11) model to study transcriptional signatures upon short-term expression of AF4-MLL
- Figure 4.3.2.1: Cloning of t(4;11) fusion genes and generation of cellular t(4;11) model
- Figure 4.3.2.2: Presence of t(4;11) fusion transgene vectors throughout experimental time points
- Figure 4.3.3.1: AF4-MLL promotes expression of pseudogenes and non-annotated genes
- Figure 4.3.3.2: Lost AF4-MLL-induced signature of up-regulated genes reappears over time
- Figure 4.3.4.1: AF4-MLL activates *de novo* genes and shut down genes
- Figure 4.3.5.1: Gene expression analysis reveals correlation between *in vitro* t(4;11) model and *in vivo* gene sets of infant B-ALL patients
- Figure 4.3.6.1: Modelling putative modes of action of t(4;11) fusion proteins during leukemogenesis using k means based clusters enables the identification of novel AF4-MLL-associated genes
- Figure 4.4.1.1: t(4;11) fusion proteins elevate expression of the majority of mitochondrial genes
- Figure 4.4.2.1: t(4;11) fusion proteins play a minor role in mitochondrial respiration *in vitro*
- Figure 4.5.1.1: A cellular t(4;11) model to study accessibility of chromatin upon short-term expression of AF4-MLL

Figure 4.5.2.1: Short-term expression of AF4-MLL alters chromatin accessibility

Figure 4.5.2.2: Briefly expressed AF4-MLL exerts not only a lasting effect on the transcriptome and chromatin, but also facilitates up-regulation of genes in less accessible chromatin regions

Figure 4.5.3.1: A cellular t(4;11) model to study t(4;11) fusion proteins individually

Figure 4.5.3.2: MLL-AF4 and AF4-MLL act in different ways on chromatin

Figure 4.5.3.3: Interplay of MLL-AF4 and AF4-MLL mediate long-term impact on chromatin

Tables

Table 1.4.1: Strategies to inhibit MLL fusion proteins.

Table 2.1.: Cell lines

Table 2.2.: Bacterial strains

Table 2.3.: Oligonucleotides

Table 2.4.1: Primary antibodies

Table 2.4.2: Secondary antibodies

Table 2.5: Enzymes

Table 2.6: Plasmids

Table 2.7: Commercial kits

Table 2.8: Reagents

Table 2.9.1: Buffers

Table 2.9.2: Media

8. REFERENCES

Agraz-Doblas, A., Bueno, C., Bashford-Rogers, R., Roy, A., Schneider, P., Bardini, M., Ballerini, P., Cazzaniga, G., Moreno, T., Revilla, C., et al. (2019). Unraveling the cellular origin and clinical prognostic markers of infant B-cell acute lymphoblastic leukemia using genome-wide analysis. *Haematologica* *104*, 1176–1188. <https://doi.org/10.3324/haematol.2018.206375>.

Ahmad, K., Katryniok, C., Scholz, B., Merkens, J., Löscher, D., Marschalek, R., and Steinhilber, D. (2014). Inhibition of class I HDACs abrogates the dominant effect of MLL-AF4 by activation of wild-type MLL. *Oncogenesis* *3*, e127–e127. <https://doi.org/10.1038/oncsis.2014.39>.

Ahmad, K., Scholz, B., Capelo, R., Schweighöfer, I., Kahnt, A.S., Marschalek, R., and Steinhilber, D. (2015). AF4 and AF4-MLL mediate transcriptional elongation of 5-lipoxygenase mRNA by 1, 25-dihydroxyvitamin D3. *Oncotarget* *6*, 25784. .

Alachkar, H., Mutonga, M.B.G., Metzeler, K.H., Fulton, N., Malnassy, G., Herold, T., Spiekermann, K., Bohlander, S.K., Hiddemann, W., Matsuo, Y., et al. (2014). Preclinical efficacy of maternal embryonic leucine-zipper kinase (MELK) inhibition in acute myeloid leukemia. *Oncotarget* *5*, 12371–12382. .

Alanazi, B., Munje, C.R., Rastogi, N., Williamson, A.J.K., Taylor, S., Hole, P.S., Hodges, M., Doyle, M., Baker, S., Gilkes, A.F., et al. (2020). Integrated nuclear proteomics and transcriptomics identifies S100A4 as a therapeutic target in acute myeloid leukemia. *Leukemia* *34*, 427–440. <https://doi.org/10.1038/s41375-019-0596-4>.

Almamun, M., Levinson, B.T., van Swaay, A.C., Johnson, N.T., McKay, S.D., Arthur, G.L., Davis, J.W., and Taylor, K.H. (2015). Integrated methylome and transcriptome analysis reveals novel regulatory elements in pediatric acute lymphoblastic leukemia. *Epigenetics* *10*, 882–890. <https://doi.org/10.1080/15592294.2015.1078050>.

Anderlini, P., Luna, M., Kantarjian, H.M., O'Brien, S., Pierce, S., Keating, M.J., and Estey, E.H. (1996). Causes of initial remission induction failure in patients with acute myeloid leukemia and myelodysplastic syndromes. *Leukemia* *10*, 600–608. .

Andersson, A.K., Ma, J., Wang, J., Chen, X., Gedman, A.L., Dang, J., Nakitandwe, J., Holmfeldt, L., Parker, M., Easton, J., et al. (2015). The landscape of somatic mutations in infant MLL-rearranged acute lymphoblastic leukemias. *Nat. Genet.* *47*, 330–337. <https://doi.org/10.1038/ng.3230>.

Artinger, E.L., Mishra, B.P., Zaffuto, K.M., Li, B.E., Chung, E.K.Y., Moore, A.W., Chen, Y., Cheng, C., and Ernst, P. (2013). An MLL-dependent network sustains hematopoiesis. *Proc. Natl. Acad. Sci. U. S. A.* *110*, 12000–12005. <https://doi.org/10.1073/pnas.1301278110>.

Asteriti, I.A., De Mattia, F., and Guarguaglini, G. (2015). Cross-Talk between AURKA and Plk1 in Mitotic Entry and Spindle Assembly. *Front. Oncol.* *5*. .

- Bai, Z., Woodhouse, S., Kim, D., Lundh, S., Sun, H., Deng, Y., Xiao, Y., Barrett, D.M., Myers, R.M., Grupp, S.A., et al. (2021). Single-cell antigen-specific activation landscape of CAR T infusion product identifies determinants of CD19 positive relapse in patients with ALL. 2021.04.15.440005. <https://doi.org/10.1101/2021.04.15.440005>.
- Balasubramanian, S., Verner, E., and Buggy, J.J. (2009). Isoform-specific histone deacetylase inhibitors: The next step? *Cancer Lett.* 280, 211–221. <https://doi.org/10.1016/j.canlet.2009.02.013>.
- Balgobind, B.V., Raimondi, S.C., Harbott, J., Zimmermann, M., Alonzo, T.A., Auvrignon, A., Beverloo, H.B., Chang, M., Creutzig, U., and Dworzak, M.N. (2009). Novel prognostic subgroups in childhood 11q23/MLL-rearranged acute myeloid leukemia: results of an international retrospective study. *Blood J. Am. Soc. Hematol.* 114, 2489–2496. .
- Bannister, A.J., and Kouzarides, T. (1996). The CBP co-activator is a histone acetyltransferase. *Nature* 384, 641–643. .
- Barretto, N.N., Karahalios, D.S., You, D., and Hemenway, C.S. (2014). An AF9/ENL-targeted peptide with therapeutic potential in mixed lineage leukemias. *J. Exp. Ther. Oncol.* 10, 293–300. .
- Barry, E.R., Corry, G.N., and Rasmussen, T.P. (2010). Targeting DOT1L action and interactions in leukemia: the role of DOT1L in transformation and development. *Expert Opin. Ther. Targets* 14, 405–418. <https://doi.org/10.1517/14728221003623241>.
- Beck, J.D., Reidenbach, D., Salomon, N., Sahin, U., Türeci, Ö., Vormehr, M., and Kranz, L.M. (2021). mRNA therapeutics in cancer immunotherapy. *Mol. Cancer* 20, 69. <https://doi.org/10.1186/s12943-021-01348-0>.
- Bene, M.C., Castoldi, G., Knapp, W., Ludwig, W.D., Matutes, E., Orfao, A., and van't Veer, M.B. (1995). Proposals for the immunological classification of acute leukemias. European Group for the Immunological Characterization of Leukemias (EGIL). *Leukemia* 9, 1783–1786. .
- Benedikt, A., Baltruschat, S., Scholz, B., Bursen, A., Arrey, T.N., Meyer, B., Varagnolo, L., Müller, A.M., Karas, M., Dingermann, T., et al. (2011). The leukemogenic AF4–MLL fusion protein causes P-TEFb kinase activation and altered epigenetic signatures. *Leukemia* 25, 135–144. <https://doi.org/10.1038/leu.2010.249>.
- Bernhard, D., Skvortsov, S., Tinhofer, I., Hübl, H., Greil, R., Csordas, A., and Kofler, R. (2001). Inhibition of histone deacetylase activity enhances Fas receptor-mediated apoptosis in leukemic lymphoblasts. *Cell Death Differ.* 8, 1014–1021. <https://doi.org/10.1038/sj.cdd.4400914>.
- Bhatia, P., Singh, M., Singh, A., Sharma, P., Trehan, A., and Varma, N. (2021). Epigenetic analysis reveals significant differential expression of miR-378C and miR-128-2-5p in a cohort of relapsed pediatric B-acute lymphoblastic leukemia cases. *Int. J. Lab. Hematol.* 43, 1016–1023. <https://doi.org/10.1111/ijlh.13477>.

- Bhatla, T., Wang, J., Morrison, D.J., Raetz, E.A., Burke, M.J., Brown, P., and Carroll, W.L. (2012). Epigenetic reprogramming reverses the relapse-specific gene expression signature and restores chemosensitivity in childhood B-lymphoblastic leukemia. *Blood* 119, 5201–5210. <https://doi.org/10.1182/blood-2012-01-401687>.
- Bier, C., Knauer, S.K., Klapthor, A., Schweitzer, A., Reik, A., Krämer, O.H., Marschalek, R., and Stauber, R.H. (2011). Cell-based Analysis of Structure-Function Activity of Threonine Aspartase 1 *. *J. Biol. Chem.* 286, 3007–3017. <https://doi.org/10.1074/jbc.M110.161646>.
- Bitoun, E., Oliver, P.L., and Davies, K.E. (2007). The mixed-lineage leukemia fusion partner AF4 stimulates RNA polymerase II transcriptional elongation and mediates coordinated chromatin remodeling. *Hum. Mol. Genet.* 16, 92–106. <https://doi.org/10.1093/hmg/ddl444>.
- Bohannon, R.A., Miller, D.G., and Diamond, H.D. (1963). Vincristine in the Treatment of Lymphomas and Leukemias*. *Cancer Res.* 23, 613–621. .
- Bolden, J.E., Peart, M.J., and Johnstone, R.W. (2006). Anticancer activities of histone deacetylase inhibitors. *Nat. Rev. Drug Discov.* 5, 769–784. <https://doi.org/10.1038/nrd2133>.
- Borkin, D., He, S., Miao, H., Kempinska, K., Pollock, J., Chase, J., Purohit, T., Malik, B., Zhao, T., Wang, J., et al. (2015). Pharmacologic Inhibition of the Menin-MLL Interaction Blocks Progression of MLL Leukemia In Vivo. *Cancer Cell* 27, 589–602. <https://doi.org/10.1016/j.ccell.2015.02.016>.
- Breese, E.H., Krupski, C., Nelson, A.S., Perentesis, J.P., and Phillips, C.L. (2021). Use of CD19-directed CAR T-Cell Therapy in an Infant With Refractory Acute Lymphoblastic Leukemia. *J. Pediatr. Hematol. Oncol.* 43, 152–154. <https://doi.org/10.1097/MPH.0000000000001857>.
- Britten, O., Ragusa, D., Tosi, S., and Mostafa Kamel, Y. (2019). MLL-Rearranged Acute Leukemia with t(4;11)(q21;q23)—Current Treatment Options. Is There a Role for CAR-T Cell Therapy? *Cells* 8, 1341. <https://doi.org/10.3390/cells8111341>.
- Broeker, P.L., Harden, A., Rowley, J.D., and Zeleznik-Le, N. (1996). The Mixed Lineage Leukemia (MLL) Protein Involved in 11 q23 Translocations Contains a Domain that Binds Cruciform DNA and Scaffold Attachment Region (SAR) DNA. In *Molecular Aspects of Myeloid Stem Cell Development*, (Springer), pp. 259–268.
- Bueno, C., Montes, R., Catalina, P., Rodríguez, R., and Menendez, P. (2011). Insights into the cellular origin and etiology of the infant pro-B acute lymphoblastic leukemia with MLL-AF4 rearrangement. *Leukemia* 25, 400–410. <https://doi.org/10.1038/leu.2010.284>.
- Bueno, C., Calero-Nieto, F.J., Wang, X., Valdés-Mas, R., Gutiérrez-Agüera, F., Roca-Ho, H., Ayllon, V., Real, P.J., Arambilet, D., Espinosa, L., et al. (2019). Enhanced hemato-endothelial specification during human embryonic differentiation through developmental cooperation between AF4-MLL and MLL-AF4 fusions. *Haematologica* 104, 1189–1201. <https://doi.org/10.3324/haematol.2018.202044>.

- Bursen, A., Moritz, S., Gaussmann, A., Moritz, S., Dingermann, T., and Marschalek, R. (2004). Interaction of AF4 wild-type and AF4-MLL fusion protein with SIAH proteins: indication for t(4;11) pathobiology? *Oncogene* 23, 6237–6249. <https://doi.org/10.1038/sj.onc.1207837>.
- Bursen, A., Schwabe, K., Ruster, B., Henschler, R., Ruthardt, M., Dingermann, T., and Marschalek, R. (2010). The AF4{middle dot}MLL fusion protein is capable of inducing ALL in mice without requirement of MLL{middle dot}AF4. *Blood* 115, 3570–3579. <https://doi.org/10.1182/blood-2009-06-229542>.
- Cao, F., Townsend, E.C., Karatas, H., Xu, J., Li, L., Lee, S., Liu, L., Chen, Y., Ouillette, P., Zhu, J., et al. (2014). Targeting MLL1 H3K4 Methyltransferase Activity in Mixed-Lineage Leukemia. *Mol. Cell* 53, 247–261. <https://doi.org/10.1016/j.molcel.2013.12.001>.
- Carlet, M., Völse, K., Vergalli, J., Becker, M., Herold, T., Arner, A., Liu, W.-H., Dill, V., Fehse, B., Baldus, C.D., et al. (2020). In vivo inducible reverse genetics in patients' tumors to identify individual therapeutic targets. *BioRxiv* 2020.05.02.073577. <https://doi.org/10.1101/2020.05.02.073577>.
- Carlet, M., Völse, K., Vergalli, J., Becker, M., Herold, T., Arner, A., Senft, D., Jurinovic, V., Liu, W.-H., Gao, Y., et al. (2021). In vivo inducible reverse genetics in patients' tumors to identify individual therapeutic targets. *Nat. Commun.* 12, 5655. <https://doi.org/10.1038/s41467-021-25963-z>.
- Caslini, C., Alarcón, As., Hess, J.L., Tanaka, R., Murti, K.G., and Biondi, A. (2000). The amino terminus targets the mixed lineage leukemia (MLL) protein to the nucleolus, nuclear matrix and mitotic chromosomal scaffolds. *Leukemia* 14, 1898–1908. <https://doi.org/10.1038/sj.leu.2401933>.
- Caslini, C., Yang, Z., El-Osta, M., Milne, T.A., Slany, R.K., and Hess, J.L. (2007). Interaction of MLL amino terminal sequences with menin is required for transformation. *Cancer Res.* 67, 7275–7283. <https://doi.org/10.1158/0008-5472.CAN-06-2369>.
- Ceccacci, E., and Minucci, S. (2016). Inhibition of histone deacetylases in cancer therapy: lessons from leukaemia. *Br. J. Cancer* 114, 605–611. <https://doi.org/10.1038/bjc.2016.36>.
- Čermáková, K., Tesina, P., Demeulemeester, J., El Ashkar, S., Méreau, H., Schwaller, J., Řezáčová, P., Veverka, V., and De Rijck, J. (2014). Validation and Structural Characterization of the LEDGF/p75–MLL Interface as a New Target for the Treatment of MLL-Dependent Leukemia. *Cancer Res.* 74, 5139–5151. <https://doi.org/10.1158/0008-5472.CAN-13-3602>.
- Chandrasekharappa, S.C., and Teh, B.T. (2003). Functional studies of the MEN1 gene. *J. Intern. Med.* 253, 606–615. .
- Chandrasekharappa, S.C., Guru, S.C., Manickam, P., Olufemi, S.-E., Collins, F.S., Emmert-Buck, M.R., Debelenko, L.V., Zhuang, Z., Lubensky, I.A., and Liotta, L.A. (1997). Positional cloning of the gene for multiple endocrine neoplasia-type 1. *Science* 276, 404–407. .

Cheah, J.J.C., Brown, A.L., Schreiber, A.W., Feng, J., Babic, M., Moore, S., Young, C.-C., Fine, M., Phillips, K., Guandalini, M., et al. (2019). A novel germline SAMD9L mutation in a family with ataxia-pancytopenia syndrome and pediatric acute lymphoblastic leukemia. *Haematologica* 104, e318–e321. <https://doi.org/10.3324/haematol.2018.207316>.

ChemoMetec A/S. (2003). Annexin V Assay using the NucleoCounter® NC-3000™ System. Application note No 3017 Rev 14.

Chen, C., Hilden, J., Frestedt, J., Domer, P., Moore, R., Korsmeyer, S., and Kersey, J. (1993). The chromosome 4q21 gene (AF-4/FEL) is widely expressed in normal tissues and shows breakpoint diversity in t(4;11)(q21;q23) acute leukemia. *Blood* 82, 1080–1085. <https://doi.org/10.1182/blood.V82.4.1080.1080>.

Chen, D., Zheng, J., Gerasimcik, N., Lagerstedt, K., Sjögren, H., Abrahamsson, J., Fogelstrand, L., and Mårtensson, I.-L. (2016). The Expression Pattern of the Pre-B Cell Receptor Components Correlates with Cellular Stage and Clinical Outcome in Acute Lymphoblastic Leukemia. *PLOS ONE* 11, e0162638. <https://doi.org/10.1371/journal.pone.0162638>.

Chen, D.Y., Liu, H., Takeda, S., Tu, H.-C., Sasagawa, S., Van Tine, B.A., Lu, D., Cheng, E.H.-Y., and Hsieh, J.J.-D. (2010). Taspase1 Functions as a Non-Oncogene Addiction Protease that Coordinates Cancer Cell Proliferation and Apoptosis. *Cancer Res.* 70, 5358–5367. <https://doi.org/10.1158/0008-5472.CAN-10-0027>.

Chen, Z., Shojaee, S., Buchner, M., Geng, H., Lee, J.W., Klemm, L., Titz, B., Graeber, T.G., Park, E., Tan, Y.X., et al. (2015). Signalling thresholds and negative B-cell selection in acute lymphoblastic leukaemia. *Nature* 521, 357–361. <https://doi.org/10.1038/nature14231>.

Chunsong, H., Yuling, H., Li, W., Jie, X., Gang, Z., Qiuping, Z., Qingping, G., Kejian, Z., Li, Q., Chang, A.E., et al. (2006). CXC Chemokine Ligand 13 and CC Chemokine Ligand 19 Cooperatively Render Resistance to Apoptosis in B Cell Lineage Acute and Chronic Lymphocytic Leukemia CD23+CD5+ B Cells. *J. Immunol.* 177, 6713–6722. <https://doi.org/10.4049/jimmunol.177.10.6713>.

Commities, W., Haggard, M.E., Fernbach, D.J., Holcomb, T.M., Sutow, W.W., Vietti, T.J., and Windmiller, J. (1968). Vincristine in acute leukemia of childhood. *Cancer* 22, 438–444. [https://doi.org/10.1002/1097-0142\(196808\)22:2<438::AID-CNCR2820220222>3.0.CO;2-M](https://doi.org/10.1002/1097-0142(196808)22:2<438::AID-CNCR2820220222>3.0.CO;2-M).

Consolaro, F., Basso, G., Ghaem-Magami, S., Lam, E.W.-F., and Viola, G. (2015). FOXM1 is overexpressed in B-acute lymphoblastic leukemia (B-ALL) and its inhibition sensitizes B-ALL cells to chemotherapeutic drugs. *Int. J. Oncol.* 47, 1230–1240. <https://doi.org/10.3892/ijo.2015.3139>.

Cools, J. (2012). Improvements in the survival of children and adolescents with acute lymphoblastic leukemia. *Haematologica* 97, 635–635. <https://doi.org/10.3324/haematol.2012.068361>.

- Cruz-Miranda, G.M., Hidalgo-Miranda, A., Bárcenas-López, D.A., Núñez-Enríquez, J.C., Ramírez-Bello, J., Mejía-Aranguré, J.M., and Jiménez-Morales, S. (2019). Long Non-Coding RNA and Acute Leukemia. *Int. J. Mol. Sci.* 20, 735. <https://doi.org/10.3390/ijms20030735>.
- Daigle, S.R., Olhava, E.J., Therkelsen, C.A., Basavapathruni, A., Jin, L., Boriack-Sjodin, P.A., Allain, C.J., Klaus, C.R., Raimondi, A., and Scott, M.P. (2013). Potent inhibition of DOT1L as treatment of MLL-fusion leukemia. *Blood* 122, 1017–1025. .
- Davezac, N., Baldin, V., Blot, J., Ducommun, B., and Tassan, J.-P. (2002). Human pEg3 kinase associates with and phosphorylates CDC25B phosphatase: a potential role for pEg3 in cell cycle regulation. *Oncogene* 21, 7630–7641. <https://doi.org/10.1038/sj.onc.1205870>.
- Davidson, G., and Niehrs, C. (2010). Emerging links between CDK cell cycle regulators and Wnt signaling. *Trends Cell Biol.* 20, 453–460. <https://doi.org/10.1016/j.tcb.2010.05.002>.
- Dawson, M.A., Prinjha, R.K., Dittmann, A., Giotopoulos, G., Bantscheff, M., Chan, W.-I., Robson, S.C., Chung, C., Hopf, C., Savitski, M.M., et al. (2011). Inhibition of BET recruitment to chromatin as an effective treatment for MLL-fusion leukaemia. *Nature* 478, 529–533. <https://doi.org/10.1038/nature10509>.
- Delgado, M.D., and León, J. (2010). Myc Roles in Hematopoiesis and Leukemia. *Genes Cancer* 1, 605–616. <https://doi.org/10.1177/1947601910377495>.
- Deo, R. (2017). Maternal Embryonic Leucine Zipper Kinase (MELK) as a Novel Therapeutic Target in the Treatment of Acute Lymphoblastic Leukemia. M.S.
- Deshpande, A.J., Bradner, J., and Armstrong, S.A. (2012). Chromatin modifications as therapeutic targets in MLL-rearranged leukemia. *Trends Immunol.* 33, 563–570. .
- Di Micco, R., Fontanals-Cirera, B., Low, V., Ntziachristos, P., Yuen, S.K., Lovell, C.D., Dolgalev, I., Yonekubo, Y., Zhang, G., Rusinova, E., et al. (2014). Control of Embryonic Stem Cell Identity by BRD4-Dependent Transcriptional Elongation of Super-Enhancer-Associated Pluripotency Genes. *Cell Rep.* 9, 234–247. <https://doi.org/10.1016/j.celrep.2014.08.055>.
- Djabali, M., Selleri, L., Parry, P., Bower, M., Young, B.D., and Evans, G.A. (1992). A trithorax-like gene is interrupted by chromosome 11q23 translocations in acute leukaemias. *Nat. Genet.* 2, 113–118. <https://doi.org/10.1038/ng1092-113>.
- Dobbins, S.E., Sherborne, A.L., Ma, Y.P., Bardini, M., Biondi, A., Cazzaniga, G., Lloyd, A., Chubb, D., Greaves, M.F., and Houlston, R.S. (2013). The silent mutational landscape of infant MLL-AF4 pro-B acute lymphoblastic leukemia. *Genes. Chromosomes Cancer* 52, 954–960. <https://doi.org/10.1002/gcc.22090>.
- Döhner, H., Estey, E.H., Amadori, S., Appelbaum, F.R., Büchner, T., Burnett, A.K., Dombret, H., Fenaux, P., Grimwade, D., Larson, R.A., et al. (2010). Diagnosis and management of acute myeloid leukemia in adults: recommendations from an international

expert panel, on behalf of the European LeukemiaNet. *Blood* 115, 453–474. <https://doi.org/10.1182/blood-2009-07-235358>.

Dombret, H., and Gardin, C. (2016). An update of current treatments for adult acute myeloid leukemia. *Blood* 127, 53–61. <https://doi.org/10.1182/blood-2015-08-604520>.

Dou, Y., Milne, T.A., Tackett, A.J., Smith, E.R., Fukuda, A., Wysocka, J., Allis, C.D., Chait, B.T., Hess, J.L., and Roeder, R.G. (2005). Physical association and coordinate function of the H3 K4 methyltransferase MLL1 and the H4 K16 acetyltransferase MOF. *Cell* 121, 873–885. .

Downing, J.R., Head, D.R., Raimondi, S.C., Carroll, A.J., Curcio-Brint, A.M., Motroni, T.A., Hulshof, M.G., Pullen, D.J., and Domer, P.H. (1994). The der(11)-encoded MLL/AF-4 fusion transcript is consistently detected in t(4;11)(q21;q23)-containing acute lymphoblastic leukemia. *Blood* 83, 330–335. .

Dreyer, Z.E., Hilden, J.M., Jones, T.L., Devidas, M., Winick, N.J., Willman, C.L., Harvey, R.C., Chen, I.-M., Behm, F.G., Pullen, J., et al. (2015). Intensified chemotherapy without SCT in infant ALL: Results from COG P9407 (Cohort 3). *Pediatr. Blood Cancer* 62, 419–426. <https://doi.org/10.1002/psc.25322>.

Druker, B.J. (2002). Inhibition of the Bcr-Abl tyrosine kinase as a therapeutic strategy for CML. *Oncogene* 21, 8541–8546. <https://doi.org/10.1038/sj.onc.1206081>.

Dunwell, T., Hesson, L., Rauch, T.A., Wang, L., Clark, R.E., Dallol, A., Gentle, D., Catchpoole, D., Maher, E.R., Pfeifer, G.P., et al. (2010). A Genome-wide screen identifies frequently methylated genes in haematological and epithelial cancers. *Mol. Cancer* 9, 44. <https://doi.org/10.1186/1476-4598-9-44>.

Dutertre, S., Cazales, M., Quaranta, M., Froment, C., Trabut, V., Dozier, C., Mirey, G., Bouché, J.-P., Theis-Febvre, N., Schmitt, E., et al. (2004). Phosphorylation of CDC25B by Aurora-A at the centrosome contributes to the G2-M transition. *J. Cell Sci.* 117, 2523–2531. <https://doi.org/10.1242/jcs.01108>.

Eckschlager, T., Plch, J., Stiborova, M., and Hrabeta, J. (2017). Histone Deacetylase Inhibitors as Anticancer Drugs. *Int. J. Mol. Sci.* 18, 1414. <https://doi.org/10.3390/ijms18071414>.

Eguchi, M., Eguchi-Ishimae, M., Knight, D., Kearney, L., Slany, R., and Greaves, M. (2006). MLL chimeric protein activation renders cells vulnerable to chromosomal damage: An explanation for the very short latency of infant leukemia. *Genes. Chromosomes Cancer* 45, 754–760. <https://doi.org/10.1002/gcc.20338>.

Emerenciano, M., Meyer, C., Mansur, M.B., Marschalek, R., Pombo-de-Oliveira, M.S., and Leukaemia, B.C.S.G. of I.A. (2013). The distribution of MLL breakpoints correlates with outcome in infant acute leukaemia. *Br. J. Haematol.* 161, 224–236. .

Erfurth, F.E., Popovic, R., Grembecka, J., Cierpicki, T., Theisler, C., Xia, Z.-B., Stuart, T., Diaz, M.O., Bushweller, J.H., and Zeleznik-Le, N.J. (2008). MLL protects CpG clusters from

methylation within the *Hoxa9* gene, maintaining transcript expression. *Proc. Natl. Acad. Sci.* *105*, 7517–7522. <https://doi.org/10.1073/pnas.0800090105>.

Ernst, P., Wang, J., Huang, M., Goodman, R.H., and Korsmeyer, S.J. (2001). MLL and CREB bind cooperatively to the nuclear coactivator CREB-binding protein. *Mol. Cell. Biol.* *21*, 2249–2258. .

Ernst, P., Mabon, M., Davidson, A.J., Zon, L.I., and Korsmeyer, S.J. (2004). An MLL-dependent Hox program drives hematopoietic progenitor expansion. *Curr. Biol.* *14*, 2063–2069. .

Felix, C.A., Lange, B.J., and Chessells, J.M. (2000). Pediatric acute lymphoblastic leukemia: challenges and controversies in 2000. *ASH Educ. Program Book 2000*, 285–302. .

Ferreirós-Vidal, I., Carroll, T., Taylor, B., Terry, A., Liang, Z., Bruno, L., Dharmalingam, G., Khadayate, S., Cobb, B.S., Smale, S.T., et al. (2013). Genome-wide identification of Ikaros targets elucidates its contribution to mouse B-cell lineage specification and pre-B-cell differentiation. *Blood* *121*, 1769–1782. <https://doi.org/10.1182/blood-2012-08-450114>.

Filippakopoulos, P., Qi, J., Picaud, S., Shen, Y., Smith, W.B., Fedorov, O., Morse, E.M., Keates, T., Hickman, T.T., Felletar, I., et al. (2010). Selective inhibition of BET bromodomains. *Nature* *468*, 1067–1073. <https://doi.org/10.1038/nature09504>.

Fleischmann, K.K., Pagel, P., Schmid, I., and Roscher, A.A. (2014). RNAi-mediated silencing of MLL-AF9 reveals leukemia-associated downstream targets and processes. *Mol. Cancer* *13*, 27. <https://doi.org/10.1186/1476-4598-13-27>.

Fong, C.Y., Gilan, O., Lam, E.Y.N., Rubin, A.F., Ftouni, S., Tyler, D., Stanley, K., Sinha, D., Yeh, P., Morison, J., et al. (2015). BET inhibitor resistance emerges from leukaemia stem cells. *Nature* *525*, 538–542. <https://doi.org/10.1038/nature14888>.

Frestedt, J.L., Hilden, J.M., Moore, R.O., and Kersey, J.H. (1996). Differential expression of AF4/FEL mRNA in human tissues. *Genet. Anal. Biomol. Eng.* *12*, 147–149. [https://doi.org/10.1016/1050-3862\(95\)00127-1](https://doi.org/10.1016/1050-3862(95)00127-1).

Fu, Z., Malureanu, L., Huang, J., Wang, W., Li, H., van Deursen, J.M., Tindall, D.J., and Chen, J. (2008). Plk1-dependent phosphorylation of FoxM1 regulates a transcriptional programme required for mitotic progression. *Nat. Cell Biol.* *10*, 1076–1082. <https://doi.org/10.1038/ncb1767>.

van Galen, J.C., Kuiper, R.P., van Emst, L., Levers, M., Tijchon, E., Scheijen, B., Waanders, E., van Reijmersdal, S.V., Gilissen, C., van Kessel, A.G., et al. (2010). BTG1 regulates glucocorticoid receptor autoinduction in acute lymphoblastic leukemia. *Blood* *115*, 4810–4819. <https://doi.org/10.1182/blood-2009-05-223081>.

Garcia-Manero, G., Assouline, S., Cortes, J., Estrov, Z., Kantarjian, H., Yang, H., Newsome, W.M., Miller, W.H., Rousseau, C., Kalita, A., et al. (2008). Phase 1 study of the oral isotype specific histone deacetylase inhibitor MGCD0103 in leukemia. *Blood* *112*, 981–989. <https://doi.org/10.1182/blood-2007-10-115873>.

- Gardner, R., Wu, D., Cherian, S., Fang, M., Hanafi, L.-A., Finney, O., Smithers, H., Jensen, M.C., Riddell, S.R., Maloney, D.G., et al. (2016). Acquisition of a CD19-negative myeloid phenotype allows immune escape of MLL-rearranged B-ALL from CD19 CAR-T-cell therapy. *Blood* 127, 2406–2410. <https://doi.org/10.1182/blood-2015-08-665547>.
- Garrido Castro, P., van Roon, E.H.J., Pinhanços, S.S., Trentin, L., Schneider, P., Kerstjens, M., te Kronnie, G., Heidenreich, O., Pieters, R., and Stam, R.W. (2018). The HDAC inhibitor panobinostat (LBH589) exerts in vivo anti-leukaemic activity against MLL-rearranged acute lymphoblastic leukaemia and involves the RNF20/RNF40/WAC-H2B ubiquitination axis. *Leukemia* 32, 323–331. <https://doi.org/10.1038/leu.2017.216>.
- Gaussmann, A., Wenger, T., Eberle, I., Bursen, A., Bracharz, S., Herr, I., Dingermann, T., and Marschalek, R. (2007). Combined effects of the two reciprocal t(4;11) fusion proteins MLL·AF4 and AF4·MLL confer resistance to apoptosis, cell cycling capacity and growth transformation. *Oncogene* 26, 3352–3363. <https://doi.org/10.1038/sj.onc.1210125>.
- Geng, H., Brennan, S., Milne, T.A., Chen, W.-Y., Li, Y., Hurtz, C., Kweon, S.-M., Zickl, L., Shojaee, S., Neuberg, D., et al. (2012). Integrative epigenomic analysis identifies biomarkers and therapeutic targets in adult B-acute lymphoblastic leukemia. *Cancer Discov.* 2, 1004–1023. <https://doi.org/10.1158/2159-8290.CD-12-0208>.
- Geng, H., Hurtz, C., Lenz, K.B., Chen, Z., Baumjohann, D., Thompson, S., Goloviznina, N.A., Chen, W.-Y., Huan, J., LaTocha, D., et al. (2015). Self-Enforcing Feedback Activation between BCL6 and Pre-B Cell Receptor Signaling Defines a Distinct Subtype of Acute Lymphoblastic Leukemia. *Cancer Cell* 27, 409–425. <https://doi.org/10.1016/j.ccell.2015.02.003>.
- Ghelli Luserna Di Rorà, A., Beeharry, N., Imbrogno, E., Ferrari, A., Robustelli, V., Righi, S., Sabattini, E., Verga Falzacappa, M.V., Ronchini, C., Testoni, N., et al. (2018). Targeting WEE1 to enhance conventional therapies for acute lymphoblastic leukemia. *J. Hematol. Oncol. J Hematol Oncol* 11, 99. <https://doi.org/10.1186/s13045-018-0641-1>.
- Gillert, E., Leis, T., Repp, R., Reichel, M., Hösch, A., Breitenlohner, I., Angermüller, S., Borkhardt, A., Harbott, J., Lampert, F., et al. (1999). A DNA damage repair mechanism is involved in the origin of chromosomal translocations t(4;11) in primary leukemic cells. *Oncogene* 18, 4663–4671. <https://doi.org/10.1038/sj.onc.1202842>.
- Godfrey, L., Crump, N.T., Thorne, R., Lau, I.-J., Repapi, E., Dimou, D., Smith, A.L., Harman, J.R., Telenius, J.M., Oudelaar, A.M., et al. (2019). DOT1L inhibition reveals a distinct subset of enhancers dependent on H3K79 methylation. *Nat. Commun.* 10, 2803. <https://doi.org/10.1038/s41467-019-10844-3>.
- Gómez-Casares, M.T., García-Alegria, E., López-Jorge, C.E., Ferrándiz, N., Blanco, R., Alvarez, S., Vaqué, J.P., Bretones, G., Caraballo, J.M., Sánchez-Bailón, P., et al. (2013). MYC antagonizes the differentiation induced by imatinib in chronic myeloid leukemia cells through downregulation of p27KIP1. *Oncogene* 32, 2239–2246. <https://doi.org/10.1038/onc.2012.246>.
- Goroshchuk, O., Vidarsdottir, L., Björklund, A.-C., Hamil, A.S., Kolosenko, I., Dowdy, S.F., and Palm-Apergi, C. (2020). Targeting Plk1 with siRNAs in primary cells from pediatric B-

cell acute lymphoblastic leukemia patients. *Sci. Rep.* *10*, 2688. <https://doi.org/10.1038/s41598-020-59653-5>.

Grembecka, J., He, S., Shi, A., Purohit, T., Muntean, A.G., Sorenson, R.J., Showalter, H.D., Murai, M.J., Belcher, A.M., Hartley, T., et al. (2012). Menin-MLL inhibitors reverse oncogenic activity of MLL fusion proteins in leukemia. *Nat. Chem. Biol.* *8*, 277–284. <https://doi.org/10.1038/nchembio.773>.

Grey, W., Ivey, A., Milne, T.A., Haferlach, T., Grimwade, D., Uhlmann, F., Voisset, E., and Yu, V. (2018). The Cks1/Cks2 axis fine-tunes Mll1 expression and is crucial for MLL-rearranged leukaemia cell viability. *Biochim. Biophys. Acta BBA - Mol. Cell Res.* *1865*, 105–116. <https://doi.org/10.1016/j.bbamcr.2017.09.009>.

Gu, Y., Nakamura, T., Alder, H., Prasad, R., Canaani, O., Cimino, G., Croce, C.M., and Canaani, E. (1992). The t (4; 11) chromosome translocation of human acute leukemias fuses the ALL-1 gene, related to *Drosophila trithorax*, to the AF-4 gene. *Cell* *71*, 701–708.

Gu, Y., Shen, Y., Gibbs, R.A., and Nelson, D.L. (1996). Identification of FMR2, a novel gene associated with the FRAXE CCG repeat and CpG island. *Nat. Genet.* *13*, 109–113.

Guest, E., Yoo, B., Kostadinov, R., Farooqi, M.S., Farrow, E., Gibson, M., Miller, N., Shah, K., Pastinen, T., and Brown, P.A. (2019). Single Cell Sequencing Reveals Heterogeneity of Gene Expression in KMT2A Rearranged Infant ALL at Relapse Compared to Diagnosis. *Blood* *134*, 2756. <https://doi.org/10.1182/blood-2019-131999>.

Guo, L., Liu, J., Yang, Y., Zeng, Y., Yuan, F., Zhong, F., Jin, Y., Wan, R., and Liu, W. (2021). Purple sweet potato anthocyanins elicit calcium overload-induced cell death by inhibiting the calcium-binding protein S100A4 in acute lymphoblastic leukemia. *Food Biosci.* *42*, 101214. <https://doi.org/10.1016/j.fbio.2021.101214>.

Haery, L., Thompson, R.C., and Gilmore, T.D. (2015). Histone acetyltransferases and histone deacetylases in B- and T-cell development, physiology and malignancy. *Genes Cancer* *6*, 184–213. <https://doi.org/10.18632/genesandcancer.65>.

Han, Q., Ma, J., Gu, Y., Song, H., Kapadia, M., Kawasawa, Y.I., Dovat, S., Song, C., and Ge, Z. (2019). RAG1 high expression associated with IKZF1 dysfunction in adult B-cell acute lymphoblastic leukemia. *J. Cancer* *10*, 3842–3850. <https://doi.org/10.7150/jca.33989>.

Harrison, C.J., Hills, R.K., Moorman, A.V., Grimwade, D.J., Hann, I., Webb, D.K.H., Wheatley, K., de Graaf, S.S.N., van den Berg, E., Burnett, A.K., et al. (2010). Cytogenetics of childhood acute myeloid leukemia: United Kingdom Medical Research Council Treatment trials AML 10 and 12. *J. Clin. Oncol. Off. J. Am. Soc. Clin. Oncol.* *28*, 2674–2681. <https://doi.org/10.1200/JCO.2009.24.8997>.

Heald, R., McLoughlin, M., and McKeon, F. (1993). Human wee1 maintains mitotic timing by protecting the nucleus from cytoplasmically activated Cdc2 kinase. *Cell* *74*, 463–474. [https://doi.org/10.1016/0092-8674\(93\)80048-j](https://doi.org/10.1016/0092-8674(93)80048-j).

- Heizmann, B., Kastner, P., and Chan, S. (2013). Ikaros is absolutely required for pre-B cell differentiation by attenuating IL-7 signals. *J. Exp. Med.* *210*, 2823–2832. <https://doi.org/10.1084/jem.20131735>.
- Hess, J.L. (2004). MLL: a histone methyltransferase disrupted in leukemia. *Trends Mol. Med.* *10*, 500–507. .
- Hilden, J.M., Dinndorf, P.A., Meerbaum, S.O., Sather, H., Villaluna, D., Heerema, N.A., McGlennen, R., Smith, F.O., Woods, W.G., Salzer, W.L., et al. (2006). Analysis of prognostic factors of acute lymphoblastic leukemia in infants: report on CCG 1953 from the Children's Oncology Group. *Blood* *108*, 441–451. <https://doi.org/10.1182/blood-2005-07-3011>.
- Hirota, T., Kunitoku, N., Sasayama, T., Marumoto, T., Zhang, D., Nitta, M., Hatakeyama, K., and Saya, H. (2003). Aurora-A and an interacting activator, the LIM protein Ajuba, are required for mitotic commitment in human cells. *Cell* *114*, 585–598. [https://doi.org/10.1016/s0092-8674\(03\)00642-1](https://doi.org/10.1016/s0092-8674(03)00642-1).
- Holleman, A., Cheok, M.H., den Boer, M.L., Yang, W., Veerman, A.J.P., Kazemier, K.M., Pei, D., Cheng, C., Pui, C.-H., Relling, M.V., et al. (2004). Gene-Expression Patterns in Drug-Resistant Acute Lymphoblastic Leukemia Cells and Response to Treatment. *N. Engl. J. Med.* *351*, 533–542. <https://doi.org/10.1056/NEJMoa033513>.
- House, C.M., Frew, I.J., Huang, H.-L., Wiche, G., Traficante, N., Nice, E., Catimel, B., and Bowtell, D.D. (2003). A binding motif for Siah ubiquitin ligase. *Proc. Natl. Acad. Sci.* *100*, 3101–3106. .
- Hsieh, H.-Y., Jia, W., Jin, Z., Kidoya, H., and Takakura, N. (2020). High expression of PSF1 promotes drug resistance and cell cycle transit in leukemia cells. *Cancer Sci.* *111*, 2400–2412. <https://doi.org/10.1111/cas.14452>.
- Hsieh, J.J.-D., Ernst, P., Erdjument-Bromage, H., Tempst, P., and Korsmeyer, S.J. (2003a). Proteolytic cleavage of MLL generates a complex of N- and C-terminal fragments that confers protein stability and subnuclear localization. *Mol. Cell. Biol.* *23*, 186–194. <https://doi.org/10.1128/MCB.23.1.186-194.2003>.
- Hsieh, J.J.-D., Cheng, E.H.-Y., and Korsmeyer, S.J. (2003b). Taspase1: a threonine aspartase required for cleavage of MLL and proper HOX gene expression. *Cell* *115*, 293–303. .
- Iacobucci, I., Iraci, N., Messina, M., Lonetti, A., Chiaretti, S., Valli, E., Ferrari, A., Papayannidis, C., Paoloni, F., Vitale, A., et al. (2012). IKAROS Deletions Dictate a Unique Gene Expression Signature in Patients with Adult B-Cell Acute Lymphoblastic Leukemia. *PLOS ONE* *7*, e40934. <https://doi.org/10.1371/journal.pone.0040934>.
- Isnard, P., Coré, N., Naquet, P., and Djabali, M. (2000). Altered lymphoid development in mice deficient for the mAF4 proto-oncogene. *Blood J. Am. Soc. Hematol.* *96*, 705–710. .
- Isoyama, K., Eguchi, M., Hibi, S., Kinukawa, N., Ohkawa, H., Kawasaki, H., Kosaka, Y., Oda, T., Oda, M., Okamura, T., et al. (2002). Risk-directed treatment of infant acute

lymphoblastic leukaemia based on early assessment of MLL gene status: results of the Japan Infant Leukaemia Study (MLL96). *Br. J. Haematol.* *118*, 999–1010. <https://doi.org/10.1046/j.1365-2141.2002.03754.x>.

Jiménez-P, R., Martín-Cortázar, C., Kourani, O., Chiodo, Y., Cordoba, R., Domínguez-Franjo, M.P., Redondo, J.M., Iglesias, T., and Campanero, M.R. (2018). CDCA7 is a critical mediator of lymphomagenesis that selectively regulates anchorage-independent growth. *Haematologica* *103*, 1669–1678. <https://doi.org/10.3324/haematol.2018.188961>.

Jude, C.D., Climer, L., Xu, D., Artinger, E., Fisher, J.K., and Ernst, P. (2007). Unique and independent roles for MLL in adult hematopoietic stem cells and progenitors. *Cell Stem Cell* *1*, 324–337. <https://doi.org/10.1016/j.stem.2007.05.019>.

Kannan, S., Aitken, M.J.L., Herbrich, S.M., Golfman, L.S., Hall, M.G., Mak, D.H., Burks, J.K., Song, G., Konopleva, M., Mullighan, C.G., et al. (2019). Antileukemia Effects of Notch-Mediated Inhibition of Oncogenic PLK1 in B-Cell Acute Lymphoblastic Leukemia. *Mol. Cancer Ther.* *18*, 1615–1627. <https://doi.org/10.1158/1535-7163.MCT-18-0706>.

Kawagoe, R., Kawagoe, H., and Sano, K. (2002). Valproic acid induces apoptosis in human leukemia cells by stimulating both caspase-dependent and -independent apoptotic signaling pathways. *Leuk. Res.* *26*, 495–502. [https://doi.org/10.1016/S0145-2126\(01\)00151-5](https://doi.org/10.1016/S0145-2126(01)00151-5).

Kerry, J., Godfrey, L., Repapi, E., Tapia, M., Blackledge, N.P., Ma, H., Ballabio, E., O’Byrne, S., Ponthan, F., Heidenreich, O., et al. (2017). MLL-AF4 Spreading Identifies Binding Sites that Are Distinct from Super-Enhancers and that Govern Sensitivity to DOT1L Inhibition in Leukemia. *Cell Rep.* *18*, 482–495. <https://doi.org/10.1016/j.celrep.2016.12.054>.

Ketzer, F., Abdelrasoul, H., Vogel, M., Marienfeld, R., Müschen, M., Jumaa, H., Wirth, T., and Ushmorov, A. (2022). CCND3 is indispensable for the maintenance of B-cell acute lymphoblastic leukemia. *Oncogenesis* *11*, 1–12. <https://doi.org/10.1038/s41389-021-00377-0>.

Kim, E., Hurtz, C., Koehrer, S., Wang, Z., Balasubramanian, S., Chang, B.Y., Müschen, M., Davis, R.E., and Burger, J.A. (2017). Ibrutinib inhibits pre-BCR+ B-cell acute lymphoblastic leukemia progression by targeting BTK and BLK. *Blood* *129*, 1155–1165. <https://doi.org/10.1182/blood-2016-06-722900>.

Klitz, W., Gragert, L., and Trachtenberg, E. (2012). Spectrum of HLA associations: the case of medically refractory pediatric acute lymphoblastic leukemia. *Immunogenetics* *64*, 409–419. <https://doi.org/10.1007/s00251-012-0605-5>.

Klossowski, S., Miao, H., Kempinska, K., Wu, T., Purohit, T., Kim, E., Linhares, B.M., Chen, D., Jih, G., Perkey, E., et al. (2020). Menin inhibitor MI-3454 induces remission in MLL1-rearranged and NPM1-mutated models of leukemia. *J. Clin. Invest.* *130*, 981–997. <https://doi.org/10.1172/JCI129126>.

Kowarz, E., Burmeister, T., Lo Nigro, L., Jansen, M.W.J.C., Delabesse, E., Klingebiel, T., Dingermann, T., Meyer, C., and Marschalek, R. (2007). Complex MLL rearrangements in

t(4;11) leukemia patients with absent AF4 · MLL fusion allele. *Leukemia* 21, 1232–1238. <https://doi.org/10.1038/sj.leu.2404686>.

Kowarz, E., Löscher, D., and Marschalek, R. (2015). Optimized Sleeping Beauty transposons rapidly generate stable transgenic cell lines. *Biotechnol. J.* 10, 647–653. <https://doi.org/10.1002/biot.201400821>.

Krebs in Deutschland 2017/2018 - Robert Koch Institute, and Zentrum für Krebsregisterdaten Krebs in Deutschland 2017/2018.

Krivtsov, A.V., Feng, Z., Lemieux, M.E., Faber, J., Vempati, S., Sinha, A.U., Xia, X., Jesneck, J., Bracken, A.P., Silverman, L.B., et al. (2008). H3K79 Methylation Profiles Define Murine and Human MLL-AF4 Leukemias. *Cancer Cell* 14, 355–368. <https://doi.org/10.1016/j.ccr.2008.10.001>.

Krivtsov, A.V., Evans, K., Gadrey, J.Y., Eschle, B.K., Hatton, C., Uckelmann, H.J., Ross, K.N., Perner, F., Olsen, S.N., Pritchard, T., et al. (2019). A Menin-MLL Inhibitor Induces Specific Chromatin Changes and Eradicates Disease in Models of MLL-Rearranged Leukemia. *Cancer Cell* 36, 660-673.e11. <https://doi.org/10.1016/j.ccell.2019.11.001>.

Kühn, A.C. (2017). Untersuchung der molekularbiologischen Relevanz des Transkriptionsfaktors IRX1 im Kontext einer MLL-AF4-assoziierten Leukämie. PhD Thesis. Johann Wolfgang Goethe-Universität Frankfurt am Main.

Kühn, A., Löscher, D., and Marschalek, R. (2016). The IRX1/HOXA connection: insights into a novel t (4; 11)-specific cancer mechanism. *Oncotarget* 7, 35341. .

Kumar, A.R., Yao, Q., Li, Q., Sam, T.A., and Kersey, J.H. (2011). t(4;11) leukemias display addiction to MLL-AF4 but not to AF4-MLL. *Leuk. Res.* 35, 305–309. <https://doi.org/10.1016/j.leukres.2010.08.011>.

Langdon, W.Y., Harris, A.W., Cory, S., and Adams, J.M. (1986). The c-myc oncogene perturbs B lymphocyte development in E μ -myc transgenic mice. *Cell* 47, 11–18. .

Laranjeira, A.B.A., de Vasconcellos, J.F., Sodek, L., Spago, M.C., Fornazim, M.C., Tone, L.G., Brandalise, S.R., Nowill, A.E., and Yunes, J.A. (2012). IGFBP7 participates in the reciprocal interaction between acute lymphoblastic leukemia and BM stromal cells and in leukemia resistance to asparaginase. *Leukemia* 26, 1001–1011. <https://doi.org/10.1038/leu.2011.289>.

Li, X., Li, D., Zhuang, Y., Shi, Q., Wei, W., Zhang, H., and Ju, X. (2013). [The expression and regulatory mechanism of microRNA-708 in pediatric common B-cell acute lymphoblastic leukemia]. *Zhonghua Xue Ye Xue Za Zhi Zhonghua Xueyexue Zazhi* 34, 138–143. .

Li, Y., Yang, W., Devidas, M., Winter, S.S., Kesserwan, C., Yang, W., Dunsmore, K.P., Smith, C., Qian, M., Zhao, X., et al. (2021). Germline RUNX1 variation and predisposition to childhood acute lymphoblastic leukemia. *J. Clin. Invest.* 147898. <https://doi.org/10.1172/JCI147898>.

- Liang, K., Volk, A.G., Haug, J.S., Marshall, S.A., Woodfin, A.R., Bartom, E.T., Gilmore, J.M., Florens, L., Washburn, M.P., and Sullivan, K.D. (2017). Therapeutic targeting of MLL degradation pathways in MLL-rearranged leukemia. *Cell* 168, 59–72. .
- Lin, C., Smith, E.R., Takahashi, H., Lai, K.C., Martin-Brown, S., Florens, L., Washburn, M.P., Conaway, J.W., Conaway, R.C., and Shilatifard, A. (2010). AFF4, a component of the ELL/P-TEFb elongation complex and a shared subunit of MLL chimeras, can link transcription elongation to leukemia. *Mol. Cell* 37, 429–437. .
- Lin, S., Luo, R.T., Ptasinska, A., Kerry, J., Assi, S.A., Wunderlich, M., Imamura, T., Kaberlein, J.J., Rayes, A., Althoff, M.J., et al. (2016). Instructive Role of MLL-Fusion Proteins Revealed by a Model of t(4;11) Pro-B Acute Lymphoblastic Leukemia. *Cancer Cell* 30, 737–749. <https://doi.org/10.1016/j.ccell.2016.10.008>.
- Liu, G.J., Cimmino, L., Jude, J.G., Hu, Y., Witkowski, M.T., McKenzie, M.D., Kartal-Kaess, M., Best, S.A., Tuohey, L., Liao, Y., et al. (2014). Pax5 loss imposes a reversible differentiation block in B-progenitor acute lymphoblastic leukemia. *Genes Dev.* 28, 1337–1350. <https://doi.org/10.1101/gad.240416.114>.
- Liu, X., Barrett, D.M., Jiang, S., Fang, C., Kalos, M., Grupp, S.A., June, C.H., and Zhao, Y. (2016). Improved anti-leukemia activities of adoptively transferred T cells expressing bispecific T-cell engager in mice. *Blood Cancer J.* 6, e430. <https://doi.org/10.1038/bcj.2016.38>.
- Lugo, T.G., Pendergast, A.-M., Muller, A.J., and Witte, O.N. (1990). Tyrosine kinase activity and transformation potency of bcr-abl oncogene products. *Science* 247, 1079–1082. .
- Luo, Z., Gao, X., Lin, C., Smith, E.R., Marshall, S.A., Swanson, S.K., Florens, L., Washburn, M.P., and Shilatifard, A. (2015). Zic2 Is an Enhancer-Binding Factor Required for Embryonic Stem Cell Specification. *Mol. Cell* 57, 685–694. <https://doi.org/10.1016/j.molcel.2015.01.007>.
- Ma, C., and Staudt, L.M. (1996). LAF-4 encodes a lymphoid nuclear protein with transactivation potential that is homologous to AF-4, the gene fused to MLL in t (4; 11) leukemias.
- Mahotka, C., Bhatia, S., Kollet, J., and Grinstein, E. (2018). Nucleolin promotes execution of the hematopoietic stem cell gene expression program. *Leukemia* 32, 1865–1868. <https://doi.org/10.1038/s41375-018-0090-4>.
- Maillard, I., Chen, Y.-X., Friedman, A., Yang, Y., Tubbs, A.T., Shestova, O., Pear, W.S., and Hua, X. (2009). Menin regulates the function of hematopoietic stem cells and lymphoid progenitors. *Blood* 113, 1661–1669. <https://doi.org/10.1182/blood-2009-01-135012>.
- Major, M.L., Lepe, R., and Costa, R.H. (2004). Forkhead Box M1B Transcriptional Activity Requires Binding of Cdk-Cyclin Complexes for Phosphorylation-Dependent Recruitment of p300/CBP Coactivators. *Mol. Cell. Biol.* 24, 2649–2661. <https://doi.org/10.1128/MCB.24.7.2649-2661.2004>.

- Mann, G., Attarbaschi, A., Schrappe, M., De Lorenzo, P., Peters, C., Hann, I., De Rossi, G., Felice, M., Lausen, B., Leblanc, T., et al. (2010). Improved outcome with hematopoietic stem cell transplantation in a poor prognostic subgroup of infants with mixed-lineage-leukemia (MLL)-rearranged acute lymphoblastic leukemia: results from the Interfant-99 Study. *Blood* 116, 2644–2650. <https://doi.org/10.1182/blood-2010-03-273532>.
- Marschalek, R. (2011a). It takes two-to-leukemia: about addictions and requirements. *Leuk. Res.* 35, 424–425. <https://doi.org/10.1016/j.leukres.2010.10.003>.
- Marschalek, R. (2011b). Mechanisms of leukemogenesis by MLL fusion proteins. *Br. J. Haematol.* 152, 141–154. <https://doi.org/10.1111/j.1365-2141.2010.08459.x>.
- Marschalek, R. (2015). MLL Leukemia and Future Treatment Strategies. *Arch. Pharm. (Weinheim)* 348, 221–228. <https://doi.org/10.1002/ardp.201400449>.
- Marschalek, R. (2016). Systematic Classification of Mixed-Lineage Leukemia Fusion Partners Predicts Additional Cancer Pathways. *Ann. Lab. Med.* 36, 85. <https://doi.org/10.3343/alm.2016.36.2.85>.
- Marschalek, R. (2019). Another piece of the puzzle added to understand t(4;11) leukemia better. *Haematologica* 104, 1098–1100. <https://doi.org/10.3324/haematol.2018.213397>.
- Maude, S.L., Laetsch, T.W., Buechner, J., Rives, S., Boyer, M., Bittencourt, H., Bader, P., Verneris, M.R., Stefanski, H.E., Myers, G.D., et al. (2018). Tisagenlecleucel in Children and Young Adults with B-Cell Lymphoblastic Leukemia. *N. Engl. J. Med.* 378, 439–448. <https://doi.org/10.1056/NEJMoa1709866>.
- McCalmont, H., Li, K.L., Jones, L., Toubia, J., Bray, S.C., Casolari, D.A., Mayoh, C., Samaraweera, S.E., Lewis, I.D., Prinjha, R.K., et al. (2020). Efficacy of combined CDK9/BET inhibition in preclinical models of MLL-rearranged acute leukemia. *Blood Adv.* 4, 296–300. <https://doi.org/10.1182/bloodadvances.2019000586>.
- Melko, M., Douguet, D., Bensaid, M., Zongaro, S., Verheggen, C., Gecz, J., and Bardoni, B. (2011). Functional characterization of the AFF (AF4/FMR2) family of RNA-binding proteins: insights into the molecular pathology of FRAXE intellectual disability. *Hum. Mol. Genet.* 20, 1873–1885. <https://doi.org/10.1093/hmg/ddr069>.
- Meyer, C., Kowarz, E., Schneider, B., Oehm, C., Klingebiel, T., Dingermann, T., and Marschalek, R. (2006). Genomic DNA of leukemic patients: target for clinical diagnosis of MLL rearrangements. *Biotechnol. J. Healthc. Nutr. Technol.* 1, 656–663. .
- Meyer, C., Hofmann, J., Burmeister, T., Gröger, D., Park, T.S., Emerenciano, M., Pombo de Oliveira, M., Renneville, A., Villarese, P., Macintyre, E., et al. (2013). The MLL recombinome of acute leukemias in 2013. *Leukemia* 27, 2165–2176. <https://doi.org/10.1038/leu.2013.135>.
- Meyer, C., Burmeister, T., Gröger, D., Tsaur, G., Fehina, L., Renneville, A., Sutton, R., Venn, N.C., Emerenciano, M., Pombo-de-Oliveira, M.S., et al. (2018). The MLL recombinome of acute leukemias in 2017. *Leukemia* 32, 273–284. <https://doi.org/10.1038/leu.2017.213>.

- Milne, T.A. (2017). Mouse models of MLL leukemia: recapitulating the human disease. *Blood* 129, 2217–2223. <https://doi.org/10.1182/blood-2016-10-691428>.
- Milne, T.A., Briggs, S.D., Brock, H.W., Martin, M.E., Gibbs, D., Allis, C.D., and Hess, J.L. (2002). MLL Targets SET Domain Methyltransferase Activity to Hox Gene Promoters. *Mol. Cell* 10, 1107–1117. [https://doi.org/10.1016/S1097-2765\(02\)00741-4](https://doi.org/10.1016/S1097-2765(02)00741-4).
- Mirguet, O., Gosmini, R., Toum, J., Clément, C.A., Barnathan, M., Brusq, J.-M., Mordaunt, J.E., Grimes, R.M., Crowe, M., Pineau, O., et al. (2013). Discovery of Epigenetic Regulator I-BET762: Lead Optimization to Afford a Clinical Candidate Inhibitor of the BET Bromodomains. *J. Med. Chem.* 56, 7501–7515. <https://doi.org/10.1021/jm401088k>.
- Mootha, V.K., Lindgren, C.M., Eriksson, K.-F., Subramanian, A., Sihag, S., Lehar, J., Puigserver, P., Carlsson, E., Ridderstråle, M., Laurila, E., et al. (2003). PGC-1 α -responsive genes involved in oxidative phosphorylation are coordinately downregulated in human diabetes. *Nat. Genet.* 34, 267–273. <https://doi.org/10.1038/ng1180>.
- Moriyama, T., Yang, W., Smith, C., Pui, C.-H., Evans, W.E., Relling, M.V., Bhatia, S., and Yang, J.J. (2021). Comprehensive characterization of pharmacogenetic variants in TPMT and NUDT15 in children with acute lymphoblastic leukemia. *Pharmacogenet. Genomics* 32, 60–66. <https://doi.org/10.1097/FPC.0000000000000453>.
- Mueller, D., Bach, C., Zeisig, D., Garcia-Cuellar, M.-P., Monroe, S., Sreekumar, A., Zhou, R., Nesvizhskii, A., Chinnaiyan, A., and Hess, J.L. (2007). A role for the MLL fusion partner ENL in transcriptional elongation and chromatin modification. *Blood J. Am. Soc. Hematol.* 110, 4445–4454. .
- Mullighan, C.G., Kennedy, A., Zhou, X., Radtke, I., Phillips, L.A., Shurtleff, S.A., and Downing, J.R. (2007). Pediatric acute myeloid leukemia with NPM1 mutations is characterized by a gene expression profile with dysregulated HOX gene expression distinct from MLL-rearranged leukemias. *Leukemia* 21, 2000–2009. <https://doi.org/10.1038/sj.leu.2404808>.
- Mullighan, C.G., Su, X., Zhang, J., Radtke, I., Phillips, L.A.A., Miller, C.B., Ma, J., Liu, W., Cheng, C., Schulman, B.A., et al. (2009). Deletion of IKZF1 and prognosis in acute lymphoblastic leukemia. *N. Engl. J. Med.* 360, 470–480. <https://doi.org/10.1056/NEJMoa0808253>.
- Muñoz-López, A., Romero-Moya, D., Prieto, C., Ramos-Mejía, V., Agraz-Doblas, A., Varela, I., Buschbeck, M., Palau, A., Carvajal-Vergara, X., Giorgetti, A., et al. (2016). Development Refractoriness of MLL-Rearranged Human B Cell Acute Leukemias to Reprogramming into Pluripotency. *Stem Cell Rep.* 7, 602–618. <https://doi.org/10.1016/j.stemcr.2016.08.013>.
- Murai, M.J., Chruszcz, M., Reddy, G., Grembecka, J., and Cierpicki, T. (2011). Crystal structure of menin reveals binding site for mixed lineage leukemia (MLL) protein. *J. Biol. Chem.* 286, 31742–31748. <https://doi.org/10.1074/jbc.M111.258186>.
- Myoumoto, A., Nakatani, K., Koshimizu, T., Matsubara, H., Adachi, S., and Tsujimoto, G. (2007). Glucocorticoid-induced granzyme A expression can be used as a marker of

glucocorticoid sensitivity for acute lymphoblastic leukemia therapy. *J. Hum. Genet.* *52*, 328–333. <https://doi.org/10.1007/s10038-007-0119-4>.

Nakamura, T., Alder, H., Gu, Y., Prasad, R., Canaani, O., Kamada, N., Gale, R.P., Lange, B., Crist, W.M., and Nowell, P.C. (1993). Genes on chromosomes 4, 9, and 19 involved in 11q23 abnormalities in acute leukemia share sequence homology and/or common motifs. *Proc. Natl. Acad. Sci.* *90*, 4631–4635. .

Nakamura, T., Mori, T., Tada, S., Krajewski, W., Rozovskaia, T., Wassell, R., Dubois, G., Mazo, A., Croce, C.M., and Canaani, E. (2002). ALL-1 is a histone methyltransferase that assembles a supercomplex of proteins involved in transcriptional regulation. *Mol. Cell* *10*, 1119–1128. .

Ng, S.Y.-M., Yoshida, T., Zhang, J., and Georgopoulos, K. (2009). Genome-wide lineage-specific transcriptional networks underscore Ikaros-dependent lymphoid priming in hematopoietic stem cells. *Immunity* *30*, 493–507. <https://doi.org/10.1016/j.immuni.2009.01.014>.

Nilson, I., LöCHNER, K., Siegler, G., Greil, J., Beck, J.D., Fey, G.H., and Marschalek, R. (1996). Exon/intron structure of the human ALL-1 (MLL) gene involved in translocations to chromosomal region 11q23 and acute leukaemias. *Br. J. Haematol.* *93*, 966–972. <https://doi.org/10.1046/j.1365-2141.1996.d01-1748.x>.

Nilson, I., Reichel, M., Ennas, M.G., Greim, R., Knörr, C., Siegler, G., Greil, J., Fey, G.H., and Marschalek, R. (1997). Exon/intron structure of the human AF-4 gene, a member of the AF-4/LAF-4/FMR-2 gene family coding for a nuclear protein with structural alterations in acute leukaemia. *Br. J. Haematol.* *98*, 157–169. .

Nold-Petry, C.A., Lo, C.Y., Rudloff, I., Elgass, K.D., Li, S., Gantier, M.P., Lotz-Havla, A.S., Gersting, S.W., Cho, S.X., Lao, J.C., et al. (2015). IL-37 requires the receptors IL-18R α and IL-1R8 (SIGIRR) to carry out its multifaceted anti-inflammatory program upon innate signal transduction. *Nat. Immunol.* *16*, 354–365. <https://doi.org/10.1038/ni.3103>.

Nowell, P.C. (1976). The Clonal Evolution of Tumor Cell Populations. *Science* *194*, 23–28. <https://doi.org/10.1126/science.959840>.

Okabe, H., Satoh, S., Furukawa, Y., Kato, T., Hasegawa, S., Nakajima, Y., Yamaoka, Y., and Nakamura, Y. (2003). Involvement of PEG10 in human hepatocellular carcinogenesis through interaction with SIAH1. *Cancer Res.* *63*, 3043–3048. .

Okada, Y., Feng, Q., Lin, Y., Jiang, Q., Li, Y., Coffield, V.M., Su, L., Xu, G., and Zhang, Y. (2005). hDOT1L links histone methylation to leukemogenesis. *Cell* *121*, 167–178. .

Ott, C.J., Kopp, N., Bird, L., Paranal, R.M., Qi, J., Bowman, T., Rodig, S.J., Kung, A.L., Bradner, J.E., and Weinstock, D.M. (2012). BET bromodomain inhibition targets both c-Myc and IL7R in high-risk acute lymphoblastic leukemia. *Blood* *120*, 2843–2852. <https://doi.org/10.1182/blood-2012-02-413021>.

Park, S., Osmers, U., Raman, G., Schwantes, R.H., Diaz, M.O., and Bushweller, J.H. (2010). The PHD3 Domain of MLL Acts as a CYP33-Regulated Switch between MLL-

Mediated Activation and Repression,. *Biochemistry* 49, 6576–6586. <https://doi.org/10.1021/bi1009387>.

Patel, A., Dharmarajan, V., Vought, V.E., and Cosgrove, M.S. (2009). On the Mechanism of Multiple Lysine Methylation by the Human Mixed Lineage Leukemia Protein-1 (MLL1) Core Complex *♦. *J. Biol. Chem.* 284, 24242–24256. <https://doi.org/10.1074/jbc.M109.014498>.

Patmasiriwat, P., Fraizer, G., Kantarjian, H., and Saunders, G.F. (1999). WT1 and GATA1 expression in myelodysplastic syndrome and acute leukemia. *Leukemia* 13, 891–900. <https://doi.org/10.1038/sj.leu.2401414>.

Picaud, S., Da Costa, D., Thanasopoulou, A., Filippakopoulos, P., Fish, P.V., Philpott, M., Fedorov, O., Brennan, P., Bunnage, M.E., Owen, D.R., et al. (2013). PFI-1, a Highly Selective Protein Interaction Inhibitor, Targeting BET Bromodomains. *Cancer Res.* 73, 3336–3346. <https://doi.org/10.1158/0008-5472.CAN-12-3292>.

Pieters, R., Schrappe, M., De Lorenzo, P., Hann, I., De Rossi, G., Felice, M., Hovi, L., LeBlanc, T., Szczepanski, T., Ferster, A., et al. (2007). A treatment protocol for infants younger than 1 year with acute lymphoblastic leukaemia (Interfant-99): an observational study and a multicentre randomised trial. *The Lancet* 370, 240–250. [https://doi.org/10.1016/S0140-6736\(07\)61126-X](https://doi.org/10.1016/S0140-6736(07)61126-X).

Pieters, R., De Lorenzo, P., Ancliffe, P., Aversa, L.A., Brethon, B., Biondi, A., Campbell, M., Escherich, G., Ferster, A., Gardner, R.A., et al. (2019). Outcome of infants younger than 1 year with acute lymphoblastic leukemia treated with the interfant-06 protocol: Results from an international phase III randomized study. *J. Clin. Oncol. Off. J. Am. Soc. Clin. Oncol.* 37, 2246–2256. <https://doi.org/10.1200/JCO.19.00261>.

Pikman, Y., and Stegmaier, K. (2018). Targeted therapy for fusion-driven high-risk acute leukemia. *Blood* 132, 1241–1247. <https://doi.org/10.1182/blood-2018-04-784157>.

Pless, B., Oehm, C., Knauer, S., Stauber, R.H., Dingermann, T., and Marschalek, R. (2011). The heterodimerization domains of MLL—FYRN and FYRC—are potential target structures in t (4; 11) leukemia. *Leukemia* 25, 663. .

Poulard, C., Kim, H.N., Fang, M., Kruth, K., Gagnieux, C., Gerke, D.S., Bhojwani, D., Kim, Y.-M., Kampmann, M., Stallcup, M.R., et al. (2019). Relapse-associated AURKB blunts the glucocorticoid sensitivity of B cell acute lymphoblastic leukemia. *Proc. Natl. Acad. Sci.* 116, 3052–3061. <https://doi.org/10.1073/pnas.1816254116>.

Prasad, R., Yano, T., Sorio, C., Nakamura, T., Rallapalli, R., Gu, Y., Leshkowitz, D., Croce, C.M., and Canaani, E. (1995). Domains with transcriptional regulatory activity within the ALL1 and AF4 proteins involved in acute leukemia. *Proc. Natl. Acad. Sci.* 92, 12160–12164. .

Prieto, C., Marschalek, R., Kühn, A., Bursen, A., Bueno, C., and Menéndez, P. (2017). The AF4-MLL fusion transiently augments multilineage hematopoietic engraftment but is not sufficient to initiate leukemia in cord blood CD34+cells. *Oncotarget* 8, 81936–81941. <https://doi.org/10.18632/oncotarget.19567>.

- Pui, C.-H., and Evans, W.E. (2013). A 50-Year Journey to Cure Childhood Acute Lymphoblastic Leukemia. *Semin. Hematol.* 50, 185–196. <https://doi.org/10.1053/j.seminhematol.2013.06.007>.
- Pui, C.-H., Gaynon, P.S., Boyett, J.M., Chessells, J.M., Baruchel, A., Kamps, W., Silverman, L.B., Biondi, A., Harms, D.O., Vilmer, E., et al. (2002). Outcome of treatment in childhood acute lymphoblastic leukaemia with rearrangements of the 11q23 chromosomal region. *The Lancet* 359, 1909–1915. [https://doi.org/10.1016/S0140-6736\(02\)08782-2](https://doi.org/10.1016/S0140-6736(02)08782-2).
- Qasim, W., Zhan, H., Samarasinghe, S., Adams, S., Amrolia, P., Stafford, S., Butler, K., Rivat, C., Wright, G., Somana, K., et al. (2017). Molecular remission of infant B-ALL after infusion of universal TALEN gene-edited CAR T cells. *Sci. Transl. Med.* 9, eaaj2013. <https://doi.org/10.1126/scitranslmed.aaj2013>.
- Rego, E.M., and Pandolfi, P.P. (2002). Reciprocal products of chromosomal translocations in human cancer pathogenesis: key players or innocent bystanders? *Trends Mol. Med.* 8, 396–405. [https://doi.org/10.1016/s1471-4914\(02\)02384-5](https://doi.org/10.1016/s1471-4914(02)02384-5).
- Reichel, M., Gillert, E., Nilson, I., Siegler, G., Greil, J., Fey, G.H., and Marschalek, R. (1998). Fine structure of translocation breakpoints in leukemic blasts with chromosomal translocation t(4;11): the DNA damage-repair model of translocation. *Oncogene* 17, 3035–3044. <https://doi.org/10.1038/sj.onc.1202229>.
- Reichel, M., Gillert, E., Breitenlohner, I., Repp, R., Greil, J., Beck, J.D., Fey, G.H., and Marschalek, R. (1999). Rapid Isolation of Chromosomal Breakpoints from Patients with t(4;11) Acute Lymphoblastic Leukemia: Implications for Basic and Clinical Research1. *Cancer Res.* 59, 3357–3362. .
- Reichel, M., Gillert, E., Breitenlohner, I., Angermüller, S., Fey, G.H., Marschalek, R., Repp, R., Greil, J., and Beck, J.D. (2001). Rapid isolation of chromosomal breakpoints from patients with t(4;11) acute lymphoblastic leukemia: implications for basic and clinical research. *Leukemia* 15, 286–288. <https://doi.org/10.1038/sj.leu.2402018>.
- Reisenauer, M.R., Anderson, M., Huang, L., Zhang, Z., Zhou, Q., Kone, B.C., Morris, A.P., LeSage, G.D., Dryer, S.E., and Zhang, W. (2009). AF17 competes with AF9 for binding to Dot1a to up-regulate transcription of epithelial Na⁺ channel α . *J. Biol. Chem.* 284, 35659–35669. .
- Relling, M.V., Hancock, M.L., Boyett, J.M., Pui, C.H., and Evans, W.E. (1999). Prognostic importance of 6-mercaptopurine dose intensity in acute lymphoblastic leukemia. *Blood* 93, 2817–2823. .
- Robison, L.L., Sather, H.N., Coccia, P.F., Nesbit, M.E., and Hammond, C.D. (1980). Assessment of the interrelationship of prognostic factors in childhood acute lymphoblastic leukemia: A report from Childrens Cancer Study Group. *J. Pediatr. Hematol. Oncol.* 2, 5–14. .
- Rössler, T., and Marschalek, R. (2013). An alternative splice process renders the MLL protein either into a transcriptional activator or repressor. *Pharm.- Int. J. Pharm. Sci.* 68, 601–607. .

- Rouce, R.H., Shaim, H., Sekine, T., Weber, G., Ballard, B., Ku, S., Barese, C., Murali, V., Wu, M.-F., Liu, H., et al. (2016). The TGF- β /SMAD pathway is an important mechanism for NK cell immune evasion in childhood B-acute lymphoblastic leukemia. *Leukemia* 30, 800–811. <https://doi.org/10.1038/leu.2015.327>.
- Ruike, Y., Katsuma, S., Hirasawa, A., and Tsujimoto, G. (2007). Glucocorticoid-induced alternative promoter usage for a novel 5' variant of granzyme A. *J. Hum. Genet.* 52, 172–178. <https://doi.org/10.1007/s10038-006-0099-9>.
- Sabiani, S., Geppert, T., Engelbrecht, C., Kowarz, E., Schneider, G., and Marschalek, R. (2015). Unraveling the Activation Mechanism of Taspase1 which Controls the Oncogenic AF4–MLL Fusion Protein. *EBioMedicine* 2, 386–395. <https://doi.org/10.1016/j.ebiom.2015.04.009>.
- Sanjuan-Pla, A., Bueno, C., Prieto, C., Acha, P., Stam, R.W., Marschalek, R., and Menéndez, P. (2015). Revisiting the biology of infant t(4;11)/MLL-AF4+ B-cell acute lymphoblastic leukemia. *Blood* 126, 2676–2685. <https://doi.org/10.1182/blood-2015-09-667378>.
- Sanjuan-Pla, A., Romero-Moya, D., Prieto, C., Bueno, C., Bigas, A., and Menendez, P. (2016). Intra-Bone Marrow Transplantation Confers Superior Multilineage Engraftment of Murine Aorta-Gonad Mesonephros Cells Over Intravenous Transplantation. *Stem Cells Dev.* 25, 259–265. <https://doi.org/10.1089/scd.2015.0309>.
- Satoh, Y., Yokota, T., Sudo, T., Kondo, M., Lai, A., Kincade, P.W., Kouro, T., Iida, R., Kokame, K., Miyata, T., et al. (2013). The Satb1 protein directs hematopoietic stem cell differentiation toward lymphoid lineages. *Immunity* 38, 1105–1115. <https://doi.org/10.1016/j.immuni.2013.05.014>.
- Schmiegelow, K., Schrøder, H., Gustafsson, G., Kristinsson, J., Glomstein, A., Salmi, T., and Wranne, L. (1995). Risk of relapse in childhood acute lymphoblastic leukemia is related to RBC methotrexate and mercaptopurine metabolites during maintenance chemotherapy. *Nordic Society for Pediatric Hematology and Oncology. J. Clin. Oncol. Off. J. Am. Soc. Clin. Oncol.* 13, 345–351. <https://doi.org/10.1200/JCO.1995.13.2.345>.
- Schwarzer, A., Emmrich, S., Schmidt, F., Beck, D., Ng, M., Reimer, C., Adams, F.F., Grasedieck, S., Witte, D., Käbler, S., et al. (2017). The non-coding RNA landscape of human hematopoiesis and leukemia. *Nat. Commun.* 8, 218. <https://doi.org/10.1038/s41467-017-00212-4>.
- Sharaf-Eldein, M., Elghannam, D., Elderiny, W., and Abdel-Malak, C. (2018). Prognostic Implication of MIF Gene Expression in Childhood Acute Lymphoblastic Leukemia. *Clin. Lab.* 64, 1429–1437. <https://doi.org/10.7754/Clin.Lab.2018.180308>.
- Shi, A., Murai, M.J., He, S., Lund, G., Hartley, T., Purohit, T., Reddy, G., Chruszcz, M., Grembecka, J., and Cierpicki, T. (2012). Structural insights into inhibition of the bivalent menin-MLL interaction by small molecules in leukemia. *Blood* 120, 4461–4469. <https://doi.org/10.1182/blood-2012-05-429274>.

- Shukla, N., Wetmore, C., O'Brien, M.M., Silverman, L.B., Brown, P., Cooper, T.M., Thomson, B., Blakemore, S.J., Daigle, S., Suttle, B., et al. (2016). Final Report of Phase 1 Study of the DOT1L Inhibitor, Pinometostat (EPZ-5676), in Children with Relapsed or Refractory MLL-r Acute Leukemia. *Blood* 128, 2780. <https://doi.org/10.1182/blood.V128.22.2780.2780>.
- Siegel, D.A., Richardson, L.C., Henley, S.J., Wilson, R.J., Dowling, N.F., Weir, H.K., Tai, E.W., and Buchanan Lunsford, N. (2020). Pediatric cancer mortality and survival in the United States, 2001-2016. *Cancer* 126, 4379–4389. <https://doi.org/10.1002/cncr.33080>.
- Silveira, V.S., Scrideli, C.A., Moreno, D.A., Yunes, J.A., Queiroz, R.G.P., Toledo, S.C., Lee, M.L.M., Petrilli, A.S., Brandalise, S.R., and Tone, L.G. (2013). Gene expression pattern contributing to prognostic factors in childhood acute lymphoblastic leukemia. *Leuk. Lymphoma* 54, 310–314. <https://doi.org/10.3109/10428194.2012.710330>.
- Srinivasan, R.S., Nesbit, J.B., Marrero, L., Erfurth, F., LaRussa, V.F., and Hemenway, C.S. (2004). The synthetic peptide PFWT disrupts AF4–AF9 protein complexes and induces apoptosis in t(4;11) leukemia cells. *Leukemia* 18, 1364–1372. <https://doi.org/10.1038/sj.leu.2403415>.
- von Stackelberg, A., Locatelli, F., Zugmaier, G., Handgretinger, R., Trippett, T.M., Rizzari, C., Bader, P., O'Brien, M.M., Brethon, B., Bhojwani, D., et al. (2016). Phase I/Phase II Study of Blinatumomab in Pediatric Patients With Relapsed/Refractory Acute Lymphoblastic Leukemia. *J. Clin. Oncol.* 34, 4381–4389. <https://doi.org/10.1200/JCO.2016.67.3301>.
- Stam, R.W., Hubeek, I., den Boer, M.L., Buijs-Gladdines, J.G.C. a. M., Creutzig, U., Kaspers, G.J.L., and Pieters, R. (2006). MLL gene rearrangements have no direct impact on Ara-C sensitivity in infant acute lymphoblastic leukemia and childhood M4/M5 acute myeloid leukemia. *Leukemia* 20, 179–182. <https://doi.org/10.1038/sj.leu.2404031>.
- Stam, R.W., Bohlander, S., Kirschner-Schwabe, R., Arentsen-Peters, S., Pieters, R., Dingermann, T., and Marschalek, R. (2007). A Novel Approach for Analyzing Gene Expression Profiles Defines Two Distinct Subgroups of t(4;11) Positive Infant Acute Lymphoblastic Leukemia Patients. *Blood* 110, 4282. <https://doi.org/10.1182/blood.V110.11.4282.4282>.
- Stam, R.W., Schneider, P., Hagelstein, J.A.P., van der Linden, M.H., Stumpel, D.J.P.M., de Menezes, R.X., de Lorenzo, P., Valsecchi, M.G., and Pieters, R. (2010a). Gene expression profiling-based dissection of MLL translocated and MLL germline acute lymphoblastic leukemia in infants. *Blood* 115, 2835–2844. <https://doi.org/10.1182/blood-2009-07-233049>.
- Stam, R.W., Schneider, P., Hagelstein, J.A.P., van der Linden, M.H., Stumpel, D.J.P.M., de Menezes, R.X., de Lorenzo, P., Valsecchi, M.G., and Pieters, R. (2010b). Gene expression profiling-based dissection of MLL translocated and MLL germline acute lymphoblastic leukemia in infants. *Blood* 115, 2835–2844. <https://doi.org/10.1182/blood-2009-07-233049>.

- Stein, E.M., Garcia-Manero, G., Rizzieri, D.A., Tibes, R., Berdeja, J.G., Savona, M.R., Jongen-Lavrenic, M., Altman, J.K., Thomson, B., Blakemore, S.J., et al. (2018). The DOT1L inhibitor pinometostat reduces H3K79 methylation and has modest clinical activity in adult acute leukemia. *Blood* 131, 2661–2669. <https://doi.org/10.1182/blood-2017-12-818948>.
- Steinhilber, D., and Marschalek, R. (2017). How to effectively treat acute leukemia patients bearing MLL-rearrangements? *Biochem. Pharmacol.*
- Stumpel, D.J.P.M., Schneider, P., Seslija, L., Osaki, H., Williams, O., Pieters, R., and Stam, R.W. (2012). Connectivity mapping identifies HDAC inhibitors for the treatment of t(4;11)-positive infant acute lymphoblastic leukemia. *Leukemia* 26, 682–692. <https://doi.org/10.1038/leu.2011.278>.
- Subramanian, A., Tamayo, P., Mootha, V.K., Mukherjee, S., Ebert, B.L., Gillette, M.A., Paulovich, A., Pomeroy, S.L., Golub, T.R., Lander, E.S., et al. (2005). Gene set enrichment analysis: a knowledge-based approach for interpreting genome-wide expression profiles. *Proc. Natl. Acad. Sci. U. S. A.* 102, 15545–15550. <https://doi.org/10.1073/pnas.0506580102>.
- Sun, Q.-Y., Ding, L.-W., Tan, K.-T., Chien, W., Mayakonda, A., Lin, D.-C., Loh, X.-Y., Xiao, J.-F., Meggendorfer, M., Alpermann, T., et al. (2017). Ordering of mutations in acute myeloid leukemia with partial tandem duplication of MLL (MLL-PTD). *Leukemia* 31, 1–10. <https://doi.org/10.1038/leu.2016.160>.
- Suraweera, A., O'Byrne, K.J., and Richard, D.J. (2018). Combination Therapy With Histone Deacetylase Inhibitors (HDACi) for the Treatment of Cancer: Achieving the Full Therapeutic Potential of HDACi. *Front. Oncol.* 8 .
- Symeonidou, V., Jakobczyk, H., Bashanfer, S., Malouf, C., Fotopoulou, F., Kotecha, R.S., Anderson, R.A., Finch, A.J., and Ottersbach, K. (2021). Defining the fetal origin of MLL-AF4 infant leukemia highlights specific fatty acid requirements. *Cell Rep.* 37, 109900. <https://doi.org/10.1016/j.celrep.2021.109900>.
- Szczepański, T., Harrison, C.J., and van Dongen, J.J. (2010). Genetic aberrations in paediatric acute leukaemias and implications for management of patients. *Lancet Oncol.* 11, 880–889. .
- Takeda, S., Chen, D.Y., Westergard, T.D., Fisher, J.K., Rubens, J.A., Sasagawa, S., Kan, J.T., Korsmeyer, S.J., Cheng, E.H.-Y., and Hsieh, J.J.-D. (2006). Proteolysis of MLL family proteins is essential for Taspase1-orchestrated cell cycle progression. *Genes Dev.* 20, 2397–2409. <https://doi.org/10.1101/gad.1449406>.
- Takeuchi, M., Miyoshi, H., Asano, N., Yoshida, N., Yamada, K., Yanagida, E., Moritsubo, M., Nakata, M., Umeno, T., Suzuki, T., et al. (2019). Human leukocyte antigen class II expression is a good prognostic factor in adult T-cell leukemia/lymphoma. *Haematologica* 104, 1626–1632. <https://doi.org/10.3324/haematol.2018.205567>.

- Taki, T., Kano, H., Taniwaki, M., Sako, M., Yanagisawa, M., and Hayashi, Y. (1999). AF5q31, a newly identified AF4-related gene, is fused to MLL in infant acute lymphoblastic leukemia with ins (5; 11)(q31; q13q23). *Proc. Natl. Acad. Sci.* *96*, 14535–14540. .
- Taylor, G.M., Hussain, A., Lightfoot, T.J., Birch, J.M., Eden, T.O.B., and Greaves, M.F. (2008). HLA-associated susceptibility to childhood B-cell precursor ALL: definition and role of HLA-DPB1 supertypes. *Br. J. Cancer* *98*, 1125–1131. <https://doi.org/10.1038/sj.bjc.6604257>.
- Thomas, M., Geßner, A., Vornlocher, H.-P., Hadwiger, P., Greil, J., and Heidenreich, O. (2005). Targeting MLL-AF4 with short interfering RNAs inhibits clonogenicity and engraftment of t(4;11)-positive human leukemic cells. *Blood* *106*, 3559–3566. <https://doi.org/10.1182/blood-2005-03-1283>.
- Thompson, P., Urayama, K., Zheng, J., Yang, P., Ford, M., Buffler, P., Chokkalingam, A., Lightfoot, T., and Taylor, M. (2014). Differences in Meiotic Recombination Rates in Childhood Acute Lymphoblastic Leukemia at an MHC Class II Hotspot Close to Disease Associated Haplotypes. *PLOS ONE* *9*, e100480. <https://doi.org/10.1371/journal.pone.0100480>.
- Townsend, E.C., DeSouza, T., Murakami, M.A., Montero, J., Stevenson, K., Christie, A.L., Christodolou, A.N., Vojinovic, U., Kopp, N., Barzaghi-Rinaudo, P., et al. (2015). The MDM2 Inhibitor NVP-CGM097 Is Highly Active in a Randomized Preclinical Trial of B-Cell Acute Lymphoblastic Leukemia Patient Derived Xenografts. *Blood* *126*, 797. <https://doi.org/10.1182/blood.V126.23.797.797>.
- Trentin, L., Giordan, M., Dingermann, T., Basso, G., Te Kronnie, G., and Marschalek, R. (2009). Two independent gene signatures in pediatric t(4;11) acute lymphoblastic leukemia patients. *Eur. J. Haematol.* *83*, 406–419. <https://doi.org/10.1111/j.1600-0609.2009.01305.x>.
- U, M., Shen, L., Oshida, T., Miyauchi, J., Yamada, M., and Miyashita, T. (2004). Identification of novel direct transcriptional targets of glucocorticoid receptor. *Leukemia* *18*, 1850–1856. <https://doi.org/10.1038/sj.leu.2403516>.
- Uckun, F.M., Qazi, S., Ozer, Z., Garner, A.L., Pitt, J., Ma, H., and Janda, K.D. (2011). Inducing apoptosis in chemotherapy-resistant B-lineage acute lymphoblastic leukaemia cells by targeting HSPA5, a master regulator of the anti-apoptotic unfolded protein response signalling network. *Br. J. Haematol.* *153*, 741–752. <https://doi.org/10.1111/j.1365-2141.2011.08671.x>.
- Vega-García, N., Malatesta, R., Estella, C., Pérez-Jaume, S., Esperanza-Cebollada, E., Torreadell, M., Català, A., Gassiot, S., Berruenco, R., Ruiz-Llobet, A., et al. (2018). Paediatric patients with acute leukaemia and KMT2A (MLL) rearrangement show a distinctive expression pattern of histone deacetylases. *Br. J. Haematol.* *182*, 542–553. <https://doi.org/10.1111/bjh.15436>.
- Vester, S.K., Beavil, R.L., Lynham, S., Beavil, A.J., Graham, D.S.C., McDonnell, J.M., and Vyse, T.J. (2021). Nucleolin acts as the receptor for C1QTNF4 and supports C1QTNF4-

mediated innate immunity modulation. *J. Biol. Chem.* 296. <https://doi.org/10.1016/j.jbc.2021.100513>.

Völse, K. (2020). Role of the t(4;11) fusion proteins MLL/AF4 and AF4/MLL for survival and growth of patient-derived xenograft leukemia cells in vivo. Technische Universität München.

Waanders, E., Scheijen, B., Meer, L.T. van der, Reijmersdal, S.V. van, Emst, L. van, Kroeze, Y., Sonneveld, E., Hoogerbrugge, P.M., Kessel, A.G. van, Leeuwen, F.N. van, et al. (2012). The Origin and Nature of Tightly Clustered BTG1 Deletions in Precursor B-Cell Acute Lymphoblastic Leukemia Support a Model of Multiclonal Evolution. *PLOS Genet.* 8, e1002533. <https://doi.org/10.1371/journal.pgen.1002533>.

Wang, C.-J., Jia, M.-Z., Deng, L.-P., Li, W.-J., Zhang, Q., Zhang, T.-J., Li, S.-Y., Cui, L., and Li, Z.-G. (2022). Interaction between CASP8AP2 and ZEB2-CtBP2 Regulates the Expression of LEF1. *Pediatr. Hematol. Oncol.* 0, 1–12. <https://doi.org/10.1080/08880018.2022.2033369>.

Wang, E.S., Altman, J.K., Pettit, K., De Botton, S., Walter, R.P., Fenaux, P., Burrows, F., Tomkinson, B.E., Martell, B., and Fathi, A.T. (2020). Preliminary Data on a Phase 1/2A First in Human Study of the Menin-KMT2A (MLL) Inhibitor KO-539 in Patients with Relapsed or Refractory Acute Myeloid Leukemia. *Blood* 136, 7–8. <https://doi.org/10.1182/blood-2020-134942>.

Wang, F., Demir, S., Gehringer, F., Osswald, C.D., Seyfried, F., Enzenmüller, S., Eckhoff, S.M., Maier, T., Holzmann, K., Debatin, K.-M., et al. (2018). Tight regulation of FOXO1 is essential for maintenance of B-cell precursor acute lymphoblastic leukemia. *Blood* 131, 2929–2942. <https://doi.org/10.1182/blood-2017-10-813576>.

Wang, W., Li, Y., Gao, L., Xu, S.-H., Gong, M., Huang, F.-Z., Li, Z.-L., Chen, Y.-R., and Ma, Y.-G. (2014). [Significance of CD37 expression in malignant B cells]. *Zhongguo Shi Yan Xue Ye Xue Za Zhi* 22, 644–647. <https://doi.org/10.7534/j.issn.1009-2137.2014.03.013>.

Watanabe, N., Broome, M., and Hunter, T. (1995). Regulation of the human WEE1Hu CDK tyrosine 15-kinase during the cell cycle. *EMBO J.* 14, 1878–1891. <https://doi.org/10.1002/j.1460-2075.1995.tb07180.x>.

Weisberg, E., Manley, P.W., Cowan-Jacob, S.W., Hochhaus, A., and Griffin, J.D. (2007). Second generation inhibitors of BCR-ABL for the treatment of imatinib-resistant chronic myeloid leukaemia. *Nat. Rev. Cancer* 7, 345–356. <https://doi.org/10.1038/nrc2126>.

Wilhelm, A., and Marschalek, R. (2021). The role of reciprocal fusions in MLL-r acute leukemia: studying the chromosomal translocation t(4;11). *Oncogene* 40, 6093–6102. <https://doi.org/10.1038/s41388-021-02001-2>.

Wilkinson, A.C., Ballabio, E., Geng, H., North, P., Tapia, M., Kerry, J., Biswas, D., Roeder, R.G., Allis, C.D., Melnick, A., et al. (2013). RUNX1 Is a Key Target in t(4;11) Leukemias that Contributes to Gene Activation through an AF4-MLL Complex Interaction. *Cell Rep.* 3, 116–127. <https://doi.org/10.1016/j.celrep.2012.12.016>.

- Witkowski, M.T., Dolgalev, I., Evensen, N.A., Ma, C., Chambers, T., Roberts, K.G., Sreeram, S., Dai, Y., Tikhonova, A.N., Lasry, A., et al. (2020). Extensive Remodeling of the Immune Microenvironment in B Cell Acute Lymphoblastic Leukemia. *Cancer Cell* 37, 867-882.e12. <https://doi.org/10.1016/j.ccell.2020.04.015>.
- Xia, Z.-B., Anderson, M., Diaz, M.O., and Zeleznik-Le, N.J. (2003). MLL repression domain interacts with histone deacetylases, the polycomb group proteins HPC2 and BMI-1, and the corepressor C-terminal-binding protein. *Proc. Natl. Acad. Sci.* 100, 8342–8347. <https://doi.org/10.1073/pnas.1436338100>.
- Yamada, M., Hirasawa, A., Shiojima, S., and Tsujimoto, G. (2003). Granzyme A mediates glucocorticoid-induced apoptosis in leukemia cells. *FASEB J. Off. Publ. Fed. Am. Soc. Exp. Biol.* 17, 1712–1714. <https://doi.org/10.1096/fj.02-1116fje>.
- Yang, Q., Rasmussen, S.A., and Friedman, J.M. (2002). Mortality associated with Down's syndrome in the USA from 1983 to 1997: a population-based study. *The Lancet* 359, 1019–1025. .
- Yang, Y., Xue, K., Li, Z., Zheng, W., Dong, W., Song, J., Sun, S., Ma, T., and Li, W. (2018). c-Myc regulates the CDK1/cyclin B1 dependent-G2/M cell cycle progression by histone H4 acetylation in Raji cells Corrigendum in /10.3892/ijmm.2019.4318. *Int. J. Mol. Med.* 41, 3366–3378. <https://doi.org/10.3892/ijmm.2018.3519>.
- Yano, T., Nakamura, T., Blechman, J., Sorio, C., Dang, C.V., Geiger, B., and Canaani, E. (1997). Nuclear punctate distribution of ALL-1 is conferred by distinct elements at the N terminus of the protein. *Proc. Natl. Acad. Sci.* 94, 7286–7291. <https://doi.org/10.1073/pnas.94.14.7286>.
- Yokoyama, A. (2015). Molecular mechanisms of MLL-associated leukemia. *Int. J. Hematol.* 101, 352–361. <https://doi.org/10.1007/s12185-015-1774-4>.
- Yokoyama, A., and Cleary, M.L. (2008). Menin critically links MLL proteins with LEDGF on cancer-associated target genes. *Cancer Cell* 14, 36–46. .
- Yokoyama, A., Kitabayashi, I., Ayton, P.M., Cleary, M.L., and Ohki, M. (2002). Leukemia proto-oncoprotein MLL is proteolytically processed into 2 fragments with opposite transcriptional properties. *Blood* 100, 3710–3718. <https://doi.org/10.1182/blood-2002-04-1015>.
- Yokoyama, A., Wang, Z., Wysocka, J., Sanyal, M., Aufiero, D.J., Kitabayashi, I., Herr, W., and Cleary, M.L. (2004). Leukemia Proto-Oncoprotein MLL Forms a SET1-Like Histone Methyltransferase Complex with Menin To Regulate Hox Gene Expression. *Mol. Cell. Biol.* 24, 5639–5649. <https://doi.org/10.1128/MCB.24.13.5639-5649.2004>.
- Yokoyama, A., Somerville, T.C.P., Smith, K.S., Rozenblatt-Rosen, O., Meyerson, M., and Cleary, M.L. (2005). The menin tumor suppressor protein is an essential oncogenic cofactor for MLL-associated leukemogenesis. *Cell* 123, 207–218. <https://doi.org/10.1016/j.cell.2005.09.025>.

- Yokoyama, A., Ficara, F., Murphy, M.J., Meisel, C., Hatanaka, C., Kitabayashi, I., and Cleary, M.L. (2013). MLL Becomes Functional through Intra-Molecular Interaction Not by Proteolytic Processing. *PLoS ONE* 8, e73649. <https://doi.org/10.1371/journal.pone.0073649>.
- Zhang, W., Xia, X., Reisenauer, M.R., Hemenway, C.S., and Kone, B.C. (2006). Dot1a-AF9 complex mediates histone H3 Lys-79 hypermethylation and repression of ENaC α in an aldosterone-sensitive manner. *J. Biol. Chem.* 281, 18059–18068. .
- Zhang, Y., Zhou, X., Li, Y., Xu, Y., Lu, K., Li, P., and Wang, X. (2018). Inhibition of maternal embryonic leucine zipper kinase with OTSSP167 displays potent anti-leukemic effects in chronic lymphocytic leukemia. *Oncogene* 37, 5520–5533. <https://doi.org/10.1038/s41388-018-0333-x>.
- Zhao, Z., Wang, L., Volk, A.G., Birch, N.W., Stoltz, K.L., Bartom, E.T., Marshall, S.A., Rendleman, E.J., Nestler, C.M., and Shilati, J. (2019). Regulation of MLL/COMPASS stability through its proteolytic cleavage by *taspase1* as a possible approach for clinical therapy of leukemia. *Genes Dev.* 33, 61–74. .
- Zheng, J. (2013). Oncogenic chromosomal translocations and human cancer (review). *Oncol. Rep.* 30, 2011–2019. <https://doi.org/10.3892/or.2013.2677>.
- Zhong, Y., Yang, J., Xu, W.W., Wang, Y., Zheng, C.-C., Li, B., and He, Q.-Y. (2017). KCTD12 promotes tumorigenesis by facilitating CDC25B/CDK1/Aurora A-dependent G2/M transition. *Oncogene* 36, 6177–6189. <https://doi.org/10.1038/onc.2017.287>.
- Zhou, H., Spicuglia, S., Hsieh, J.J.-D., Mitsiou, D.J., Høiby, T., Veenstra, G.J.C., Korsmeyer, S.J., and Stunnenberg, H.G. (2006). Uncleaved TFIIA Is a Substrate for Taspase 1 and Active in Transcription. *Mol. Cell. Biol.* 26, 2728–2735. <https://doi.org/10.1128/MCB.26.7.2728-2735.2006>.
- Zipursky, A., Peeters, M., and Poon, A. (1987). Megakaryoblastic leukemia and Down's syndrome: a review. *Pediatr. Hematol. Oncol.* 4, 211–230. .

9. STATUTORY DECLARATION

Eidesstattliche Erklärung

Hiermit erkläre ich, Alexander Wilhelm, die hier vorgelegte Dissertation mit dem Thema

“The role of reciprocal fusions in *MLL-r* acute leukemia: studying the chromosomal translocation t(4;11)”

selbständig angefertigt und mich anderer Hilfsmittel als der in ihr angegebenen nicht bedient habe, insbesondere, dass alle Entlehnungen aus anderen Schriften mit Angabe der betreffenden Schrift gekennzeichnet sind.

Ich versichere, die Grundsätze der guten wissenschaftlichen Praxis beachtet und nicht die Hilfe einer kommerziellen Promotionsvermittlung in Anspruch genommen zu haben.

Frankfurt am Main, den

.....

Unterschrift

10. CURRICULUM VITAE

Alexander Wilhelm

Born on 10 April, 1991
 Brinkstr. 65, 63069 Offenbach
 +49 (0) 15771914007
 a.wilhelm@stud.uni-frankfurt.de



EDUCATION

- | | |
|--|--------------------------|
| <p>Universitätsklinikum Frankfurt Goethe-Universität, Frankfurt, Germany</p> <ul style="list-style-type: none"> · Researcher at the Institute of Medical Virology in the laboratory of Dr. Marek Widera · Establishment of a fast and versatile SARS-CoV-2 virus culture using the Sleeping Beauty Technology · Rapid analysis of neutralizing antibody immunity against SARS-CoV-2 variants of concern · Wastewater-based surveillance of SARS-CoV-2 variants of concern | <p>since 04/2020</p> |
| <p>Goethe Universität Frankfurt, Frankfurt, Germany</p> <ul style="list-style-type: none"> · PhD thesis: <i>“The role of reciprocal fusions in MLL-r acute leukemia: studying the chromosomal translocation t(4;11)”</i> · Institute for Pharmaceutical Biology in the laboratory of Prof. Rolf Marschalek | <p>since 01/2018</p> |
| <p>Ruprecht-Karls-Universität Heidelberg, Heidelberg, Germany</p> <ul style="list-style-type: none"> · M.Sc. Molecular and Cellular Biology – Final grade: 1,5 · Master thesis: „The role of the E3 ubiquitin ligase hyperplastic discs (Hyd) in regulating Histone H3-like centromeric protein A (CENP-A).“ · Zentrum für Molekulare Biologie der Universität Heidelberg (ZMBH) in the laboratory of Dr. Sylvia Erhardt | <p>10/2014 – 03/2017</p> |
| <p>Karl-Franzens-Universität Graz, Graz, Austria</p> <ul style="list-style-type: none"> · B.Sc. Molecular biology – Final grade: 1,8 · Institut für Molekulare Biowissenschaften (IMB) · Bachelor thesis: „Interactions of Phages and Human Pathogen Viruses with Biofilms“. Supervision: Prof. Günther Koraimann and Prof. Klaus-Dieter Kühn | <p>02/2011 – 07/2014</p> |

Leibniz Gymnasium Offenbach, *Offenbach, Germany*

08/2001 – 06/2010

- Abitur – Final grade: 2,0
- Advanced courses: Politics and economy, Biology

11. LIST OF PUBLICATIONS

Publications

1. Demirdizen E, Spiller-Becker M, Förtsch A, Wilhelm A, Corless S, Bade D, Bergner A, Hessling B, Erhardt S, 2019. Localization of Drosophila CENP-A to non-centromeric sites depends on the NuRD complex. *Nucleic Acids Res.* 2019 Dec 16;47(22):11589-11608.
2. Shin D, Mukherjee R, Grewe D, Bojkova D, Baek K, Bhattacharya A, Schulz L, Widera M, Mehdipour A R, Tascher G, Geurink P P, Wilhelm A, van der Heden van Noort G J, Ovaa H, Müller S, Knobloch K-P, Rajalingam K, Schulman B A, Cinatl J, Hummer G, Ciesek S, Dikic I. 2020. Papain-like protease regulates SARS-CoV-2 viral spread and innate immunity. *Nature.* 2020 Nov;587(7835):657-662.
3. Widera M, Wilhelm A, Toptan T, Raffel J M, Kowarz E, Roesmann F, Grözing F, Siemund A L, Luciano V, Külp M, Reis J, Bracharz S, Pallas C, Ciesek S, Marschalek R. Generation of a Sleeping Beauty transposon-based cellular system for rapid and sensitive screening for compounds and cellular factors limiting SARS-CoV-2 replication. *Frontiers in Microbiology.* 2021
4. Wilhelm A, Widera M, Grikscheit K, Toptan T, Schenk B, Pallas C, Metzler M, Kohmer N, Hoehl S, Helfritz FA, Wolf T, Goetsch U, Ciesek S. Reduced Neutralization of SARS-CoV-2 Omicron Variant by Vaccine Sera and Monoclonal Antibodies. *medRxiv.* 2021
5. Wilhelm A, Toptan T, Pallas C, Wolf T, Goetsch U, Gottschalk R, Vehreschild M JGT, Ciesek S, Widera M. Antibody-mediated neutralization of authentic SARS-CoV-2 B.1.617 variants harboring L452R and T478K/E484Q. *Viruses.* 2021
6. Carlet M, Völse K, Vergalli J, Becker M, Herold T, Arner A, Liu W-H, Dill V, Fehse B, Baldus C D, Bastian L, Lenk L, Schewe D M, Bagnoli J W, Wilhelm A, Marschalek R, Jost P J, Miehting C, Riecken K, Schmidt-Supprian M, Binder V, Jeremias I. In vivo inducible reverse genetics in patients' tumors to identify individual therapeutic targets, *Nature Communications.* 2021

7. Widera M, Wilhelm A, Hoehl S, Pallas C, Kohmer N, Wolf T, Rabenau H F, Corman V, Drosten C, Vehreschild M JGT, Goetsch U, Gottschalk R, Ciesek S. Limited neutralization of authentic severe acute respiratory syndrome coronavirus 2 variants carrying E484K in vitro. *Journal of Infectious Diseases*. 2021
8. Wilhelm A, Marschalek R. The role of reciprocal fusions in MLL-r acute leukemia: studying the chromosomal translocation t(4;11). *Oncogene*. 2021
9. Wilhelm A, Pallas C, Marschalek R, Widera M. Detection and Quantification of SARS-CoV-2 by Real-Time RT-PCR Assay. *Methods Mol Biol*. 2022
10. Wilhelm A, Widera M, Grikscheit K, Toptan T, Schenk B, Pallas C, Metzler M, Kohmer N, Hoehl S, Marschalek R, Herrmann E, Helfritz FA, Wolf T, Goetsch U, Ciesek S. Limited Neutralisation of the SARS-CoV-2 Omicron Subvariants BA.1 and BA.2 by Convalescent and Vaccine Serum and monoclonal antibodies. *EbioMedicine*. 2022
11. Grikscheit K, Rabenau H, Ghodatrian Z, Widera M, Wilhelm A, Toptan Grabmair T, Hoehl S, Layer E, Helfritz F, Ciesek S. Characterization of antibody and T-cell response after second booster vaccination. *Viruses*. 2022
12. Wilhelm A, Schot J, Meinert-Berning C, Agrawal S, Bastian D, Orschler L, Ciesek S, Teichgräber B, Wintgens T, Lackner S, Weber FA, Widera M. Wastewater Surveillance Allows Early Detection of SARS-CoV-2 Omicron in North Rhine-Westphalia, Germany. *Science of the Total Environment*. 2022
13. Wilhelm A, Schot J, Meinert-Berning C, Agrawal S, Bastian D, Orschler L, Ciesek S, Teichgräber B, Wintgens T, Lackner S, Weber FA, Widera M. Early Detection of SARS-CoV-2 Omicron BA. 4/5 in German wastewater. *Viruses*. 2022
14. Veleanu A, Kelch MA, Ye C, Flohr M, Wilhelm A, Widera M, Martinez-Sobrido L, Ciesek S, Toptan T. Molecular Analyses of Clinical Isolates and Recombinant SARS-CoV-2 Carrying B.1 and B.1.617.2 Spike Mutations Suggest a Potential Role of Non-Spike Mutations in Infection Kinetics. *Viruses*. 2022

Meeting Abstracts

Talks

1. Wilhelm A, Marschalek R. Investigating HDACi and dnTASP1 for the treatment of t(4;11) leukemic cells. Annual Meeting Kind-Phillip-Foundation of Leukemia Research, Wilsede. 2019
2. Wilhelm A, Marschalek R. Role of reciprocal fusions in *MLL-r* acute leukemia: studying t(4; 11) fusion proteins. Annual Meeting Kind-Phillip-Foundation of Leukemia Research 2020, Wilsede
3. Wilhelm A, Schot J, Meinert-Berning C, Dolny R, Bastian D, Wintgens T, Weber FA, Widera M. Wastewater Surveillance Allows Early Detection of SARS-CoV-2 Omicron in North Rhine-Westphalia, Germany. 31th Annual Meeting of the Society for Virology. 2022

Poster

1. Wilhelm A, Marschalek R. Significance of the reciprocal AF4-MLL fusion protein in t(4;11) acute lymphoblastic leukemia. the 25th Congress of the European Hematology Association. 2020
2. Wilhelm A, Toptan Grabmair T, Raffel J, Kowarz E, Roesmann F, Siemund AL, Luciano V, Kulp M, Reis J, Bracharz S, Pallas C, Wolf T, Ciesek S, Marschalek R, Widera M. Generation of a Sleeping Beauty transposon-based cellular system for rapid and sensitive identification of SARS-CoV-2 host dependency and restriction factors. 30th Annual Meeting of the Society for Virology. 2021
3. Wilhelm A, Grikscheit K, Toptan T, Schenk B, Roesmann F, Pallas C, Kowarz E, Metzler M, Kohmer N, Hoehl S, E, Helfritz FA, Wolf T, Marschalek R, Goetsch U, Ciesek S., Widera M. Rapid analysis of waning neutralizing antibody immunity against SARS-CoV-2 variants of concern using the A549-AT infectious model. 31th Annual Meeting of the Society for Virology. 2022

12. ACKNOWLEDGEMENTS

First of all, I want to thank my doctoral supervisor Rolf for his supervision and unfailing support. Especially I am grateful for his patience during the COVID-19 pandemics which kept us all quite busy doing science in hemato-oncology but also medical virology. Rolf has given me all the freedom to pursue my projects and offered me his valuable scientific guidance whenever needed.

I am especially thankful to Prof. Dr. Robert Fürst for being my second referee.

I would like to particularly thank Dr. Bruno Lopes and Fabian Roesmann for reading my thesis but also your friendship.

I also would like to thank Dr. Eric Kowarz and Dr. Claus Meyer for great and helpful discussions.

I gladly thank my collaboration partners Kerstin Völse and Prof. Dr. Irmela Jeremias, Dr. Constantin Kondak and Prof. Dr. Jochen Klein, Dr. Klaus Hoffmeier, Dr. Fabian Grunz, Alejandro Rodríguez, Lukas Jost, Mohammed Alkhatib and Dr. Björn Rotter.

My thanks also go to all the members of the Marschalek Lab for being a special team. I want to especially acknowledge the support of Jennifer Reis for scientific but also non-scientific support and for being a wonderful colleague. I also would like to thank Dr. Ilse Zündorf, Silvia Bracharz for your excellent support in cell-culturing and Patrizia Larghero, Dr. Iris Bischoff-Kont and Mareike Lang for your help and guidance.

I want to thank Dr. Marek Widera and Prof. Dr. Sandra Ciesek for the opportunity to pursue relevant and interesting SARS-CoV-2 research. Especially I want to thank Dr. Marek Widera for critical input, very helpful directions and valuable scientific guidance.

I also want to thank all my colleagues at the Institute for Medical Virology and especially Dr. Tuna Toptan Grabmair, Dr. Sandra Westhaus, Dr. Katharina Grikscheit, Christiane Pallas, Fabian Roesmann, Prof. Dr. Denisa Bojkova, Johanna Raffel, Irina Jakobsche, Andrei Veleanu and Marco Bechtel for your help in the laboratory and support during numerous demanding projects.

My thanks go to the outstanding and enthusiastic students Jonas Schmidt and Wai Lam Kwan and Irene Ballesteros.

My sincere thanks go also to Prof. Dr. Klaus-Dieter Kühn for encouraging me all over the years.

Most importantly, very special thanks to my entire family, in particular to my wife Giannina and to my son Maximilian, for their support during the dual workload during the COVID-19 pandemics.

Gracias Pecesita, por haber creído en mí.